THE AS-LAID EMBEDMENT OF SUBSEA PIPELINES

by

Zachary J. Westgate

M.S.C.E.

A thesis submitted for the degree of

Doctor of Philosophy

The University of Western Australia

School of Civil and Resource Engineering

May 2013

ABSTRACT

The behaviour of a subsea pipeline is strongly influenced by its level of embedment into the seabed. In deep water, the in-service embedment of a pipeline is mainly controlled by the lay process during installation. The as-laid embedment is notoriously difficult to assess, due to uncertainties associated with the near surface soil properties, the dynamic movement of the pipe caused by the sea state and resulting vessel motion, and the large-deformation nature of pipe-soil interaction at the seabed. Prior to this work, the industry approach to assessing as-laid embedment was to first assess the static embedment as if the pipe were lowered statically onto the seabed, allowing for the effect of the pipe catenary on the touchdown load, and then to amplify this embedment by an empirical adjustment factor, not linked directly to the soil conditions, pipe properties or lay process.

Data sets obtained from as-laid field surveys of subsea pipelines were combined with numerical simulations of offshore pipe laying and physical model testing of the dynamic pipe embedment process to investigate the mechanisms that govern the as-laid embedment of seabed pipelines. The field surveys comprise embedment data for five different pipelines from three different hydrocarbon-producing regions. The pipeline properties, soil conditions, lay vessel characteristics, and sea states varied widely across the five case studies, which allowed benchmarking of existing and newly proposed calculation methods for assessing as-laid embedment. The numerical simulations were used to assist with interpretation of the field surveys, by simulating the pipe response due to the measured vessel motions and sea states. The physical model testing, performed in a geotechnical centrifuge, involved well-controlled idealisations of different aspects of the lay process.

New methods for assessing as-laid embedment have been proposed, which treat more rigorously the processes that control the embedment of a pipe into the seabed. The new calculation methods explicitly account for the influences of the governing soil and pipeline properties. It is shown that a reasonable estimate of as-laid pipeline embedment can be made using the fully remoulded soil strength combined with a theoretically-rigorous solution for the vertical bearing capacity. However, it is also shown, through physical modelling, that this is a simplification of the real behaviour. Combined vertical-horizontal loading caused by pipe movement in the touchdown zone also

contributes to the embedment process, and is compensated by only partial remoulding of the surrounding soil. Calculation methods with differing levels of complexity are used to back-analyse the field and model test observations. These methods represent significant advances in the understanding of pipe-soil interaction and offer improvements to subsea pipeline design. They have already found application in practice.

PUBLICATIONS ARISING FROM THIS THESIS

In accordance with regulations of the University of Western Australia, this thesis is organised as a series of academic papers that describe the work performed during the PhD candidature. Chapters 1 and 8 comprise the Introduction and Conclusions chapters, respectively. These chapters are University requirements and were not submitted for publication. As is customary, these chapters have been prepared solely by the candidate. All six of the remaining chapters have been published, and were prepared by the candidate with assistance from the co-authors. Full bibliographic details are provided below. Overall, the candidate is the lead author on all publications arising from this body of work, and is responsible for more than 90% of the content presented in this thesis.

- **Chapter 2:** Westgate, Z.J., White, D.J. & Randolph, M.F. (2009). Video observations of dynamic embedment during pipelaying in soft clay. *Proc. Offshore Mechanics and Arctic Engineering Conf.*, Honolulu, USA, June 1-5, Paper OMAE2009-79814.

  The video review and back-analysis of observed pipeline embedment was performed solely by the candidate. Both co-authors contributed to the write-up of this chapter, after a full initial draft was prepared by the candidate.

- **Chapter 3:** Westgate, Z.J., Randolph, M.F., White D.J. & Li, S. (2010). The influence of seastate on as-laid pipeline embedment: a case study. *Applied Ocean Research*, Vol. 32, No. 3, pp. 321-331.

  Preliminary data processing was performed by the last co-author, which was checked and back-analysed by the candidate. The numerical simulations were performed solely by the candidate. The second and third co-authors contributed to the write-up of this chapter, after a full initial draft was prepared by the candidate.

- **Chapter 4:** Westgate, Z.J., White, D.J., Randolph, M.F. & Brunning, P. (2010). Pipeline laying and embedment in soft fine-grained soils: field observations and numerical simulations. *Proc. Offshore Technology Conf.*, Paper OTC20407.

  All data processing and interpretation was performed by the candidate. The video review and numerical simulations were performed solely by the candidate.

The second, third and fourth co-authors contributed to the write-up of this chapter, after a full initial draft was prepared by the candidate.

- **Chapter 5:** Westgate, Z.J., Randolph, M.F., White, D.J. & Brunning, P. (2010). Theoretical, numerical and field studies of offshore pipeline sleeper crossings. *Proc.2nd Int. Sym. Frontiers in Offshore Geotechnics*, Perth.

  All data processing and interpretation was performed by the candidate. An initial draft analysis of the theoretical aspects of this chapter was performed by the second co-author, which was checked and extended to the sleeper crossing application by the candidate. The numerical simulations were performed solely by the candidate. The second and third co-authors contributed to the write-up of this chapter, after a full initial draft was prepared by the candidate.

- **Chapter 6:** Westgate, Z.J., White, D.J. & Randolph, M.F. (2012). Field observations of as-laid pipeline embedment in carbonate sediments, *Géotechnique*, Vol. 62, No. 9, pp. 787-798.

  The data processing and interpretation was performed by the candidate. Interpretation of the geotechnical data within this chapter was performed primarily by the candidate with assistance from the co-authors, both of whom also contributed to the write-up of this chapter, after a full initial draft was prepared by the candidate.

- **Chapter 7:** Westgate, Z.J., White, D.J. & Randolph, M.F. (2013). Modelling the embedment process during offshore pipe laying on fine-grained soils, *Canadian Geotechnical J.*, Vol. 50, No. 1, pp. 15-27.

  The physical model testing presented in this chapter was performed by the candidate, with assistance from the second author. The second co-author contributed to the write-up of this chapter after a full initial draft was prepared by the candidate, and the third co-author provided review comments.

The stated contributions above have been agreed with the co-authors of each paper, and full permission has been granted by each co-author to include the relevant paper within this thesis.

Zachary J Westgate, candidate……

Professor David J White, coordinating supervisor……

ACKNOWLEDGEMENTS

There are many individuals that, through their support and encouragement, made the work presented in this thesis possible.

Firstly, I acknowledge the financial support provided through the Endeavour International Postgraduate Research Scholarship program, as well as the financial support provided by the Shacklock Top-Up Scholarship and Samaha Research Scholarship. I am also grateful to COFS for providing additional financial support during my studies.

I extend special thanks to industry colleagues Paul Brunning and Andrew Pearce for supporting with aspects of this thesis. I also thank Colin Blundell of Orcina Ltd. for assistance with the OrcaFlex numerical model development.

I thank my advisors Dave White and Mark Randolph, for their inspiration, guidance, and patience during this work. I am very fortunate to have been able to work with both of you, and look forward to working together in the future.

I thank the COFS technical department for assisting with the physical model testing phase of this work, especially Bart, Don, Shane, Dave, and Phil. Your collective expertise in all things technical is second to none. I also thank the COFS administration department for making life easier when it came to form signing and all things bureauocratic, specifically Eileen, Monica and Lisa.

While I would like to list all of the individuals whose friendship and camaraderie have made for an enjoyable experience during my four years at COFS, I trust you know who you are and I provide here a gentle reminder: the morning coffee club, the brewing cohort, the surf club, the Friday ‘arvo’ table sessions, and all of those who I was fortunate enough to meet during your travels through Perth.

Finally, I thank my partner and best friend Tara for taking a leap of faith and agreeing to move our little family across the world for a few years. While difficult at times, hopefully we have come out of this experience with good memories and broader minds.

To my daughter Mason Isabella, I hope someday you will appreciate (and still remember) your life in Australia. This thesis is dedicated to you…

TABLE OF CONTENTS

LIST OF TABLES

LIST OF FIGURES

NOMENCLATURE

The nomenclature presented throughout this thesis has been adopted with the aim of maintaining consistency with previously published work. Inevitably, there may be instances throughout the thesis where a specific parameter has used different notation, or where specific notation refers to two different parameters in different chapters. These are noted below.

List of Symbols

∞	infinity
a	fitting parameter in static penetration response
A	foundation area
A_s	area of pipeline below mudline
B	effective pipe-soil contact width (including effect of soil heave)
b	fitting parameter in static penetration response
c_v	vertical coefficient of consolidation
D	pipe diameter
D'	pipe-soil contact width (excluding effect of soil heave)
E	elastic modulus of pipeline
E	passive energy of pipe response during lateral motion (Chapter 1)
f_b	buoyancy factor in bearing capacity solution
f_{dyn}	dynamic embedment factor (also expressed as F_{dyn} in Chapters 2 and 3)
f_{lay}	touchdown lay factor
g	acceleration due to gravity
H	horizontal pipe-soil contact force (per unit length)
h	sleeper height above seabed (Chapter 5)

h	wave height (Chapter 3)
h/D	normalised heave height above seabed
H_s	significant wave height
i	cycle number for drained embedment calculation
I	second moment of area of pipeline
k	linearised soil stiffness, defined as V_{max}/w
k_{qc}	cone resistance gradient
k_{qnet}	net cone resistance gradient
k_{qTbar}	T-bar resistance gradient
k_{su}	undrained shear strength gradient
k_{su-ini}	initial undrained shear strength gradient
k_{su-op}	operative shear strength gradient
k_{vp}	plastic bearing stiffness
L	distance between sleeper and touchdown point (Chapter 5)
L	length of the touchdown zone (Chapter 3)
M	dimensionless bearing modulus
N	T-bar cycle number
N_{95}	number of T-bar cycles to achieve 95% strength degradation
$N_{95,rem}$	number of T-bar cycles to achieve 95% strength degradation due to remoulding (Chapter 7)
$N_{95,str}$	number of T-bar cycles to achieve 95% strength degradation due to soil structure (Chapter 7)
N_b	bearing capacity factor for soil buoyancy
N_c	bearing capacity factor for soil strength (undrained conditions) (also referred to as N_{cV} in Chapter 4)

$N_{cV\text{-}H}$	bearing capacity factor for combined vertical and horizontal loading (undrained conditions)
N_{kt}	cone bearing factor
N_q	bearing capacity factor (drained conditions)
N_{Tbar}	T-bar bearing factor
N_{TDZ}	number of cycles of pipe motion in touchdown zone
p	submerged pipe weight
Q	normalised net cone resistance
q_c	measured cone penetration resistance
q_{net}	net cone penetration resistance
q_{Tbar}	T-bar penetration resistance
$q_{Tbar\text{-}ini}$	initial T-bar penetration resistance
q_{ult}	ultimate bearing capacity
R	correlation coefficient
r	discounting parameter for pipe penetration into undisturbed soil (Chapter 7)
S	wave steepness
S_t	cyclic sensitivity of soil (also referred to as $S_{t\text{-}cyc}$ in Chapter 7)
$S_{t,in\text{-}out}$	ratio of the initial penetration resistance to the initial extraction resistance
s_u	undrained shear strength
$s_{u\text{-}ini}$	initial shear strength (also referred to as $s_{u\text{-}initial}$ in Chapter 4)
$s_{u\text{-}int}$	intact shear strength
s_{um}	mudline strength intercept
$s_{u\text{-}op}$	operative shear strength (also referred to as $s_{u\text{-}mob}$ in Chapter 4)

$s_{u\text{-}rem}$	fully remoulded shear strength
T	normalised time factor (Chapter 6)
T	wave period (Chapter 3)
t/D	normalised trench depth (below nominal seabed elevation)
T_0	static bottom tension in pipeline
T_{95}	normalised time factor to achieve 95% consolidation
t	time during which a pipe element passes through the touchdown zone
t_{cyc}	period of cyclic pipe motion
t_{swell}	swell period (also referred to as T_p in Chapter 7)
u	centre-to-peak horizontal pipe displacement amplitude
u_{max}/D	maximum normalised horizontal displacement amplitude occurring at the front of the touchdown zone
$(u/D)_{far\text{-}field}$	normalised lateral distance to far-field seabed
$(u/D)_{heave}$	normalised lateral distance to peak seabed heave elevation
$(u/D)_{LDZ}$	normalised horizontal peak-to-peak oscillation amplitude through lay down zone
$(u/D)_{trench}$	normalised lateral distance to edge of trench
u_i	initial average excess pore pressure
U_N	normalised average pore pressure ratio
v	lay rate
V	vertical pipe-soil contact force (per unit length)
V_{avg}	average vertical pipe-soil contact force during cycles of vertical motion (per unit length)
V_{dyn}	maximum dynamic vertical pipe-soil contact force (per unit length)

V_{max}	maximum vertical pipe-soil contact force (per unit length)
V_{min}	minimum vertical pipe-soil contact force (per unit length)
V_{ult}	ultimate vertical bearing capacity (per unit length)
$(V/V_{max})_{pp}$	parallel point
w	pipe embedment
W'	submerged weight of pipeline (per unit length)
$(w/D)_{BOT}$	normalised pipe embedment relative to local seabed elevation (referred to as $(w/D)_l$ in Chapter 2)
$(w/D)_{deep}$	normalised depth to deep flow round behaviour
$(w/D)_{dynamic}$	normalised pipe embedment due to lay effects
$(w/D)_{dynamic/intact}$	normalised pipe embedment calculated using dynamic catenary force and intact shear strength
$(w/D)_{dynamic/remolded}$	normalised pipe embedment calculated using dynamic catenary force and remolded shear strength
$(w/D)_{max}$	normalised maximum pipe embedment
$(w/D)_{MSB}$	normalised pipe embedment relative to nominal seabed elevation (referred to as $(w/D)_g$ in Chapter 2)
$(w/D)_{static/intact}$	normalised pipe embedment calculated using static catenary force and intact shear strength
$(w/D)_{static/remolded}$	normalised pipe embedment calculated using static catenary force and remolded shear strength
w_{avg}	the average pipe embedment between initial embedment value and current embedment value
$w_{calculated}$	calculated pipe embedment
$w_{dynamic}$	pipe embedment due to dynamic pipe motions
w_{heave}	pipe embedment below top of soil heave

w_{local}	pipe embedment relative to local seabed elevation
$w_{nominal}$	pipe embedment relative to nominal seabed elevation
$w_{observed}$	pipe embedment from as-laid survey (also referred to as $w_{as\text{-}laid}$ in Chapter 4)
w_{static}	pipe embedment from static penetration
x	distance along pipeline (Chapter 5)
x	distance from start of lay down zone to current touchdown zone (Chapter 6)
x_{LDZ}	length of lay down zone
z_w	water depth
Δu	current average excess pore pressure
$\Delta u/D$	incremental horizontal pipe displacement
Δu_2	measured pore pressure at cone shoulder
Δw_i	incremental (drained) static pipe embedment
$\Sigma(s/D)$	cumulative normalised total pipe displacement
$\Sigma(u/D)$	cumulative normalised horizontal pipe displacement
$(\Sigma s/D)_{95}$	cumulative normalised total pipe displacement to achieve 95% degradation
$(\Sigma u/D)_{95}$	cumulative normalised horizontal pipe displacement to achieve 95% degradation
$\Sigma\Delta w_i$	cumulative pipe embedment for cycles 1 through i
$\Sigma\Delta w_{i-1}$	cumulative pipe embedment for cycles 1 through i-1
α	fitting parameter in dissipation response
α_N	strength degradation parameter
β	fitting parameter in dissipation response (Chapter 6)

β	attenuation factor in horizontal lpipe oscillation model (Chapter 7)
δ_{op}	operative strength degradation factor
δ_{rem}	fully remoulded strength degradation factor
δ_{str}	component of strength degradation due to the loss of soil structure
ϕ	lay angle relative to horizontal
γ'	effective unit weight of soil
γ	total unit weight of soil
κ	fitting parameter in assessment of horizontal oscillation amplitude
λ	slope of flow rule (Chapter 7)
λ	characteristic length (also referred to as λ_{TDZ} in Chapter 6)
σ'_{v0}	in situ vertical effective stress
ζ	depth discounting parameter

List of Abbreviations

BOT	bottom of trench
CPT	cone penetration test
HTHP	high-temperature, high-pressure
KP	kilometre point
MSB	mean sea bed
NEPP	normalised excess pore pressure
PZ	process zone
RAO	response amplitude operator

SCR	steel catenary riser
TDP	touchdown point
TDZ	touchdown zone
TOP	top of pipe

CHAPTER 1. INTRODUCTION

Subsea pipelines are a significant component of offshore hydrocarbon developments. Recent advances in the offshore industry have led to complex pipeline design issues, such as lateral buckling and axial walking, which require consideration of the self-burial, or as-laid embedment, of a subsea pipeline. The magnitude of as-laid embedment also influences other aspects of subsea pipeline design, including exposure to lateral loading (from deep sea landslides for example), flow assurance (via the insulation provided by the soil), and hydrodynamic stability. For some of these design aspects, there is no single conservative approach to assess pipeline embedment. It is therefore necessary to assess the full range in expected embedment, including consideration of the influence from the pipe laying process on the as-laid embedment.

1.1 THESIS OBJECTIVES

The goals of this research were to (i) develop an improved understanding of the mechanisms that lead to pipeline embedment during offshore pipe laying and (ii) use this knowledge to guide the development of new calculation methods for assessing as-laid pipeline embedment. To do this, several different activities were performed, comprising:

1. Back-analyses of as-laid pipeline embedment from field surveys;
2. Numerical simulations of pipeline laying;
3. Physical model testing of idealised pipe laying simulations.

The back-analyses of the field surveys provided the raw data from which general observations and trends of as-laid embedment were interpreted, allowing a benchmark against which the numerical simulations and physical model testing could then be compared. The observations from the field surveys, which included video footage of the touchdown zone as well as sonar seabed scans, were used to guide the input parameters for both the numerical simulations and physical model testing.

The field surveys were performed for real pipelines in real soils, carried out across different regions, using different types of lay vessels, and under different pipe catenary configurations. These varying conditions provided a wide-ranging data set against

which the calculation framework developed during this work was then compared. This work was aimed at investigating as-laid embedment in fine-grained soils (i.e. clays, silts, and muds), which are prevalent in deep water frontiers. However, during the course of the work, additional field data for a site that included coarse-grained soils (i.e. silty sands and sands) became available (as presented in Chapter 6).

1.2 THESIS ORGANISATION

This thesis is organised as a series of published academic papers in accordance with the policies of the University of Western Australia. Forewords preceding each chapter provide a brief discussion on how the work of each chapter fits within the broader thesis objectives. A summary of the thesis organisation is presented on Figure 1.1, and a summary of the contents of each chapter is provided below.

- Chapter 1 is the introductory chapter that provides an overview of as-laid pipeline embedment, states the thesis objectives and key areas of research, and describes the organisation of the thesis. As is common for a thesis by papers, the literature review is divided amongst the individual chapters, highlighting the key studies relevant to the particular focus of each chapter. However, a brief overarching literature review is included in this chapter to provide the reader with a general understanding of the previous research on the subject of as-laid pipeline embedment.

- Chapter 2 presents observations from video footage of touchdown zone monitoring during an as-laid survey for a heavy pipeline laid in shallow water at a soft silty clay site in the North Sea. This chapter, published as a peer-reviewed conference paper, provides evidence of dynamic lay effects and how they influence the resulting as-laid embedment during various lay processes, providing a scene-setting overview of the challenges of this topic.

  Westgate, Z.J., White, D.J. & Randolph, M.F. (2009). Video observations of dynamic embedment during pipelaying in soft clay. *Proc. Offshore Mechanics and Arctic Engineering Conf.*, Honolulu, USA, June 1-5, Paper OMAE2009-79814.

- Chapter 3 presents the results of a detailed field survey back-analysis that was performed for a light pipeline at the North Sea site. This chapter, published as a

journal paper, discusses the results of numerical simulations that illustrate the influence of the sea state on as-laid pipeline embedment, and provides statistical insights into the key drivers of as-laid embedment in fine-grained soils.

Westgate, Z.J., Randolph, M.F., White D.J. & Li, S. (2010). The influence of seastate on as-laid pipeline embedment: a case study. *Applied Ocean Research*, Vol. 32, No. 3, pp. 321-331.

- Chapter 4 presents, in summary form, the results from the first field survey back-analysis at the North Sea site (from Chapters 2 and 3), together with the results of the second field survey back-analysis for a network of pipelines at a soft clay site offshore West Africa. This chapter, published as a conference paper, discusses the key observations and interpreted trends from the back-analyses, which were used to guide the development of a simple framework for assessing as-laid pipeline embedment in fine-grained soils.

  Westgate, Z.J., White, D.J., Randolph, M.F. & Brunning, P. (2010). Pipeline laying and embedment in soft fine-grained soils: field observations and numerical simulations. *Proc. Offshore Technology Conf.*, Paper OTC20407.

- Chapter 5 presents a study of a specific pipe laying application – a buckle initiator, or 'sleeper', crossing – using a subset of the field data introduced in Chapter 4. This chapter, published as a peer-reviewed conference paper, illustrates the influence of lay process asymmetry and dynamic lay effects on as-laid pipe embedment adjacent to offshore sleepers, using theoretical and numerical analyses. The results are compared to field survey data of an as-laid pipeline adjacent to a sleeper from the West African site. These comparisons help to illustrate how the different tools and levels of analysis available to engineers can be used in practice.

  Westgate, Z.J., Randolph, M.F., White, D.J. & Brunning, P. (2010). Theoretical, numerical and field studies of offshore pipeline sleeper crossings. *Proc.2nd Int. Sym. Frontiers in Offshore Geotechnics*, Perth.

- Chapter 6 presents the results of the third field survey back-analysis, comprising a pipeline laid in carbonate sediments offshore Australia. This chapter, published as a journal paper, extends the scope of the pipe embedment problem from soft

clayey fine-grained soils (i.e. as found at the North Sea and West African sites) through to fine-grained carbonate silt and stiff coarse-grained carbonate sands. In addition to confirming the broader conclusions from the first two back-analyses, this chapter addresses the effects of soil drainage on as-laid pipeline embedment, and provides guidance for determining the boundaries between undrained and drained soil conditions during pipeline laying.

Westgate, Z.J., White, D.J. & Randolph, M.F. (2012). Field observations of as-laid pipeline embedment in carbonate sediments, *Géotechnique*, Vol. 62, No. 9, pp. 787-798.

- Chapter 7 presents the results of physical centrifuge model tests that were performed to further investigate the different dynamic embedment mechanisms in fine-grained soils by isolating pipe motions in different directions and with varying amplitudes. This chapter, published as a journal paper, discusses how these insights were used to guide the development of a model to track pipe embedment through cycles of vertical pipe loading and horizontal pipe displacement in fine-grained soils. This model is a more sophisticated procedure for calculating pipe embedment than the approaches described in the preceding chapters. The model is benchmarked against the three field survey back-analyses presented in the earlier chapters of this thesis.

  Westgate, Z.J., White, D.J. & Randolph, M.F. (2013). Modelling the embedment process during offshore pipe laying on fine-grained soils, *Canadian Geotechnical J.*, Vol. 50, No. 1, pp. 15-27.

- Chapter 8 is the closing chapter that, in the same manner as the introductory chapter, provides a summary discussion of the research presented throughout this thesis and highlights the key conclusions. The candidate's original contributions to knowledge are described, and aspects of the research that deserve further investigation are identified.

1.3 LITERATURE REVIEW

As customary for a thesis by papers, a brief literature review is included in this chapter that provides the reader with background information that was necessarily excluded from the individual chapters due to paper length restrictions.

1.3.1 Subsea pipeline laying

Several textbooks (e.g. Bai 2001, Bræstrup & Andersen 2005, Palmer & King 2008) and related papers (e.g. Palmer et al. 1974, Pesce et al. 1998, Lenci & Callegari 2005) discuss the subsea pipeline laying process in detail. Provided below is a summary of this lay process.

In order to install a subsea pipeline, pipe sections normally manufactured onshore are loaded onto a pipe lay vessel. They are then welded together (and subsequently coated with insulation, plastic, or concrete) in assembly-line fashion on what is referred to as a 'firing line'. The fully constructed pipeline is then fed onto a lay ramp, which can be nearly vertical as in the J-lay method (Figure 1.2a), or initially horizontal as in the S-lay method (Figure 1.2b). The latter method uses a 'stinger' as the lay ramp in order to reduce stresses in the overbend region of the pipeline as it leaves the vessel. There are also hybrid lay vessels which can be characterised as steep S-lay or shallow J-lay vessels (Perinet & Frazer 2007), as well as other lay methods such as the reel lay method and the tow and placement method.

The choice of lay vessel depends on several factors, including the pipeline properties, pipe weight, water depth, vessel availability and cost. The lay vessel (and by extension the lay method) can significantly affect the magnitude of vertical (in-plane) and horizontal (out-of-plane) pipeline motions occurring at the lay ramp, due to the moderation of the sea state according to the dynamic response of the vessel. While lay vessel designs have been able to reduce the effects of the sea state during laying through lay ramp location and articulation (e.g. Frazer 2006), it is these dynamic pipe motions that drive the as-laid pipeline embedment at the seabed.

The pipe lay rate governs the exposure period of the pipeline to these motions. Typical pipe laying rates can vary by an order of magnitude, due to the differences in pipe laying operations, welding and coating capabilities and requirements, and station-keeping abilities. Lay rates for S-lay vessels can exceed several kilometres per day, and have generally doubled over the past two decades due to increased efficiency in welding processes (Lund 2000a). Lay rates for J-lay are often less than for S-lay, due to the increased pipe handling and shorter firing line arising from the lay ramp geometry.

The reel lay method is similar to the J-lay method due to lack of an overbend through the water column, but is only used with relatively flexible pipelines of small diameter.

This method allows the pipeline to be constructed onshore and pre-installed around a spool on the vessel. This significantly increases the lay rate, which effectively reduces the exposure of the pipeline to the effects of the sea state. The towing and placement method usually utilises two lay vessels in tandem, sequentially installing lengths of pipeline onto the seabed. This method does not subject the pipeline to significant dynamic motion as the pipeline is suspended by a cable or chain. Nor does it subject the pipeline to high force concentrations, as the pipeline remains relatively horizontal during the lay process.

In the J-lay or S-lay method, as the pipeline exits the lay ramp or stinger, it oscillates through the water column and eventually contacts the seabed at what is referred to as the touchdown zone (Figure 1.3a). Through the touchdown zone and process zone, which are collectively defined as the length of seabed between the forward touchdown point and the location where pipe motions cease, the vertical force, V, imposed on the seabed becomes greater than the submerged weight of the pipeline, p, due to the pipe stiffness and curvature (Figure 1.3b). This force concentration attenuates through the process zone, defined as the length of seabed between the trailing touchdown point and the as-laid zone, where the pipeline rests on the seabed under a force equal to its submerged weight.

1.3.2 Dynamic lay effects

The lay vessel dynamics and pipeline properties influence what are referred to as dynamic lay effects. These comprise horizontal (out-of-plane) and vertical (in-plane) pipeline loads and movements, the magnitude of which vary through the touchdown and process zones (Figure 1.4). For example, the horizontal pipeline displacement gradually reduces through both of these zones (Figure 1.4a). The dynamic vertical force can be less than zero where the pipe is lifted away from the seabed (if an uplift force, or suction, can be sustained), but V remains compressive through the process zone (Figure 1.4b). Numerical software packages such as OFFPIPE and OrcaFlex are now used routinely in pipeline design to model these pipeline loads and displacements during pipeline laying (Malahy 1996, Orcina 2009).

Field studies have provided insights into the effect of these dynamic movements on as-laid embedment. For example, Lund (2000b) published a field survey back-analysis for a large diameter pipeline laid in fine-grained soil, showing that a shallow trench forms

around the pipeline during typical sea state conditions, with as-laid embedment equal to a fraction of the pipeline diameter. Surveys of steel catenary risers (SCRs) have also provided further insights, showing that trenches up to several diameters in both depth and lateral extent can result from long term exposure to dynamic movements where the pipe touches down on the seabed (Bridge & Howells 2007). While an SCR is analogous to a pipeline suspended from a lay vessel, it generally undergoes larger motions than as-laid pipelines due to the influence of major storm events (during which pipeline laying would be halted). These movements have been shown to exceed several diameters within the touchdown zone (Thethi & Moros 2001, Clukey et al. 2005).

1.3.3 Historical development

Offshore pipeline construction and installation increased significantly during the 1970s as the number of offshore hydrocarbon developments in the Gulf of Mexico and North Sea expanded. In response to this, early research work primarily investigated pipeline response to storm loading as pipelines were located in shallow waters on the continental shelves (e.g. Lammert et al. 1989). This led to significant improvements in understanding pipe-soil interaction in relation to hydrodynamic stability.

Some of the earliest published work on pipe-soil interaction (Reese & Casbarian 1968, Small et al. 1971) linked pipe embedment to the ultimate bearing capacity of the soil, extending analytical solutions for shallow foundation analysis (e.g. Prandtl 1921, Skempton 1951) to pipeline design using empirical adjustments. The use of plasticity theory to predict pipe penetration directly was introduced by Karal (1977), which was subsequently refined following analyses of lateral pile response (Randolph & Houlsby 1984), to more accurate solutions given by Murff et al. (1989).

This early work laid the foundation for the bulk of the experimental studies done in the late 1980s through the joint industry projects (JIPs) of PIPESTAB (e.g. Brennodden et al. 1986; Wagner et al. 1987; Hale et al. 1989) and the American Gas Association's (AGA) Pipeline Research Committee (PRC) (e.g. Allen et al. 1989). PIPESTAB was the first major JIP that examined both vertical and horizontal pipeline response to environmental loading conditions. Much of the work on pipeline embedment from this project was collated into empirical solutions for pipe embedment and lateral response in clays (Verley & Lund 1995) and sands (Verley & Sotberg 1994).

As SCRs became an integral part of offshore developments following the introduction of floating platforms, two other major JIPs developed: the STRIDE (Steel Risers in Deepwater Environments) JIP and the CARISIMA (Catenary Riser/Soil Interaction Model for Global Riser Analysis) JIP. The experimental work from these two JIPs focused primarily on cyclic vertical pipeline-seabed interaction on clay seabeds using large scale field trials (Bridge 2005) and experimental 1-g testing (e.g. Fontaine et al. 2004), and has produced pipe-soil interaction models for pipe penetration up to several diameters (Bridge et al. 2004, Clukey et al. 2005, Aubeny et al. 2006, Randolph & Quiggin 2009).

As developments moved into deeper water, and operating conditions moved to higher temperature and pressure, other pipeline design issues arose, such as lateral buckling and axial walking (Bruton et al. 2006), as well as lateral loading from submarine mudslides and landslides (Swanson & Jones 1982). The SAFEBUCK (Safe Design of Pipelines with Lateral Buckling) JIP was established to investigate these issues, focusing on the lateral response of pipelines subject to buckling, and the associated axial pipe-soil interaction.

Reflecting the new challenges associated with the transition to deep water and high pressure high temperature (HPHT) pipelines, Cathie et al. (2005) summarised the state-of the art on pipeline geotechnics, covering the basic aspects of several key issues relating to subsea pipeline design, but with only cursory discussion on dynamic lay effects. A more detailed paper on dynamic pipeline embedment (Randolph & White 2008a) provided review of recent studies on shallow seabed soil characterisation (White & Randolph 2007), pipe-soil bearing capacity (Aubeny et al. 2005, Merifield et al. 2009), pipeline catenary behaviour (Pesce et al. 1998; Lenci & Callegari 2005), and physical model testing of dynamic lay effects (Cheuk & White 2008). While the key aspects of dynamic pipeline embedment during offshore pipeline laying were identified, the Randolph & White (2008a) paper highlighted the difficulty in quantifying dynamic lay effects.

1.3.4 Design tools

Following the developments arising from the hydrodynamic stability work in the 1980s, two offshore pipeline design codes emerged: the AGA Pipeline Design Guidelines and Software (Allen et al. 1989), and Det Norske Veritas's (DNV) Recommended Practice

for On-Bottom Stability Design of Submarine Pipelines (RP-E305) (DNV 1988). Although the more commonly-adopted method was the DNV RP-E305 (Lund 2000a), both methods were based on the same experimental model test database developed through the PIPESTAB JIP. A comparison of the two methods showed that while they shared several similarities in using history-dependent pipe-soil interaction models for hydrodynamic analyses, there were key differences related to the calculation of pipe embedment (Hale et al. 1991). For example, while both models were solely empirical and conservative in regards to the ultimate lateral pipe-soil resistance (relative to the model test database), the DNV model consistently predicted less embedment than the AGA model.

In 2007, DNV published the updated design code RP-F109: On-bottom Stability Design of Submarine Pipelines (DNV 2007). This version superseded their RP-E305 design code, and included several updates for pipe embedment related to lateral stability, as well as commentary on pipe-soil interaction in carbonate soils. While a significant change was the inclusion of empirical reduction factors for hydrodynamic loading due to pipe embedment, the accuracy of these factors has been shown to be limited, based on recent numerical simulations (An et al. 2011). Furthermore, the revised code provides no prescriptive guidance for calculating the pipe penetration due to dynamic lay effects. While DNV have also published RP-F105: Free-spanning Sections of Submarine Pipelines (DNV 2006), which recognises the dynamic nature of pipeline installation and recommends including the effects of the pipe catenary on the pipe-seabed contact force, no specific guidance is provided in this code either. Because of this, pipeline engineers have had to adopt very conservative ranges of pipe embedment for use in design, often resorting to advanced physical and numerical modelling techniques (e.g. White & Gaudin 2008, Gaudin & White 2009) to narrow this range in order make their pipeline designs feasible.

1.3.5 Contributions to pipeline embedment

There are four general contributions to as-laid pipeline embedment (excluding mechanical trenching). These comprise:

- Static embedment due to the submerged weight of the pipe and the vertical pipe-soil force concentration from the pipe catenary, i.e. the static lay effect.

- Dynamic embedment due to pipe motions in the touchdown zone, i.e. dynamic lay effects.
- Pipe settlement due to primary consolidation and creep of the soil beneath the pipe.
- Soil erosion due to sediment mobility and dispersion, causing further pipe embedment due to loss of soil from beneath the pipe and/or build-up of soil adjacent to the pipe.

1.3.6 The pipeline catenary

The static force imposed on a segment of pipeline during installation is due to the additive components of the submerged pipeline weight and the force concentration due to the pipe catenary (Figure 1.3b). This enhanced pipe-soil contact force, V_{max}, normalised by the diameter, D, and undrained shear strength at the pipe invert, s_u, governs static embedment in fine-grained soils. Values of V_{max}/s_uD can vary from less than 1 to values as high as 7 or more for typical pipelines in soft soils. The general shape of this non-linear static penetration response is shown on Figure 1.5.

The vertical force concentration in the touchdown zone can be determined from standard catenary solutions, coupled to idealised elastic or plastic models for the seabed response (Palmer et al. 1974; Pesce et al. 1998; Lenci & Callegari 2005; Randolph & White 2008a, Palmer 2009). The vertical force concentration is a function of the pipeline submerged weight per unit length, p, water depth, z_w, and lay angle, ϕ, which are used to determine the horizontal pipeline tension, T_0. These are interrelated through the following:

$$\frac{T_0}{z_w p} = \frac{\cos\phi}{1-\cos\phi} \tag{1.1}$$

From Pesce et al. (1998), the tension can then be used to calculate the characteristic length, λ, based on the pipeline stiffness, EI, as follows:

$$\lambda = \sqrt{\frac{EI}{T_0}} \tag{1.2}$$

where E is the elastic modulus and I is the second moment of area of the pipeline.

The characteristic length, λ, reflects the extent of the zone where the bending stiffness of the pipeline affects the catenary shape. It is a similar order of magnitude to the distance from the TDP to the point where the pipeline becomes approximately horizontal, beyond the TDP (Figure 1.3a). As the seabed stiffness decreases, that distance increases as the TDP moves closer to the vessel. If the seabed is assumed to behave elastically, with a stiffness, k = V/w, where w is the pipe embedment, then the normalised seabed stiffness, K, can be defined as:

$$K = \frac{\lambda^2 k}{T_0} \tag{1.3}$$

The force concentration factor, V_{max}/p, can then be calculated using the approximate solution (Randolph & White 2008a):

$$\frac{V_{max}}{p} \approx 0.6 + 0.4K^{0.25} \tag{1.4}$$

This relationship is accurate for normalised tension (i.e. $T_0/\lambda p$) values greater than about 3 (Randolph & White 2008a). The magnitude of V_{max}/p can be greater than 4 for shallow to medium water depths (Cathie et al. 2005, White & Randolph 2007), but for deep water with soft sediments it rarely exceeds about 2.5 (Randolph & White 2008a), and reduces with pipe embedment (since the equivalent secant elastic stiffness reduces).

1.3.7 Static embedment

The static bearing capacity of a pipeline on fine-grained soil is a well understood problem, drawing on almost a century of research related to the bearing capacity of strip footings (e.g. Prandtl 1921, Skempton 1951, Green 1954, Brinch Hansen 1970, Davis & Booker 1973) and laterally-loaded piles (Randolph & Houlsby 1984, Martin & Randolph 2006). Research directly related to pipe bearing capacity has included experimental studies (Wantland et al. 1979, Aubeny & Dunlap 2003, Verley & Lund 1995, Cheuk & White 2008, Dingle et al. 2008, Cheuk & White 2011), theoretical solutions (Murff et al. 1989, Randolph & White 2008b, Cheuk et al. 2008, Merifeld et al. 2009), and numerical analyses (Aubeny et al. 2005, Wang et al. 2010, Chatterjee et al. 2010, 2012).

Merifield et al. (2009) have investigated pipe penetration using numerical analyses, and developed theoretically-based solutions for the bearing capacity of a pipe in fine-grained soil, expressed in simplified form as:

$$\frac{V}{D} = N_c s_u + N_b \gamma' w \tag{1.5}$$

where N_c and N_b are bearing capacity factors for soil strength and buoyancy, respectively.

The value of N_c for various structural elements (i.e. pipes, piles, strip footings) is influenced by the interface roughness, soil strength heterogeneity and embedment (Davis & Booker 1973, Randolph & Houlsby 1984, Murff et al. 1989, Martin & Randolph 2006).

Aubeny et al. (2005) showed that N_c can be related to pipe embedment directly using the power law, so that in weightless soil:

$$\frac{V}{s_u D} = N_c = a\left(\frac{w}{D}\right)^b \tag{1.6}$$

where a and b are empirical fitting parameters shown to range from a = 4.4 to 7.4 and b = 0.15 to 0.37 based on numerical analyses for wished-in-place pipes (Aubeny et al. 2005). Numerical analyses of pipe penetration using the RITSS (remeshing and interpolation technique with small strain, Hu & Randolph 1998) large deformation finite element method, which falls into the Arbitrary Langrangian-Eulerian (ALE) category, show that these coefficients are also dependent on the tendency for soil flow around the pipe (Barbosa-Cruz & Randolph 2005), as well as the strain rate and strain softening (Chatterjee et al. 2010, 2012). The typical shape of the static pipe penetration response for fine-grained soils is illustrated in Figure 1.5.

Merifield et al. (2009) showed that the penetration resistance due to buoyancy can be significant, quantified using the buoyancy factor N_b, expressed as:

$$N_b = \frac{f_b A_s}{Dw} \tag{1.7}$$

The submerged area of the pipe, A_s, can be enhanced by soil heave adjacent to the pipe. For purely static loading, the heave height can be up to 50% of the nominal pipe embedment, as shown numerically and experimentally (Dingle et al. 2008, Wang et al.

2010). This contribution to the penetration resistance is approximated using the buoyancy coefficient, f_b, which can be expressed as:

$$f_b = \max\left[1{,}1 + 0.5\left(1 - \frac{w/D}{(w/D)_{deep}}\right)\right] \tag{1.8}$$

where $(w/D)_{deep}$ is the transition depth where a deep flow-round mechanism occurs (White et al. 2010). Values of f_b can exceed 2, but are typically assumed equal to 1.5 for routine calculations (Randolph & White 2008a).

Experimental studies have also investigated the static penetration of a pipe on fine-grained soils. For example, Verley & Lund (1995) compiled the test data from PIPESTAB and AGA/PRC and derived the following expression, suggesting that static pipe penetration was primarily a function of the shear strength and the (total) soil unit weight:

$$\frac{w}{D} = 0.0071\left(\frac{V}{s_u D}\left(\frac{s_u}{D\gamma}\right)^{0.3}\right)^{3.2} + 0.062\left(\frac{V}{s_u D}\left(\frac{s_u}{D\gamma}\right)^{0.3}\right)^{0.7} \tag{1.9}$$

More recent data from the SAFEBUCK JIP (Bruton et al. 2008) proposed a direct relationship for pipe embedment based on the normalised vertical load, expressed as:

$$\frac{w}{D} = f\left(\frac{V}{s_u D}\right)^g \tag{1.10}$$

where f is taken as the soil sensitivity, S_t, divided by the constant 15, and g is equal to 2. These empirical solutions have been shown to predict poorly the true static bearing response, and were probably mistakenly skewed due to deficiencies in assessment of the near surface soil strength and the pipe penetration during the associated experimental studies (Randolph & White 2008a).

1.3.8 Dynamic embedment

The industry approach to assessing dynamic pipeline embedment remains empirical, using a dynamic embedment factor, f_{dyn}, defined as:

$$f_{dyn} = \frac{w_{as-laid}}{w_{static}} \tag{1.11}$$

where w_{static} is the static embedment that is calculate based on V_{max}, which accounts for the concentration of vertical load in the touchdown zone. Values of f_{dyn} have been shown to range from about 1 to 3 for soft fine-grained soils (Bruton et al. 2007) and 5 to 8 for stiff fine-grained soils (Lund 2000b).

The primary dynamic embedment mechanisms in fine-grained soils are softening, combined vertical and horizontal loading, and trenching of the seabed soil (Figure 1.6). The softening mechanism reduces the soil strength, thus decreasing the bearing capacity of the seabed along with the combined loading. During cyclic separation of the pipeline from the seabed, water entrainment into the soil can further reduce the soil strength (Ghazzaly & Lim 1975, White & Randolph 2007, Gaudin & White 2009). During horizontal pipe motions, displacement of the soil, or trenching, can lower the local seabed elevation, thus reducing the buoyancy component of the bearing capacity (Aubeny et al. 2006, Merifield et al. 2009).

Early studies investigating hydrodynamic stability of offshore pipelines have provided a large database of dynamic pipe-soil interaction in fine-grained soils (Wantland et al. 1979, Wagner et al. 1987, Brennodden et al. 1989, Morris et al. 1988, Dunlap et al. 1990, Hale et al. 1992, Morris et al. 1992). Wantland et al. (1979) was one of the first to carry out experimental field testing of dynamic embedment, and showed that the observed embedment values for a range of pipe weights agreed with the embedment predicted using the remoulded shear strength at the pipe invert depth. Based on model tests of horizontal pipe motion, Morris et al. (1988) proposed an embedment prediction model based on cycle-by-cycle superposition, similar in concept to soil strength degradation models used in shallow foundation analysis (Andersen 1991). Verley & Lund (1995) compiled the data from these early studies and derived a relationship to predict dynamic embedment in fine-grained soils:

$$\left(\frac{w}{D}\right)_{dynamic} = 0.097\left(\frac{E}{s_u D^2}\right)^{0.279}\left(\frac{V}{s_u D}\right)^{0.637}\left(\frac{u}{D}\right)^{-0.25} \tag{1.12}$$

where E is the work done by the assumed passive component of the horizontal resistance. They also derived a solution to predict the maximum achievable embedment based on the horizontal oscillation amplitude:

$$\left(\frac{w}{D}\right)_{max} = 1.1\left(\frac{V}{s_u D}\right)\left(\frac{s_u}{\gamma D}\right)^{0.54}\left(\frac{u}{D}\right)^{0.17} \quad (1.13)$$

These solutions were often cumbersome to implement, due to the history-dependent energy parameters. In addition, the test database was limited to pipe embedment values less than 0.3D.

Recent high quality centrifuge model testing for the SAFEBUCK JIP has investigated pipe embedment during pipe laying simulations (Cheuk & White 2008), illustrating how the sensitivity of the soil and the amplitude of the vertical pipe loads and horizontal pipe motions influence embedment. Related centrifuge studies (Dingle et al. 2008) utilising particle image velocimetry (White et al. 2003) showed that the soil deformation patterns under combined loading were consistent with previously derived plasticity-based solutions, transitioning from the Murff et al. (1989) wedge mechanism at shallow embedment to the 'Martin' mechanism at deeper embedment (Martin & Randolph 2006). Closer inspection of the deformations revealed intermittent shear banding, similar to that observed during numerical modelling of strain-softening soil reported by Zhou et al (2008). Using links to plasticity theory based on the work of Randolph & White (2008b), Cheuk et al. (2008), and Merifield et al. (2008), Cheuk & White (2011) proposed a method to calculate dynamic pipe embedment on a cycle-by-cycle basis. Their model, which determines the pipe trajectory during horizontal oscillations, incorporates the effects of cumulative shear strain on the soil strength degradation, linked to strength degradation around a T-bar penetrometer (Einav & Randolph 2005, Randolph et al. 2007, Zhou & Randolph 2009).

These recent studies highlight the complexity of the soil deformation during dynamic pipe embedment. Other effects present in fine-grained soils include strain rate effects (Aubeny & Shi 2007, Lehane et al. 2009, Chatterjee et al. 2012) and partial drainage, which can limit the degree of soil softening due to reconsolidation and strength gain between cycles of loading (White & Randolph 2007; Hodder et al. 2008, White & Hodder 2010). This can influence the potential magnitude of dynamic pipe embedment, as well as the lateral breakout resistance (Bruton et al. 2007).

1.3.9 Summary of literature

Over the past several decades, increasing development of offshore oil and gas fields into deeper water has led to new pipeline design challenges, such as lateral buckling, axial

walking and flow assurance of subsea pipelines. These new challenges have provided the impetus for significant research into pipe-soil interaction with a particular focus on quantifying the as-laid embedment of subsea pipelines. Early studies that focused on the static and dynamic behaviour of subsea pipelines exposed to environmental loading showed that the bearing capacity response of a pipeline can be analysed in a similar manner to that of a shallow strip footing. Insights from lateral pile loading analysis led to development of plasticity-based theoretical solutions for pipe-soil interaction, both for purely vertical loading and for combined horizontal and vertical loading.

Dynamic vertical pipe-soil interaction models were developed following investigations into the behaviour of steel catenary risers in the touchdown zone, the geometry of which is analogous to a pipeline catenary during installation. These models illustrated how cyclic vertical penetration softened the soil, leading to increased penetration with each cycle. Observations of steel catenary risers showed that continued cyclic vertical motion, combined with horizontal oscillations, resulted in trenches forming around the riser pipe up to several diameters in width and depth. Field survey back-analyses showed similar trench development during pipeline laying, albeit on a smaller scale due to the relatively short exposure period to cyclic motions.

From the field and model scale observations and analytical solutions, empirical and theoretically-based models have been developed to predict dynamic pipeline embedment in fine-grained soils. However, there remain significant uncertainties regarding the soil parameters used in these models, not least of which is the appropriate value of the soil strength to use in bearing capacity analyses, which changes due to soil softening during pipe laying. A further key challenge associated with offshore pipeline laying is the additional uncertainty associated with the sea state and pipeline dynamics at the seabed. This uncertainty hampers the development of theoretical models to predict as-laid embedment. Because of this, there is no generally accepted robust methodology for assessing as-laid pipe embedment.

At the start of this research, the standard industry practice was to calculate the pipe embedment via a static calculation, and then to amplify this embedment by an empirical adjustment factor, not linked to the soil conditions, pipe properties or lay process (see, for example, the version of the SAFEBUCK industry guideline that was issued in 2007, Boreas Consultants (2007)). The work described in this thesis has led to improved

techniques for assessing pipeline embedment, which have been adopted in the current version of the SAFEBUCK Guideline, referencing research from this thesis.

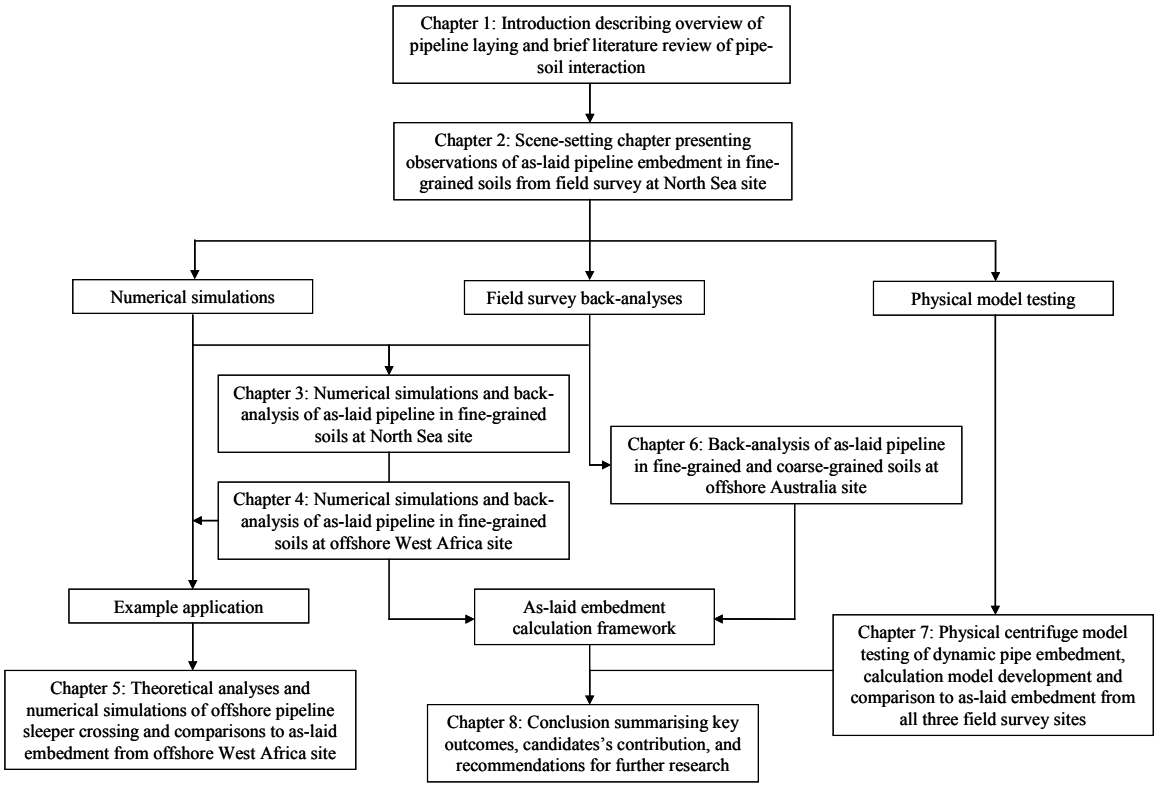

Figure 1.1. Thesis organisation chart

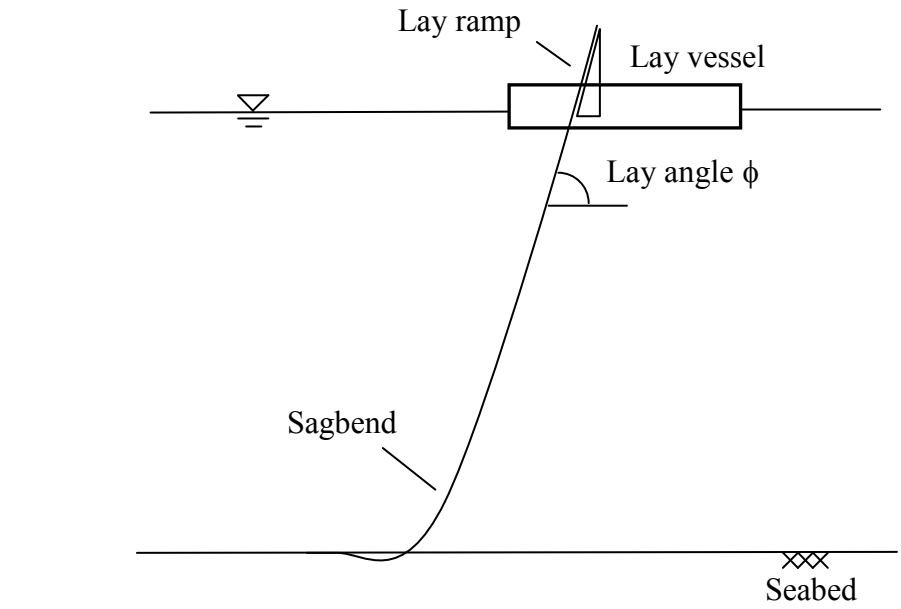

(a)

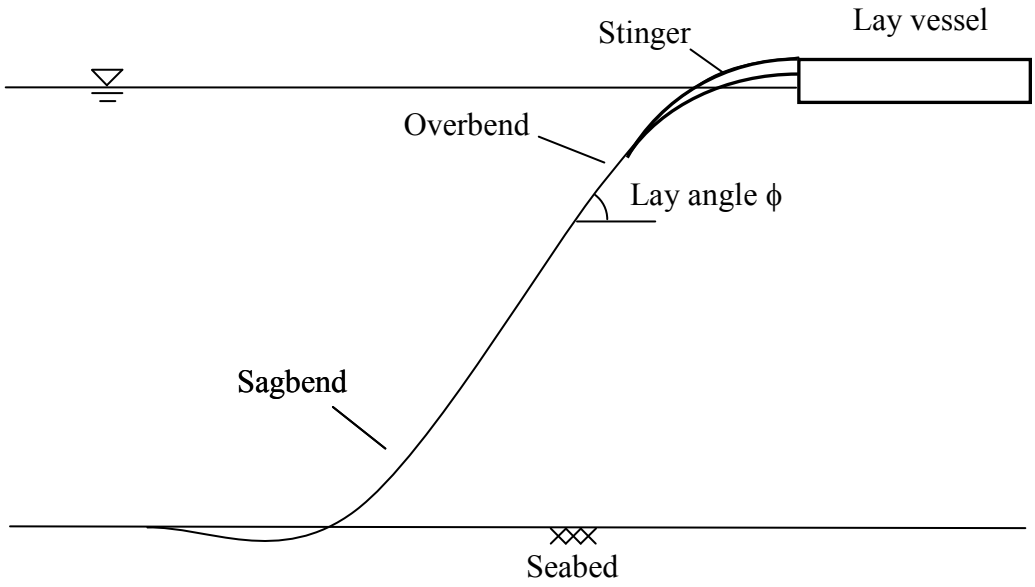

(b)

Figure 1.2. Illustration of pipeline laying methods: (a) J-lay and (b) S-lay

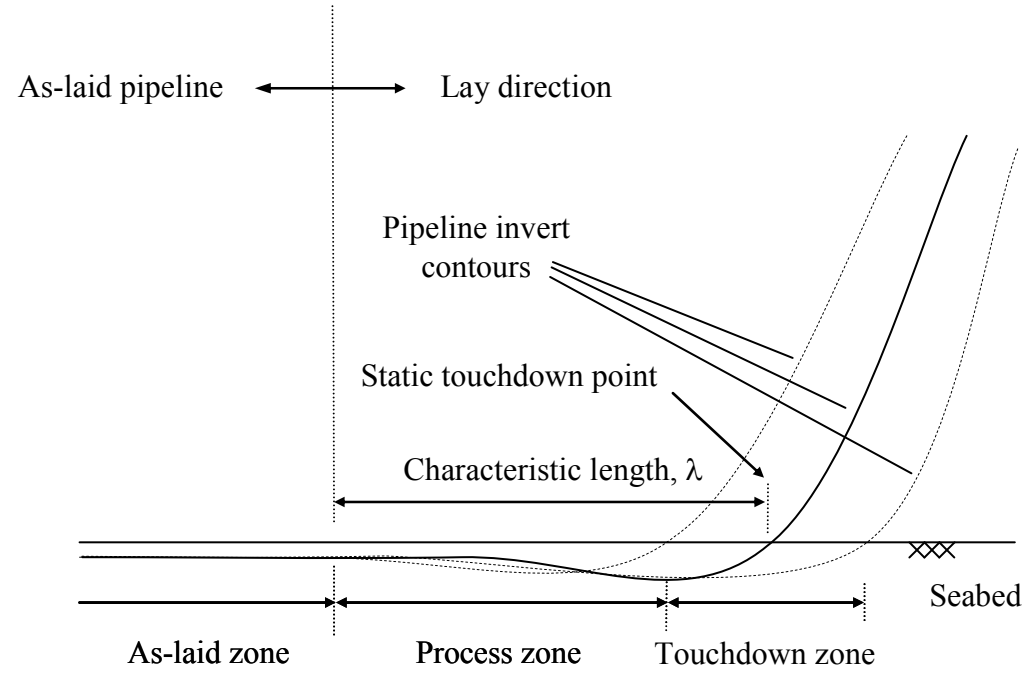

(a)

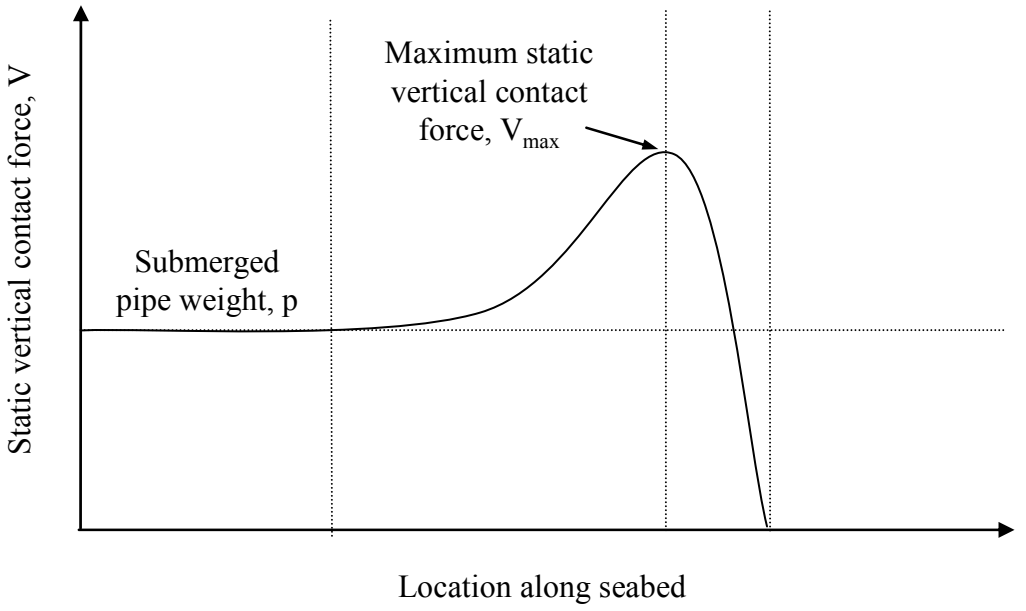

(b)

Figure 1.3. Illustration of (a) seabed zones and (b) static lay effect at seabed

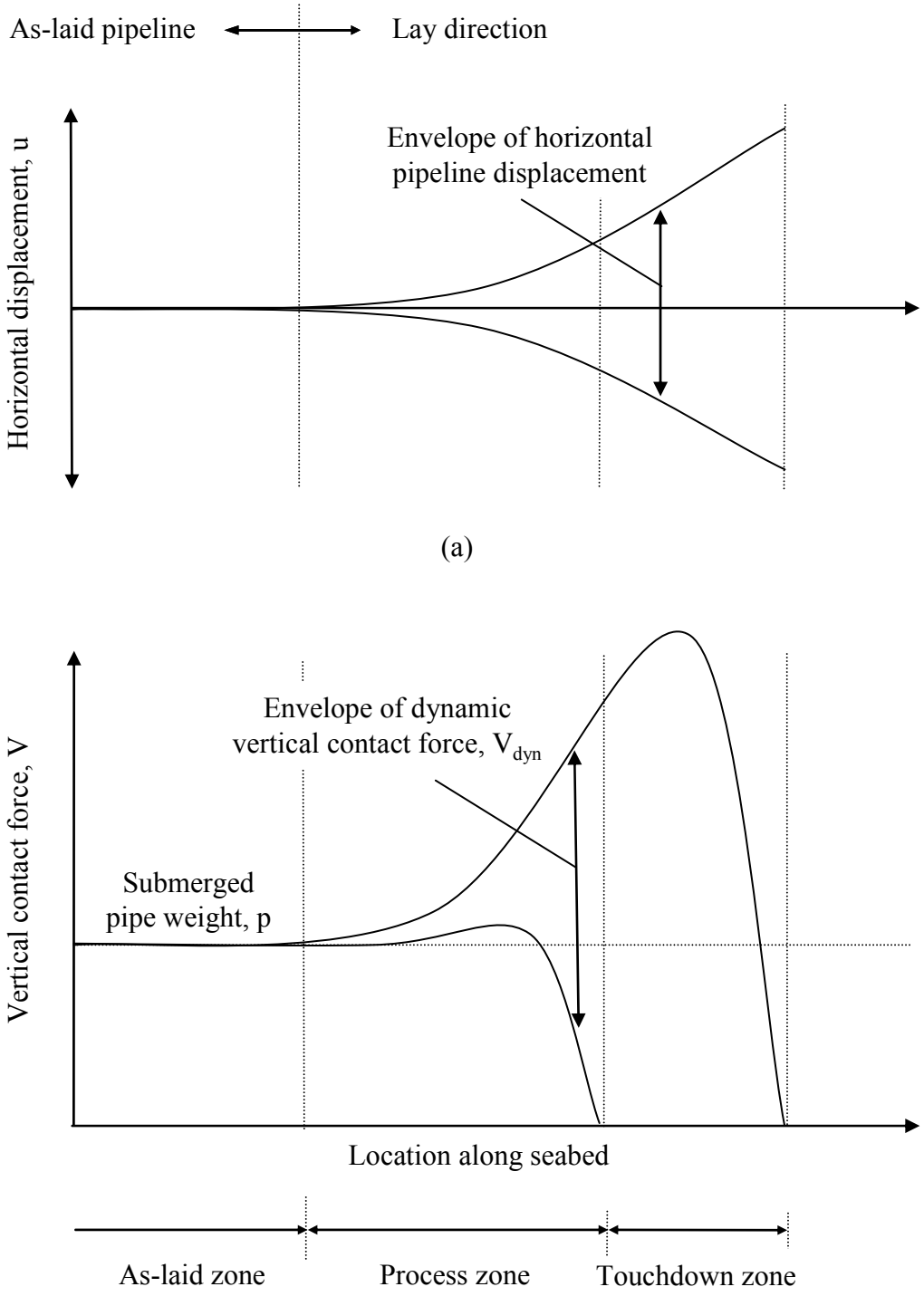

Figure 1.4. Dynamic lay effects at seabed showing (a) horizontal lay effect and (b) vertical lay effect

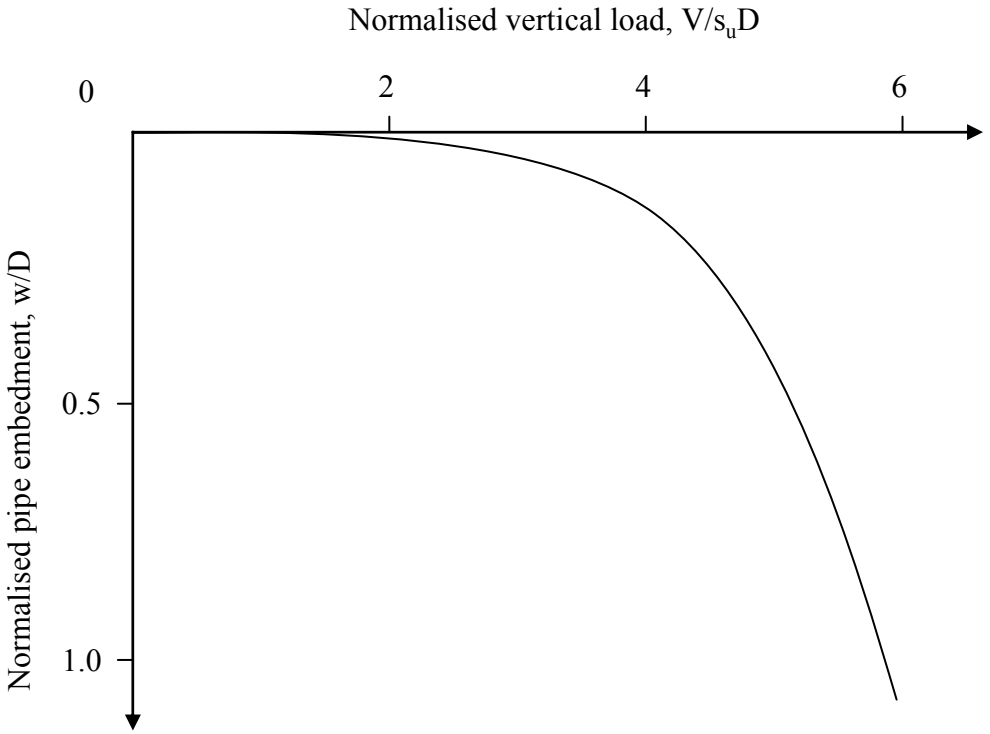

Figure 1.5. Typical static penetration response

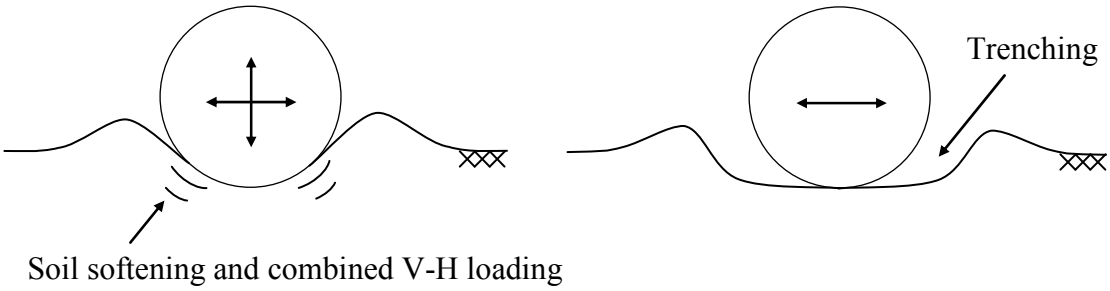

Figure 1.6. Dynamic pipe embedment mechanisms

CHAPTER 2. VIDEO OBSERVATIONS OF DYNAMIC EMBEDMENT DURING PIPELAYING IN SOFT CLAY

The paper presented in this chapter introduces the pipe laying process and illustrates a set of as-laid embedment observations from a heavy pipeline installed in the North Sea. Three variations of the lay process are highlighted: normal pipeline laying, downtime events, and pipeline lay down.

The first variation, normal pipeline laying, refers to periods of pipe laying when the pipeline is being alternately welded together and paid out with regular forward progress of the lay vessel. The second variation, downtime events, refers to significant periods of time when the lay vessel stops advancing forward due to mechanical breakdown or onerous weather, or where in-line structures are being connected to the pipeline. In these cases, the exposure of the pipeline to cyclic motion in the touchdown zone can increase both in duration and severity. The third variation, the pipeline lay down process, is when the pipeline is removed from the lay ramp and is then lowered to the seabed using a chain or cable supported by an on-board crane. This process affects the pipeline catenary response in two ways: (i) there is an instantaneous reduction in lay effects as the pipeline is 'disconnected' from the lay ramp, and (ii) there is a gradual reduction in the vertical pipe-soil contact force concentration in the touchdown zone.

The observations of these three processes in this chapter highlight the different levels of exposure of the pipeline to dynamic lay effects, and provide a basis for back-calculating dynamic embedment factors from as-laid field survey data. The heavy weight of the pipeline, which in this case is piggy-backed (i.e. there is a second smaller pipeline connected to it), allowed for clear distinctions between the different processes. While the observations are limited to this single pipeline over a short section of a lay route, this initial study provides a scene-setting basis for the remainder of the activities performed as part of this thesis.

Westgate, Z.J., White, D.J. & Randolph, M.F. (2009). Video observations of dynamic embedment during pipelaying in soft clay. *Proc. Offshore Mechanics and Arctic Engineering Conf.*, Honolulu, USA, June 1-5, Paper OMAE2009-79814.

2.1 ABSTRACT

The as-laid embedment of a pipeline is an important parameter that affects many aspects of pipeline design. Offshore pipelaying is a dynamic process that causes pipelines to embed deeper than predicted based on static penetration models. This additional embedment is due to cyclic pipeline motions at the seabed that soften and displace the soil. This study presents observations from an ROV-based video survey of dynamic pipeline motion and as-laid embedment. The pipeline had a diameter of 12 inches and was installed from a J-lay vessel in 140 m water depth onto soft clay. The observations illustrate typical trends of embedment and seabed disturbance. Different lay conditions were encountered including downtime events and laydown of the final section of pipeline using a chain. From these observations, the effect of the dynamic behavior is quantified. The results show that in this case dynamic lay effects resulted in an as-laid embedment that was an order of magnitude greater than that from the submerged pipeline self weight alone, and was up to five times greater than the static embedment accounting for the vertical stress concentration from the pipeline catenary.

2.2 INTRODUCTION

2.2.1 Role of pipeline embedment in design

The as-laid embedment of a pipeline is a key design parameter. The magnitude of embedment affects the on-bottom stability of the pipeline during environmental loading, and the lateral buckling and axial walking behavior during thermal cycles. In addition, the further embedded the pipeline is, the less susceptible it is to lateral loading. Also, the geometry of the seabed immediately adjacent to the pipeline – i.e. the presence of heave or a local trench – affects the pipe-soil interaction forces and also the thermal insulation of the pipeline.

The as-laid embedment of a pipeline can be assessed by considering the static bearing capacity of the seabed. However, due to the dynamic aspects of the laying process, the as-laid embedment is generally significantly greater than predicted in this way, particularly on soft clay soils. A large increase in as-laid embedment can result from relatively few cycles of pipeline motion as the soil is softened and displaced by the dynamic movement during the pipelaying process. Large numbers of cycles can cause a

trench to form around the pipe, similar to observations within the touchdown zone of steel catenary risers (SCRs) (Bridge & Howells 2007).

There is little published data of the as-laid embedment of on-bottom pipelines, and few studies have aimed to back-analyze the lay process in order to quantify the dynamic behavior. It is usual for an as-laid survey to be conducted but this type of data has rarely been published. There are potential benefits of back-analyzing these measurements due to the important influence of as-laid embedment on many aspects of pipeline design.

2.2.2 Objectives and scope of this study

This paper presents a back-analysis of the dynamic pipeline motion during laying and the resulting as-laid embedment for a 12 inch diameter pipeline laid on soft clay in the North Sea. Data from a remotely-operated vehicle (ROV)-based video survey is coupled with a dynamic analysis of the lay process. The study provides insights into the geometry of the deformed seabed due to the dynamic pipeline movement and clarifies the phenomena observed during as-laid cross-profiler surveys (e.g. Lund 2000b) and video surveys of SCR trenches (e.g. Bridge & Howells 2007). The seastate and lay vessel activity during the lay process is known, allowing the governing aspects of dynamic embedment to be determined. Due to the approximate nature of measurements derived from video surveys, the values of embedment are presented to a low precision, but sufficient to reveal the strong influence of dynamic processes.

2.3 ASSESSMENT OF DYNAMIC EMBEDMENT

2.3.1 Survey method

The survey was carried out using a video recorder aboard an ROV. Footage from three camera angles was obtained to provide port, center, and starboard views of the pipeline. The ROV followed immediately behind the lay vessel, progressing according to the pipe lay rate. The touchdown zone was reached on several occasions allowing the dynamic pipeline motion to be observed, before these lengths of pipeline were re-surveyed to capture the final as-laid embedment. This paper focuses on the final 1.3 km of the lay route, which highlights three different phases of the lay process. These include (i) normal lay operations, (ii) downtime events (such as pipeline repair or end connection preparations), and (iii) final laydown of the pipe onto the seafloor, by a length of chain.

The latter two cases particularly highlight the influence of lay effects: a downtime event represents an increased period of dynamic activity while the end of the final laydown phase involves static embedment of the pipeline without seastate or catenary effects.

2.3.2 Site conditions

The site is located in the North Sea within the Witch Ground area, in a water depth of approximately 140 m. The upper soil stratigraphy within the Witch Ground area is characterized as medium plasticity soft silty clay. The near surface stratigraphy consists of a very soft silty clay layer (undrained strength, s_u ~ 1 kPa, ~200 mm thick). Below this layer, the silty clay becomes stiffer (s_u of 10 to 20 kPa, to a depth of 1 m). In addition, seafloor depressions, or pockmarks, are scattered in the area, up to 200 m in diameter and 4 m deep. This resulted in spanning pipeline segments and local increases in embedment on the shoulders of the span due to the increased normal contact force between the pipeline and the seabed, i.e. the vertical stress concentration. An approximation of the undrained shear strength profile using a mudline strength intercept of zero and a strength gradient of 10 kPa/m captures the transition between the two layers. The effective unit weight γ' of the soil varied between 6.5 and 8.5 kN/m^3, with an average γ' of 7.5 kN/m^3 adopted for use in predicting the static embedment.

2.3.3 Lay vessel description

The lay vessel was the Acergy Falcon. This is a dynamically positioned vessel, 153 m in length (162 m at the layramp) and 21 m in width. A J-lay ramp was used with a pipe departure angle of approximately 68 degrees to the horizontal. The lay ramp is fixed to the vessel stern, so vessel motions from the seastate created large changes in pipeline tension at the lay ramp, significantly influencing pipeline motions at the seabed.

2.3.4 Pipeline and lay geometry

The 12 inch steel pipeline had an overall outside diameter of 0.39 m (Table 2.1). Attached to the pipeline was a smaller 3 inch piggyback pipeline, resulting in a total submerged weight, W', of approximately 0.59 kN/m. The nominal vertical stress imposed by the pipe, defined as the submerged weight per unit length divided by the pipe diameter, was therefore 1.5 kPa.

The geometry of the pipeline catenary in the vertical plane is shown in Figure 2.1, at the point on the lay route where the pipe was connected to a chain for laydown of the final

section. The horizontal distance between the lay ramp and the static touchdown point was 165 m, termed the layback length. The catenary length (i.e. the length of the suspended pipeline), was 235 m.

Using standard catenary equations (e.g. Randolph & White 2008a), the vertical stress concentration factor within the touchdown zone can be estimated based on the soil bearing capacity (and therefore the initial plastic stiffness), the pipeline rigidity and the pipeline tension. Based on static numerical analyses carried out using OrcaFlex software (Orcina 2009) during the design phase for this pipeline, the tension at the layramp was estimated as approximately 155 kN, while at the seabed it was approximately 50 kN. This assessment results in an estimated maximum stress concentration factor in the touchdown zone of approximately 2.5, implying a maximum bearing pressure of 3.75 kPa. This calculation neglects the dynamic aspects of pipelaying, arising from the vessel motions and the resulting change in pipeline tension, as well as softening of the soil due to remolding.

2.4 DYNAMIC RESPONSE

2.4.1 Metocean conditions

The metocean conditions relevant to pipelaying are primarily wave height and wave heading due to their combined effects on vessel motions. Current loading is a secondary factor, which can result in dynamic pipeline motions (e.g. vortex-induced vibrations (VIV) under high current loads). This behavior is more relevant to SCR response. For the 1.3 km lay route segment analyzed in this paper, three metocean readings were obtained at 6 hour intervals. These described the seastate as calm, progressing from beam seas to head-quartering seas. The significant wave height, H_s, increased from 1 m to 1.5 m.

2.4.2 Vessel response

The response of the vessel to wave loading is characterized by the response amplitude operators (RAOs) particular to the vessel. Vessel motions change the pipeline tension on the lay ramp. These motions, combined with the pipeline rigidity and the catenary response, drive the pipeline motion at the touchdown point. From analyses using OrcaFlex, the vessel motions during the pipelay were calculated to be small, with

maximum heave, surge and sway values of less than 0.1 m at the layramp. No measurements of vessel motions were obtained.

2.4.3 Observed pipeline motions

Through the mechanical response of the lay ramp and the catenary, vessel motion is translated into pipeline motion in the touchdown zone, with both seastates (i.e. beam and quartering) imposing significant vertical and horizontal pipeline oscillations. ROV video observations showed that both conditions caused cyclic pipeline–seabed separation, i.e. 'breakaway', at the touchdown point.

Seven episodes of pipeline motion during the lay process were observed as the ROV progressed into the touchdown zone. The pipeline motion for each episode is presented in Table 2.2, together with the corresponding seastate. The duration of each observation episode was very limited, ranging from approximately 1 to 10 wave periods (~5 to 50 sec). The pipeline movement was often partially obscured by sediment plumes. The amplitude of the motion ranged from 0.05D (peak-to-peak) up to 0.2D in both the vertical and horizontal directions.

With this limited number of observations, it was not possible to discern a systematic difference in the pipeline response for different wave heights or headings. The pipeline motions were also highly erratic, with occasional larger displacements occurring during intervals of more regular oscillations. The latter effect was particularly evident during the final episode associated with preparations for laydown. In this instance, the pipeline displaced vertically upwards by approximately 0.5D, pulling the adjacent berm of heaved soil into the underlying trench.

2.5 SURVEY OBSERVATIONS

2.5.1 Idealized seabed profile

An idealized cross-section of the deformed seabed was developed to define key embedment parameters for both heaved seabed profiles and trenched seabed profiles (Figure 2.2). The embedment of the pipeline is defined by a local value, relative to the immediately adjacent seabed $(w/D)_l$, and a global value, relative to the undisturbed or far-field seabed, $(w/D)_g$. If the seabed has heaved adjacent to the pipe, then $(w/D)_l > (w/D)_g$. If a trench is present, then $(w/D)_l < (w/D)_g$. In some instances, both a trench and heave can be present; in this case, the heave height does not contribute to local

embedment due to the separation provided by the trench. Heave height and trench depth are denoted as h/D and t/D respectively.

The ROV videos were then used to assess approximate values for each parameter at different locations. The pipeline diameter was used to provide scale in each image. Due to the approximate nature of the observations, increments of one-quarter of the diameter (0.25D) were used, including a range where appropriate (e.g. 0.25D to 0.5D). Typical values for the embedment parameters have been quantified from the ROV video footage for three pipelay conditions, to highlight the differences between (i) normal laying (KP 39.450-40.500), (ii) downtime events (KP 40.505-40.535) and (iii) final laydown (KP > 40.535) (Table 2.3).

For the normal lay conditions (i.e. no trench), the difference between the volume of soil displaced by the pipeline and the volume of heaved soil, based on these derived values, is always less than 5% (Table 2.3). This agreement is excellent considering the approximations involved. Note that this only applies to non-trenched profiles, as the majority of trenched sections exhibited significant soil volume loss.

2.5.2 Normal lay conditions

For the majority of the lay route segment analyzed (KP 39.450-40.500), normal lay conditions prevailed, in this case corresponding to an average lay rate of approximately 100 m/hr. Although the seastate varied slightly during these periods, the pipeline embedment was relatively consistent, ranging from 0.5D to 0.75D, based on assessment of ROV video still images about every 10 m along the lay route segment (Table 2.3). The video footage suggests that during beam seas with wave heights of 1 m, the lateral motions of the pipeline were slightly larger than during head-quartering seas with wave heights of 1.2 m, resulting in slightly higher pipeline penetration and larger vertical and lateral heave extent. For the latter seastate, the pipeline penetration was the least of the observed values (~0.5D), also with minimal heave. As the head-quartering waves increased to 1.5 m, the pipeline penetration increased (~0.75D), with little change to the heave profile.

2.5.3 Downtime conditions

During the laying process, there were three downtime events due to repairs and one event associated with preparing the pipeline for final lay down. The pipeline repairs were all about 20 minutes in duration, and did not appear to affect the pipeline

embedment. The lay down preparation event lasted for approximately 10 hours based on the vessel log record. During this time, the higher sea state (head-quartering with H_s of 1.5 m) prevailed. Based on the estimated wave period of between 4 and 6 seconds, the number of vessel oscillations and hence cyclic pipeline motions at the touchdown point was in the range 6000 to 9000 cycles for the lay down preparation event. The ROV observations showed that this duration of dynamic movement had a significant effect on the seabed profile. This behavior, during a long break in laying, is similar to the very early stages of SCR trench formation.

The catenary geometry during this downtime event (with the average touchdown point being at KP 40.515) is illustrated in Figure 2.1. In this paper, the region behind the average TDP (towards the laid pipeline) where dynamic embedment occurs is termed the process zone. This zone was approximately 15 m in length, based on the video footage. The region towards the vessel from the average TDP is termed the touchdown zone (TDZ), and was approximately 20 m in length. Note that this is a local definition for convenience, as the TDZ typically refers to the zone between the minimum and maximum TDP. The remaining 215 m of the pipeline route, during which the pipe was lowered to the seabed via a chain, is referred to as the catenary, or lay down, zone. The former description refers to the pipeline position during the downtime event, while the latter refers to the pipeline following the downtime event.

The geometry of the seabed in the process and touchdown zones related to the downtime preparations for lay down is illustrated in Figure 2.3, in plan and profile. In profile, the pipeline was laid in the base of a ladle-shaped trench with the maximum embedment occurring in the process zone at about KP 40.510, just behind the mean TDP. The pipeline embedment then reduced gradually through the TDZ towards the catenary (lay down) zone. In plan, the pipeline was fully embedded in the process zone just behind the TDP. In front of the mean TDP was a wide trench. The trench reduced in depth before transitioning into seabed heave, created during the lay down stage.

The following sections describe the changing seabed profile through each of these zones. Figure 2.4 shows the observed images and idealized interpretations of the changing seabed profile for selected points along the lay route illustrated in Figure 2.3, as well as for a segment towards the end of the pipeline within the lay down zone (KP 40.700). The line types used to highlight the key features of the disturbed seabed

geometry are defined in Figure 2.3. Only the center views have been included; however the port and starboard views were instrumental in interpreting vertical seabed scaling.

2.5.4 Process zone

The changing seabed geometry along the process zone spans lay route segments KP 40.500 up to KP 40.515. The idealized seabed profile for KP 40.500 represents a typical seabed profile for normal lay conditions, as it was located sufficiently far from the TDP not to be affected by the cyclic motion during the downtime event. Moving through the process zone, the embedment almost doubled to a maximum of approximately 1D at KP 40.510, which coincided with the maximum vertical stress concentration. At this point the combination of high (maximum) pipe-seabed normal contact force and small amplitude dynamic lateral motion lead to maximum burial of the pipe. There was no open trench adjacent to the pipe, indicating the small range of dynamic lateral motion.

2.5.5 Touchdown zone

The changing seabed geometry along the touchdown zone spans lay route segments KP 40.515 to KP 40.535. Moving away from the mean TDP (KP 40.515) towards the vessel, the pipeline embedment reduced relative to the original seabed level and also the local soil level, as a trench opened out with the pipe-soil contact line lying below the original seabed elevation (i.e. $(w/D)_l < (w/D)_g$). The local pipe embedment, i.e. relative to the trench floor, was negligible along most of the touchdown zone, suggesting that during each lateral movement the pipeline ploughed a new layer of soil from the trench floor.

In the center of the touchdown zone, the trench was widest, approximately 2D in width at the trench floor and 3D in width at the trench surface. No heave was observed along this interval and it was clear from the video footage that all displaced soil from the trench was lost. Some of this sediment appeared to have been dispersed onto the top of the pipe in the process zone.

2.5.6 Laydown zone

During laydown of the final pipeline section, the pipe was lowered through the water column, supported by a chain. The vertical stress concentration would have progressively reduced during this operation due to the decrease in the pipeline curvature

in the touchdown zone, until the pipe-soil contact force, V, was simply the submerged pipe weight, W′. Opposing this effect was the reduction in pipeline tension when the pipeline was removed from the lay ramp. The stress concentration factor may have initially increased, before decaying to unity (so that V = W′) as the last joint was laid on the seabed. Also, the dynamic motion caused by the seastate reduced due to the flexibility of the chain supporting the pipeline.

The changing seabed geometry for the lay down zone spans lay route segments KP 40.435 to KP 40.750, the end of the pipeline. The embedment within the lay down zone (~0.25D) was significantly less than the embedment during normal laying. The duration of the lay down was approximately 25 minutes, resulting in a lay rate of ~500 m/hr, or five times the normal lay rate. This effect alone reduced the exposure of the pipeline to the sea state-induced action (i.e. the number of cyclic pipeline motions) by a factor of five, in addition to the reduced stress concentration and intensity of dynamic motion.

At the start of the lay down zone (KP 40.535), the local embedment was ~0.25D, with a maximum heave height of 0.25D located at a 0.25D offset from the pipe. The embedment progressively reduced and the heave decreased as dynamic effects became negligible. At the end of the lay down zone the local and global embedment values were less than 0.25D, and appeared to be closer to 0.1D from the port and starboard viewing angles.

2.6 DISCUSSION

2.6.1 Effects of lay condition on dynamic embedment

The catenary behavior, sea state, and the level of exposure to cycles of dynamic motions had a significant effect on as-laid pipeline embedment and the adjacent seabed profile. As the sea state was generally calm throughout this pipe laying operation, it was clear that even minor vessel and pipeline motions resulted in significant additional embedment relative to the static penetration from the submerged pipe weight alone. The observed dynamic embedment is compared to the embedment at the beginning of the fast lay down period, allowing the ratio between the dynamic embedment and the embedment from static load alone (with catenary effects) to be derived. This ratio, F_{dyn}, is commonly termed the dynamic embedment factor (Bruton et al. 2008). At the end of

the lay down period, the catenary effects were negligible, and embedment from the submerged pipe weight alone was observed.

Firstly, it is useful to calculate the static embedment based on theoretical considerations, although the limited soils data and the layered stratigraphy hampered the precision of this estimate. Merifield et al. (2009) derived accurate solutions for the static penetration resistance of a pipeline on undrained soil, validated by plasticity limit analysis and numerical modeling. The recommended bearing capacity parameters account for soil buoyancy, accentuated by heave, during pipeline penetration. This solution links the vertical pipe-soil force per unit length, V, to the embedment, w/D, via the following bearing capacity expression:

$$\frac{V}{Ds_u} = N_c + N_b \frac{\gamma' D}{s_u} \tag{2.1}$$

where, for pipes, N_c is a power law function of w/D (Aubeny et al. 2005, Merifield et al. 2009), γ' and s_u are the soil submerged weight and undrained strength respectively, and N_b is the buoyancy factor:

$$N_b = f_b \frac{A_s}{Dw} \tag{2.2}$$

A_s is the area of soil displaced by the pipeline, calculated as:

$$A_s = \frac{D^2}{4}\left[\sin^{-1}\sqrt{4\frac{w}{D}\left(1-\frac{w}{D}\right)} - 2\left(1-2\frac{w}{D}\right)\sqrt{\frac{w}{D}\left(1-\frac{w}{D}\right)}\right] \tag{2.3}$$

Based on numerical analyses, f_b is taken as 1.5 (Merifield et al. 2009). To use these equations with a strength profile increasing with depth, an iterative process is required to ensure compatibility between the calculated vertical load, V, which is the submerged pipe weight, W', enhanced by the catenary stress concentration, and an equivalent 'plastic' seabed stiffness, V/w, derived from this expression (which affects the stress concentration factor).

Based on the pipeline properties, the normalized pipe-soil contact force (V/s_uD) is equal to 4.0. This results in a predicted static penetration of approximately 0.2D at an invert shear strength of 0.8 kPa, assuming a smooth pipe-soil interface roughness. This value is very close to the observed embedment for the initial part of the lay down segment (KP 40.550), supporting the hypothesis that dynamic lay effects did not have a

significant influence on the lay down segment of the route. If the vertical stress concentration from the pipe catenary shape is ignored, and only the submerged pipe weight is considered, V/s_uD reduces to 3.3 leading to a predicted static penetration of approximately 0.1D at an invert shear strength of 0.5 kPa. This is a reduction of 50% from the full catenary-induced embedment, and is also very close to the observed response (w/D ~0.1) for the final laydown segment at KP 40.700. There was therefore an order of magnitude difference between the embedment due to the pipe weight alone and the as-laid embedment from a downtime event, which was enhanced by both the catenary-induced stress concentration and dynamic lay effects.

As the lay down condition likely included a nominal degree of cyclic exposure, the theoretical penetration of 0.2D from the bearing capacity model represents the best estimate of the true static embedment (including the catenary effect). The resulting dynamic embedment factors for lay down, normal laying and downtime conditions ranged from just greater than 1 up to 5. As shown in Table 2.4, these factors generally increase with the number of cycles of dynamic motion, and it is likely that the values also depended on the amplitude of the dynamic motion and would be influenced by the sensitivity of the soil.

The calculated values of embedment are sensitive to the soil strength profile, which is subject to uncertainty due to the limited available data. However, this uncertainty does not affect the key conclusion, which is that the embedment resulting from the vertical stress concentration and the dynamic motion far exceeds the embedment based on the submerged pipe weight alone.

2.6.2 Effects of lay condition on heave and trenching

The disturbed seabed surface profiles were highly dependent on the dynamic motion of the pipeline. Within the touchdown zone the seabed heave, which was up to 0.5D in height, created additional pipeline embedment. However, the shape of the heave profile varied significantly, and was typically offset from the pipeline, in some cases indicating the direction of the final lateral pipeline movement.

Where the amplitude of dynamic motion was negligible, the heave remained in contact with the pipe (e.g. Figure 2.4, KP 40.550). Where the lateral motion was moderate (~0.2D), heave was not in contact with the pipe (e.g. Figure 2.4, KP 40.500). With sufficient lateral motions of moderate amplitude, the heave was entirely eroded and a

trench formed adjacent to the pipe. During such periods (e.g. a downtime event), a steep trench wall formed close to the pipe furthest from the vessel where the lateral movement was smaller (e.g. Figure 2.4, KP 40.520). Moving towards the vessel, the trench widened and the side slopes flattened, reflecting the remolding and softening of the soil due to the lateral pipeline motion (e.g. Figure 2.4, KP 40.530).

2.7 CONCLUSIONS

This study has presented observations of pipeline embedment, seabed heave profiles and trench formation during a typical pipe laying operation on soft clay in 140 m water depth. The results indicate that the magnitude of embedment and the local seabed disturbance were highly dependent on the dynamic motion of the hanging pipeline, which were determined by the lay vessel and sea state. Approximate mean values of as-laid embedment have been derived from survey video footage for different sections along the pipeline route that includes normal laying conditions, downtime events, and also the final lay down of the pipeline end.

In normal laying conditions the as-laid embedment was about 2.5 to 4 times greater than the static embedment due to the submerged pipe weight and the static stress concentration created by the catenary. When a downtime event increased the exposure of the pipeline to dynamic motion, this ratio increased to 5. A trench was observed to form around the pipe during this downtime period. This large trench, 0.75D in depth and 2D in width, developed within 10 hours even though the amplitude of the lateral pipeline motion was an order of magnitude less than the trench width (~0.2D). These ratios of as-laid dynamic to static embedment were governed by the vessel motion transmitted down the pipe catenary and the resistance offered by the seabed, which depends on the soil properties. The values reported in this paper are not necessarily applicable to other conditions, but highlight the dominant influence of dynamic lay effects on as-laid pipeline embedment in soft clay.

Table 2.1. Pipeline properties

Outside Steel Diameter	0.3239 m
Steel Grade	ISO 3183-3 L450QC
Wall Thickness	17.5 mm
Coating 1	0.15 mm FBE
Coating 2 and 3	2.15 mm PP
Overall Outside Diameter	0.3285 m
Unit Weight in Air[1]	1.51 kN/m
Submerged Unit Weight (empty)[1]	0.59 kN/m

Note: [1] includes weight of the 3 inch piggyback line

Table 2.2. Observed pipeline motions (from ROV video footage)

KP (km)	Time and date stamp	Lay condition	Significant wave height, H_s (m)	Wave direction ("seas")	Peak-to-peak amplitude of dynamic motion	
					Vertical, w/D	Horizontal, u/D
39.582	4/15/08 8:57	Normal	1	Beam	0.1	0.1
39.737	4/15/08 10:22	Normal	1.2	Head-quartering	-	0 to 0.1
40.100	4/15/08 14:38	Normal	1.2	Head-quartering	0.05 to 0.2	0.05
40.188	4/15/08 16:00	Normal	1.5	Head-quartering	-	0 to 0.02
40.386	4/15/08 17:55	Normal	1.5	Head-quartering	0.1	0.05 to 0.1
40.515	4/15/08 19:30	Downtime	1.5	Head-quartering	0.2	0.2

Table 2.3. Summary of typical as-laid parameters (as defined in Figure 2.2)

Lay Condition	$(w/D)_g$	h/D	$(u/D)_{heave}$	$(u/D)_{far\text{-}field}$	Displaced Seabed Area (m^2)	Heave Area (m^2)
Laydown	0 to 0.25	0 to 0.25	0.5 to 0.75	0.75 to 1.25	0.06	0.06
Normal Lay	0.5 to 0.75	0.25 to 0.5	0.75 to 1.0	1.25 to 1.75	0.39	0.38
Downtime	1.0	0.5	1.0 to 1.25	1.75 to 2.0	0.70	0.69

Table 2.4. Back-calculated dynamic embedment factors

Lay Condition	No. of Cycles	$(w/D)_g$	F_{dyn}
Static + catenary effect (theoretical)	-	0.2	1
Static + catenary effect (observed during lay down)	~20	.25	1.25
Dynamic embedment (observed during normal lay)	~100 (minimum)	.5	2.5
	~1000 (maximum)	.75	3.75
Dynamic embedment (observed during downtime)	~5000 to 10000	1	5

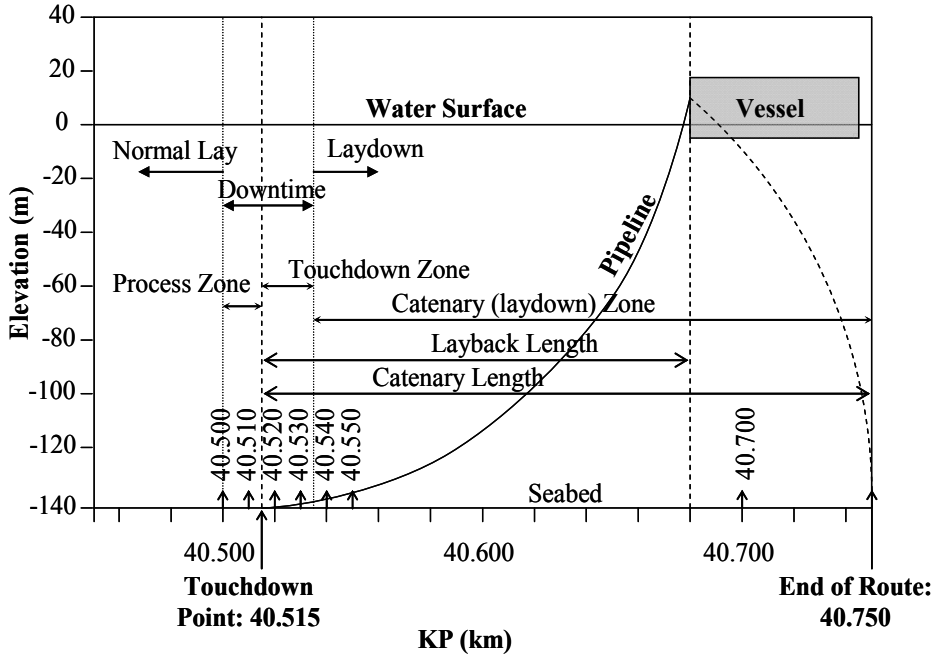

Figure 2.1. Catenary geometry during laydown preparations

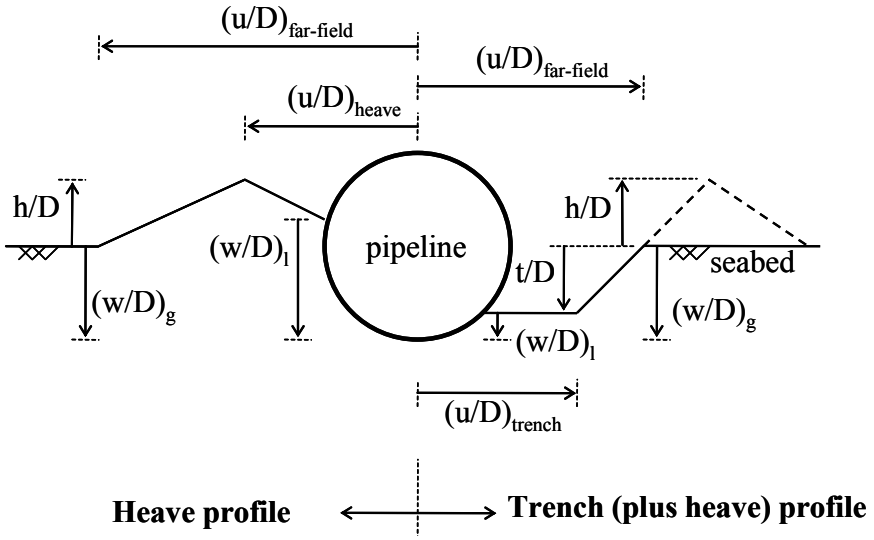

Figure 2.2. Definition of seabed profiles

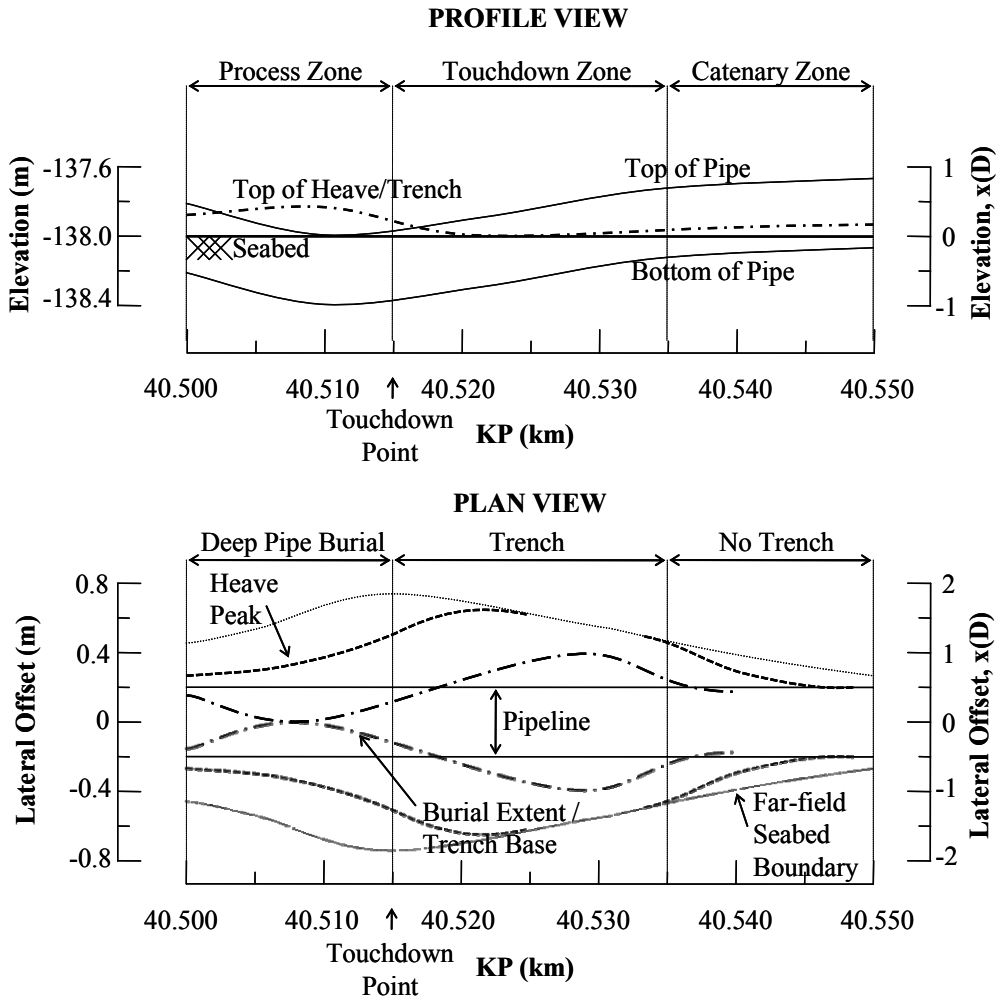

Figure 2.3. Seabed disturbance created near touchdown point during downtime for lay down preparations

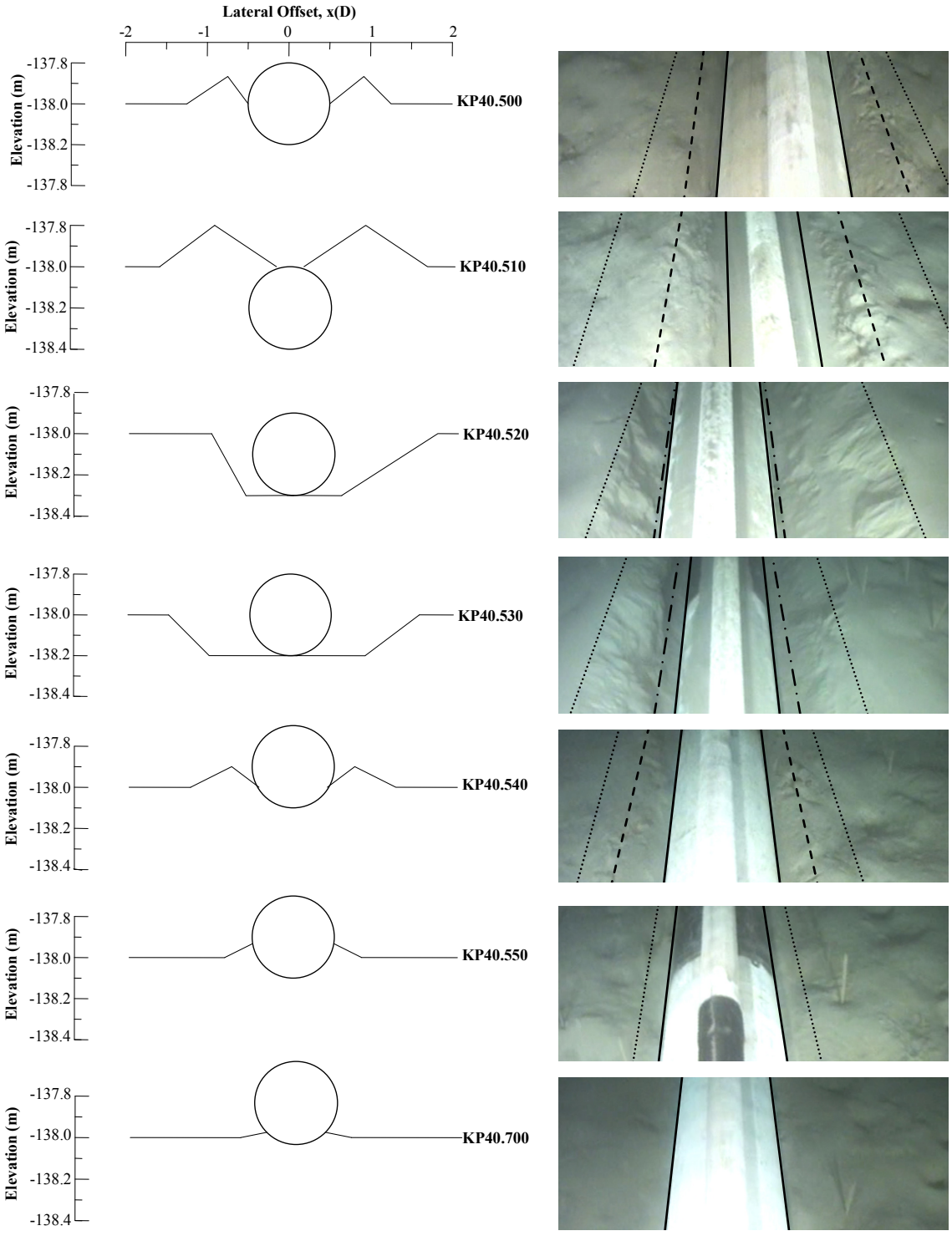

Figure 2.4. Idealized and observed seabed profiles

CHAPTER 3. THE INFLUENCE OF SEASTATE ON AS-LAID PIPELINE EMBEDMENT: A CASE STUDY

The paper presented in this chapter describes a back-analysis for a lighter as-laid pipeline from the North Sea site described in Chapter 2. The observations from Chapter 2 suggested that dynamic lay effects can result in significantly more pipe embedment compared to a statically-placed pipeline on the seabed (by up to a factor of 5 in that case). To explore dynamic lay effects further, specifically those related to the varying vertical contact force through the touchdown zone, numerical simulations of pipeline laying were performed using the commercially-available offshore modelling software package OrcaFlex. In these analyses, the specific pipeline properties and the OrcaFlex model of the real lay vessel, provided by the project donor, were used. Stationary pipelay simulations were performed (i.e. the lay vessel remained in one position) using idealisations of the observed sea state that occurred during the installation.

The analyses show that for the observed sea states, the vertical pipe-soil contact force along the touchdown zone varies significantly. Statistical relationships between the different sea states, the lay vessel motions and the as-laid embedment are presented. These relationships allow a qualitative assessment of the dominant mechanisms associated with the sea state – vessel – pipeline interactions that affect as-laid pipe embedment in fine-grained soils.

Westgate, Z.J., Randolph, M.F., White D.J. & Li, S. (2010). The influence of seastate on as-laid pipeline embedment: a case study. *Applied Ocean Research*, Vol. 32, No. 3, pp. 321-331.

3.1 ABSTRACT

The as-laid embedment of an offshore pipeline is an important parameter for design as it affects lateral and axial stability, exposure to environmental loads, and thermal insulation. For soft clay seabeds, the as-laid embedment can be significantly higher than predicted using methods based on the static penetration resistance due to dynamic lay effects. There are very few published field surveys showing the as-laid embedment of a pipeline following installation. Back-analysis of field survey data has the potential to improve existing design methods, as well as gain insights into the effects of the installation conditions, including the vessel response, the lay angle and tension, weather and seastate, and downtime events. This study describes the as-laid field survey carried out for a 12-inch flowline installed on a soft clay seabed in the North Sea. The dynamic lay effects are examined by studying the influence of seastate, manifested through the vessel response which leads to pipeline motions at the seabed. The findings show that a clear correlation exists between seastate and pipeline embedment. The ratio between the mean observed embedment and the embedment that would be predicted using a conventional static penetration analysis (termed the dynamic embedment factor, F_{dyn}) ranged from 2.5 up to 4 for normal pipelay conditions, increasing with wave height. Downtime events, during which pipelay is temporarily suspended, significantly increase the embedment. In this study they led to maximum embedment values greater than one diameter, corresponding to F_{dyn} of up to 10, due to the larger numbers of cyclic pipeline motions at the seabed.

3.2 INTRODUCTION

During offshore pipeline installation, pipeline motions at the seabed increase the pipeline embedment above that predicted by static penetration models, even allowing for the vertical force concentration where the pipeline contacts the seabed (Bruton et al. 2006). Pipeline motions at the seabed are a function of several factors, including seastate, vessel response, lay ramp configuration, pipeline rigidity, water depth and seabed stiffness. Experimental studies on model pipe segments have shown that small oscillations of a pipeline resting on a soft clay seabed can result in significantly increased pipeline embedment (e.g. Cheuk & White 2008). However, only limited field data from pipeline route surveys showing as-laid embedment and profiles of the surrounding seabed have been published, preventing quantification of this behaviour.

Lund (2000b) provided one such case study for the installation of the 40-inch (1 m) diameter Zeepipe 2B pipeline, and concluded that dynamic embedment is primarily a function of lateral cyclic motions, which were estimated to be of limited amplitude (~0.5 diameters, 0.5D, peak to peak). Lund's study also illustrated the effect of vessel downtime on dynamic embedment. Greater embedment was observed (> 1D) due to the higher exposure, from a larger number of cyclic oscillations of the pipeline that occurred whilst the vessel was stationary. Related studies on steel catenary risers (Bridge & Howells 2007) have shown that even greater embedment – up to several diameters – can result from long-term vertical and horizontal cyclic motions.

This paper presents an analysis of dynamic lay effects and the resulting pipeline embedment during installation of a 12-inch (0.39 m external diameter including coatings) steel flowline in a water depth of ~140 m in the North Sea. The paper provides insights, based on numerical analyses, into the source of dynamic lay effects and how vessel motions at the sea surface translate to pipeline motions at the seabed. Measurements of pipeline embedment along the lay route are compared to the changing seastate during installation, providing the link between seastate, vessel motion, pipeline motion, and the resulting pipeline embedment, allowing a quantitative study of dynamic lay effects. The observed pipeline embedment is also compared to static penetration models, resulting in back-calculated dynamic embedment factors (F_{dyn}) for a range of lay conditions.

3.3 SURVEY FACTUAL INFORMATION

3.3.1 Location

The flowline was installed in the UK North Sea sector, approximately 210 km northeast of Aberdeen. The water depth along the 25 km lay route varied from 134 m to 153 m. The field is located in the Witch Ground Graben of the northern North Sea. The seabed exhibits extensive pockmarking, with individual depressions extending up to 200 m wide and up to 4 m deep. Pockmarks significantly increase the complexity of back-analysing the as-laid pipeline embedment, as sharp localised changes in embedment can affect individual values. Pockmarks can become infilled over time, resulting in large variations in sediment consistency along the lay route, which also affect the magnitude of pipeline embedment. Evidence of this pockmark evolution is clear based on seismic surveys carried out in the Witch Ground area (Harrington 1985).

3.3.2 Geotechnical data

The geotechnical site investigation along the pipeline route included 11 shallow cone penetrometer tests (CPTs) and 10 vibrocores spaced evenly over 25 km. The soil conditions along the layroute are similar, characterised by a medium plasticity marine clay seabed, consistent with the general conditions of the Witch Ground area (Paul & Jobson 1991). The surface stratigraphy comprises a thin very soft silty clay layer within the upper 0.2 m (the Glenn Member), transitioning to soft silty clay with thin interbedded sand layers below 0.2 m (the Witch Member). The soil properties for these layers are shown in Table 3.1. Since the thickness of the shallower Glenn Member corresponds to about half the pipeline diameter, this layered stratigraphy may have influenced the observed pipeline embedment.

3.3.3 Vessel and pipeline data

The Acergy Falcon pipelay vessel (formerly named the Seaway Falcon) was used for the installation. The dynamically-positioned vessel measures 153 m in length (162 m at the lay ramp) and 21 m in breadth. The lay ramp is located at the vessel stern, which was set to a lay angle of 68 degrees from horizontal for this pipelay, resulting in a J-lay pipe catenary (Figure 3.1). As the lay ramp is fixed to the vessel stern, the seastate strongly affects the generation of pipeline motions.

The pipeline is a coated steel production flowline with an outer diameter of approximately 0.39 m (Table 3.2). The empty submerged unit weight of the pipeline is 0.22 kN/m, which corresponds to a specific gravity of 1.18 and a nominal contact stress (acting on the full diameter) of 0.56 kPa. The pipeline was installed in the empty condition. The layback length varied from 171 m at the shallowest water depth (134 m) to 190 m at the deepest water depth (153 m), with the corresponding pipe catenary length ranging from 238 m to 267 m, respectively (Figure 3.1). This lay angle is relatively shallow for a J-lay catenary; for deep water pipelay, the lay angle is generally much steeper, approaching angles of 85 degrees or more.

3.3.4 Metocean conditions

The metocean data gathered during the pipelay included the wind, wave, and current magnitudes and headings, with readings obtained at 6-hour intervals. The seastate magnitudes and headings are shown in Figure 3.2 (note that the wind speed has been reduced by a factor of 10 for plotting purposes whereas the current is unscaled). The

vessel heading remained steady at approximately 75 degrees. The current heading was highly variable, with no clear trend evident. The wave and wind headings were well-correlated, transitioning from head seas in the early stages of the lay to stern seas towards the end of the lay. At several sections along the lay route, beam and quartering seastates were prevalent.

No data on wave period were obtained so the period, T, has been estimated using simplified hydrodynamic relationships based on the wave height, h, and the wave steepness, S. For a low amplitude sinusoidal wave on deep water (the water depth for this installation was considered deep as the wavelength was less than half the water depth), the period is calculated as

$$T = \sqrt{\frac{2\pi h}{gS}} \tag{3.1}$$

The wave steepness is a function of the water depth, wave height, and wind speed, ranging from extreme values of 1/7 to 1/25 (Tucker & Pitt 2001). Using wave steepness relationships based on JONSWAP data, values between 1/16 and 1/25 are calculated, whilst from Pierson-Moskowitz wave theory, a fully-developed seastate has a constant steepness value equal to 1/19.7. For this study, a wave steepness of 1/18 was adopted.

3.4 NUMERICAL ANALYSIS

3.4.1 Analysis methodology

OrcaFlex, a commercial software package for numerical analysis of offshore marine systems with specific capabilities for pipelay analysis, was used to model vessel and pipeline motions during installation. The pipe catenary was modelled in 10 m sections, further divided into 1 m sections near the seabed. The environmental data input into the analysis was based on the observed metocean conditions during the installation. An average water depth of 144 m was adopted.

A non-linear seabed soil model in OrcaFlex (version 9.2e) was used as it models the dynamic aspects of the vertical pipe-soil interaction on soft clay more accurately than a linear seabed model (Randolph & Quiggin 2009). The non-linear penetration resistance is based on a power law expression for the nominal bearing capacity factor, $N_c = V/Ds_u$,

with V being the vertical force per unit length, D the pipeline diameter and s_u the undrained shear strength at the pipeline invert, expressed by Aubeny et al. (2005) as

$$N_c = a\left(\frac{w}{D}\right)^b \tag{3.2}$$

where w is the pipeline penetration into the seabed. The OrcaFlex default values of $a = 6$ and $b = 0.25$ were adopted. Other parameters of the model relating to suction resistance, cyclic uplift and repenetration were also taken as the default values (see model details in Randolph & Quiggin 2009, Orcina 2009).

The undrained shear strength profile of the seabed was idealised using a zero strength intercept at the mudline and a strength gradient of 10 kPa/m, determined from the site investigation data. The horizontal resistance of the seabed was modelled using a moderately low friction factor, μ, equal to 0.35.

A Dean Stream non-linear regular wave model was adopted as it is considered suitable for all regular waves. Incremental wave heights of 1 m were analysed up to 4 m (the maximum observed significant wave height, H_s), plus a nominal minimum value of H_s = 0.3 m, for each of the following five wave headings (relative to the longitudinal axis forward of the vessel) to capture the range in observed seastate:

- Stern seas: 0 deg
- Stern-quartering seas: 45 deg
- Beam seas: 90 deg
- Head-quartering seas: 135 deg
- Head seas: 180 deg

3.4.2 Vessel response

Figure 3.3 shows the vessel motion response spectra at the base of the lay ramp based on the vessel response amplitude operators (RAOs) that were derived specifically for the Acergy Falcon. The angular motions of the vessel govern the displacement motions at the stern, with pitch being the dominant motion, resulting in heave amplitudes of up to 1 m per metre wave height at the base of the lay ramp. Under beam seas, the vessel roll governs the pipeline motion creating sway at the base of the lay ramp, whilst under

quartering seas, the vessel yaw results in similar sway amplitudes at the lay ramp. The peak surge and heave motions are generally in phase (i.e. they occur concurrently), especially for head and stern seas, while the sway is out of phase relative to surge and heave for all wave headings. Dynamic positioning was not considered in calculation of the vessel motions as it affects only surge and sway motions which were not the dominant motions at the lay ramp. This is discussed further in Section 3.5.

3.4.3 Pipeline response

The static pipeline condition was modelled in OrcaFlex by setting the initial position of the vessel to obtain the design horizontal pipeline tension at the seabed (~18 kN). The static pipeline parameters include the lay (or declination) angle, effective tension, shear force, bending moment, penetration (including the penetration normalised by the pipeline diameter) and vertical force concentration, defined as the vertical pipe-soil contact force per unit length, V, normalised by the submerged pipe self-weight per unit length, p. These parameters are presented in Figure 3.4 as a function of the pipeline arclength (i.e. catenary length) off the vessel. The arclength scale is reduced for the penetration and force concentration plots to highlight the zone of seabed contact. The touchdown point (TDP) was located at an arclength of ~250 m, with a maximum static penetration of 0.047 m (0.12D) occurring 9 m behind the TDP and coinciding with the maximum vertical force concentration factor – denoted V_{max}/p – of 3.25. Note that the residual pipeline embedment shown in Figure 3.4 is not realistic as the simulation does not consider the continuous laying process (i.e. it is a snapshot of the catenary-induced response at a fixed vessel position).

The dynamic lay effects imposed from the vessel can be divided into two processes: (i) vertical pipeline oscillations, which create a force concentration at the (deeper) extreme of each cycle and (ii) horizontal pipeline oscillations. The vertical pipeline oscillations consist of (i) separation cases, in which the pipe breaks away from the seabed (so V reduces to zero), and (ii) contact cases, for which V remains positive and the pipeline does not lift off the seabed. The length of pipe-seabed 'breakaway' is termed the touchdown zone (TDZ), or the distance between the extreme TDPs. Beyond the TDZ (i.e. towards the laid pipeline), vertical and horizontal pipeline motions occur, but the pipeline remains in contact with the seabed. This zone is termed the process zone (PZ). Within the PZ, the force concentration factor gradually reduces to unity, and significant pipeline motions cease.

A detailed representation of these two processes is shown in Figure 3.5 using beam seas up to a wave height of 3 m (for clarity) as an example, with the static TDP shown in relation to the dynamic TDZ. The static TDP is the location where the pipe touches down on the seabed in the static configuration, in the absence of any sea state. This figure illustrates the change in the force concentration, V/p, and the horizontal oscillation amplitude, u/D, along the pipeline catenary for three different wave heights. The maximum force concentration factor and length of the TDZ increase with wave height (Figure 3.5a). For example, for a wave height of 3 m, the maximum force concentration factor is about 6.5, and the length of the TDZ is 43 m. The location of the maximum force concentration is also dependent on the wave height, and affects the interaction of vertical and lateral pipeline motions. For this pipelay, the maximum force concentration was located within the PZ (i.e. beyond the maximum TDP) for wave heights less than 2 m, whilst for larger wave heights it was located within the TDZ. The maximum force concentration factor is a calculated value, based on hydrodynamic theory using regular waves. In reality, random sea state conditions frequently increase the instantaneous maximum force concentration factor, but also increase the frequency of the forces that are lower in magnitude than the average. As the analysis considers average conditions observed over large time/space intervals (e.g. several hundreds of metres of lay route for each set of averaged embedment data), these less significant effects can be neglected in this study.

The horizontal oscillation amplitude, u/D, – defined as half the difference between the maximum and minimum calculated out-of-plane pipe displacements normalised by the pipe diameter – also increases with wave height, but is amplified along the catenary for small wave heights (H_s = 1 m) and is attenuated for larger wave heights (Figure 3.5b, lower plot). For the observed sea states, u/D was generally smaller than ±0.3 within the TDZ, and smaller than ±0.15 at the point of maximum force concentration (Figure 3.5b, upper plot). Horizontal oscillations combined with pipeline-seabed breakaway can cause the TDP to wander laterally, eroding seabed heave during concurrent cycles of vertical motion. Beam and quartering seas, for which this interaction was most likely, prevailed over nearly 50% of the lay route, as presented in Figure 3.2.

From this type of analysis, a representative maximum force concentration factor can be determined for each wave height and heading (Figure 3.6). Clearly, V_{max}/p is strongly governed by the sea state. The number of cycles, N, of vertical pipe oscillations

experienced by a single element of the pipeline at the lay ramp during normal lay can be calculated based on the wave period, T, the length of the element being considered, L, and the vessel lay rate, v, as

$$N = \frac{(L/v)}{T} \tag{3.3}$$

For example, based on the average lay rate of 100 m/hour (or approximately 2.5 km/day) and the average wave period of 5 seconds, the number of cycles of motion for a 3 m beam sea was about 320 cycles, calculated using the 43 m length of TDZ. The number of cycles of additional vertical pipe motions at the seabed is then dependent on the dynamic response of the pipeline catenary. However, only a small fraction of these cycles also include the high force concentration factor of $V_{max}/p = 6.5$.

It is difficult, from this numerical analysis alone, to determine whether the horizontal pipe oscillations would be similar in number to the vertical oscillations, due to the effects of increasing embedment on lateral pipe-soil interaction. Similarly, it is unknown whether smaller amplitude horizontal oscillations within the short zone of maximum force concentration would result in greater pipe embedment than larger amplitude oscillations under less vertical loading towards the front of the TDZ. This is due to the repeated separation and re-attachment of the pipe to the seabed in the TDZ which will tend to entrain water into the soil and pump very soft soil away from the pipe. These two effects will tend to increase the pipe embedment in a manner that is not captured by existing pipe-soil interaction models. It is understood however, from physical modelling of dynamic pipe embedment, that the relatively few cycles of motion within the short zone of maximum force concentration will generate a significantly greater increase in embedment than the later cycles (of similar amplitude) imposed in the final section of the PZ, where the vertical force is lower (Cheuk & White 2008).

3.5 PIPELINE EMBEDMENT DATA

Cross-sectional profiles of the seabed around the as-laid pipeline were obtained using a remotely-operated underwater vehicle (ROV) which followed the vessel during the pipelay. The cross-profiler obtained seabed profile scans at intervals of approximately 1.6 m along the length of the pipeline, deriving elevation values for 5 discrete points along a cross-section: (a) two elevations 3 m to either side of the pipeline representing

the mean seabed elevations (MSB); (b) two local elevations adjacent to the pipeline, termed the bottom of trench elevations (BOT); and (c) one data point for the top of the pipeline (TOP). The measurements were obtained with a resolution of 0.025D, or approximately 0.01 m. These definitions are shown in Figure 3.7, for three types of idealised seabed profiles. The commonly-used terminology of BOT representing the local seabed elevation can be misleading because it implies the presence of a trench adjacent to the pipe. In this case the BOT elevation lies below the MSB elevation (Figure 3.7c). If the pipe is not within a trench, but instead seabed heave exists adjacent to the pipe, then the BOT elevation is above the MSB elevation (Figure 3.7a).

The embedment data profile along the lay route is presented in Figure 3.8, showing the running average values (for clarity) of nominal penetration w_{MSB} and local penetration w_{BOT}, defined as shown in Figure 3.7. Penetration is in metres; positive values correspond to increasing penetration. Seabed heave adjacent to the pipeline, evident from values of w_{BOT} greater than w_{MSB}, prevailed over 70% the lay route. The average seabed heave during calm seas equalled ~0.1D. During higher seas, or during downtime events, seabed heave was not observed based on these measurements. Instead, a trench formed adjacent to the pipeline, with a depth equal to the nominal embedment less the local embedment, i.e. w_{MSB}-w_{BOT}. Trench formation is due to a combination of increased overall pipeline motions, but more specifically increased horizontal pipe oscillation amplitudes. Also evident along the lay route were several suspended pipeline spans – which appear within the cross-profiler data as a negative embedment – corresponding to the seabed pockmarks, and several local increases in embedment that generally corresponded to downtime events.

Although there is significant scatter in the penetration data, it is clear in Figure 3.8 that the as-laid pipeline embedment was significantly influenced by the sea state, which drove the vessel motions. Heave and pitch were the dominant vessel motions, as expected based on the response spectra shown in Figure 3.3. The vessel motions occurring during pipe lay govern the change in pipeline tension at the lay ramp. In this case, the theoretical horizontal component of the pipeline tension was 37% of the total pipeline tension (based on the cosine of the lay angle). Under static conditions this value is approximately constant along the suspended catenary, and eventually reduces to zero following contact with the seabed. The effective tension at the seabed – which is approximately equivalent to the horizontal component due to the catenary shape – was

calculated in OrcaFlex, and is also plotted in Figure 3.8. The minimum pipeline tension decreased significantly due to vessel motions during the lay process, tending towards compression for severe sea states. Depending on the seabed stiffness, this behaviour can create a significant increase in the vertical force concentration (Pesce et al. 1998). For a rigid seabed, as the effective tension decreases the force concentration increases exponentially. For a compliant seabed, the pipeline embeds deeper as the effective tension reduces, and the force concentration increases, but by less than for a rigid seabed due to the reduction in pipeline curvature. For the latter case, an upper bound force concentration factor close to or slightly larger than the static maximum value is more realistic. As the tension was not measured during the installation, it is not possible to determine the actual horizontal tension in the pipeline.

3.5.1 Detailed examination of data

Portions of the lay route were examined in detail to assess the relative influence of the two principal mechanisms of dynamic embedment: (1) softening of the soil through remoulding, and (2) ploughing of the soil to form a trench around the pipeline. From examination of the vessel log, there were several events during which pipelay was temporarily suspended. These 'downtime' events increased the exposure of the pipeline to the sea state (i.e. the number of cycles of pipe motion increased), and were associated with various activities common to the pipelay process, such as equipment repairs, weather-related standby, and abandonment and recovery events. In this case, abandonment and recovery events caused the most severe exposure – up to several hours duration.

Table 3.3 shows the sea state, lay route location, and the resulting embedment values for eight different cases. Each case can be linked to one of the three types of idealised seabed profiles (Figure 3.7). For normal lay, cases 1 and 4 lead to significant seabed heave adjacent to the pipeline (Figure 3.7a). This scenario was prevalent where the horizontal pipe oscillations were small (u/D smaller than ±0.1). It is unlikely that the lateral position of the TDP changed for these cases. For cases 2 and 3, the seabed heave was partially eroded by pipe motions induced by the higher sea state during normal lay (Figure 3.7b). This erosion of the seabed heave indicates lateral movement of the TDP due to pipeline-seabed separation (i.e. breakaway) and moderate horizontal oscillations (u/D equal to ±0.2). For downtime cases 5 to 8, a trench formed adjacent to the

pipeline (Figure 3.7c), where large numbers of cycles were combined with moderate to large horizontal oscillations. Trenches deeper than one pipe diameter were observed.

The reported survey data do not fully capture the seabed cross-section geometry, as they are based only on five elevation measurements. However, supported by ROV video survey analysis for a similar pipeline installed in the same development (Westgate et al. 2009), the idealised seabed profiles shown in Figure 3.7 are indeed representative of the general cross-sections. Only by considering further analysis of the cross-profiler scans can the full cross-section, including the lateral extent of the heave or trench, be quantified.

3.5.2 Statistical analysis

The penetration data was filtered to create a dataset that could be used statistically to quantify the typical as-laid embedment and examine possible correlations between the embedment, seastate and lay activities. The filtering process eliminated all known seabed pockmarks, existing pipeline crossings (of which there were four), and major (> 1 hr) downtime events. In addition, the first and last kilometres of the layroute (i.e. 0 to 1 km, 24 to 25 km) were excluded. A histogram of the nominal pipeline embedment is shown in Figure 3.9. The mean embedment was equal to 0.37D, and ranged from 0.26D to 0.48D within one standard deviation and from 0.15D to 0.59D within two standard deviations. The average embedment values for each wave height (in increments of 1 m) fall within the range of one standard deviation, as illustrated in the following section.

Correlation coefficients between the metocean and embedment parameters were calculated to investigate relationships between the responses of the vessel and the pipeline and the nominal pipeline embedment. Table 3.4 shows the correlation coefficient, R, for each combination, with pipeline penetration most strongly linked to wave height (R = 0.37). The vessel heave, pitch, and surge each showed a similarly significant positive correlation to penetration (R = 0.32); however, the vessel sway, roll and yaw each showed very weak positive correlations to embedment (R ~ 0.04). This suggests that the vertical pipeline motions were the primary driver of pipeline embedment. The large heave and surge correlation (R = 0.94) indicated that the vertical motions were concurrent and in-phase (i.e. forward surge combined with upward heave, and vice versa), resulting in large variations in the horizontal pipeline tension. The minimum horizontal pipeline tension showed a negative correlation with embedment (R

= -0.25), as expected, but this was weaker than the link between wave height and embedment, suggesting that it is the combination of horizontal (out-of-plane) pipe oscillations and vertical (in-plane) pipe oscillations that influenced the as-laid embedment. This is evidenced by the larger (negative) correlation ($R < -0.3$) that all vessel motions (from surge through to yaw) contributed in part to the changing pipeline tension, thus the changing vertical pipe-soil force concentration.

3.5.3 Pipeline embedment trends

The local and nominal embedment values, averaged for each wave heading and wave height, are plotted in rose diagrams in Figure 3.10a and Figure 3.10b, respectively. All wave headings produced a significant increase in pipeline embedment for an increase in wave height. Head, stern and quartering seas produced the largest variations in embedment, while beam seas (for which lateral oscillations of the lay ramp occurred due to vessel sway and roll, together with vertical pipe motions from the vessel heave) produced minor changes in embedment with increasing wave height, but exhibited relatively high embedment (~0.35D) even for the calmest seas.

The correlation relationships were further explored by averaging the embedment data for all wave headings against the significant wave height and the corresponding maximum vertical force concentration factor, V_{max}/p (Figure 3.11). The significant wave height data were measured. Conversely, the force concentration factor, based on the measured data, was calculated within the OrcaFlex analysis and therefore includes an additional degree of uncertainty due to the assumptions used in the software.

There is a strong correlation between wave height and pipeline embedment, indicating that the seastate and the resulting vessel motions were a key factor controlling dynamic embedment for this pipeline catenary. Considering the similar force concentration factors of $V_{max}/p \sim 4.5$ for 1 m and 2 m wave heights, there is arguably an even stronger correlation (nearly linear) between the maximum force concentration and pipeline embedment. As the wave height and force concentration increased, the amount of heave relative to the nominal embedment decreased, i.e. $(w/D)_{MSB}$ and $(w/D)_{BOT}$ eventually converged, transitioning from the idealised seabed profile in Figure 3.7a towards the idealised profile in Figure 3.7b. For a wave height of 4 m and maximum force concentration factor of 6.5, the local and nominal embedment values were about equal. The maximum local embedment relative to the nominal embedment occurred

during calm seas, and was about 0.13D in height, or 50% of the associated nominal embedment. This is in agreement with other studies (Randolph & White 2008a).

The extent to which seabed heave results in additional area of contact around the pipe circumference (affecting the axial resistance) is unclear due to the lack of cross-profiler images provided. Observations of survey video footage suggest that the seabed heave only remains in contact with the pipe during sea states where horizontal pipe oscillations are absent (Westgate et al. 2009). For sea states that give rise to large horizontal pipe oscillations at the seabed and pipeline-seabed breakaway, the lack of seabed heave immediately adjacent to the pipe suggests that any heave was displaced, or eroded, by horizontal pipe motions in the TDZ (e.g. Case 2 in Table 3.3). This behaviour was accentuated during downtime events for which the number of cycles of motions was increased by an order of magnitude, causing a trench to form along the pipeline (Figure 3.7c, Cases 5 to 8 in Table 3.3).

3.5.4 Dynamic embedment factors

It is common practice in design for the as-laid embedment, $(w/D)_{as\text{-}laid}$, to be estimated by first calculating the static embedment, $(w/D)_{static}$, (taking into account the static catenary force concentration, and using the intact shear strength of the soil) then applying a multiplier, termed the dynamic embedment factor, F_{dyn} (Bruton et al. 2006), to give

$$\left(w/D\right)_{as-laid} = \left(w/D\right)_{static} F_{dyn} \tag{3.4}$$

F_{dyn} has been found to vary in the range 2 to 10 (Randolph & White 2008a). The static force concentration can be calculated using standard catenary equations (e.g. Lenci & Callegari 2005; Randolph & White 2008a). There are several static penetration resistance models available, which are either based on theoretical plasticity solutions (Murff et al. 1989, Aubeny et al. 2005) or which are calibrated to model test data (Verley & Lund 1995). The recent solutions reported by Merifield et al. (2009) are based on plasticity limit analysis but also account for soil buoyancy and heave. The static penetration of 0.12D and the maximum static force concentration factor of $V_{max}/p = 3.25$, as calculated in the OrcaFlex analysis, is based on the model of Aubeny et al. (2005) together with an appropriate buoyancy factor, and thus is consistent with the model of Merifield et al. (2009).

Based on this embedment value (0.12D), F_{dyn} for this pipeline ranged from a minimum average value of approximately 2.5 for calm sea states up to a maximum of 4 for high sea states under normal lay conditions (Figure 3.12). From the statistical analysis, F_{dyn} ranging from 1 to 5 could be considered for normal lay conditions, which represents two standard deviations below and above the mean embedment, respectively, over the entire lay route. Similar variations could be calculated using statistical parameters for each wave height. For downtime events, F_{dyn} values up to 10 were observed due to the high quantity of vertical and horizontal pipeline oscillations.

The dynamic embedment factor is based on the nominal pipeline embedment, and is therefore exclusive of seabed heave which results in additional local embedment. As evident for this pipeline, seabed heave can contribute up to 50% of the nominal embedment (Table 3.3). However, heave was eroded during episodes of high exposure so this additional contribution of embedment does not significantly increase the total embedment during higher sea states (Figure 3.11). This behaviour has been observed for other pipelines in the same development (Westgate et al. 2009). Therefore, if it is necessary to make an assessment of the maximum local pipe embedment, the maximum values of F_{dyn} (which lead to the highest values of nominal embedment) do not apply concurrent with the higher values of local embedment. Local embedment from seabed heave is eroded by the same process that increases the nominal embedment.

3.6 CONCLUSIONS

A back-analysis of the laying process of an on-bottom pipeline in the North Sea has provided insights into the influence of dynamic lay effects on pipeline embedment. The results provide evidence of the mechanisms of dynamic pipeline embedment during offshore pipe lay. The key contribution of this case study is the observation of a strong link between sea state and as-laid pipeline embedment. This link highlights the effect of pipeline motion at the seabed.

The following additional conclusions were determined from this study:

- Pipeline motions at the seabed, driven by sea state-induced vessel motions based on numerical analyses, were significantly affected by the dynamic response of the pipe catenary. This effect complicates the development of generalised guidance on the interaction between vessel motion and dynamic embedment.

However, modern pipelay software, such as used in this study, enables site-specific dynamic simulation of the lay process, allowing the sea state, the vessel response and the catenary behaviour to be combined into an assessment of the likely pipe-soil loads and pipeline displacements at the seabed.

- A non-linear soil model was used to assess the changes in vertical force concentration through the pipe catenary in contact with the seabed. During normal lay conditions for this pipeline, the maximum dynamic vertical force concentration factor was 6.5, which is twice the static value. This generally occurred within about 10 m of the static touchdown point. For calm seas it occurred within the process zone, where the pipeline remains in contact with the seabed, whilst for higher seas it occurred within the touchdown zone, where the pipeline separates from the seabed with each vertical cycle of motion.

- Horizontal pipeline motions were largest for beam sea conditions, attaining maximum amplitudes of approximately 0.3D in the touchdown zone, decreasing to maximum amplitudes of approximately 0.1D in the process zone. The combination of large horizontal pipeline motions and pipeline-seabed separation may have led to lateral displacement of the touchdown point. Conversely, the combination of large horizontal pipeline motions and maximum vertical pipe-soil contact forces may have lead to quicker embedment of the pipeline, due to remoulding and entrainment of water.

- The as-laid pipeline embedment resulting from normal lay conditions – corresponding to a lay rate of 1 to 3 km/day – varied between average values of 0.3 and 0.45D, increasing with wave height from H_s = 0.3 m (the nominal calm sea state) up to H_s = 4 m (the nominal maximum allowable sea state). For a given rate of laying, the pipeline embedment increased as the dynamic motion of the vessel increases.

- At several locations along the lay route, the as-laid embedment increased to more than one pipe diameter. The locations corresponded to the touchdown zone of the pipe during downtime events, including pipeline repairs and abandonment and recovery events. In general, the longer the downtime event – up to several hours in this case – the higher the pipeline embedment, which indicates an

underlying influence of the pipelay rate. These events were infrequent, and represent only a small fraction (less than ~1%) of the total lay route.

- The static embedment of the pipeline, accounting for the static force concentration on the seabed, was calculated as 0.12D using both OrcaFlex and a direct calculation method. Based on this static embedment value, $(w/D)_{static}$, the corresponding average dynamic embedment factors ($F_{dyn}=(w/D)_{as\text{-}laid}/(w/D)_{static}$) ranged from approximately 2.5 to 4 for normal lay conditions, increasing with wave height. Variations of these values (from a minimum F_{dyn} of 1 up to about 5) could be considered based on a statistical analysis of the mean embedment along the lay route. The local increases in embedment associated with downtime events correspond to F_{dyn} values up to 10.

- Seabed heave adjacent to the pipeline was evident during calm sea states (~70% of the lay route), with an average height of 0.1D, enhancing the local embedment of the pipeline. This value represents up to 50% of the nominal embedment. Due to the slight horizontal pipe oscillations present regardless of sea state, it is unlikely that the seabed heave was in direct contact with the pipeline, especially at higher nominal embedment. This presence of heave, which may or may not be in contact with the pipe, can be relevant to pipeline design calculations related to thermal insulation, axial pipe-soil resistance and exposure to seabed landslides, for example.

- Periods of very high sea states and downtime events did not result in seabed heave, but rather a decrease in the local embedment resulting from formation of a trench adjacent to the pipeline. A further study of seabed cross-sectional profiles for a similar pipeline in the same development is described by Westgate et al. (2009), which provides observations of the development of seabed heave and trenching during pipe lay.

Table 3.1. Soil conditions along the lay route

Soil Property	Glenn Member	Witch Member
Depth to Bottom of Layer (m)	~0.2	> 1
Effective Unit Weight (kN/m^3)	6.5 to 8.5	
Shear Strength Gradient (kPa/m)[1]	5 to 20	1 to 2
Sensitivity	2 to 3	

1 – Mudline strength intercept is considered negligible

Table 3.2. 12-inch flowline properties

Outside Steel Diameter	0.3239 m
Wall Thickness	15.9 mm
Coating 1	0.45 mm FBE
Coating 2	34 mm SPU
Overall Outside Diameter	0.3928 m
Unit Weight in Air	1.44 kN/m
Submerged Unit Weight (empty)	0.221 kN/m
Modulus of Elasticity, E[1]	200 GPa
Bending Rigidity, EI	36.6 MN-m^2

1 – Assumed value based on typical steel pipes

Table 3.3. Individual lay process episodes

Case	Event type	Sea state	Heading	KP (km)	$(w/D)_{MSB}$	$(w/D)_{BOT}$	Heave (h/D)
1	Normal Lay	Calm	Head/Stern	12.5	0.27	0.40	0.13
2	Normal Lay	Rough	Beam	10.1	0.44	0.44	0.00
3	Normal Lay	Rough	Head/Stern	8.1	0.42	0.46	0.04
4	Normal Lay	Rough	Quartering	14	0.37	0.47	0.11
5	Repair	Rough	Head/Stern	16.1	*0.89*	*0.48*	-0.41
6	A&R	Rough	Head/Stern	8.7	*1.07*	*0.25*	-0.81
7	A&R	Rough	Head/Stern	9.9	*0.89*	*0.25*	-0.64
8	A&R	Rough	Head/Stern	24.1	*1.15*	*0.15*	-0.99

Italics denotes an interpreted (not calculated) embedment value

Table 3.4. Correlation coefficients between penetration, sea state, and vessel response

	$(w/D)_{MSB}$	H_s	Surge	Sway	Heave	Pitch	Roll	Yaw
$(w/D)_{MSB}$	1							
H_s	0.37	1						
Surge	0.32	0.86	1					
Sway	0.04	0.20	0.10	1				
Heave	0.32	0.87	0.94	0.38	1			
Pitch	0.32	0.88	0.98	0.22	0.98	1		
Roll	0.05	0.22	0.13	0.99	0.41	0.26	1	
Yaw	0.03	0.25	0.31	0.73	0.49	0.43	0.79	1
Tension	-0.25	-0.76	-0.67	-0.51	-0.76	-0.68	-0.52	-0.32
Lay Rate	0.06	0.06	0.03	0.03	0.06	0.03	0.03	0.04

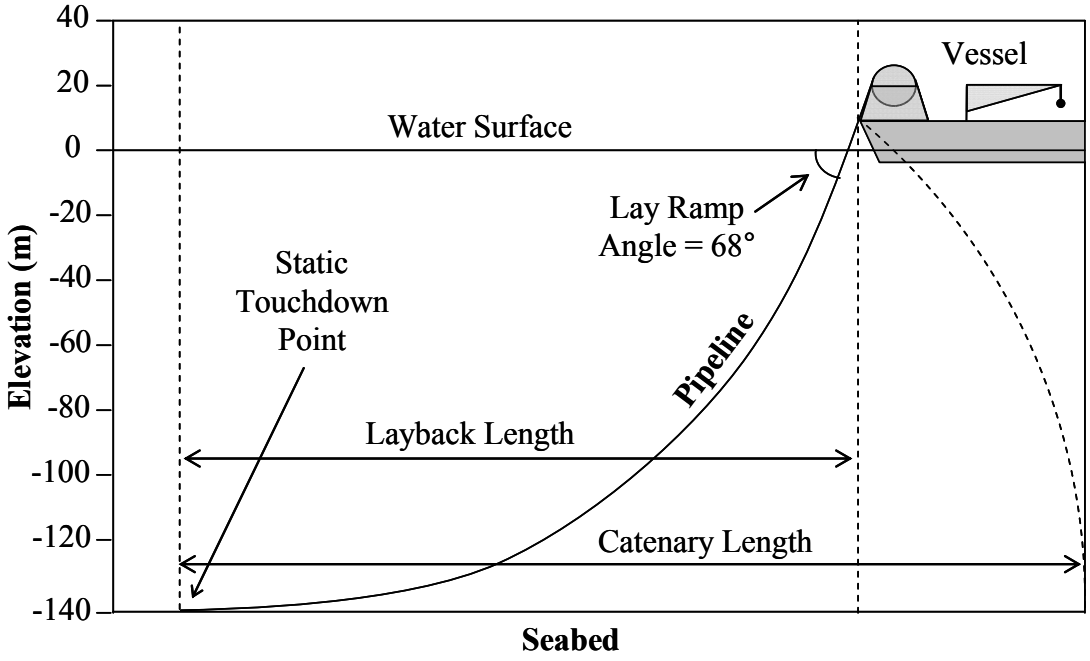

Figure 3.1. Acergy falcon vessel and lay geometry

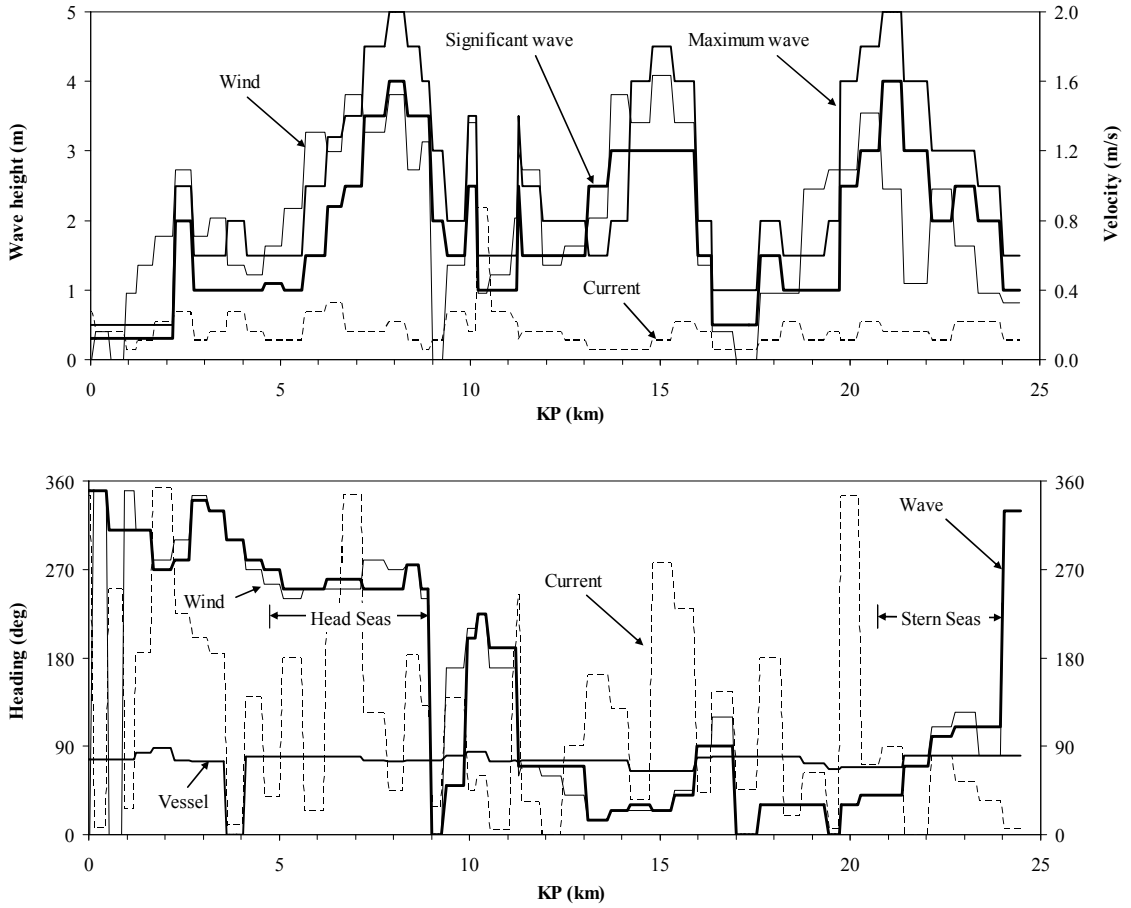

Figure 3.2. Metocean conditions during pipe lay

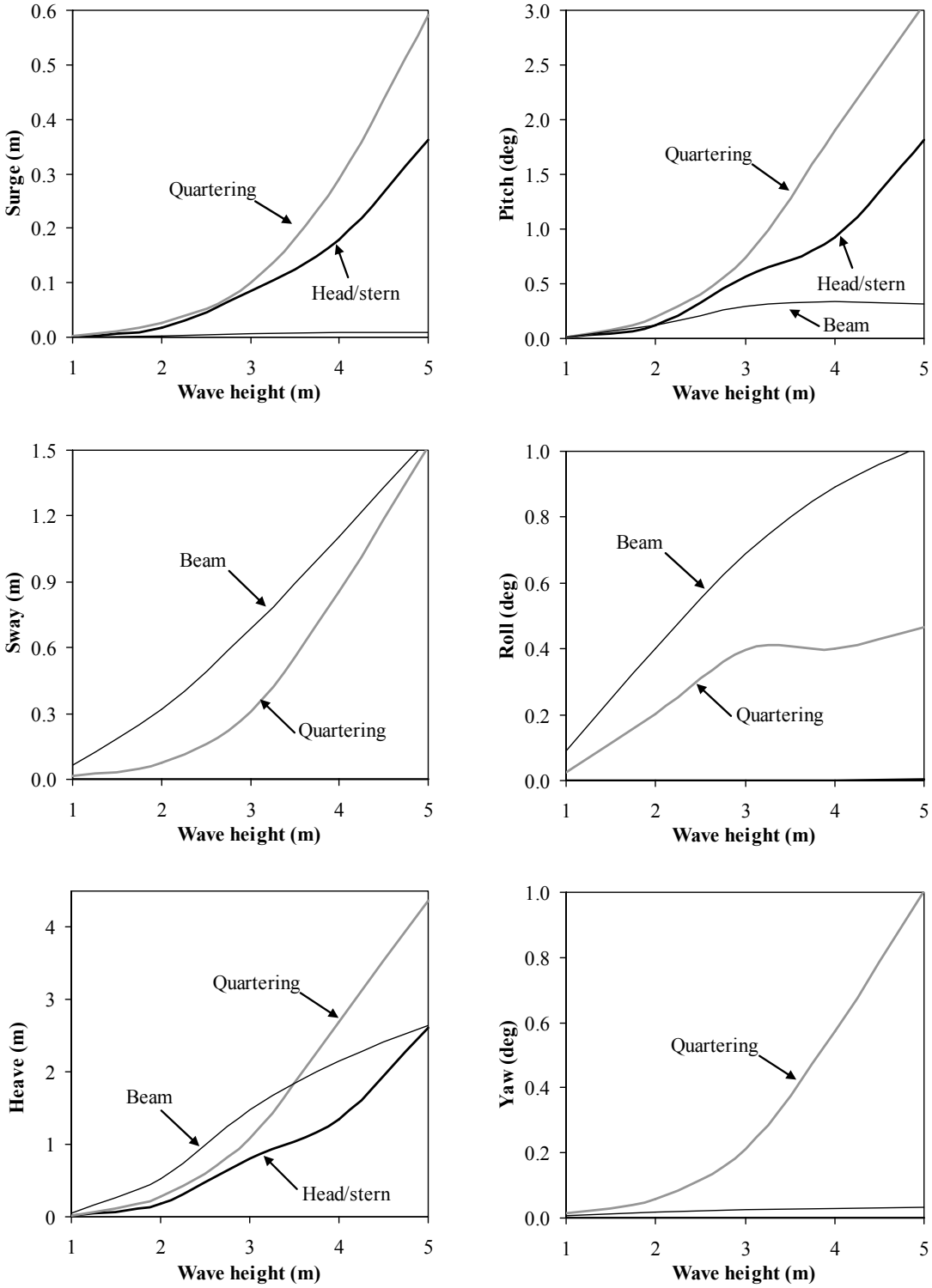

Figure 3.3. Vessel response spectra at lay ramp

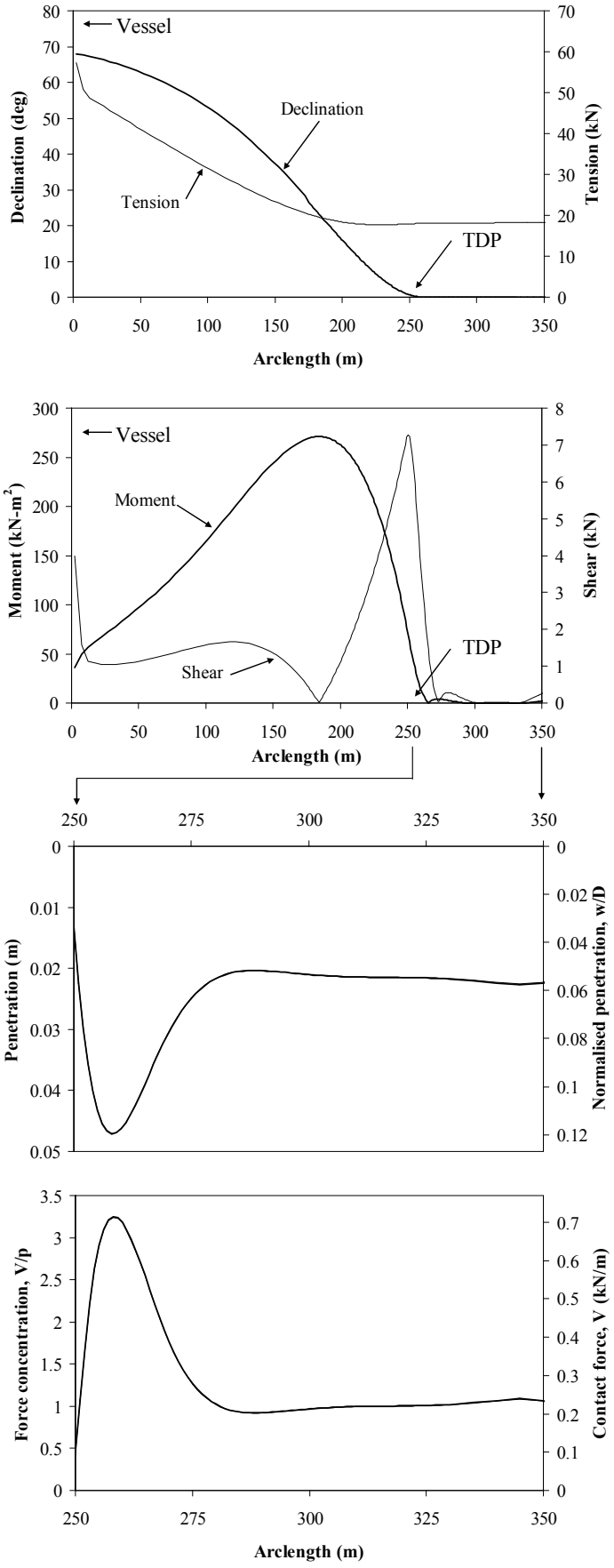

Figure 3.4. Static pipeline condition

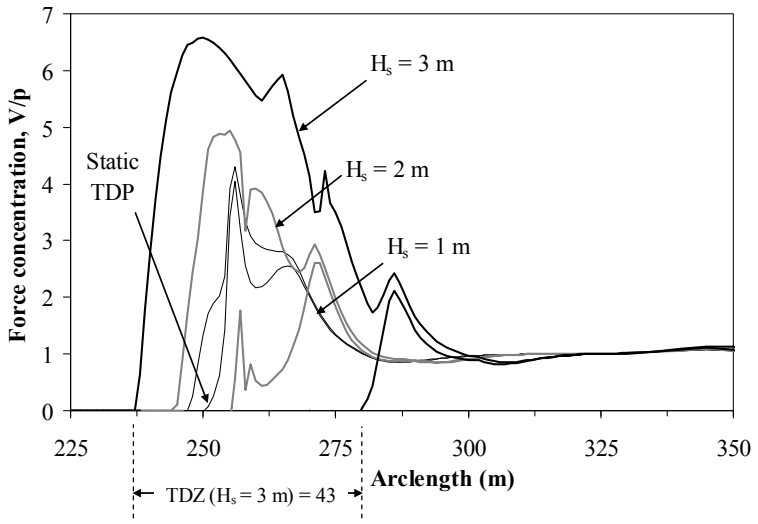

(a)

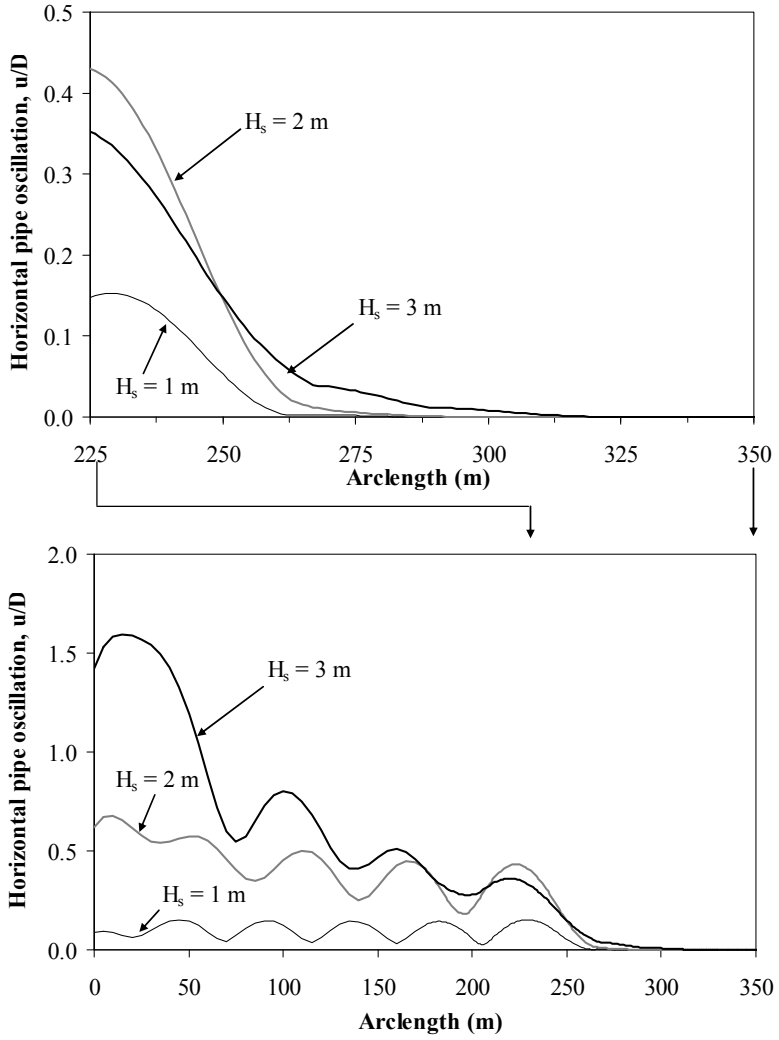

(b)

Figure 3.5. Dynamic pipeline response for beam seas

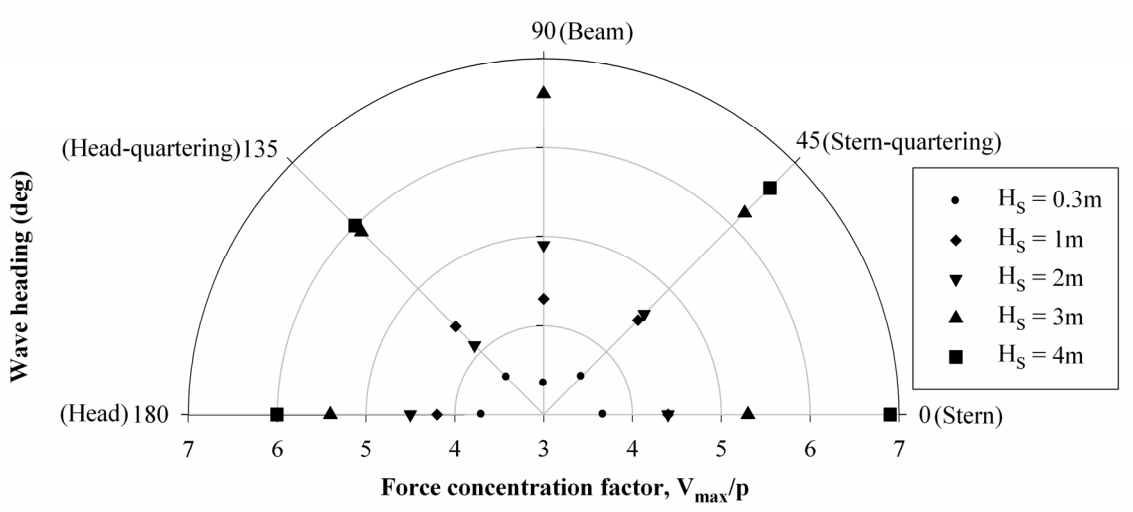

Figure 3.6. Effect of sea state on maximum force concentration factor

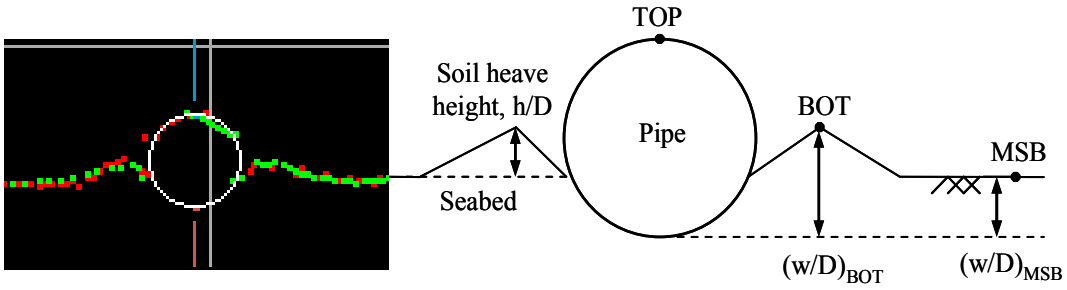

(a)

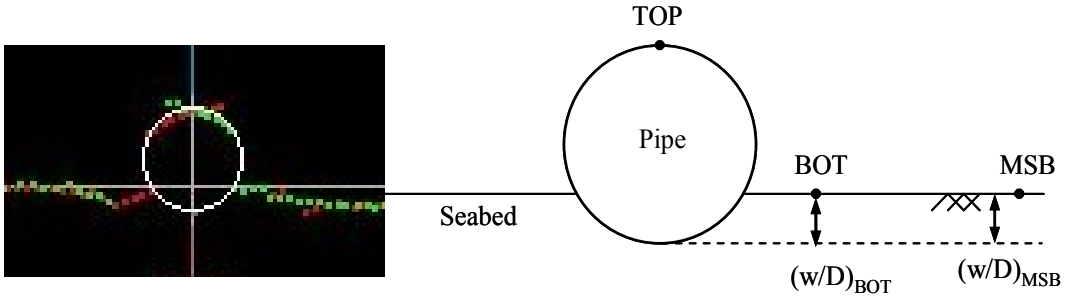

(b)

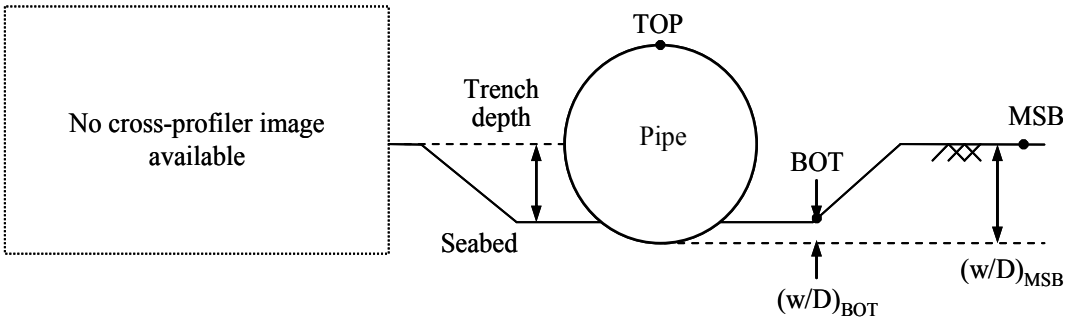

(c)

Figure 3.7. Idealised seabed profiles and example cross-profiler images

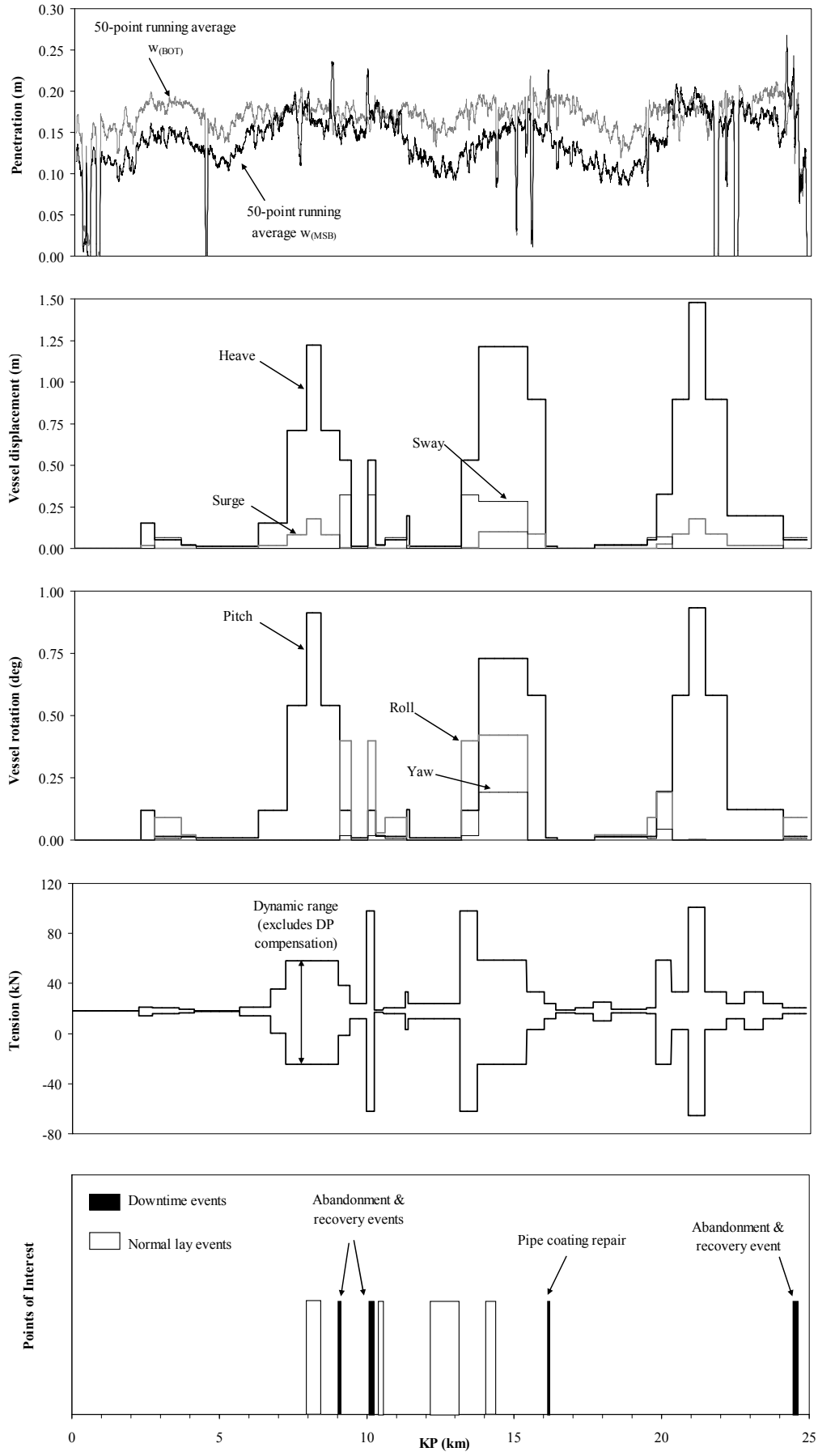

Figure 3.8. Embedment data along route

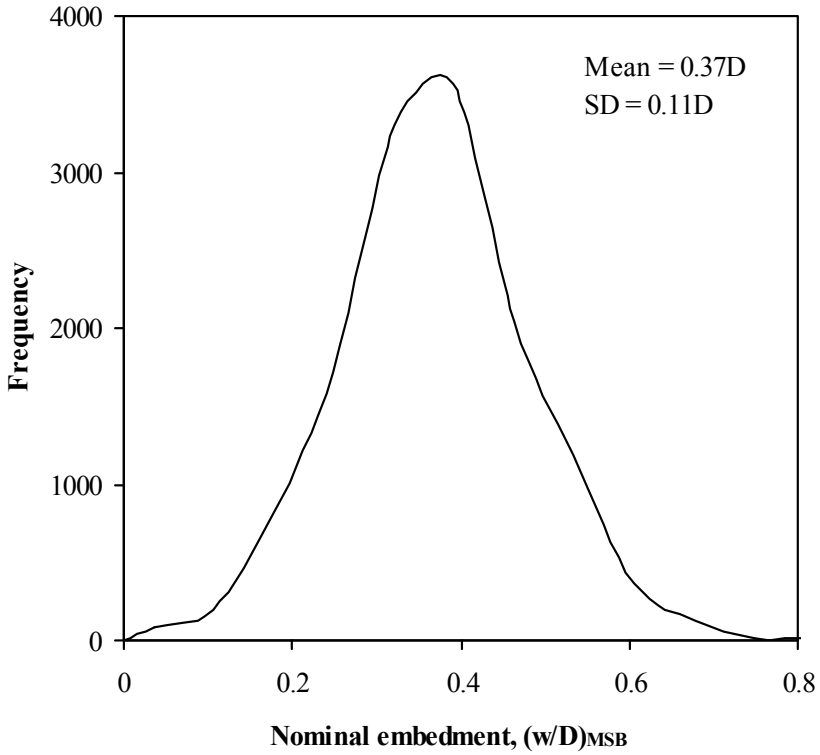

Figure 3.9. Filtered embedment data histogram

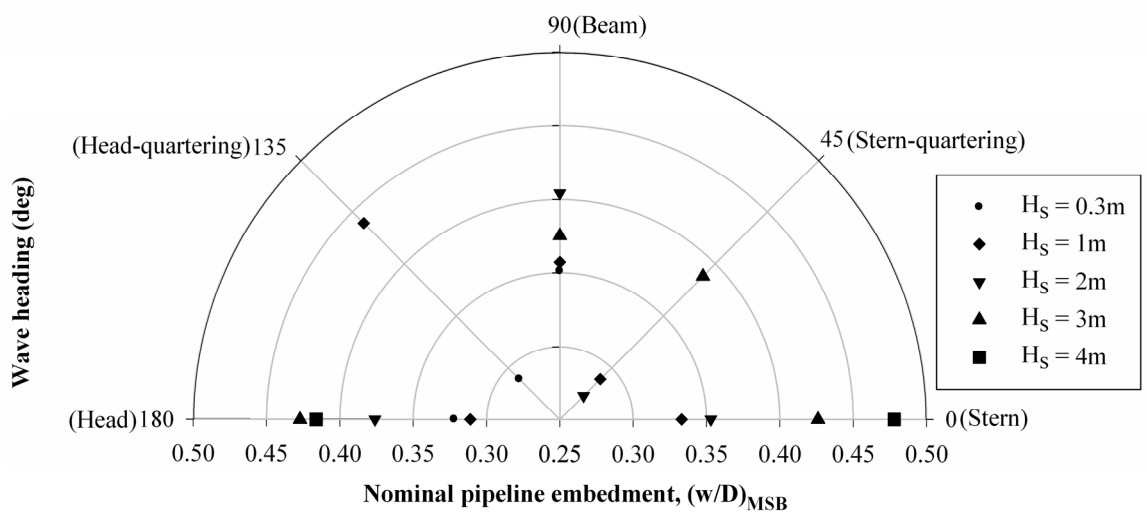

(a)

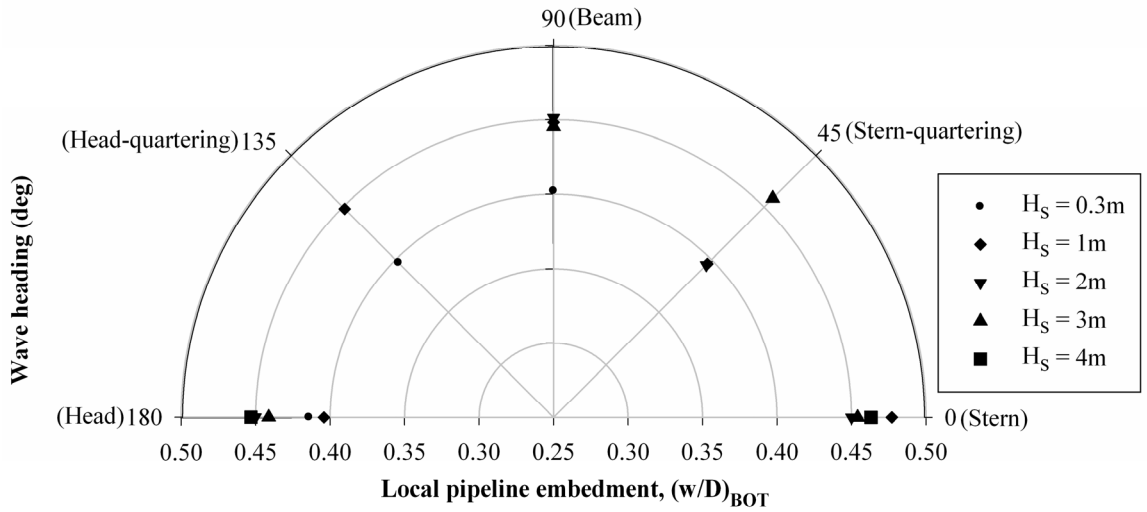

(b)

Figure 3.10. Effect of sea state on nominal and local embedment

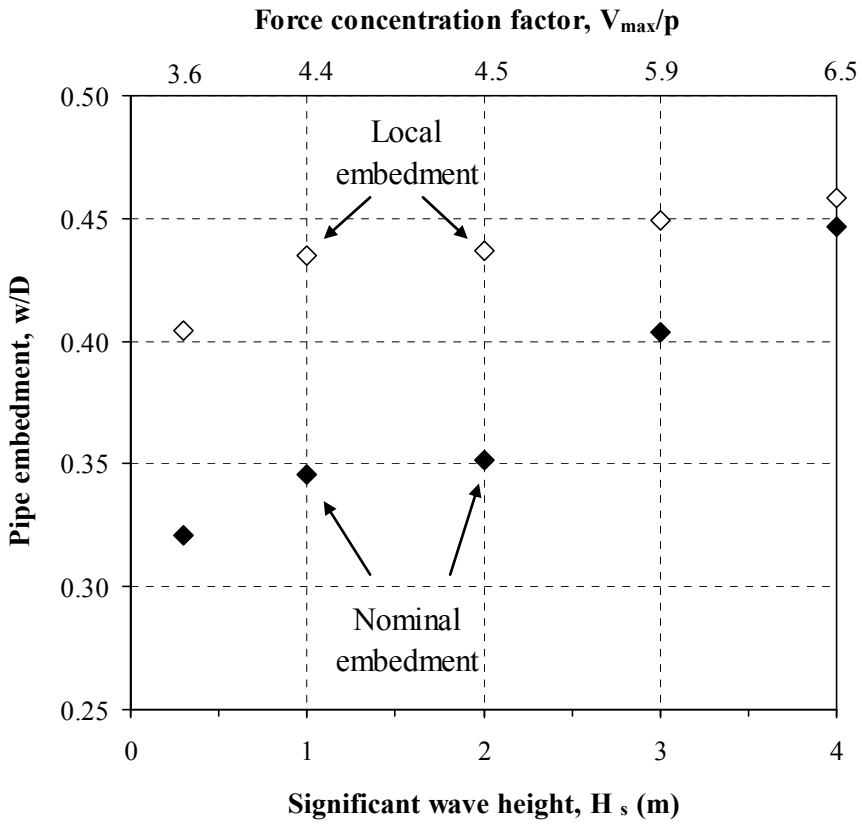

Figure 3.11. Measured and calculated pipeline embedment trends

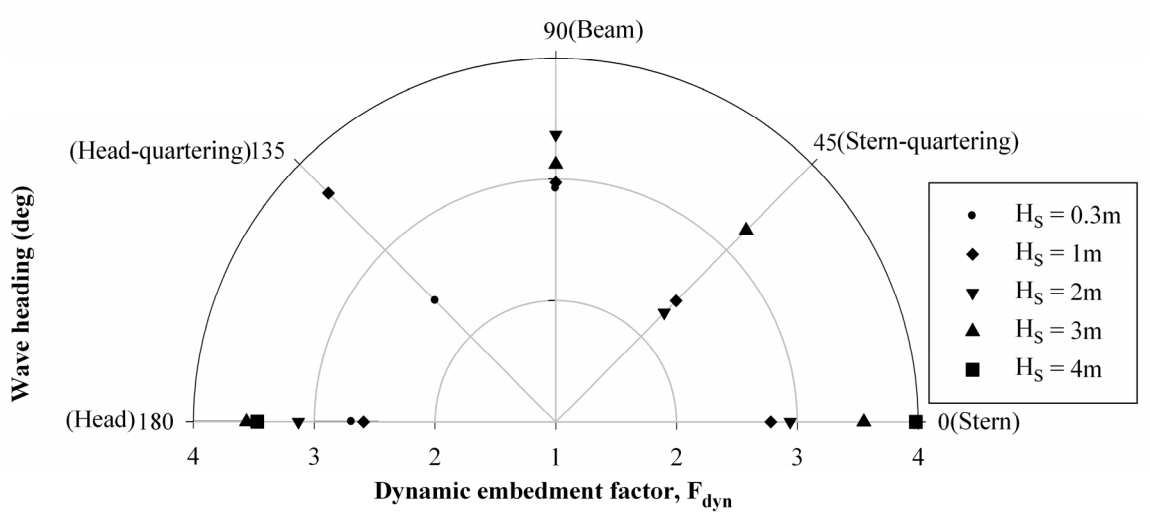

Figure 3.12. Effect of sea state on dynamic embedment factor during normal pipe lay

CHAPTER 4. PIPELINE EMBEDMENT IN SOFT FINE-GRAINED SOILS: NUMERICAL SIMULATIONS AND FIELD OBSERVATIONS

The paper presented in this chapter introduces the use of remoulded soil strength in theoretical bearing capacity solutions to calculate as-laid pipe embedment. The analyses build on the conclusions from Chapter 3 in that the dynamic pipe-soil contact force calculated numerically for each pipeline and lay condition is used directly as an input into bearing capacity calculations of as-laid embedment.

As-laid embedment data for five different pipelines are presented – two from the North Sea site described in Chapters 2 and 3 and three from a site offshore West Africa. High quality geotechnical data, comprised of cyclic T-bar test results, was used to quantify the intact and remoulded undrained shear strength of the soil for use in the calculations. Comparisons between the calculated and measured as-laid embedment values illustrate the relative effectiveness of using different combinations of soil strength (i.e. intact or remoulded) and vertical force (i.e. static or dynamic) to assess as-laid embedment.

The comparisons show that the degradation in soil strength can be linked to the pipe laying rate and the severity of the dynamic lay effects. This suggests that if certain soil properties and lay parameters are known in advance of pipeline installation, a reasonably accurate assessment of the final as-laid embedment can be made, by altering the assumed soil strength profile and vertical touchdown force appropriately. This represents a significant advancement in assessing as-laid embedment.

Westgate, Z.J., White, D.J., Randolph, M.F. & Brunning, P. (2010). Pipeline laying and embedment in soft fine-grained soils: field observations and numerical simulations. *Proc. Offshore Technology Conf.*, Paper OTC20407.

4.1 ABSTRACT

The as-laid embedment of offshore pipelines governs several aspects of pipeline design and lay route architecture. The observed as-laid embedment in soft soils is greater than would be predicted based on the static penetration resistance of the seabed using the in situ soil strength. Empirical 'dynamic embedment factors' are used to scale up this calculated embedment to estimate the as-laid value. The source of this discrepancy is dynamic lay effects, including the form and duration of any dynamic vessel and pipeline movements, and the seabed soil conditions. This study presents data to support an improved methodology to estimate the likely range of as-laid pipeline embedment. Existing theoretical models are reviewed, using as-laid pipeline survey data from five pipelines across two soft fine-grained soil sites. It is shown how the dynamic embedment in the field can be estimated by accounting separately for (i) a reduction in soil strength due to pipeline motions in the touchdown zone and (ii) an increase in the pipeline catenary bearing pressure due to vessel and pipeline dynamics. This represents a more robust methodology than the common industry practice of applying an empirical dynamic embedment factor to the calculated static embedment. Guidance on the pipeline embedment that occurs when the usual lay process is interrupted is also provided, for example at sleeper crossings and during weather-related downtime, in-line tee connections, abandonment and recovery activities, and pipeline termination assembly connections.

4.2 INTRODUCTION

The as-laid embedment of an offshore pipeline is an important design parameter, influencing pipe-soil resistance, exposure to external loading, and thermal insulation. The magnitude of the as-laid embedment in soft soils is greater than the penetration of the pipe into the seabed under its submerged weight alone. This additional embedment is due to (i) the additional vertical pipe-soil contact force from the pipeline catenary and (ii) dynamic lay effects. The additional contact force multiplier, termed the touchdown lay factor f_{lay}, can raise the contact force by a factor of four compared to the submerged pipe weight for typical pipe lay conditions (Cathie et al. 2005, Bruton et al. 2006) although factors between 1.5 and 2 are more relevant for deep water developments. In practice, a dynamic embedment factor f_{dyn} is then applied to this calculated pipe embedment to account for dynamic lay effects. Values of f_{dyn} between 1 and 10 have

been reported (Lund 2000b, Bruton et al. 2006), but there is no established basis for adopting specific values. As a result, predictions of as-laid pipe embedment can span an order of magnitude.

If the length of pipe that has just reached the seabed in the lay process – in the area referred to as the touchdown zone – is exposed to an extended duration of dynamic motions, a trench can form around the pipeline, increasing the embedment further. This is effectively the earliest stage of trench formation that is observed in the touchdown zone of a steel catenary riser (SCR). These trenches can reach several diameters in depth within the first year or two of SCR operation (Bridge & Howells 2007).

The mechanisms that govern dynamic embedment are not simple to quantify. The pipe moves cyclically within the touchdown zone due to excitation from the vessel and pipeline dynamics, softening and remolding the seabed soil. Vertical, or in-plane, pipe motions (Figure 4.1) create transient variations in the vertical pipe-soil force, associated with longitudinal translation of the touchdown point accompanied by changes in the pipe tension. The cyclic expulsion and sucking in of water between the pipe and soil during vertical motions also tends to encourage water entrainment into the soil thereby increasing the degradation of shear strength (Hodder et al. 2008, Gaudin & White 2009). Horizontal, or out-of-plane, pipe motions reduce the vertical bearing capacity of the soil due to the combined V-H loading imposed on the seabed (Merifield et al. 2008, Randolph & White 2008b, Cheuk et al. 2008), increasing the embedment required to support a given vertical load. Also, horizontal motions tend to sweep soil laterally away from the pipeline alignment, which leads to the formation of a trench around the pipeline.

Physical model testing of dynamic lay simulations have provided some insights into these mechanisms. For example, it has been shown that the rate and ultimate magnitude of embedment increase as the amplitude of pipeline motions increases (Cheuk & White 2008, 2011, Gaudin & White 2009). However, the chaotic blend of vertical and horizontal pipe motions that occur during real pipe laying makes it difficult to separate each mechanism based on field observations alone, or to model the process explicitly.

It is considered, however, that the main processes leading to dynamic embedment of the pipeline are (i) reduced shear strength and bearing capacity of the soil, accompanied by (ii) transient increases in vertical pipe bearing pressure during which transverse shear

may also be applied due to lateral movement of the pipe. There are well-established theoretical solutions for idealizations of these two mechanisms. The bearing pressure of a pipeline suspended from a lay vessel can be solved using standard catenary solutions (Pesce et al. 1998, Lenci & Callegari 2005, Randolph & White 2008a, Palmer 2009). The bearing capacity of fine-grained soils subject to pipe penetration is also a well-documented problem for which solutions exist based on plasticity limit analysis (Murff et al. 1989, Aubeny et al. 2005, Randolph & White 2008b) and numerical finite element simulations (Merifield et al. 2008, 2009, Randolph & White 2008a, White et al. 2010). These solutions have been validated by geotechnical centrifuge tests (Dingle et al. 2008, Zhou et al. 2008, Wang et al. 2010).

The bearing capacity solutions can be expressed in a normalized form as V/s_uD against w/D, where w is the pipe invert depth below the original soil surface and s_u is the soil strength at this depth (Aubeny et al. 2005, White & Randolph 2007). The solutions show that the normalized load-penetration response is sharply non-linear at shallow depths (Figure 4.2). Beyond an embedment of ~0.5D it converges slowly towards a steady value at which a deep flow round mechanism is mobilized. However, with the exception of Aubeny et al. (2005), most solutions have examined the response only to ~0.5D embedment.

Dynamic lay effects shift the load-penetration path downwards toward greater embedment through two processes. Firstly, by reducing the soil strength to below the in situ value and secondly by reducing the local seabed elevation if trenching or erosion occurs around the pipeline. An iterative combination of the standard catenary solutions and the static bearing capacity solutions provides a convenient method of assessing static pipeline embedment in fine-grained soils during pipe lay, accounting for the soil-structure interaction associated with the catenary. However, this approach still predicts embedments less than observed in the field, because the softening of the soil and the dynamic catenary behavior are both neglected.

This paper explores simple approaches to incorporate these two additional effects. The governing mechanisms of dynamic pipeline embedment are examined through the back-analysis of a set of as-laid pipeline surveys from two different soft fine-grained soil sites – one in shallow water and one in deep water – aided by numerical analysis. Suggestions are made for improved methods to assess dynamic pipeline embedment in the field for a range of lay conditions and rates.

4.3 FIELD STUDIES

As-laid surveys for 5 pipelines at two different sites have been analyzed. Site A is located in shallow water (~140 m) in the North Sea. Site B is located in deep water (~1300 m) offshore Angola. As-laid survey data was provided for one of the pipelines at Site A (Pipe A1) while touchdown monitoring and as-laid video footage from a remotely-operated vehicle (ROV) were provided for another pipeline at this site (Pipe A2). As-laid survey data were provided for 3 pipelines at Site B, including brief touchdown monitoring video footage for the lightest of these pipes (Pipe B1).

4.3.1 Soil conditions

The soil conditions through the upper 0.5 m of the seabed at the two sites are summarized in Table 4.1. The soil at Site A comprised medium plasticity silty clay and clayey silt. Cone penetrometer tests (CPTs) carried out along the pipe routes were used to determine an intact strength profile while mini-vane laboratory tests were used to assess the remolded strength. The soil at Site B comprised high plasticity clay. Cyclic T-bar penetrometer tests carried out across the site were used to determine the intact and remolded strength profiles. For each site the submerged unit weight was determined from laboratory tests.

4.3.2 Pipeline properties

The structural properties of the 5 pipelines are summarized in Table 4.2. All of the pipelines were 0.32 m (12-in) diameter steel pipes, with various wall thicknesses and coatings. The resulting range of submerged pipe weight, denoted p, is between 0.22 and 0.59 kN/m. Pipe A1 was the lightest of the 5 pipes. The other pipeline at Site A – Pipe A2 – included a 3-in pipe piggybacked to the main pipe, resulting in a heavier submerged weight. The pipe bearing pressures, p/D, for all 5 pipelines ranged from 0.56 to 1.8 kPa. All pipelines were laid empty and were surveyed prior to hydrotesting.

4.3.3 Lay vessel geometry

The Acergy Falcon lay vessel was used to install Pipe A1 and Pipe A2. The ship-shaped Falcon measures 153 m in length (162 m including the lay ramp at the vessel stern) and 21 m in breadth. Three welding stations along the fabrication line were employed to connect multiple pipe sections (37.5 m in total length) together between payout. The Falcon's lay ramp is effectively a small radius stinger that provides the

efficiency of S-lay fabrication (Perinet & Frazer 2007). The ramp was set to an angle of 67.9 degrees for the two pipelines, resulting in a relatively shallow J-lay catenary (Figure 4.3). The average lay rate for these pipelines was about 2.5 km/day (average welding cycle of about 20 minutes).

The Acergy Polaris lay vessel was used to install Pipes B1-B3. The barge-shaped Polaris measures 137 m in length and 39 m in breadth. The lay ramp for the Polaris is a tower located mid-ship. The tower has a gimbaling capability for (fixed) pitch and (live) roll, and can rotate azimuthally relative to the pipeline to keep the vessel oriented into favorable seas. This reduces the effect of the sea state on vessel and pipe motions (Perinet & Frazer 2007). The tower was set to lay angles between 82.6 and 86 degrees for the three pipelines (Figure 4.3). Pipe sections (25 m total length) were loaded into the tower for connection to the pipe catenary with an average welding cycle of 30 minutes. The typical pipe payout duration was about 5 minutes. These rates combine to give an average lay rate of about 1 km/day for these pipelines.

4.3.4 Sea states

The sea state at Site A was irregular, with significant wave heights of 0.3 to 4 m and large variations in wave heading (Table 4.2). The wave period was calculated to range between 4 and 6 seconds, depending on the wave height. For the short 1.3 km length of pipeline examined, the range of significant wave heights for Pipe A2 was less than for Pipe A1. The sea state at Site B was relatively calm and consistent in comparison to Site A, with smaller wave heights and longer wave (predominantly swell) periods. The wave heading at Site B remained oriented in a head or stern direction due to the gimbaling capability of the lay tower. The longer wave period at Site B combined with the slower average lay rate resulted in a similar number of pipeline motions to those at Site A.

4.4 OBSERVED PIPELINE MOTIONS

4.4.1 Motions at lay ramp

For Site A, the vessel motions at the lay ramp were calculated in OrcaFlex, which is a commercial software package for numerical analysis of the dynamic response of offshore systems (Orcina 2009). The response amplitude operators (RAOs) of the vessel were used to obtain lay ramp motions for given wave characteristics. The calculated lay

ramp motions were relatively large for Pipe A1 due to the stern location of the lay ramp and higher sea state. The in-phase vessel heave and pitch resulted in vertical pipe motions at the lay ramp of up to 3 m. The Pipe A2 motions at the lay ramp were limited to about 0.5 m, illustrating the highly non-linear relationship between vessel motions and wave height. For Site B, the combination of smaller wave heights, the central location of the lay ramp, and the live gimbaling ability resulted in much smaller lay ramp motions compared to Site A. However, due to the deeper water depth and longer wave period at Site B, the transfer of pipe motions at the lay ramp to those at the touchdown zone is different.

4.4.2 Motions at touchdown zone

ROV video footage at each site showed pipeline motions in the vicinity of the touchdown zone. The ranges of pipe motion for the two pipelines surveyed are shown in Figure 4.4. Pipe A2 was surveyed during beam and quartering seas with wave heights between 1 to 1.5 m. The observed pipe motions ranged from about 0.05 to 0.2D in the vertical and horizontal directions, peak to peak.

Pipe B1 was surveyed at two locations along the pipeline during stern seas with wave heights of 1.4 and 2 m. Brief plan view footage of the touchdown zone indicated minimal lateral pipe motions. For the 1.4 m waves, the vertical pipe motions increased from about ±0.05D at the mean touchdown point up to ±0.1D near the front of the touchdown zone (including pipe-seabed separation). At 10 m and 15 m in front of the mean touchdown point, the pipe remained suspended above the seabed and vertical motions increased to ±0.25D and ±0.5D, respectively. Even for the relatively minor increase in wave height to 2 m, the vertical pipe motions approximately doubled in amplitude.

4.5 OBSERVED FIELD EMBEDMENT

4.5.1 Normal lay

The as-laid pipe embedment was calculated based on 5-point ROV cross-profiler scans. Nominal values represent the pipeline embedment relative to the far-field seabed elevation, and local values represent the pipeline embedment immediately adjacent to the pipeline, as defined in Figure 4.5. Local embedment is greater than nominal embedment when seabed heave is present; but is less when a trench surrounds the

pipeline. Running averages of the nominal and local pipeline embedment for a 50 m length of pipeline (i.e. 30 data points for Site A and 50 data points for Site B) are presented in Figure 4.6. For all pipelines, the local embedment was greater than the nominal embedment except for a few locations where trenches formed adjacent to the pipeline. The magnitude of local embedment relative to the nominal embedment increased with pipe weight.

There are several sources of variation in the embedment data, linked to changes in water depth, lay tension, seabed conditions, and sea state. A key component of interest in this study is the embedment variation linked to the sea state, which represents long sections (several hundred meters) of the route. This variation reduced with increasing pipe weight. There is also a local scatter component, or noise, which reflects (i) the precision of the cross-profiler scanning system and (ii) variations in the seabed surface elevation, or roughness. This was most relevant for Pipe A1 due to the heavily pockmarked seabed at Site A. A third component was detected at Site B as a periodic variation in embedment with a frequency linked to the intermittent payout process. During welding the stationary touchdown zone is exposed to more cycles of motion compared to the advancing touchdown zone during pipe payout. This enhances the nominal embedment and reduces the local embedment. This effect can be discerned in the close-up views of Figure 4.6 showing 10-point (i.e. 10 m) averages of the cross-profiler data, where a periodicity of 25 m is evident. This periodic response was less regular for the heavier Pipes B2 and B3, and was undetectable for Pipe A1 which may be due to the larger noise component from the seabed roughness and the greater influence from the (highly variable) sea state. The latter effect led to convergence between the nominal and local embedment, or the beginning of the transition from a heaved seabed to a trenched seabed. The effect of the sea state on the embedment for Pipe A1 is further detailed in Westgate et al. (2010a).

4.5.2 Downtime events

There were several locations along the pipeline routes where pipe laying was interrupted for in-line tee and flowline termination assembly connections, abandonment and recovery events, equipment repairs or weather-related downtime. For convenience, these are all referred to as ‘downtime events’, i.e. downtime relative to the steady advancement of the vessel (and touchdown zone) during normal pipe lay. These can be identified in Figure 4.6 where the nominal embedment increased significantly over very

short (< 100 m) sections of the route. Example embedment profiles during the longer downtime events (more than a few hours) are shown in Figure 4.7. Through these zones, the nominal pipe embedment increased significantly relative to the seabed heave, eventually forming a trench adjacent to the pipe with vertical and lateral dimensions of up to 2D. A detailed illustration of this process is presented in Westgate et al. (2009) for Pipe A2. In that study, observations of pipeline embedment during the final pipe laydown sequence were presented, including the final phase of lowering the head of the pipeline onto the seabed using a chain. Observed values of static embedment (with and without the catenary force), normal lay embedment, and downtime embedment are all quantified in detail, the results of which corroborate those reported here.

At Site A, the downtime events were up to several hours in duration, while at Site B the events were up to several days in duration. Figure 4.8 shows the peak nominal embedment for each event. Interestingly, the lighter pipes exhibited the greatest embedment overall. The duration of the event, rather than the sea state, appeared to have the greatest influence on embedment but only for the lighter pipelines. The maximum embedment for the heavier pipelines was consistently just less than one pipe diameter.

Each pipeline was exposed to several thousand cycles of pipe motions in the touchdown zone during the downtime events (based on the event duration and the wave period). This represents one or two orders of magnitude more pipe motions compared to normal lay conditions. An even longer duration of motion (several months), as observed for SCRs, can result in nominal embedment to a depth of several diameters (Bridge & Howells 2007).

4.5.3 Sleeper crossings

At Site B, sleepers were employed to control lateral buckling of the pipelines. Two of the pipelines (Pipes B1 and B2) included enlarged diameter buoyancy sections at the sleeper crossings to minimize the pipeline embedment in the touchdown zones. These ultra-lightweight pipe sections were 200 m in length and had a nominal bearing pressure of about 0.03 kPa. Examples of the pipeline embedment for the standard and ultra-light pipe sections are shown in Figure 4.9. Slight differences in embedment are exhibited either side of the sleeper, with a greater maximum embedment occurring on the leading (vessel) side of the sleeper. The ultra-lightweight pipe sections attain embedment values

of ~ 0.1D, which is much greater than the pipe weight alone would create. This suggests that dynamic lay effects have a greater influence as pipe weight reduces.

The sleeper crossing process has been examined in detail in another study (Westgate et al. 2010b), which presents numerical analyses showing the basis for the slight asymmetry observed. The observations suggest that both dynamic lay effects and the sleeper crossing process itself should be considered in assessing pipeline embedment adjacent to sleepers, since this has an important influence on the lateral buckling response which the sleeper is intended to control.

4.5.4 General observations from field data

From the illustrations presented above, supported by further analysis detailed in Westgate et al. (2009, 2010a, 2010c), the lay rate has a significant effect on as-laid embedment, as shown in simplified form in Figure 4.10. The local embedment is greatest, relative to nominal embedment (i.e. $w_{local} > w_{nominal}$), when the lay rate is fast (e.g. during pipe payout). This maximum ratio between the local and nominal embedment is about 1.5, supported by other studies (Randolph & White 2008a). This is also the case for very calm seas, when pipe motions are essentially absent. As the duration over which pipeline motions in the touchdown zone increases, the nominal embedment increases relative to the local embedment, eventually converging ($w_{local} = w_{nominal}$). This convergence rate increases with sea state. If the duration of pipe motions continues (e.g. during downtime events), the nominal embedment exceeds the local embedment, creating a trench around the pipe ($w_{local} < w_{nominal}$). This response appears to be independent of the sea state for the cases studied in this paper, although some nominal amplitude vessel motions are required to induce the pipe motions in the touchdown zone.

4.6 THEORETICAL AND NUMERICAL ANALYSIS

The static pipe embedment was calculated for each of the 5 pipelines using an iterative method combining the bearing capacity solution of Merifield et al. (2009) (which accounts for enhanced soil buoyancy due to local heave) with an approximation of the standard catenary solution (Randolph & White 2008a). Figure 4.11 shows the predicted static pipeline embedment for each of the pipes at Site A and Site B, based on the intact shear strength and static lay parameters. Included in the plot are the mean nominal

embedment values during normal lay conditions as well as the peak nominal embedment values for each downtime event. Dynamic embedment factors, f_{dyn}, have been back-calculated using the usual definition: i.e. $f_{dyn} = (w/D)_{as\text{-}laid} / (w/D)_{static/intact}$, where $(w/D)_{static/intact}$ is calculated using the submerged pipe weight with the static catenary force concentration and the intact shear strength. The resulting f_{dyn} values span the range of published values, ranging from 1.5 to 4 for Site A and from 4 to 7 for Site B. These values increase with increasing sea state and reduce with increasing pipe weight. The nominal embedment that occurs during downtime events is far greater: the f_{dyn} values for these conditions range from 8 up to 60, also reducing with pipe weight.

By considering the embedment mechanisms individually, the key parameters used in the bearing capacity and catenary solutions can be adjusted to reflect the individual contributions from the mechanisms that are lumped into the dynamic embedment factors. The most important parameters are the soil shear strength and (dynamic) catenary contact force, but calculations may also include adjustment of soil buoyancy effects due to the changing shape of the seabed heave (including reduced local embedment) and reductions in the bearing capacity of the soil due to combined V-H loading. The key input parameters – undrained shear strength and vertical pipe-soil load – have been examined in detail in this study.

4.6.1 Operative undrained shear strength

The soil around the pipe undergoes softening during pipeline motions, reducing in shear strength from the intact value towards a remolded value. The progression from the intact to the remolded state can be assessed by considering the cumulative shear strain of the soil on a cycle-by-cycle basis, similar to cyclic strength assessments used in calculations of offshore foundation capacity (Andersen 1991). Cyclic T-bar tests are commonly used to assess the remolded strength of soils, and can also indicate the rate of softening with disturbance. Typically around 10 cycles of vertical T-bar motion are sufficient to fully remold most clays (White et al. 2010, Gaudin & White 2009). Figure 4.12 shows the cyclic reduction in strength recorded near the soil surface for two cyclic T-bar tests carried out in kaolin clay in a geotechnical centrifuge. During one test the T-bar remained embedded in the soil, while during the other test the T-bar was extracted from the soil on each upstroke. It is clear that repeated separation of the T-bar from the soil surface increases the rate and magnitude of strength degradation, which is attributed to entrainment of water from the free surface. Similar observations have been made

from offshore cyclic T-bar tests conducted in the upper 0.5 m of the seabed (Low et al. 2008).

The failure mechanism around an embedded T-bar penetrometer extends about 1.5 diameters in the direction of the movement (Martin & Randolph 2006, Zhou & Randolph 2009). Due to the shape similarity of pipes and T-bars, 1.5 diameters of cumulative pipe movement might create the same level of remolding in the surrounding soil as one pass of a T-bar penetrometer (Cheuk & White 2011). For small amplitude movements of a pipe, the tendency will be for some soil distant from the pipe to be exposed to a lower level of damage than during the full passage of a T-bar, so this value is likely to be an underestimate.

For typical pipeline motions occurring in the touchdown zone during laying, with peak-to-peak amplitudes 0.05D to 0.25D, one cycle of pipe movement would then be equivalent to 1/7.5 to 2/3 of a T-bar pass (or 1/15 to 1/3 of a T-bar cycle). A very approximate assessment would therefore be that 30 to 150 cycles of pipe movement would be a minimum number required to fully remold the surrounding soil. These numbers of cycles can easily be surpassed for typical pipe lay rates, suggesting that normal lay conditions have the potential to soften the seabed soil to a fully remolded state.

4.6.2 Catenary force

Adjusting the input soil strength in the bearing capacity solution alone ignores the effects of the dynamic catenary response. The vessel motions lead to static changes in geometry of the pipeline, with the touchdown point translating along the pipeline, but also dynamic axial and flexural waves that travel along the suspended pipeline (Callegari et al. 2003). These lead to combined static and dynamic changes in tension and in the contact force within the touchdown zone. The dynamic component of the catenary force can be quantified using the non-dimensional dynamic force ratio V_{dyn}/V_{static} where V_{dyn} is the maximum dynamic catenary force and V_{static} is the maximum static catenary force. The non-linear soil model in OrcaFlex (Randolph & Quiggin 2009) was used to calculate V_{dyn}/V_{static} ratios for the extreme lay configurations, shear strengths, and sea states for each pipeline. The range in values of this ratio was surprisingly narrow across a relatively wide range of input parameters, with values between 1.4 and 1.5 calculated at the two sites for moderate sea state

conditions. For higher sea states, the ratio increases up to $V_{dyn}/V_{static} > 2$ at Site A. Although wave heights up to 2.5 m were recorded at Site B, the maximum V_{dyn}/V_{static} ratio was less than 1.6 due the heavier pipelines. Since the maximum pipeline contact force reduces as the seabed stiffness reduces, using the remolded strength in the bearing capacity calculation reduces the dynamic and static contact forces, and their ratio. For this study, V_{dyn}/V_{static} values between 1.2 and 1.5 were calculated for remolded soil strengths, also increasing with sea state.

4.6.3 Comparisons of calculated and observed embedment

The following sections illustrate how the operative shear strength and the changing catenary force can be used in the bearing capacity and standard catenary solutions to provide more accurate calculations of as-laid embedment. As noted previously, comparison of the observed mean embedment, $(w/D)_{as\text{-}laid}$, and the calculated embedment $(w/D)_{static/intact}$, (i.e. calculated using the intact soil strength and the static catenary V/p) leads to back-calculated dynamic embedment factors in the range 1.5 to 4 for Site A and 4 to 7 for Site B.

Predicted embedment using fully remolded soil strength: $(w/D)_{static/remolded}$

The fully remolded shear strength gradients from the two sites (Table 4.1) were substituted into the bearing capacity solution to calculate the pipeline embedment. The calculated values for each pipeline are shown on the nominal embedment histograms in Figure 4.13. The histograms are based on the complete datasets, filtered only for downtime events and sleeper crossings. Therefore the distribution shown in the histograms includes the periodic variation in embedment due to the lay process, and noise in the data resulting from seabed undulations where relevant. For Pipe A1, the embedment calculated using the remolded soil strength and the static catenary force ($(w/D)_{static/remolded}$) is about twice the embedment calculated using the intact soil strength, but falls short of the mean observed values. For Pipe B1, $(w/D)_{static/remolded}$ is also less than the mean, but closer to the majority of observed values. The $(w/D)_{static/remolded}$ value for Pipe A2 (histogram not shown) was calculated to be 0.48 – matching the mean observed value of $(w/D)_{as\text{-}laid} \sim 0.5$ that was estimated visually from the as-laid video footage. For the remaining heavier Pipes B2 and B3, $(w/D)_{static/remolded}$ matches the observed values well, slightly overpredicting the mean $(w/D)_{as\text{-}laid}$.

For the lighter pipe at Site A, back-calculated f_{dyn} values using this embedment calculation method (i.e. $f_{dyn} = (w/D)_{as\text{-}laid}/(w/D)_{static/remolded}$) are between 1 and 2.5, increasing with sea state. For the lighter pipe at Site B, as well as the heavier pipeline at Site A, f_{dyn} values are between 1 and 1.5, also increasing with sea state. This range is narrower than the range back-calculated using the more common definition of $f_{dyn} = (w/D)_{as\text{-}laid}/(w/D)_{static/intact}$, showing that the use of remolded soil strength provides a systematic improvement in the calculated embedment. However, as the calculated embedment remains below the mean for the lighter pipes, additional embedment mechanism(s) must be present – including the dynamic catenary force.

Predicted embedment using fully remolded soil strength and dynamic catenary force: $(w/D)_{dynamic/remolded}$

The pipe embedment was recalculated for each site considering both the fully remolded strength in the bearing capacity solution and the dynamic pipe-soil contact force in the catenary solution. The resulting embedment values are shown in Figure 4.13. For Pipe A1, a separate calculation was performed for each 1 m increment in wave height, but using dynamic force ratios (V_{dyn}/V_{static}) based on the intact soil strength since the difference between the intact (10 kPa/m) and remolded (3.3 kPa/m) strength gradients has a relatively small effect on this ratio. This approach captured a wide range of observed embedment values, spanning the mean embedment ±1 standard deviation. For Pipe B1, embedment was calculated using the dynamic force ratios based on the remolded strength due to the large difference between the intact (50 kPa/m) and remolded (5 kPa/m) strength gradients. The range of calculated embedment for Pipe B1 matches the mean observed embedment well, with back-calculated f_{dyn} factors (defined as $(w/D)_{as\text{-}laid}/(w/D)_{dynamic/remolded}$) around 1. However, this same approach over-predicts the embedment of pipes B2 and B3.

Predicted embedment using operative soil strength and dynamic catenary force

By considering such variables as the lay rate (including its periodic variation due to the lay process) and the wave period – two parameters that can be estimated reasonably accurately in advance of actual installation –the likely degree of soil remolding during pipe lay can be estimated in order to assess dynamic pipeline embedment more precisely. For example, the 5-minute payout phase for the pipelines at Site B resulted in intermittent sections of the seabed being exposed to only a few cycles of vertical pipe

motion, which may have only partially remolded the soil. Considering the likely degree of remolding occurring during each phase, appropriate shear strength gradients and their respective V_{dyn}/V_{static} ratios were adopted. The fully remolded gradient was adopted for the longer welding phase while the intact gradient of 20 kPa/m was adopted for the brief payout phase, given the very low number of cycles of motion during payout and considering the average intact strength at the as-laid pipe invert elevation. Figure 4.14 shows the embedment profiles for Pipes B1-B3 from the close-up views in Figure 4.6. Included in the plots are the individual cross-profiler embedment data points and the 10-point average embedment. As shown, the calculated embedments for $(w/D)_{dynamic/intact}$ and $(w/D)_{dynamic/remolded}$ provide close matches to the field data, capturing both the lower and upper bound process-dependent pipeline embedment for each pipeline.

4.7 CONCLUSIONS

The as-laid embedment of a seabed pipeline is a critical design parameter, but one that is extremely difficult to predict reliably due to dynamic effects associated with the lay process. Accurate solutions exist for the idealized case of static penetration of a pipeline into the seabed. However, these require additional factors to model real pipe laying. These factors must account for (i) the force concentration in the touchdown zone, caused by the pipe catenary, (ii) the influence of the dynamic pipe movement in the touchdown zone – which includes remolding of the seabed soil (and in extreme cases the development of a trench around the pipe) and (iii) a dynamic amplification of the catenary force, due to the vertical pipe movement.

High quality field data of as-laid pipeline embedment for a total of 5 pipelines from two separate sites comprising soft fine-grained soil in widely differing water depths have been processed in detail, and linked to the relevant metocean conditions and pipe lay geometry. The analysis has shown that the as-laid embedment of a pipeline can be better quantified by careful scrutiny of the geotechnical data close to the seabed surface, in particular the remolded soil strength, as well as through numerical simulations of the lay process. Further theoretical analysis supported by field data for validation is required to provide more general conclusions on the optimal techniques to assess as-laid pipeline embedment. Consideration of additional dynamic embedment mechanisms, such as the effects of the changing seabed geometry and combined V-H loading on bearing capacity, may lead to further improvements in the accuracy of as-laid embedment

calculations. It has also been shown that metocean conditions and the response of the lay vessel can influence the embedment behavior, so there will inevitably be significant uncertainty in forward predictions of embedment, regardless of the accuracy of the analysis techniques.

The key conclusions of this study are:

- Estimates of the pipe embedment made using the intact soil strength and the static catenary force were less than the as-laid observations for normal pipe lay conditions by factors up to 10. Even larger factors were back-calculated for extended downtime periods where the vessel remained at a particular location along the lay route for several hours to several days. This ratio – often termed the dynamic embedment factor, f_{dyn} – varied (between 1.5 to 7) across the 5 pipelines in an inconsistent manner.

- Estimates of the pipe embedment made using the remolded soil strength and the static catenary force resulted in back-calculated f_{dyn} values between about 1 – 2.5 across all pipelines, increasing with reducing pipe weight. This approach is more reliable than the common design practice of estimating embedment based on the intact soil strength coupled with a value of f_{dyn} that aims to capture all dynamic lay effects. One implication from this observation is that the near-surface remolded soil strength profile (including the effects of water entrainment) is a more important design input that the intact soil strength profile. Cyclic T-bar or ball penetrometer tests conducted either at the seabed or in a box core provide the most effective method for establishing this information.

- In cases involving shallow water, harsh metocean conditions, or light pipelines, the dynamic catenary force concentration may also be significant. In the cases analyzed here, the dynamic component typically increased the maximum vertical pipe-soil contact force by 20 – 60%, but up to 100% was calculated for the shallow water site during the most extreme sea state. Estimates of the pipe embedment made using the remolded soil strength and the dynamic catenary force resulted in close matches to the field data in these cases.

- A stop-start payout sequence with intervening welding operations, typical of S-lay and J-lay methods, means that different sections of pipe are subjected to different durations of dynamic lay effects. A periodic variation of embedment

with a wavelength equal to the payout length, which is attributed to this mechanism, was detected at the deepwater site. This variation in embedment was bracketed by calculations that adopted the intact and remolded strength profiles, coupled with the corresponding dynamic force concentration factors. This refinement beyond the more simplistic approach of using the remolded strength and the static catenary force accounts for the dynamic force concentration as well as the varying degree of soil remolding due to the intermittent lay process.

Table 4.1. Soil conditions

Property / Parameter	Site A	Site B
In situ test	CPT	cyclic T-bar
Soil type	silty clay / clayey silt	clay
Submerged unit weight (kN/m^3)	7.5	3
Intact strength profile (kPa)	0 + 10z	0.5 + 50z[a]
Remolded strength profile (kPa)	0 + 3.3z	0 + 5z

a – this intact strength profile only applies to the upper 0.1 m; an average intact strength profile of 20 kPa/m applies over the upper 0.5 m

Table 4.2. Pipeline properties and lay conditions

Property / Parameter	Pipe A1	Pipe A2	Pipe B1	Pipe B2	Pipe B3
Outside steel diameter (m)	0.324				
Steel thickness (mm)	15.9	17.5	20.6	17.5	19.1
Coating thickness (mm)	34.5	2.3	90.5	2.6	2.6
Overall outside diameter, D (m)	0.393	0.329	0.505	0.329	0.329
Submerged pipe weight, p (kN/m)	0.221	0.59[a]	0.373	0.466	0.577
Bearing pressure, p/D (kPa)	0.56	1.80	0.74	1.42	1.75
Water depth (m)	134 - 153		1215 - 1450		
Lay ramp angle (deg)	67.9		84 - 86		82.6
Static pipe tension at seabed (kN)	18 - 20	47 - 54	34 - 57	46 - 79	106 - 112
Route length (km)	25	41[b]	23	13	21
Significant wave height (m)	0.3 - 4	1 - 1.5	0.7 - 2.5	0.6 - 1.7	0.7 - 2.4
Wave heading	Varied	Varied	Stern	Head	Stern
Lay ramp azimuth[c] (deg)	0	0	42 - 105	6-90	90

a – the higher submerged pipe weight of A2 relative to A1 is due to a 3-in pipeline piggybacked to Pipe A2; b – only the final 1.3 km was examined in this study; c – measured from stern to starboard side of vessel.

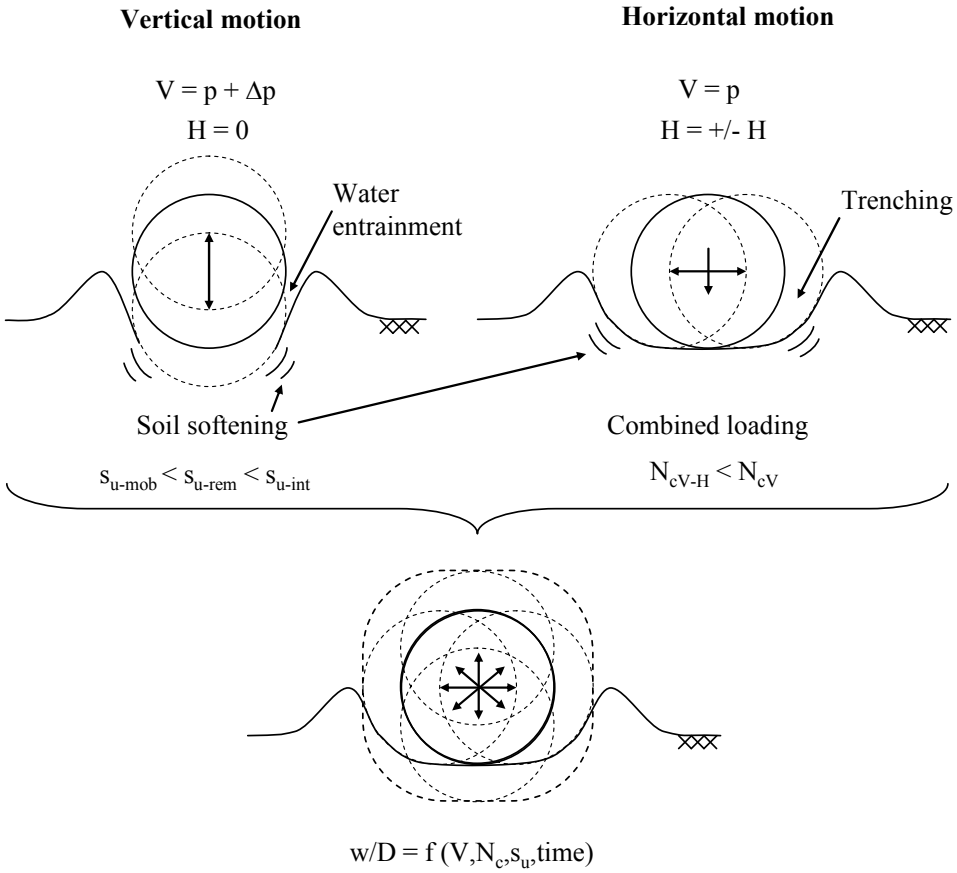

Figure 4.1. Effects of pipe motion during laying

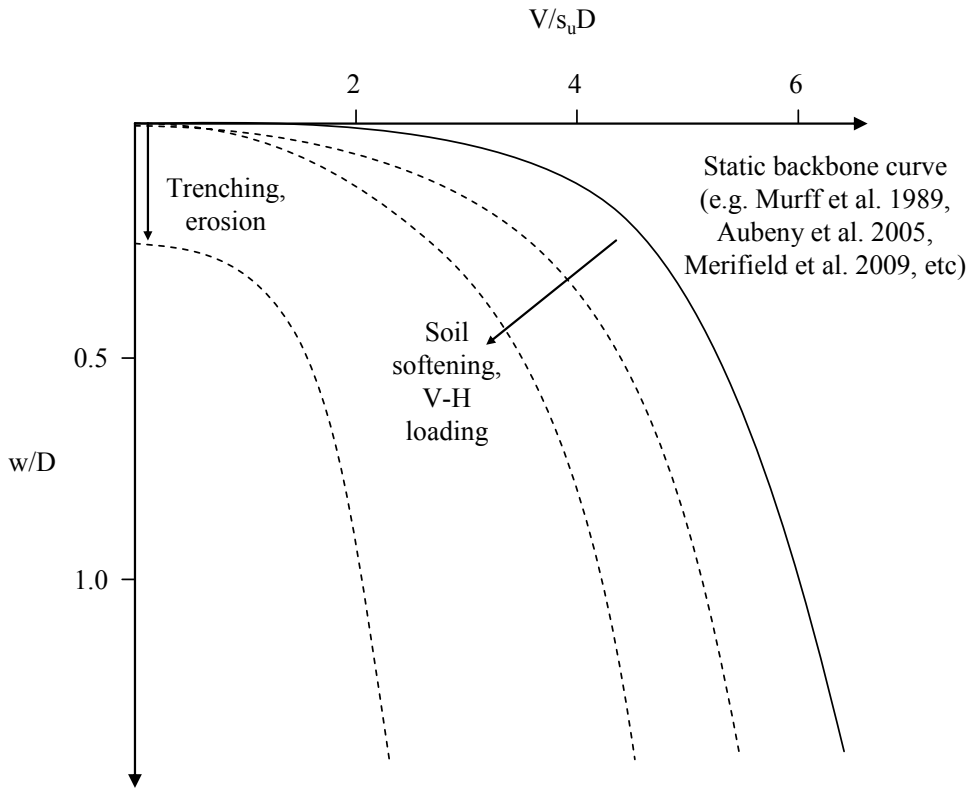

Figure 4.2. Pipe penetration response, with influence of lay effects

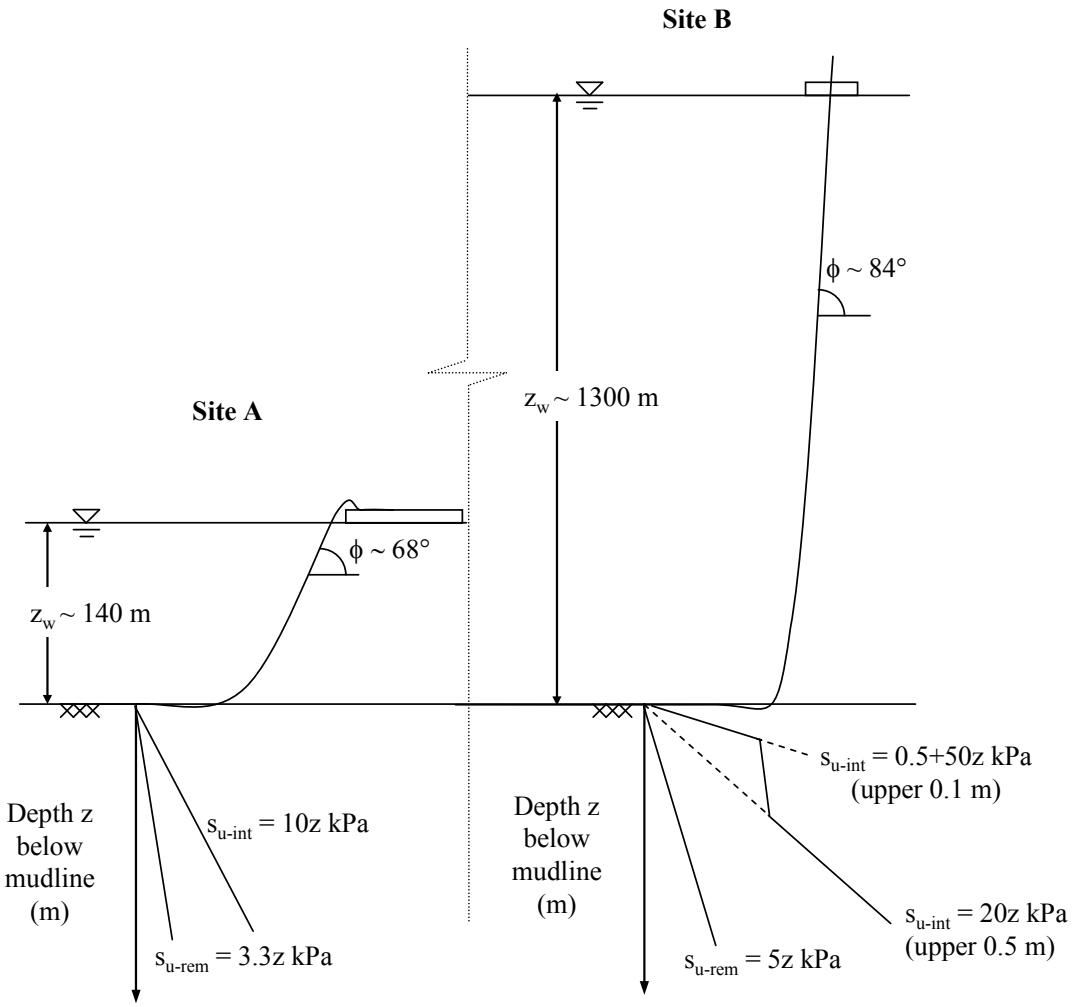

Figure 4.3. Pipe lay configurations and seabed shear strength profiles for Sites A and B (not to scale)

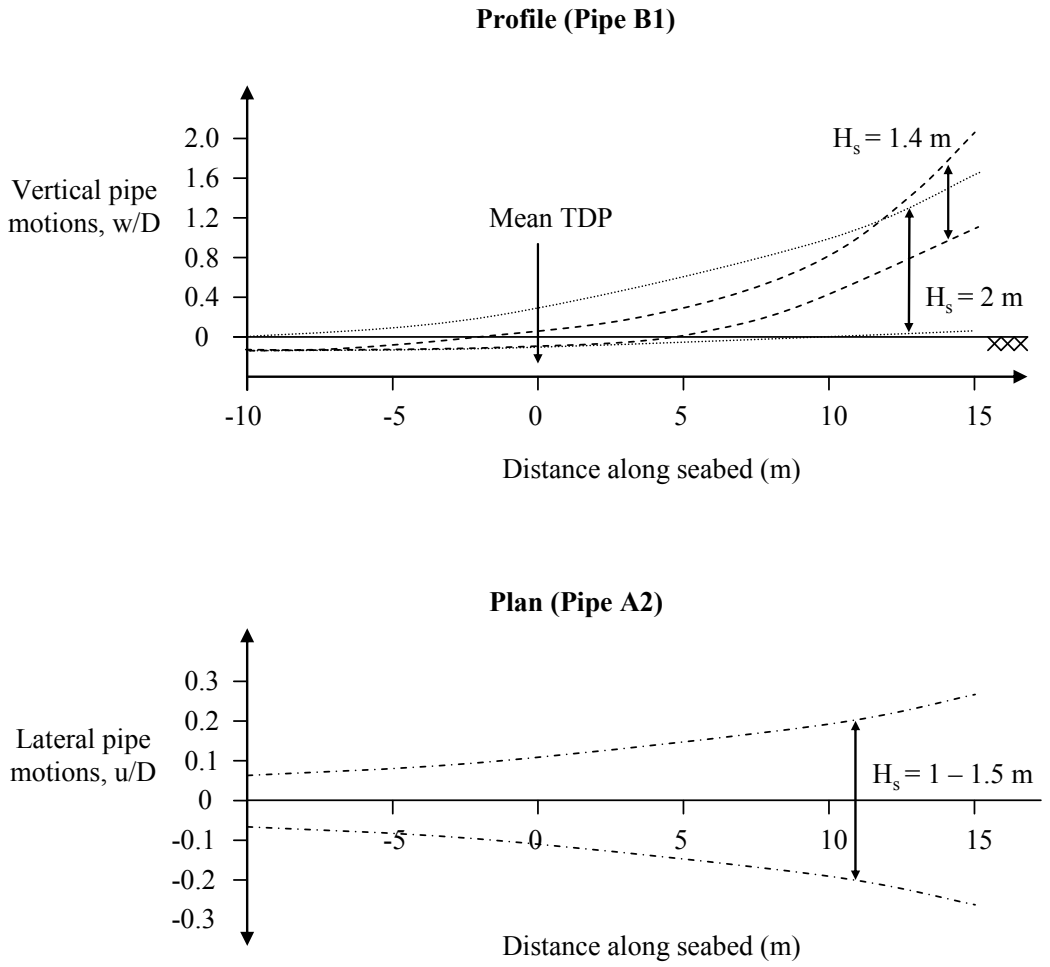

Figure 4.4. Dynamic pipeline motions from ROV video footage

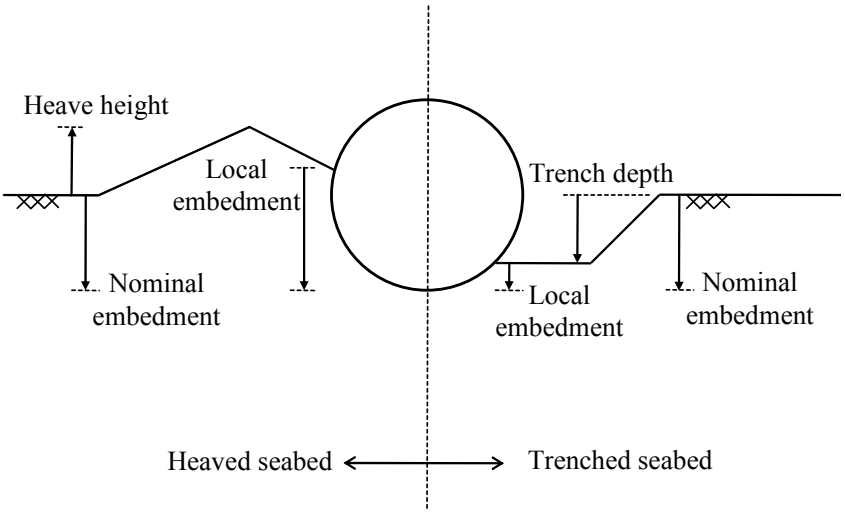

Figure 4.5. Simplified seabed cross-sections

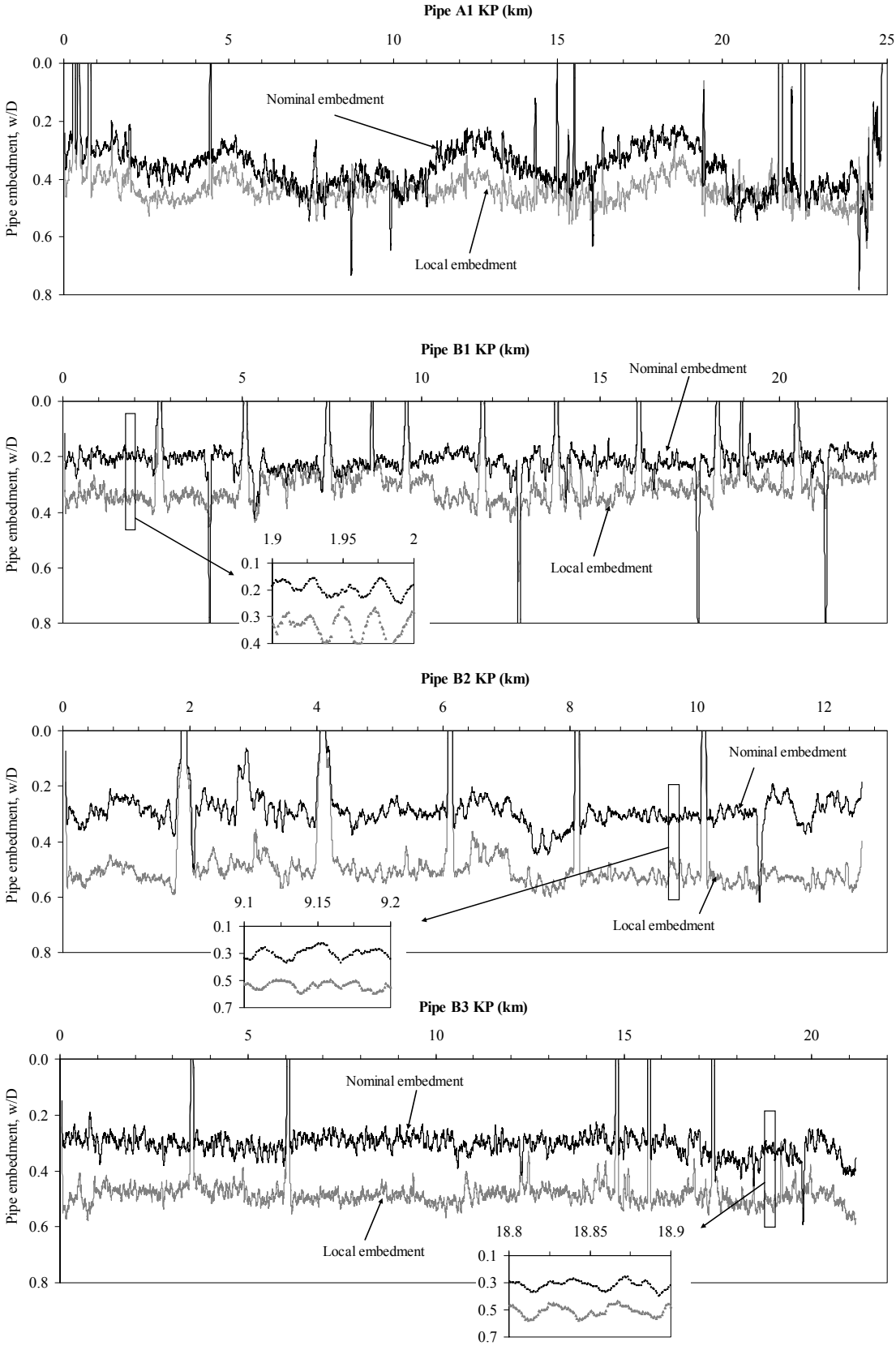

Figure 4.6. Averaged profiles of as-laid embedment

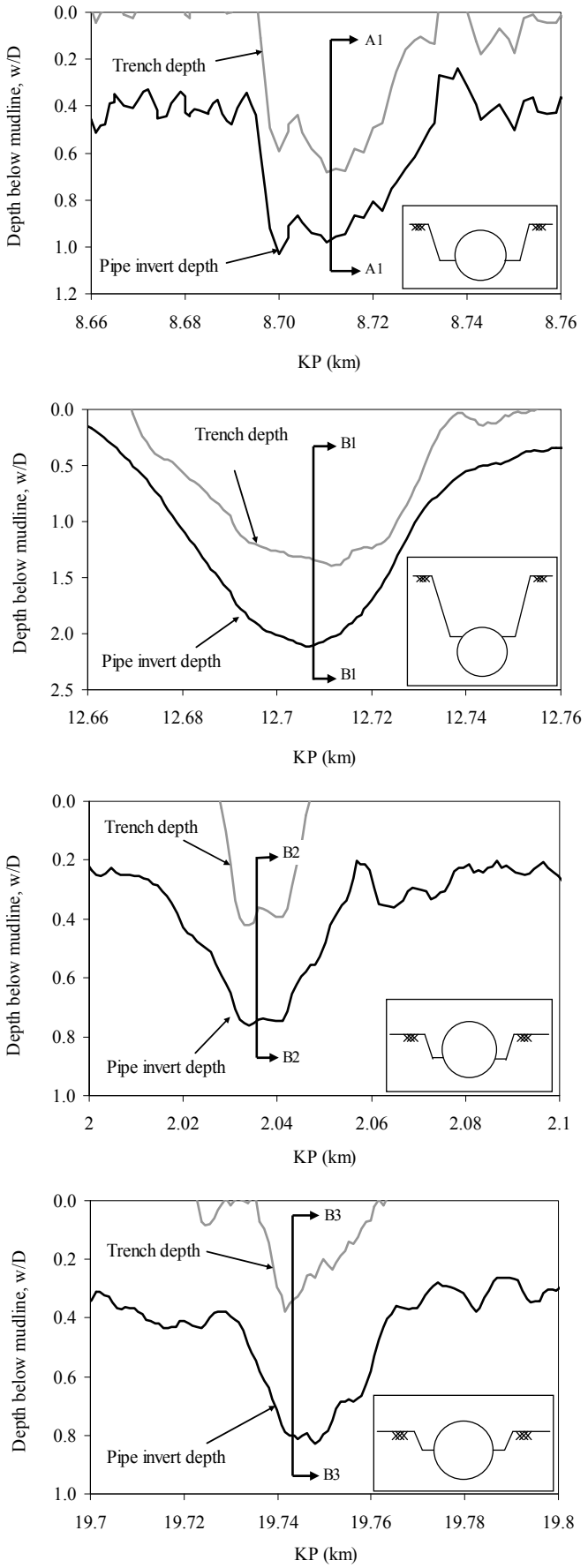

Figure 4.7. Example embedment profiles from downtime events

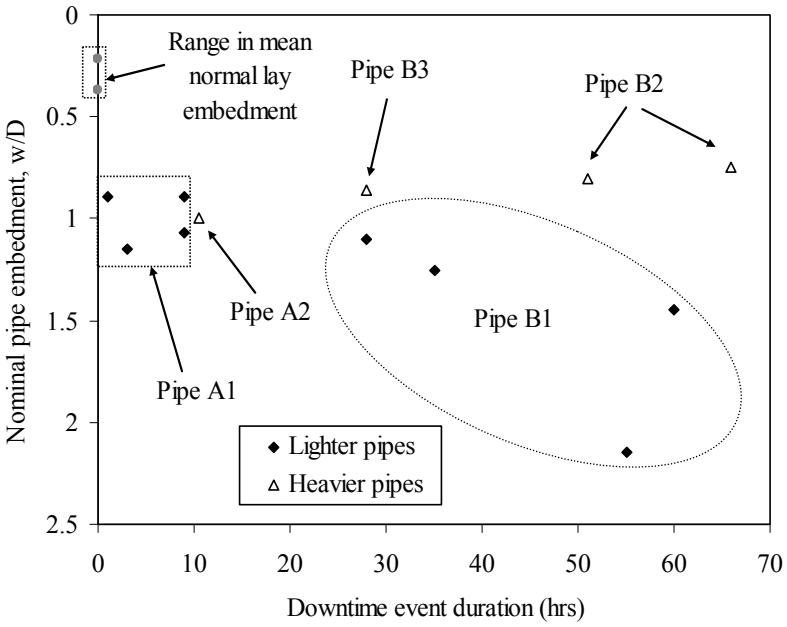

Figure 4.8. Maximum nominal embedment from downtime events

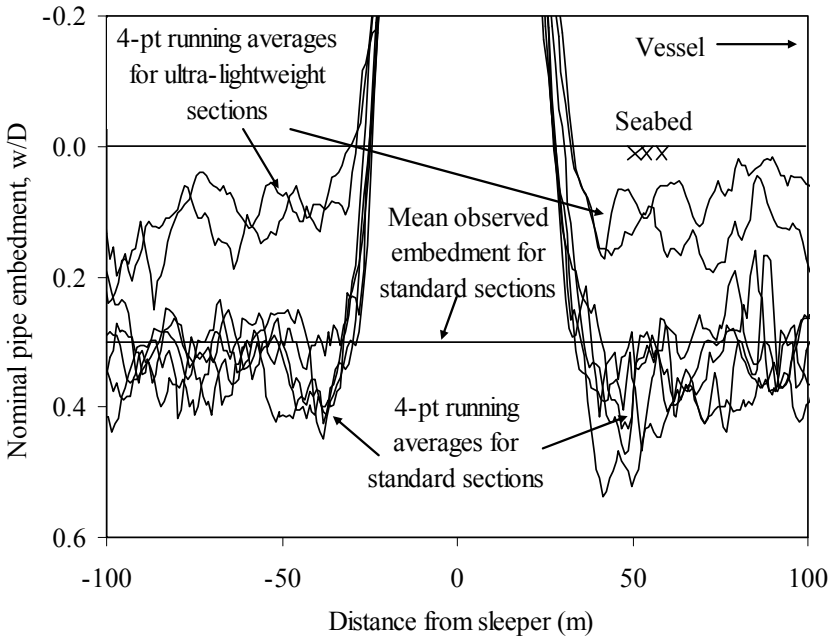

Figure 4.9. Sleeper crossing profiles

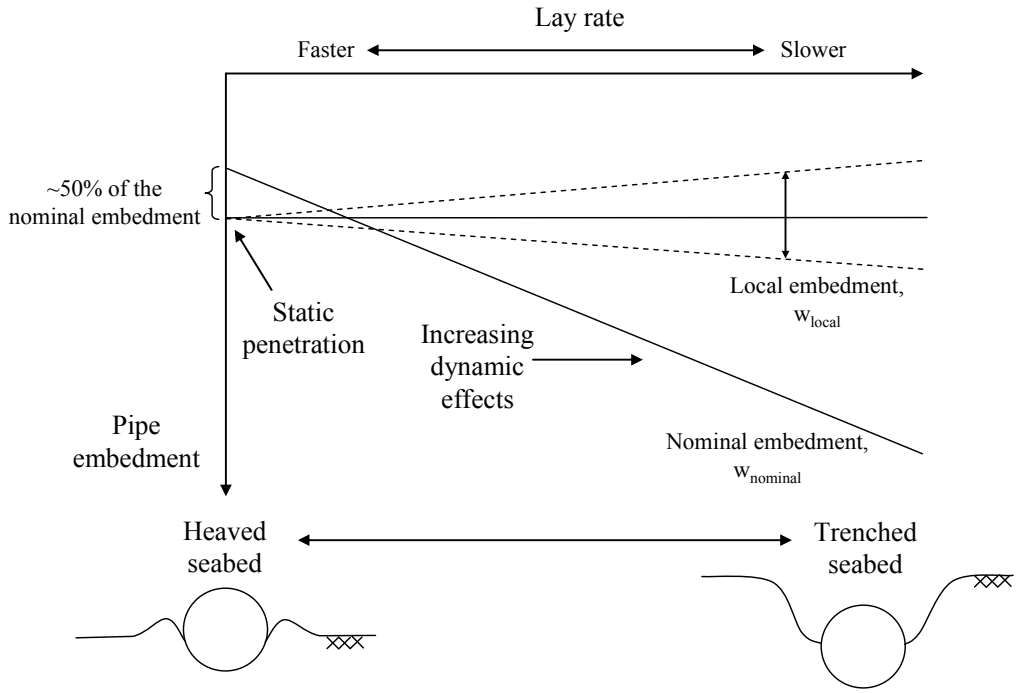

Figure 4.10. General relationship between lay rate and pipeline embedment

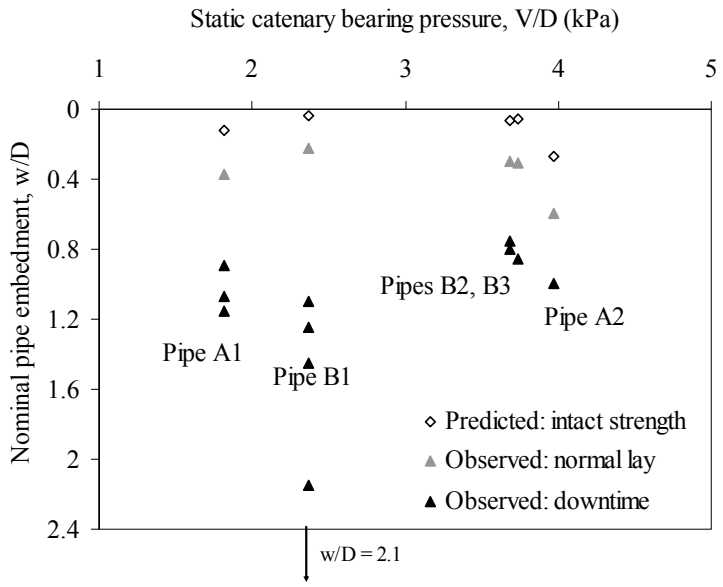

(a) Nominal as-laid embedment

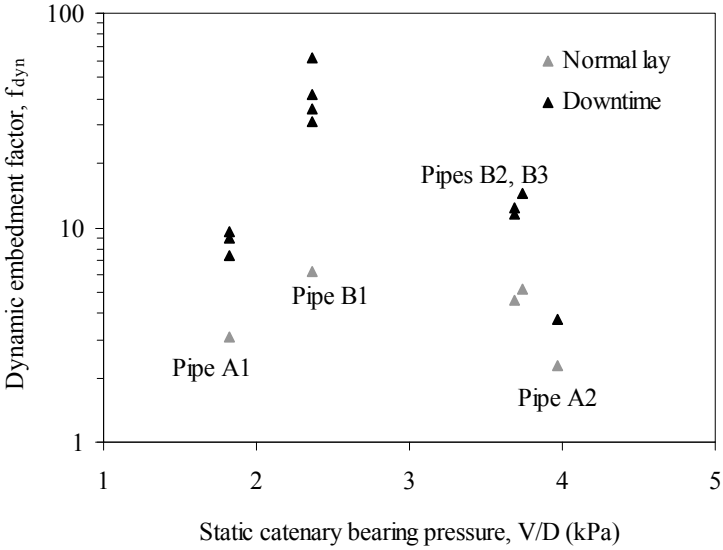

(b) Dynamic embedment factors based on $(w/D)_{static/intact}$

Figure 4.11. Summary of nominal as-laid embedment and calculated static embedment

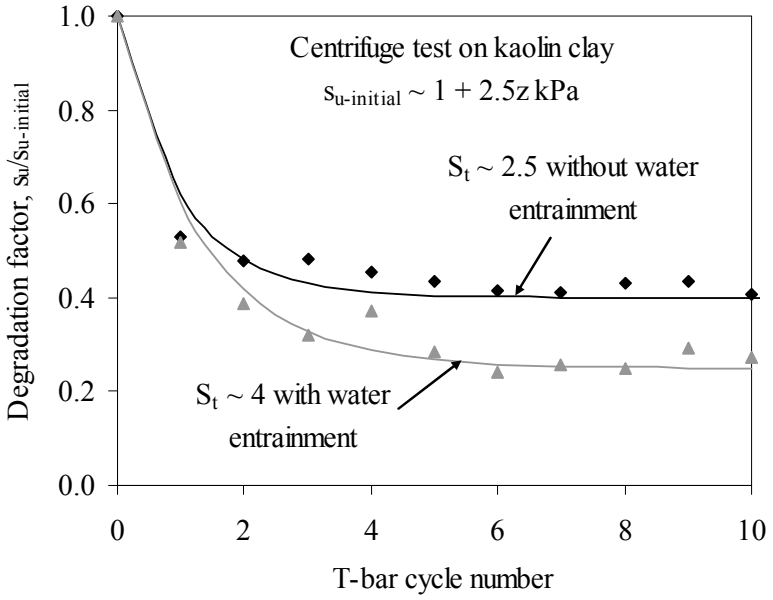

Figure 4.12. Cyclic T-bar tests showing effects of water entrainment

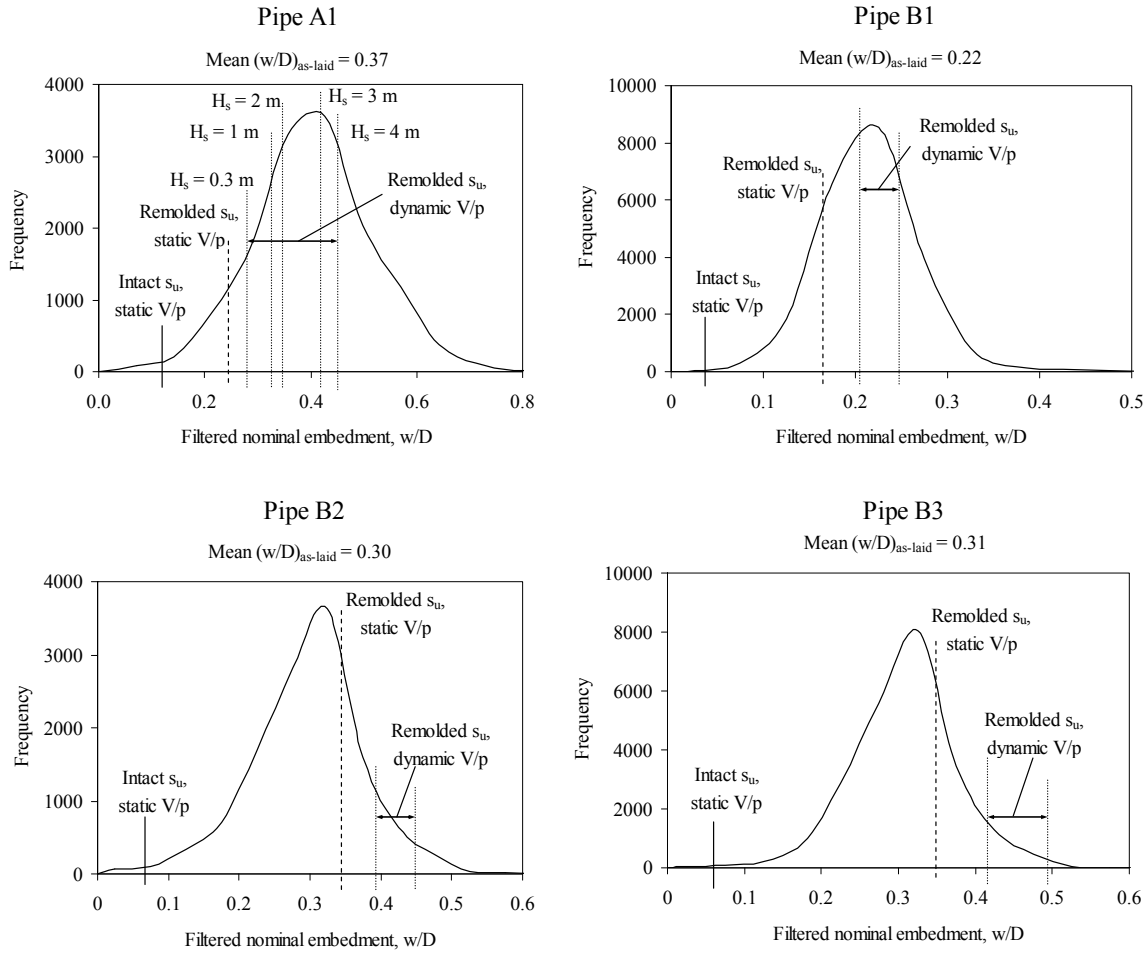

Figure 4.13. Observed embedment histograms illustrating alternative embedment assessment methods

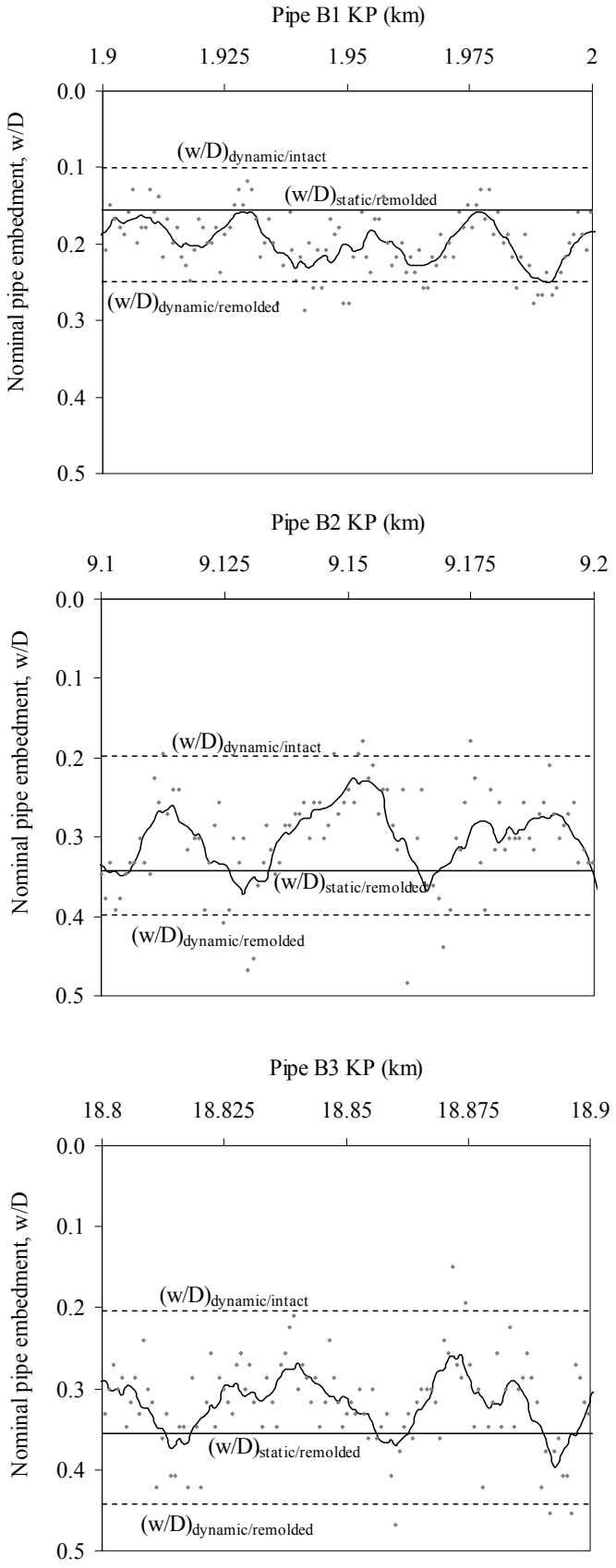

Figure 4.14. Comparison between observed periodic embedment and calculated embedment for Site B

CHAPTER 5. THEORETICAL, NUMERICAL AND FIELD STUDIES OF OFFSHORE PIPELINE SLEEPER CROSSINGS

The paper presented in this chapter is a detailed subset of analyses (for Pipe B3) from the larger set of back-analyses described in Chapter 4. The study illustrates the effects of the vertical seabed stiffness non-linearity and the mechanics of the lay process on a specific application in offshore pipe laying – the sleeper crossing – using theoretical, numerical, and empirical techniques. Theoretical catenary solutions are compared to numerical simulations of linear and non-linear seabed-pipe interaction, and these are compared to field data from the West African site. Numerical tools for pipe laying were developed in OrcaFlex, which allowed the lay vessel to progress forward while paying out the pipeline at a fixed rate, thus a maintaining constant static pipeline catenary geometry but allowing the four-dimensional effect of a 'moving' touchdown zone to be simulated directly. This also allowed the changing catenary forces and their influence on pipe embedment across a fixed seabed object to be quantified.

The analyses in this paper represent a range of simple to advanced techniques that could now be implemented by practicing engineers to investigate a specific pipe-soil-structure interaction problem. While the utility of the analyses is illustrated, it is not claimed that the specific conclusions are generally applicable, but they illustrate the complexity of the interacting mechanisms that govern as-laid embedment – particularly in the vicinity of support structures.

Westgate, Z.J., Randolph, M.F., White, D.J. & Brunning, P. (2010). Theoretical, numerical and field studies of offshore pipeline sleeper crossings. *Proc.2nd Int. Sym. Frontiers in Offshore Geotechnics*, Perth.

5.1 ABSTRACT

Offshore pipelines experience axial stresses due to internal pressure and thermal cycles during start-up and shut-down, leading to the formation of lateral buckles. Pipeline lay routes often include strategically-spaced transverse sleepers, creating a vertical imperfection from which a controlled lateral buckle can be initiated. The as-laid pipeline embedment affects the pipe-soil interaction forces and therefore the buckle initiation response. The potential for increased embedment in the touchdown zones to either side of the sleeper exists, which can cause higher than expected lateral breakout forces. The magnitude of this embedment is difficult to quantify due to dynamic lay effects and changes in catenary forces as the pipe is laid over the sleeper. Theoretical solutions for the touchdown force at a sleeper crossing are presented for the case of an elastic seabed, and are compared to as-laid survey data in soft clay. Static and dynamic numerical analyses are also presented to illustrate the changes in pipe-soil contact force as a pipe is laid across a sleeper. This provides a rationale for asymmetry observed in as-laid embedment profiles and its influence from dynamic lay effects. General guidance is provided for pipeline designers to assist the assessment of pipe-soil interaction forces in the vicinity of sleepers.

5.2 INTRODUCTION

As offshore hydrocarbon developments have progressed into deeper waters, new pipeline design issues have arisen, such as lateral buckling, which occurs due to axial pipe stresses during thermal cycles of start-up and shut-down. This has led to development of lateral buckle mitigation techniques, such as sleepers. Sleepers allow controlled buckles to occur in predetermined locations along the route by creating a vertical imperfection on which the pipeline slides laterally (Sinclair et al. 2009).

In deep water developments where soft fine-grained soils are prevalent, the lay process induces significant pipeline embedment due to dynamic lay effects (Randolph & White 2008a). As-laid field surveys (Lund 2000b, Westgate et al. 2010c) show that pipeline embedment during normal lay conditions in the field can be up to an order of magnitude greater than the predicted static pipeline embedment based on the intact soil strength. Using the remoulded strength in this calculation has been shown to predict embedment closely matching field observations (Westgate et al. 2010c).

Pipeline embedment influences the lateral breakout resistance provided by the seabed soil. Together with dynamic lay effects, the variation in pipe-soil contact force across a sleeper influences the magnitude of pipeline embedment. This can lead to differences in the lateral breakout resistance along the touchdown zones to either side of the sleeper, affecting the pipeline stresses along the buckle.

This study illustrates the variation in pipe-soil contact force in the vicinity of sleepers, and the dependence of the resulting pipeline embedment on the asymmetric and dynamic nature of the lay process. The paper presents results of theoretical analyses used to calculate the pipe-soil contact force and embedment based on the standard catenary solution, and static and dynamic numerical analyses of the lay process. These are compared to as-laid field data for a pipeline installed at a soft clay site in deep water.

5.3 THEORETICAL ANALYSES

Theoretical methods for calculating pipe-soil contact forces during pipe laying are well-established (Lenci & Callegari 2005, Palmer 2009). The governing equation for the response of a pipe being laid on an elastic seabed can be written as:

$$EI\frac{d^4w}{dx^4} - T_0\frac{d^2w}{dx^2} + kw = p \tag{5.1}$$

where E = elastic modulus, I = second moment of area, T_0 = horizontal pipe tension, p = submerged pipe weight, k = seabed soil stiffness, w = pipe embedment, and x = the distance along the pipeline.

The horizontal pipe tension is calculated based on the standard catenary solution as:

$$\frac{T_0}{z_w p} = \frac{\cos\phi}{1-\cos\phi} \tag{5.2}$$

where ϕ = the lay angle, defined as the inclination to the horizontal at the lay ramp departure point, and z_w = the water depth. The horizontal component of tension is constant along the suspended pipeline.

The pipe catenary creates a vertical force concentration at the touchdown zone expressed as the pipe-soil contact force V, normalised by the submerged pipe weight p. The ratio V/p is related to the characteristic length $\lambda = (EI/T_0)^{0.5}$, after Pesce et al. (1998).

5.3.1 The sleeper crossing problem

The as-laid sleeper crossing problem can be idealised as a beam on an elastic seabed due to the small vertical deformation of the pipeline in the vicinity of the sleeper (Figure 5.1).

For the case of a pipeline laid from a vessel, the maximum force concentration V_{max}/p in the touchdown zone may be approximated as (Randolph & White 2008a):

$$\frac{V_{max}}{p} = 0.6 + 0.4(\lambda^2 k/T_0)^{0.25} \tag{5.3}$$

For the case of a pipeline lowered from a horizontal plane above a flat seabed under zero tension, i.e. 'placed', $V_{max}/p = 1$ everywhere along the pipeline due to the absence of the catenary.

The presence of a sleeper of height h above the seabed complicates this condition due to the additional boundary conditions imposed (Figure 5.1). Visual inspection shows that deflection, slope, shear and moment are continuous at x = 0, with deflection w = 0. Similarly, at x = L, w = -h and slope = 0, which allow equation 5.1 to be solved. It is worth noting that for the extreme (though unrealistic) case of $T_0 = 0$, the character of the solution to equation 5.1 changes from a catenary to a beam solution.

Several variations of pipe lay over a sleeper were analysed, increasing in realism and computational effort (Table 5.1). Table 5.2 lists the pipeline properties and lay conditions for these analyses. These correspond to a pipeline for which the lay conditions and as-laid embedment is known (Case 8).

5.3.2 Static pipe lay and placement on linear seabed

Figure 5.2 shows the variation in V/p for the zero tension, pipe placement condition (Case 1) and the as-laid catenary tension of the real case (Case 2). For this geometry and tension there is little difference between the as-laid catenary case with tension and the zero tension placement case, with a maximum V/p equal to 1.38 and 1.5 respectively.

The adopted stiffness of k = 20 kPa for the elastic solutions is consistent with the theoretical pipe penetration prediction of Merifield et al. (2009) for an intact shear strength gradient of s_u = 20 kPa/m (negligible mudline strength intercept) as applicable to the field case discussed later. This stiffness gave a nominal embedment due to the

pipe weight p of w/D = 0.09 (i.e. w = 0.09 pipe diameters) and a maximum embedment due to the catenary contact force V of w/D = 0.13.

Reducing the seabed stiffness in the theoretical solution represents a case where the seabed has softened due to dynamic lay effects. A reduced stiffness of 8 kPa represents a fourfold drop to remoulded conditions, based on a remoulded shear strength gradient of 5 kPa/m as applicable to the field case. This decreases the maximum force concentration by ~10% so the nominal and maximum embedment values increase by less than fourfold to w/D = 0.22 and w/D = 0.27 respectively (Figure 5.3).

These solutions represent symmetric sleeper crossing cases, with the same maximum contact force and embedment on each side of the sleeper. However, the lay process is asymmetric, as illustrated conceptually in Figure 5.4. As the pipe is laid from the lay vessel, it approaches the sleeper with a catenary configuration independent of the sleeper's presence (dotted line). On the trailing side of the sleeper, the pipe lifts off of the seabed as it contacts and rotates over the sleeper (due to the pipe stiffness), causing the touchdown point to move away from the sleeper through the 'uplift zone' (dashed line to left of sleeper). On the leading (i.e. vessel) side of the sleeper, the additional weight of the suspended pipe causes the pipe to embed further compared to the nominal pipe catenary force (dashed line to right of sleeper). This load-unload mechanism results in a similar uplift zone on the leading side of the sleeper. The end result is an asymmetric embedment profile on a real (plastic) seabed (heavy solid line) which exceeds that of an idealised (elastic) seabed (light solid line).

An analysis of the lay process on a non-linear (plastic) seabed will show this asymmetry since the over-loading history will force irreversible embedment. However, the elegant elastic cases allow trends related to the lay tension and seabed stiffness to be explored – in particular the variation in force concentration in the touchdown zones.

Effects of pipe tension

Figure 5.5 shows V/p as a function of the normalised pipe tension $T_0/\lambda p$, for a seabed stiffness of k = 20 kPa. The temporary pipe-soil contact force from the pipe catenary is always greater than the final contact force after the pipeline has crossed the sleeper, with the difference increasing with reducing pipe tension.

For a horizontal tension of 103 kN, the catenary-induced contact force is 1.73 and the final sleeper-induced contact force is 1.38, a reduction of 20%. For the final pipe-

sleeper configuration, the maximum V/p reduces towards a value of 1.5 at zero tension. At this point, the maximum V/p for the catenary is infinite, but rapidly reduces for more realistic values of $T_0/\lambda p$. At high normalised tension values, both conditions converge to V/p = 1.

Effects of seabed stiffness

Figure 5.6 shows V/p as a function of the normalised seabed stiffness $K = \lambda^2 k/T_0$. As the seabed stiffness increases, both the absolute V/p values and the ratio of V/p between the two cases increase. As the stiffness reduces, V/p converges to unity. Normalised stiffness values for soft clay seabeds are typically in the range of K = 100 – 1000, but for very weak remoulded soft clays K can be lower, and for stiffer clays K can exceed 10,000.

5.4 FIELD STUDIES

Variations in pipeline embedment across sleepers were obtained from as-laid field survey data from a development in deep water with a soft clay seabed. The intact undrained shear strength gradient in the upper 0.5 m of the seabed is about 20 kPa/m, with a remoulded strength gradient of 5 kPa/m. The properties and lay conditions for the surveyed pipeline are summarised in Table 5.2. The pipeline was laid from a J-lay vessel with a lay ramp that permitted 3 degree-of-freedom rotational motion, thus minimising effects of the vessel motions on the pipe-soil contact forces.

Profiles of the as-laid normalised pipeline embedment w/D across the sleepers (Case 8) are shown in Figure 5.7, compared to the as-laid theoretical solution for the intact and remoulded strength gradients (Cases 2 and 3).

The mean embedment for this pipeline away from the sleepers was 0.31D. At the sleeper crossings, the embedment ranged from about 0.2D to 0.5D. The leading side of the sleeper exhibited slightly deeper embedment consistent with the lay process discussed in Section 2. The as-laid embedment data showed that the height of the sleeper crown h above the seabed was between 0.9 and 1.0 m, which affects the length of the hanging spans L on each side of the sleeper (Figure 5.1).

The theoretical solution for the intact seabed (Case 2) exhibits the correct shape of the embedment response, but significantly under predicts the magnitude of the embedment and over predicts the length of the hanging spans. If the remoulded strength is used in

the theoretical solution (Case 3), the embedment and span length are closer to the field values, but the asymmetry is absent.

5.5 NUMERICAL ANALYSES

The dynamic riser analysis software, OrcaFlex (Orcina 2009), was used to explore the trends shown in the field data. The first numerical analysis (Case 4) comprised static pipe lay on a linear elastic seabed. Further analyses (Cases 5, 6, 7) show the influence of non-linear seabed stiffness, a reduced strength from remoulding and vessel motions respectively. The idealised pipe properties used in the numerical model are those used in the theoretical analyses (Table 5.2).

5.5.1 Static pipe lay on linear seabed

Figure 5.8 shows the variation in V/p and w/D for the linear seabed (Case 4). The solid line shows the final profile, which matches the theoretical solution from Case 2. The dashed line shows the maximum (temporary) profile exhibited during the lay process (Figure 5.4).

As the pipe catenary approaches the sleeper, the force concentration factor is constant at V/p = 2.1, with a corresponding embedment w/D = 0.16. The final embedment reduces (elastically) to w/D = 0.09, corresponding to the submerged pipe weight. After making contact with the sleeper, V/p reduces as the pipe weight is redistributed to the sleeper and eventually to the seabed on the leading side of the sleeper. The increase in contact force on the leading side (due to the heavier catenary) is 20% higher than that on the trailing side, with a maximum V/p = 2.7. The pipe embedment for this force is w/D = 0.2.

Once the sleeper crossing is completed, the maximum force concentration factor returns to the nominal value of V/p = 2.1, for which w/D = 0.16. For the elastic seabed, the increased V/p has no effect on the final embedment. Although an asymmetric final profile cannot be predicted by the elastic seabed model, the progressive laying simulation of Case 4 shows a maximum V/p profile that is consistent with the asymmetry in the field data of as-laid embedment (Figure 5.7).

5.5.2 Static pipe lay on non-linear seabed

A non-linear seabed with the intact shear strength gradient of 20 kPa/m (mudline strength intercept of zero) was analysed for static pipe lay. The non-linear soil model in OrcaFlex has a stiff unloading response following penetration, thus capturing the effect of a previous overloading event (Randolph & Quiggin 2009). The model also captures increasing pipeline penetration with cycles of vertical loading, simulating the effects of soil softening. Default soil model parameters were used for the static analysis, which were based on intact strength profiles.

Figure 5.9 shows the range in V/p (upper plot) and w/D (lower plot) for static pipe lay across the sleeper on a non-linear intact seabed (Case 5). Also shown is the final force concentration and embedment. An uplift (transient tensile) zone is evident on both the trailing and leading sides of the sleeper, as discussed in Section 2. The final pipe embedment is close to the maximum embedment profile due to the plastic seabed deformation, and captures the asymmetry well.

A second static non-linear case was carried out for the remoulded shear strength gradient of 5 kPa/m (Case 6). The final embedment profile for this case is also shown in Figure 5.9. The weaker penetration resistance due to the lower strength gradient results in deeper pipe embedment. This final 'remoulded' embedment is closer to the mean embedment profile observed in the field and captures the asymmetry.

5.5.3 Dynamic pipe lay on non-linear seabed

Vessel-induced pipe motions result in higher transient contact forces, which (for the non-linear plastic seabed) lead to greater penetration as well as incremental pipe embedment with each cycle.

A dynamic analysis (Case 7) was carried out by adding a regular (Dean stream) significant wave height of H_s = 2 m with a wave period of 13 seconds (to match the field conditions) to the static non-linear Case 5. The vessel and pipe payout advanced at 0.1 m/s, i.e. a lay rate of 360 m/hr. This lay rate corresponds to the time period between welding operations, i.e. the minimum number of cyclic pipe motions in the touchdown zone.

The intact soil strength gradient of 20 kPa/m was adopted as the non-linear soil model accounts for incremental penetration under cyclic motions. Inspection of individual

nodes along the pipeline indicated that the force – penetration response reached near steady-state conditions within the 15 to 20 cycles of pipe motions to which it was subjected. The analysis is therefore not sensitive to the range of lay rate recorded during normal laying operations. This represents a touchdown zone length of about 23 m, which is realistic for this seabed, pipe and lay geometry.

The non-linear soil model parameters were then optimised to match the shape of the field data profiles by reducing the non-dimensional maximum suction resistance factor and increasing the non-dimensional repenetration resistance depth factor (Randolph & Quiggin 2009). Figure 5.10 shows the final embedment profile from this analysis, which provides the best match to the field data. This example illustrates how soil non-linearity and the dynamic aspects of pipeline embedment can be simulated.

5.6 CONCLUSIONS

This study has presented a series of theoretical and numerical analyses showing the variation in pipe-soil contact force and the resulting pipeline embedment in the vicinity of sleeper crossings along offshore pipelines. The results have been compared to field survey embedment data for a pipeline installed at a soft clay site in deep water.

The asymmetry within the pipe-soil contact force profiles across sleepers can only be captured realistically using non-linear seabed models that account for the loading history of the pipe-soil contact force during the sleeper crossing. Static pipe lay analysis using non-linear seabed models and a remoulded shear strength to account for dynamic lay effects provided an embedment profile that generally matched the trends in the field data. A marginally closer match to field observations was obtained using an optimised dynamic pipe lay analysis that simulated incremental penetration due to cycles of vertical pipe movement in the touchdown zone, dictated by the lay rate, sea state, and vessel and pipeline dynamics.

These analysis techniques can be used in pipeline design to determine the range of embedment likely to occur near sleepers, aiding assessment of the pipe-soil response during buckling.

Table 5.1. List of analyses

Case	Analysis	Process	Seabed stiffness/strength	Bottom tension	
1	Theoretical	Placement	Linear / intact	Zero	Increasing realism and computational effort ↓
2	Theoretical	Static lay	Linear / intact	As-laid	
3	Theoretical	Static lay	Linear / remoulded	As-laid	
4	Numerical	Static lay	Linear / intact	As-laid	
5	Numerical	Static lay	Non-linear / intact	As-laid	
6	Numerical	Static lay	Non-linear / remoulded	As-laid	
7	Numerical	Dynamic lay	Non-linear / intact	As-laid	
8	Empirical	Real pipe lay	Real soil	As-laid	

Table 5.2. Pipeline properties and lay conditions

Parameter	Idealised	Field case
Outside diameter, D (m)	0.32	0.32
Steel thickness (mm)	19	19
Bending rigidity, EI (MNm^2)	44	44
Coating thickness (mm)	0	2.6
Submerged pipe weight, p (kN/m)	0.57	0.58
Water depth, z_w (m)	1300	1240-1310
Lay angle, ϕ (deg)	83	82.6
Horizontal pipe tension, T_0 (kN)	103	106-112
Sleeper height, h (m)	0.9	0.9-1.0
Significant wave height, H_s (m)	2	0.7-2.4

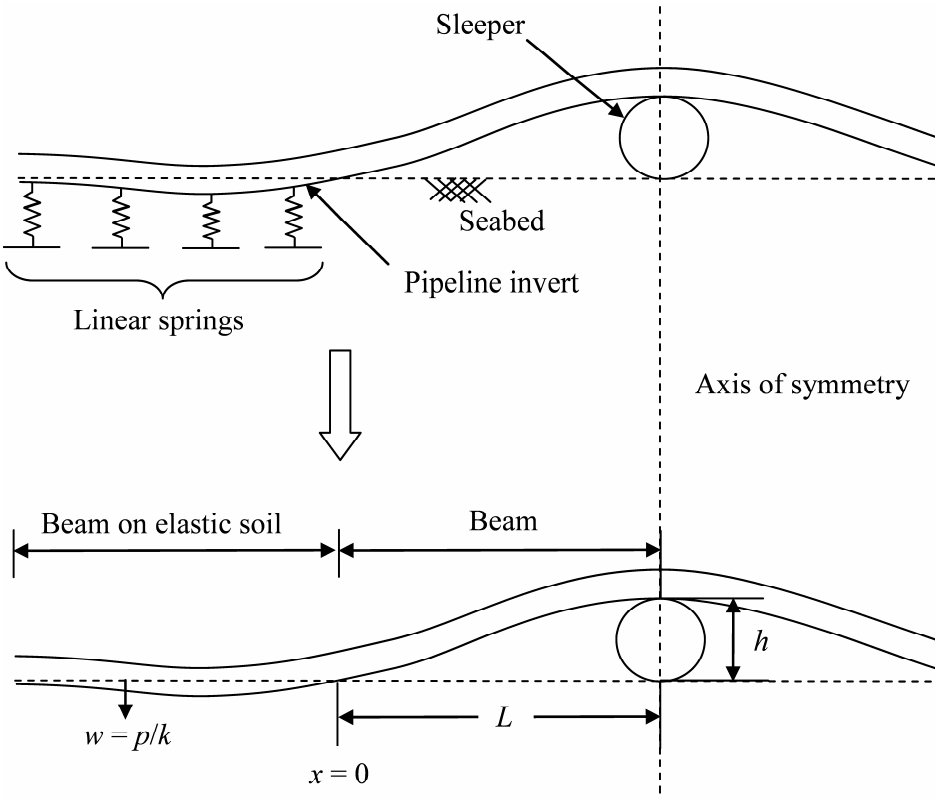

Figure 5.1. Idealised sleeper crossing (vertical scale exaggerated for clarity)

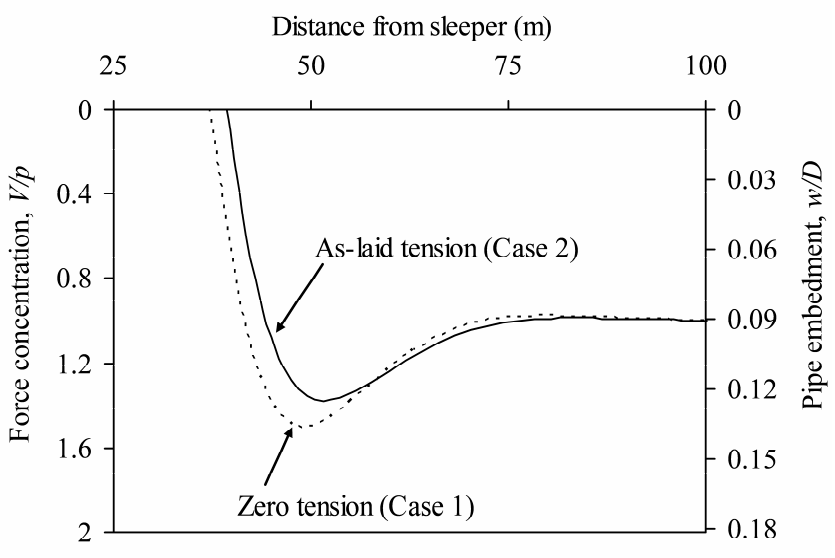

Figure 5.2. Theoretical analyses for intact seabed (Case 1 and 2)

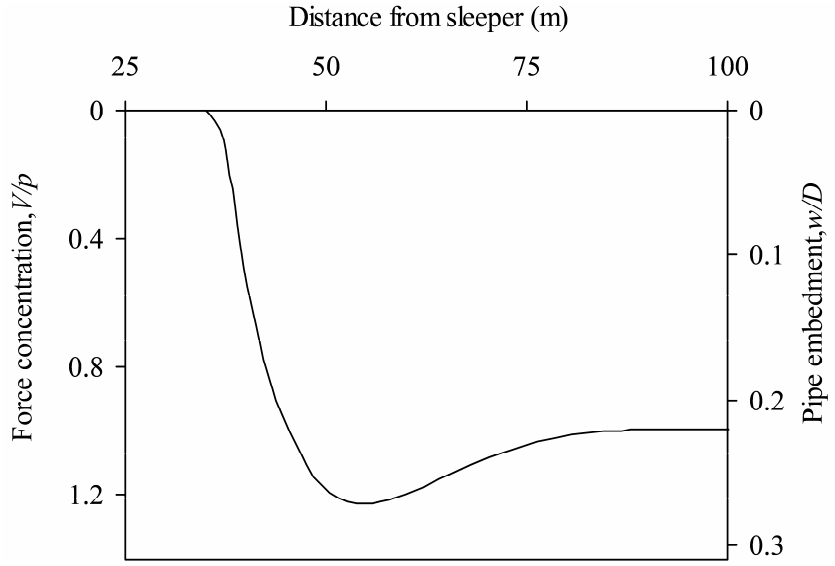

Figure 5.3. Theoretical analysis for remoulded seabed (Case 3)

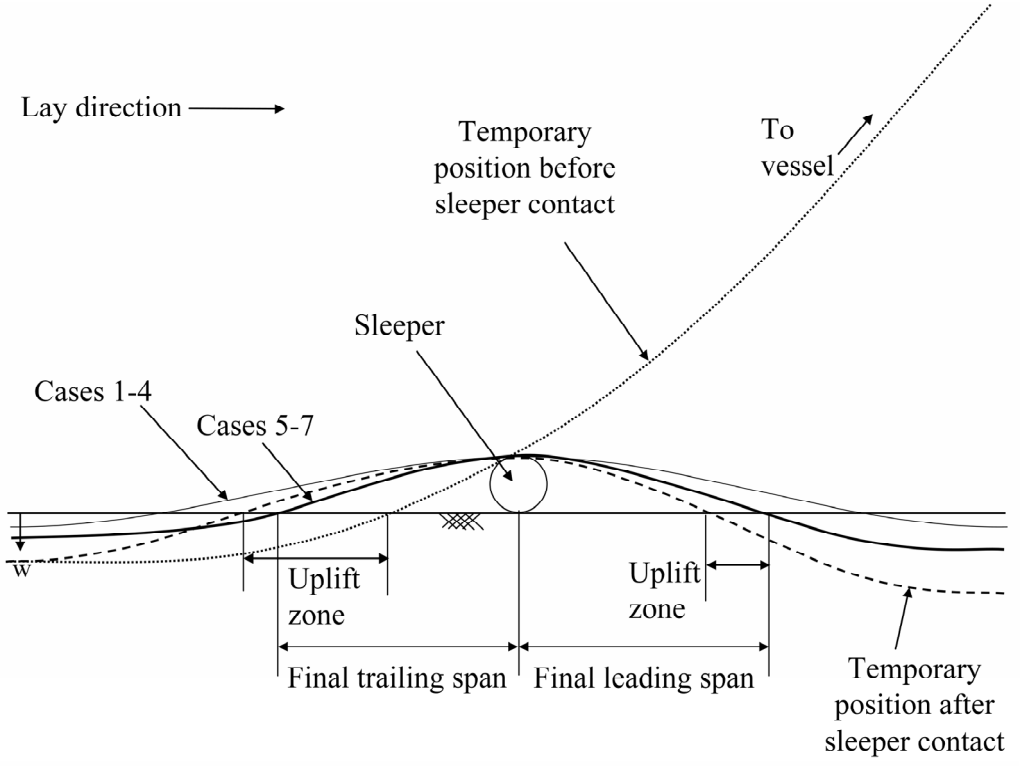

Figure 5.4. Sleeper crossing lay process (vertical scale exaggerated for clarity)

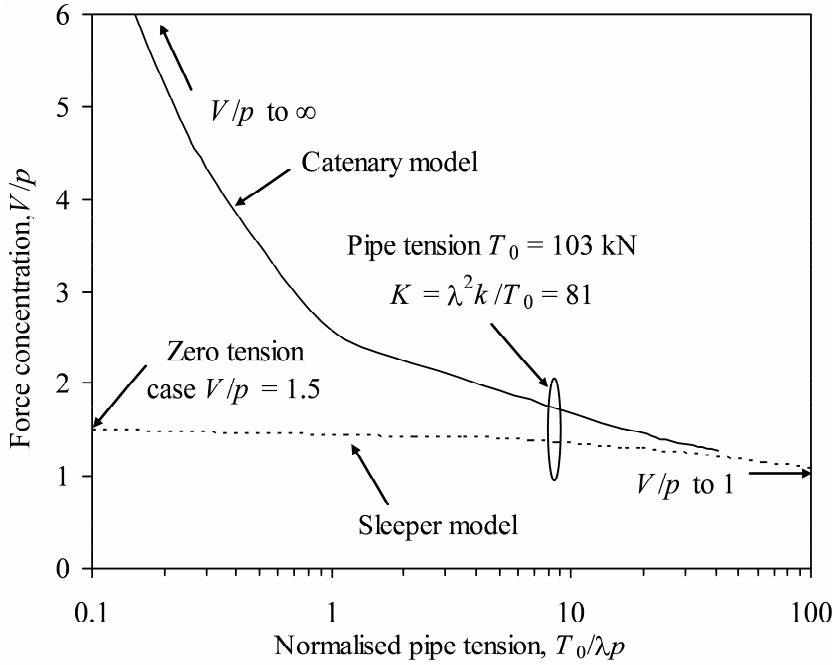

Figure 5.5. Influence of horizontal pipe tension on maximum pipe-soil contact forces

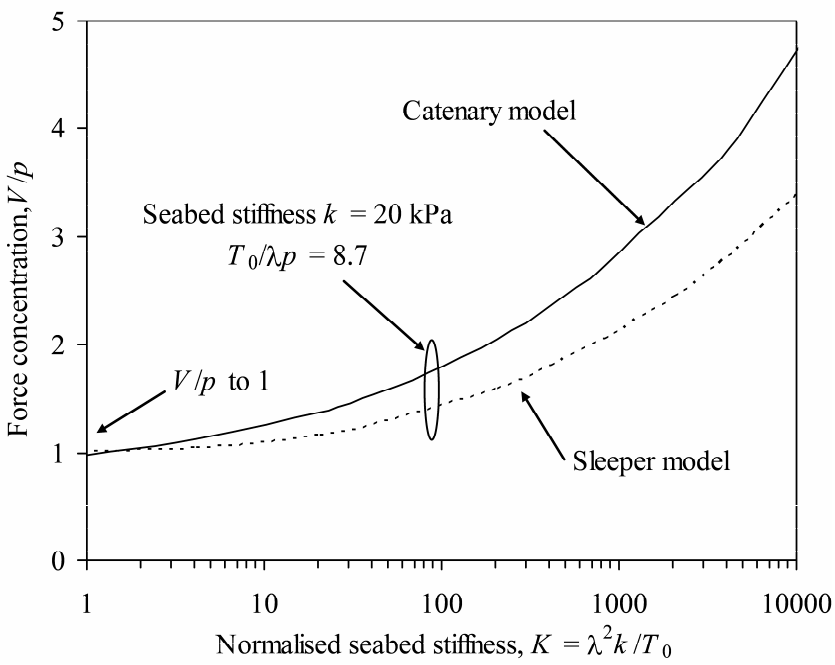

Figure 5.6. Influence of seabed stiffness on maximum pipe-soil contact forces

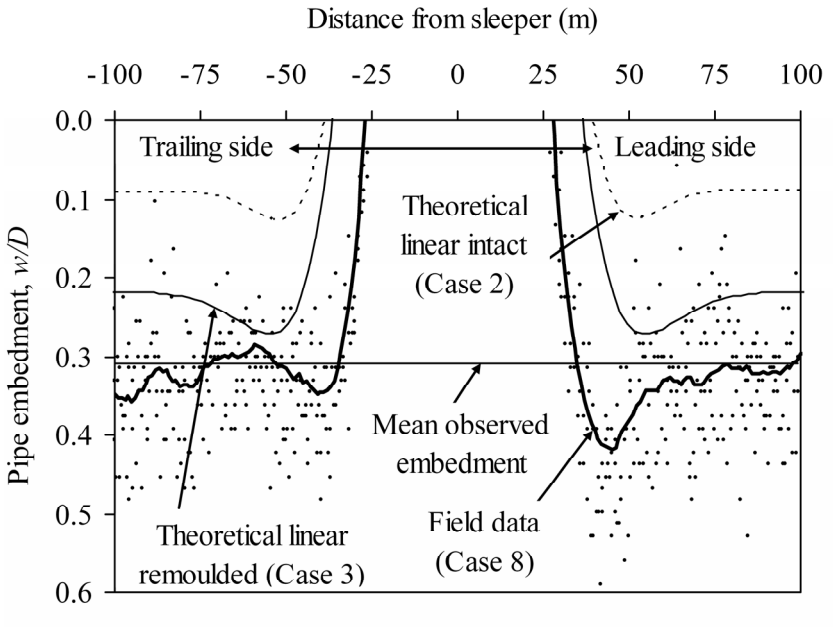

Figure 5.7. As-laid field survey embedment profiles compared to as-laid theoretical solutions (Cases 2 and 3)

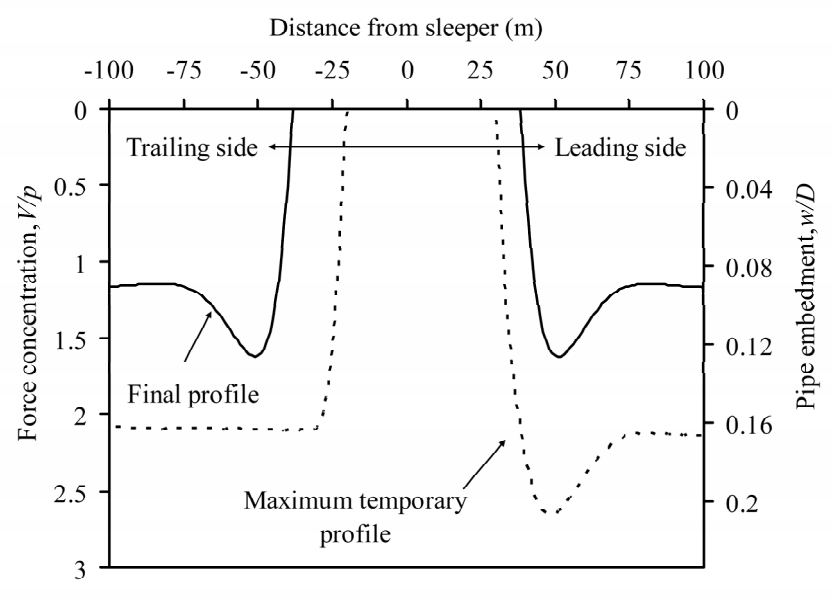

Figure 5.8. Variation in pipe-soil contact force and embedment for static pipe lay on linear intact seabed (Case 4)

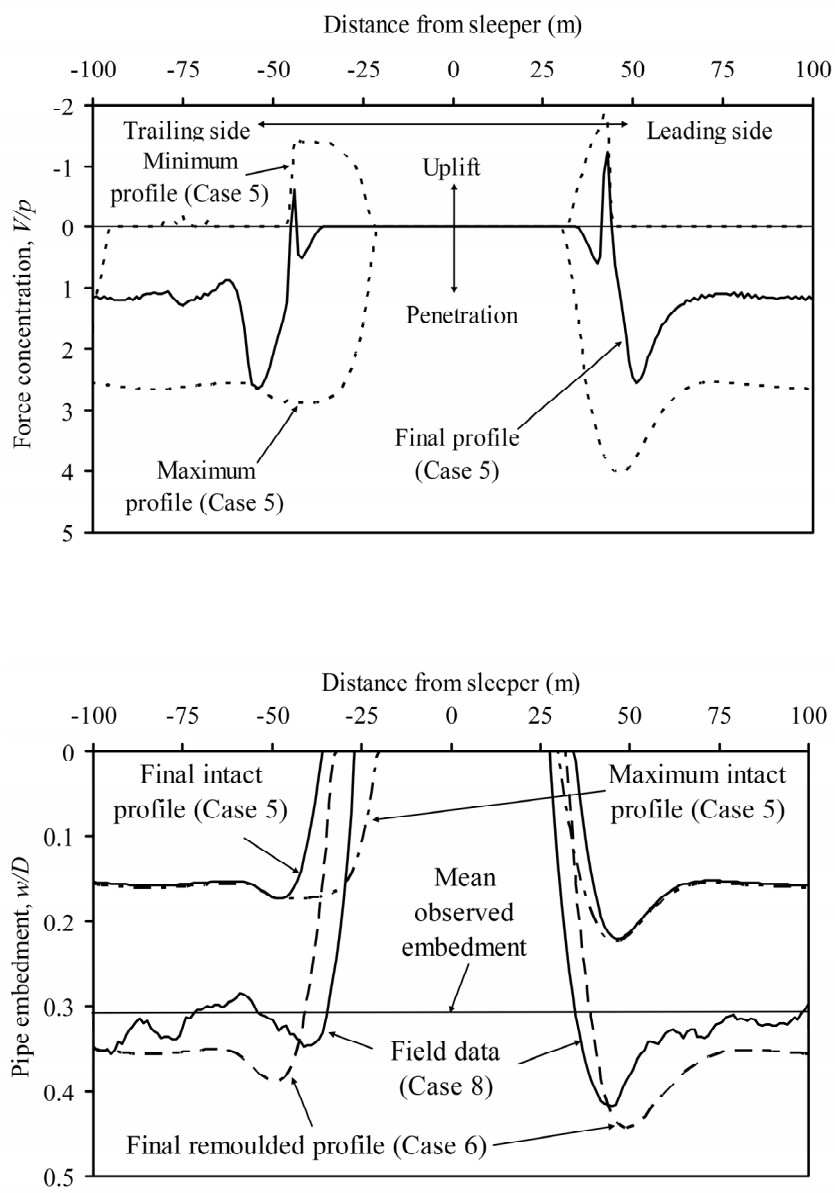

Figure 5.9. Variation in pipe-soil contact force and embedment for static pipe lay on non-linear seabed (Cases 5 and 6)

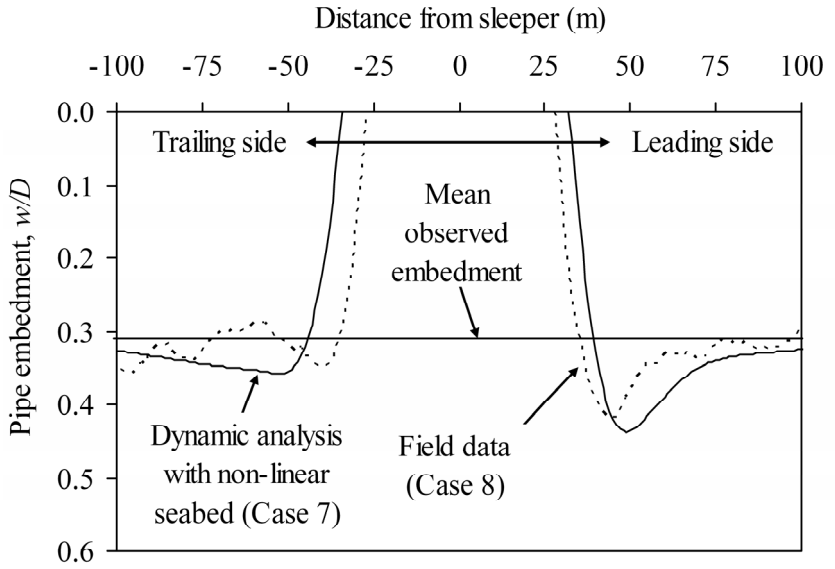

Figure 5.10. Variation in embedment for dynamic pipe lay on non-linear seabed (Case 7) compared to field survey data

CHAPTER 6. FIELD OBSERATIONS OF AS-LAID PIPELINE EMBEDMENT IN CARBONATE SEDIMENTS

The paper presented in this chapter describes the back-analysis for a third set of as-laid embedment data from a pipeline surveyed in carbonate sediments offshore Australia. The motivation to perform a third back-analysis was (i) to assess whether the trends in as-laid embedment in fine-grained carbonate soils were similar to trends in as-laid embedment in fine-grained non-carbonate soils, and (ii) to examine the embedment response in coarse-grained carbonate soils and compare this to previous assessments of pipe embedment in these soil types. A key outcome of this paper is a general framework to help determine the drainage conditions in the soil during pipeline laying, in order to determine appropriate as-laid embedment calculation methods.

The quality of the geotechnical and lay vessel data for this back-analysis were arguably better than for the other sites. Vessel motions and tension were measured during the installation on a second-by-second basis, providing valuable information on the variation in lay effects due to the sea state. However, details of the lay vessel model, which had been provided for the other sites, were not made available. This did not significantly affect the analyses as the variations in the soil conditions were more influential on the as-laid embedment, as were changes in static catenary parameters due to the large variation in water depth, which was between the two ranges of water depths at the other sites.

The conclusions from this chapter help to refine the framework for assessing as-laid embedment in fine-grained soils by further validating the use of a soil softening model that is linked to the number and amplitude of pipe motions in the touchdown zone. It was found that this type of model is important in sensitive soils, such as carbonate silts, due to the deeper embedment values predicted using the fully remoulded shear strength. Furthermore, it was found that cyclic embedment, linked to a sweeping mechanism, captured the as-laid embedment well in the coarse-grained soils, which are not subject to softening during cyclic pipe-soil interaction but rather densification during vertical loading and displacement during horizontal loading.

Westgate, Z.J., White, D.J. & Randolph, M.F. (2012). Field observations of as-laid pipeline embedment in carbonate sediments, *Géotechnique*, Vol. 62, No. 9, pp. 787-798.

6.1 ABSTRACT

Reliable prediction of the embedment of untrenched subsea pipelines is of increasing importance as hydrocarbon developments progress into deeper waters, located further from shore. Pipeline design issues such as hydrodynamic stability, lateral buckling and axial walking require accurate assessment of the pipe embedment, in order to correctly assess the pipe-soil resistance forces and the thermal insulation provided by the soil. This study presents a detailed back-analysis of the laying process and the as-laid condition of a pipeline in carbonate sediments. The pipe embedment is linked to the relevant soil properties, metocean conditions, vessel motions, and lay geometry along the route.

A cycle-by-cycle framework is proposed for the development of embedment as the pipe is subjected to oscillations during laying. The calculations use parameters obtained from standard in situ tests, and are applied across a range of soil and lay conditions along this particular pipeline route. The proposed calculation framework incorporates the effect of the lay rate and the pipeline catenary on the embedment process. It offers a significant improvement on the current practice of applying empirical multiplicative factors to the calculated static embedment in order to account for dynamic lay effects.

6.2 INTRODUCTION

Subsea pipelines represent a significant expenditure for offshore oil and gas projects. Assessing the as-laid embedment of subsea pipelines is important for several aspects of pipeline design (Cathie et al. 2005, Bruton et al. 2006). Many hydrocarbon developments are located in regions rich in carbonate soils, such as offshore Australia. However, most of the existing solutions for assessing as-laid embedment were derived for non-carbonate soils. Carbonate soils can be problematic in foundation and pipeline engineering due to their high compressibility (Jewell & Khorshid 1988). Because of this, analysis tools for siliceous soils often fail to capture the behaviour of carbonate soils adequately.

6.2.1 Assessing as-laid pipeline embedment

Theoretical solutions for pipe embedment in undrained soils based on plasticity limit analysis have been reported (Murff et al. 1989, Randolph & White 2008b), supported by

numerical simulations (Merifield et al. 2009). Centrifuge model test data have provided further insights (Dingle et al. 2008, Hodder & Cassidy 2010). Solutions for pipe embedment in drained soils have been developed experimentally from model tests in siliceous (Verley & Sotberg 1994) and carbonate sands (Zhang et al. 2002, Tian et al. 2010).

These solutions do not account for dynamic lay effects, i.e. the influence of the sea state on the lay process and the resulting pipe embedment. During laying, vessel motions cause the pipeline to oscillate within the touchdown zone, softening and displacing the soil, and increasing the transient pipe-soil contact load. These effects have been quantified in model tests (Cheuk & White 2011), but inevitably such idealisations may not fully represent field conditions. This paper provides a detailed field case study of the influence of dynamic lay effects, evaluating and extending published theories for assessing dynamic pipe embedment during laying.

6.2.2 Current state of practice

Current practice generally assesses as-laid pipeline embedment by calculating the static embedment using appropriate solutions (which incorporate an enhanced vertical load due to the pipeline catenary), and then adjusting this embedment using a multiplicative 'dynamic embedment factor', f_{dyn}, defined as:

$$f_{dyn} = \frac{w_{dynamic}}{w_{static}} \quad \text{or} \quad \frac{w_{observed}}{w_{calculated}} \tag{6.1}$$

where w is the pipe invert embedment. As indicated, f_{dyn} is essentially empirical, expressing the degree of agreement between a calculated embedment (based on a static analysis) and an observed value (influenced by dynamic effects). Reported f_{dyn} values range from 1 to 8 (Lund 2000b, Bruton et al. 2006), which have been broadly confirmed for fine-grained soils based on as-laid surveys from offshore Brazil, the North Sea, and offshore West Africa (Carneiro et al. 2010, Westgate et al. 2010a, Westgate et al. 2010c). The wide range of reported f_{dyn} in fine-grained soils, together with the dearth of guidance in coarse-grained soils or carbonate soils, suggest that this approach could usefully be replaced with embedment prediction models that are more closely linked to (i) site-specific conditions, and (ii) the underlying physical processes.

6.2.3 Objectives

This study compares field data of as-laid pipeline embedment to calculations of pipe embedment, using a combination of drained and undrained calculation methods, in order to refine these approaches and establish an improved framework for use in design. The refinements have aimed to establish links with physical processes occurring in the touchdown zone during pipeline laying. The high quality of the field data and the comprehensive monitoring of the lay process provide a rare opportunity to validate the embedment analyses against as-laid observations.

6.3 COLLATION OF DATA SETS

Data sets documenting the laying arrangements of the pipeline, the metocean conditions during laying, the as-laid pipeline embedment, and the geotechnical characteristics of the pipeline route were collated from two 5 km sections of an offshore pipeline. The data were interpreted to determine the parameters that control pipe embedment.

6.3.1 Summary of pipe laying data

The pipe laying data set included vessel logs, vessel response and pipeline tension measurements during installation, and intermittent video footage of the touchdown zone.

Two distinct route sections were considered. Region A lies along the outer continental shelf in shallow water, with a carbonate sandy seabed. Region B lies along the continental slope in deeper water, with a carbonate silty seabed. The pipe properties and lay conditions are summarised in Table 6.1.

The pipeline was S-laid over a stinger at a lay angle of 64 degrees (Figure 6.1), progressing from shallower water with pipe lengths of 12.2 m being successively paid out. Within the final 1.3 km of Region B, the pipeline was removed from the stinger and was then laid onto the seabed from a cable.

Metocean data included the significant wave height, H_s, and the swell period, t_{swell}, recorded at 6-hour intervals during the installation (Table 6.1). Vessel motions were also recorded at 6-hour intervals, while the pipeline tension was monitored at 1-second intervals. In Region A, the minimum measured transient tension was about equal to the calculated static tension, while the maximum measured transient tension was up to 30%

greater than the static values. In Region B, the calculated static tension was in the middle of the range in dynamic measured tension, but in some areas the minimum measured transient tension was up to 30% less than the static values. The relevance of these minima is that reductions in lay tension below the static value lead to greater vertical pipe-soil contact force. In this study, these reductions in tension were minor compared to the variations in the static lay conditions and soil conditions along the route, and therefore the calculated static bottom tension values, T_0, shown in Table 6.1, were used in the back-analyses presented later.

6.3.2 Summary of as-laid survey data

The as-laid embedment was surveyed 6 months after installation, with measurements obtained at 1-metre intervals along the route and at three different pipeline offsets, as illustrated in Figure 6.2. The 'near', 'local' and 'far' values of embedment along the route sections are shown in Figure 6.3 and summarised in Table 6.2. The minimum and maximum values reported in Table 6.2 are averages over 20 data points (i.e. 20 m). Illustrative cross-sections of 'near' and 'local' embedment along each route section are shown in Figure 6.4.

In Region A (Figure 6.3a), the 'near' embedment, representing the embedment relative to a datum outside of any zone of seabed disturbance during laying, was consistent along most of the route section, but approximately doubled near the end. The average 'near' embedment of the pipe invert, w, was equal to 0.06 pipeline diameters (i.e. 0.06D) (Figure 6.4a). In Region B (Figure 6.3b), the 'near' embedment was less consistent than for Region A, with an average value of 0.29D. The deepest embedment (0.7D) occurred just prior to the lay down zone due to the pause in laying as the pipeline was prepared for removal from the stinger (Figure 6.4b). Through this zone, the embedment reduced as the pipe was laid gently onto the seabed using a cable (Figure 6.4c), which is consistent with previous field studies (Westgate et al. 2009).

The 'local' embedment in Region A was greater than the 'near' embedment, with an average value of 0.08D, implying a modest level of heave (Figure 6.4a). The 'far' embedment was greater than both the 'near' and 'local' embedment, with an average value of 0.12D. This leaves some uncertainty as to which measure of embedment is most appropriate, as the seabed in this region is susceptible to sediment transport and scour. In comparisons with predicted pipeline embedment presented later, both 'near'

and ‘far’ embedment are considered, which represent the bounds of the measured values.

In Region B, the ‘local’ embedment was on average equal to the ‘near’ embedment. However, at some locations the ‘local’ embedment was greater than the ‘near’ embedment, reflecting soil heave adjacent to the pipe (Figure 6.4d). At other locations, it was less than the ‘near’ embedment, reflecting a shallow trench adjacent to the pipe (Figure 6.4e). The heave in Region B is less than that of a statically-penetrated pipe, which is likely due to softening within the heave mounds from remoulding and water entrainment. This type of behaviour is also consistent with previous field studies (Westgate et al. 2010c). The ‘far’ embedment in Region B was also greater than both the ‘near’ and ‘local’ embedment, but with a higher average value of 0.36D and showing less consistency along the route section due to local undulations in the topography.

6.3.3 Summary of geotechnical survey data

Geotechnical site investigations performed along the route comprised piezocone and T-bar penetration testing, and classification testing of soil samples. A summary of the geotechnical data and interpreted soil parameters is presented in Table 6.3.

The coarse-grained soils (coarse fraction > 0.7) in Region A are ‘carbonate’, while the fine-grained soils (fines fraction > 0.7) in Region B are ‘siliceous carbonate’ (Clark & Walker 1977). In Region B, the in situ effective unit weight of the soil, γ', ranges from 4.5 to 6 kN/m^3. In these softer soils, γ' affects the non-negligible component of penetration resistance that arises from buoyancy (Merifield et al. 2009).

Cone penetration testing was performed in both Region A and Region B. The profiles of net cone resistance, q_{net}, in the upper 0.5 m of the seabed are shown in Figure 6.5. The resistance gradients, $k_{qnet,}$ range from 3 to 6 MPa/m in Region A, and from 60 to 600 kPa/m in Region B. The soil classification chart of Schneider et al. (2008) was used to classify the soil. This chart uses the normalised net cone resistance, Q, equal to q_{net}/σ'_{v0}, where σ'_{v0} is the in situ effective vertical stress in the soil, and the normalised excess pore pressure, $\Delta u_2/\sigma'_{v0}$, where Δu_2 is the measured excess pore pressure at the cone shoulder. These values from each cone test within the upper 0.5 m of the seabed are shown in Figure 6.6. While both regions include Type 3 (transitional) soils, Region A is

predominantly Type 2 (drained sands) and Region B is predominantly Type 1 (silty and clay-sized) soils.

T-bar penetration testing was only performed in Region B. The profiles of T-bar penetration resistance, $q_{Tbar,}$ in the upper 0.5 m of the seabed are shown in Figure 6.7. The resistance gradients, k_{qTbar}, reduce from 400 kPa/m at the top of the slope down to 40 kPa/m at the bottom of the slope, with q_{Tbar}/q_{net} ratios close to 0.7. Two cyclic T-bar tests were performed in the silt. The resistance degradation response for these two tests, with the cyclic penetration resistance normalised by the initial penetration resistance, is shown in Figure 6.8. The resistance shows a rapid reduction after the initial cycle, followed by a more gradual reduction towards a stable value equal to 0.14, or a sensitivity, S_t, equal to 7.

The consolidation characteristics of the soil influence the drainage conditions around the pipe during laying. The coefficient of consolidation, c_v, was determined from oedometer testing on in situ samples, Rowe cell testing on reconstituted samples, and through empirical relationships for permeability, linked to c_v using one-dimensional consolidation theory. The c_v values range from about 400,000 to 700,000 m^2/yr in Region A and from about 10 to 1,000 m^2/yr in Region B.

6.4 BACK-ANALYSIS OF AS-LAID EMBEDMENT

Two main types of analyses were performed: (i) a consolidation assessment to determine the level of soil drainage during pipe laying, and (ii) static and cycle-by-cycle pipe embedment calculations for comparison with the as-laid embedment.

6.4.1 Soil drainage during pipe laying

Pipeline motion in the touchdown zone generally consists of superposed cycles with different periods, ranging from the wave period up to longer durations associated with pipeline catenary dynamics (Lund 2000b). Video footage showed that, on average, the period of pipe motion, t_{cyc}, approximately matched the swell period, t_{swell}, which was in the range 8 to 13 seconds. The drainage response of the soil during each cycle was assessed using the normalised time factor, T, based on the full pipe diameter, D, expressed as:

$$T = \frac{c_v t_{cyc}}{D^2} \tag{6.2}$$

This time factor was then used to assess the normalised average excess pore pressure, U_N, around a partially-embedded pipeline (Gourvenec & White 2010, Krost et al. 2011). U_N is defined as the ratio of the current average excess pore pressure, Δu, to the initial average excess pore pressure, u_i, when the pipe was initially loaded, expressed as:

$$U_N = \frac{\Delta u}{u_i} = 1 - \left(\frac{T}{T + \alpha} \right)^{\beta} \tag{6.3}$$

where α and β are fitted functions of the pipe embedment, based on the measured 'near' embedment values from the field survey in this analysis. This expression relates to dissipation of excess pore pressures created by sustained vertical load. While the pore pressure field may dissipate faster or slower under the more complex loading during laying, this uncertainty is insignificant given the large range in c_v along the route.

The U_N values are presented in Figure 6.9. In Region A, U_N was about 0.05, suggesting that any excess pore pressures could almost fully dissipate during each swell period. In Region B, U_N was about 0.95, indicating minimal dissipation. Based on this, a drained pipe bearing capacity model was adopted for Region A, while an undrained model was adopted for Region B.

6.4.2 Input parameters for assessing pipe embedment

The input parameters used in calculations of as-laid pipe embedment include the maximum vertical pipe-soil contact force in the touchdown zone, V_{max}, the cone resistance gradient, k_{qc} or k_{qnet} (to determine drained bearing capacity), the undrained shear strength gradient, k_{su} (to determine undrained bearing capacity), and the effective unit weight, γ', to determine the additional bearing capacity due to buoyancy.

Randolph & White (2008b) showed that V_{max} can be approximated as:

$$\frac{V_{max}}{W'} = 0.6 + 0.4 \left(\frac{\lambda^2 k}{T_0} \right)^{0.25} \tag{6.4}$$

for sufficiently high normalised tension, where k is the linearised seabed stiffness expressed in kN/m/m (equivalent to V_{max} divided by the pipe embedment, w) and T_0 is the bottom tension in the pipeline. The characteristic length, λ, is expressed as (Pesce et al. 1998):

$$\lambda = \sqrt{\frac{EI}{T_0}} \tag{6.5}$$

where E is the modulus of elasticity of the pipeline and I is the second moment of area of the pipe cross section. In this study, λ was equal to 27 m through Region A and ranged from 21 to 46 m through Region B.

6.4.3 Overview of embedment calculations

Pipe bearing capacity calculations were applied in three different ways in this study:

1. Firstly, static calculations were performed, to back-calculate the f_{dyn} values that would be required in these particular carbonate soils and lay conditions to match the field data.
2. Modified static calculations were then performed, to assess whether dynamic effects can be accounted for using the fully remoulded soil strength, as has been previously proposed (Westgate et al. 2010c).
3. Finally, cycle-by-cycle calculations of the accumulation of pipe embedment were performed to determine whether a more accurate method, linked to physical processes and the number of pipe motions through the touchdown zone, could be used to capture the as-laid embedment more accurately.

6.4.4 Static embedment calculations

Drained method

Centrifuge model testing of drained foundation behaviour on calcareous soil has shown that the load-penetration response is approximately linear (Finnie & Randolph 1994), and may be calculated as:

$$q_{ult} = \frac{V_{ult}}{A} = M\gamma'w \tag{6.6}$$

where q_{ult} is the ultimate bearing capacity, A is the foundation area, V_{ult} is the vertical load and M is a dimensionless bearing modulus, analogous to the surcharge bearing capacity factor, N_q. Zhang et al. (2002) extended this approach to pipelines on carbonate sand, lumping M, γ', and the pipe diameter, D, into the plastic bearing stiffness, k_{vp}, where:

$$V_{ult} = k_{vp} w \tag{6.7}$$

and

$$k_{vp} = M\gamma' D \tag{6.8}$$

with k_{vp} having units of modulus.

The chord width, D', defined in Figure 6.10, is calculated as:

$$D' = \min\left(2D\sqrt{\frac{w}{D} - \left(\frac{w}{D}\right)^2}, D \right) \tag{6.9}$$

Results from centrifuge model tests in carbonate sand show that the contact stress based on the effective pipe-soil contact width, B, (i.e. V/B) is similar to the cone resistance (Zhang et al. 2002, Tian et al. 2010). B is calculated using an increased w, representing the 'local' embedment, enhanced by the heave mounds (Figure 6.10):

$$B = \min\left(2D\sqrt{\frac{1.5w}{D} - \left(\frac{1.5w}{D}\right)^2}, D \right) \tag{6.10}$$

This idealisation is consistent with the heave profiles observed in numerical analyses of static pipe penetration (Merifield et al. 2009) and physical model tests (Dingle et al. 2008).

The final expression for the pipe bearing capacity in drained carbonate sand is expressed as:

$$\frac{V_{ult}}{B} = q_c \tag{6.11}$$

where q_c is taken at the pipe invert elevation, w. The embedment of the pipe can be established by calculating B from Equation 6.11, then solving Equation 6.10 for w. To account for the stress concentration due to the catenary, iteration with Equation 6.4 is required.

Cone-based approaches have been adopted in industry for other types of foundations, including skirted foundations (DNV 1992) and piles (API 2007). Other factors that influence the relationship between pipe penetration resistance and cone tip resistance include the difference in bearing capacity for circular (i.e. cone) and strip (i.e. pipe)

objects, as well as the progressive failure around a cone tip compared to a curved pipe surface. It is recognised that these factors can be important; however, this study evaluates the direct applicability of Equation 6.11.

Undrained method

Undrained pipe embedment was calculated using the bearing capacity expression of Merifield et al. (2009), which superimposes the penetration resistance from the soil strength and soil buoyancy. The expression is:

$$V_{ult} = N_c s_u D + f_b A_s \gamma' \tag{6.12}$$

where V_{ult} is the ultimate bearing capacity (expressed in kN/m) and N_c is the soil strength bearing capacity factor, approximated as:

$$N_c = a\left(\frac{w}{D}\right)^b \tag{6.13}$$

During pipe laying, the combination of soil softening around the pipe and the down-drag of softer surface soils creates a relatively smooth pipe-soil interface for undrained conditions. Values of a = 5.2 and b = 0.19 were adopted, which represent values that approximately account for the smooth pipe-soil interface, the soil unit weight, the penetration rate and softening of the soil during initial penetration (Chatterjee et al. 2012). To calculate $s_{u,ini}$, the penetration resistance from the T-bar testing was divided by a resistance factor, N_{Tbar}, equal to 10.5 (Stewart & Randolph 1991). The calculated shear strength gradients ranged from $k_{su,ini}$ = 4 to 38 kPa/m.

The penetration resistance due to the soil buoyancy component in Equation 6.12 is a modification of Archimedes' principle. Soil buoyancy is the product of γ' and the displaced area of soil, A_s, but is enhanced by soil heave adjacent to the pipe using the factor, f_b, taken as 1.5 (Merifield et al. 2009).

Comparison of static calculations to as-laid embedment

The calculated static embedment in Region A ranged from 0.01D to 0.02D, significantly under-predicting the observed embedment (Figure 6.11a). The back-calculated f_{dyn} values, based on Equations 6.1, 6.4, 6.10 and 6.11, ranged from 3 to 8 where the soil was 'fully drained' (from 0 to 3.9 km) (Figure 6.11b). Within the zone where less than 95% dissipation occurred, the observed embedment dramatically increased, resulting in

higher f_{dyn}. This highlights the inadequacy of static calculation methods for assessing as-laid pipe embedment in drained conditions, and provides an indication of where partially-drained conditions prevail.

The calculated static embedment in Region B, using the intact strength, also under-predicts the observed embedment (Figure 6.12a). The back-calculated f_{dyn} values, based on Equations 6.1, 6.4, 6.12 and 6.13, ranged from 2 to 3 within the zone where lay effects were present (from 0 to 3.7 km). Within the lay down zone, where lay effects are less significant, the agreement between the calculated and observed embedment improves, and eventually become equal at the end of the route. This observation indicates that the theoretical bearing capacity solution of Merifield et al. (2009) provides good embedment predictions in static conditions, and is consistent with previous field studies (Westgate et al. 2009).

6.4.5 Modified static embedment calculations

Modified static calculations were performed for Region B, using the fully remoulded strength gradient, calculated using $S_t = 7$, in the undrained bearing capacity equation (Equation 6.12) to capture the softening and trenching mechanisms in a simple way. The calculated embedment is compared to the observed embedment in Figure 6.13. Within the zone where lay effects were present (from 0 to 3.7 km), the calculated embedment using the fully remoulded strength generally agrees with the observed embedment. Within the lay down zone, the calculated embedment using the fully remoulded strength diverges from the observed embedment as the soil becomes less disturbed by the lay process. These observations are also consistent with previous field studies (Westgate et al. 2010c), and shows that use of the fully remoulded soil strength to calculate the penetration resistance captures reasonably well the as-laid embedment for normal lay conditions.

6.4.6 Cycle-by-cycle embedment calculations

The previous calculation approaches represent the state-of-the-art methods by which as-laid embedment is assessed in routine design. To explore whether a more sophisticated approach, incorporating the lay process, could provide better agreement with the observed embedment, a cycle-by-cycle calculation approach was tested. The approach uses the lay rate and the amplitude of pipe motion to determine the amount of strength

degradation in undrained conditions, or the cumulative depth of soil swept aside in drained conditions.

To calculate the number of oscillations that pipe element experiences in the touchdown zone, N_{TDZ}, the following expression was adopted:

$$N_{TDZ} = \frac{(\lambda/\text{layrate})}{t_{swell}} \tag{6.14}$$

where λ is the characteristic length (Equation 6.5) and t_{swell} is the swell period. The resulting N_{TDZ} varied over an order of magnitude, from about 40 cycles in the lay down zone, up to about 400 cycles where the lay rate reduced.

A summary of the cycle-by-cycle calculation framework is shown in Figure 6.14. In these calculations, V_{max} reduces due to the increasing pipe embedment and reducing soil stiffness, as per Equation 6.4. An iterative process is performed to establish a value of embedment that gives equal values of V_{max} (from the catenary overstress) and bearing capacity, V_{ult}, which differs for each drainage condition.

Drained method

Video footage from Region A showed that the pipe sweeps soil aside with each oscillation. To capture this embedment mechanism, a cycle-by-cycle approach was adopted that summed the incremental static pipe embedment, Δw_i, from the drained bearing capacity model, for each cycle, i, assuming that the depth of material swept aside in each oscillation was equal to this static embedment. V_{max} retains its link to the cumulative embedment, $\Sigma\Delta w_i$ (which reflects the pipe shape in the touchdown zone). The bearing capacity, V_{ult}/B, is calculated using the incremental embedment, Δw_i, and the updated cone resistance taken at the depth of the cumulative embedment, $\Sigma\Delta w_i$.

Undrained method

Video footage from Region B showed that the pipe sank into progressively softened soil. To capture this embedment mechanism, a cycle-by-cycle approach was adopted that updated the operative strength in the undrained bearing capacity model, based on the cumulative pipe displacement over the total number of cycles, N_{TDZ}. The relationship between the level of disturbance – quantified by the number of T-bar cycles, N – and the operative strength can be expressed as:

$$\frac{s_u}{s_{u-ini}} = \delta_{rem} + (1-\delta_{rem})e^{(-3N/N_{95})} \tag{6.15}$$

where δ_{rem} is the fully remoulded strength ratio. N_{95} represents the number of cycles required to degrade the soil strength by 95%. Assuming that $s_u/s_{u\text{-}int} = q_{T\text{-}bar}/q_{Tbar\text{-}ini}$, the T-bar data result in $\delta_{rem} = 0.14$ and $N_{95} = 2.5$, as shown in Figure 6.8.

To link soil remoulding from a vertically-cycled T-bar to a horizontally-cycled pipeline, it was assumed that the cumulative horizontal pipe displacement required to cause 95% remoulding of the surrounding soil, $(\Sigma u/D)_{95}$, is equivalent to:

$$(\Sigma u/D)_{95} = 2(1.5)N_{95} \tag{6.16}$$

where the factor 2 represents two passes of the T-bar for each vertical cycle, and 1.5 represents the approximate vertical extent of the failure mechanism (as a multiple of the diameter) around the T-bar (Zhou & Randolph 2009, Cheuk & White 2011). The equivalent strength degradation response for pipe laying is then:

$$\frac{s_u}{s_{u-ini}} = \delta_{rem} + (1-\delta_{rem})e^{(-3\Sigma(u/D)/(\Sigma u/D)_{95})} \tag{6.17}$$

This is only an approximate link that ignores the effects of elastic displacements and increasing penetration into undisturbed soil. However, it retains an appropriate level of simplicity for practical use.

Video footage showed that near the front of the touchdown zone, the maximum u/D was about 0.5, peak-to-peak. This amplitude reduces through the touchdown zone due to the lateral soil resistance. In the present study, u/D = 0.3 was adopted to calculate the cumulative pipe displacement during cycling. This was chosen as the representative average u/D occurring over the length of the touchdown zone, based on numerical simulations of similar pipe laying activities (Westgate et al. 2010a, 2010c).

Through the lay down zone, u/D reduces to zero due to the attenuation in lay effects. These changes include (i) a gradual reduction in the water depth below the head of the pipeline, which influences V_{max}, (ii) an immediate reduction in u/D as the pipe is transferred from the rigid stinger to the flexible cable, and (iii) an additional gradual reduction in u/D as the transfer of vessel motions through the pipeline reduces. In this study, the effect of (i) is accounted for in the static V_{max} values, based on the pipe lay

analyses that simulated the lay down process. The effect of (ii) and (iii) hold greater uncertainty, and in this study it was assumed that the horizontal oscillation amplitude through the lay down zone, $(u/D)_{LDZ}$, reduced exponentially as:

$$\left(\frac{u}{D}\right)_{LDZ} = \min\left[\frac{0.5u}{D}, \frac{0.5u}{D}\left(\frac{x_{LDZ} - x}{x_{LDZ}}\right)^{\kappa}\right] \tag{6.18}$$

where u/D is the amplitude outside of the lay down zone, x_{LDZ} is the length of the lay down zone (equal to 1.3 km), and x is the distance travelled through the lay down zone. The factor 0.5 was used to capture the effect of (ii) above, while the effect of (iii) was calibrated to the observed embedment using the fitting parameter, κ.

Characteristic behaviour of cycle-by-cycle calculations

Example profiles of cycle-by-cycle embedment calculations are presented in Figure 6.15 and illustrate the characteristic behaviour of the different calculation models. The drained calculations, using k_{qnet} = 3 and 6 MPa/m, show gradual increases in embedment (Figure 6.15a). In these calculations, both V_{max} and B reduce progressively, while q_c increases. Therefore, the depth of material swept aside with each oscillation reduces progressively, so the rate of embedment is not linear with cycle number.

The undrained calculations, using $k_{su,ini}$ = 10 kPa/m, shows that the initial rate of embedment depends markedly on the severity of the lay effects, quantified using u/D. Under normal lay conditions, the larger u/D = 0.5 results in rapid embedment to a steady state value associated with fully remoulded conditions. If u/D reduces, the rate of embedment also reduces but eventually attains an embedment associated with fully remoulded conditions. These example calculations capture the general trends observed in the field.

Comparison of cycle-by-cycle calculations to as-laid embedment

The cycle-by-cycle embedment using the variation in soil and lay conditions along each route section is compared to the observed embedment in Figure 6.16. In Region A, the cycle-by-cycle calculation is bounded by the observed 'near' and 'far' embedment, within the 'fully drained' zone (Figure 6.16a). In Region B, the cycle-by-cycle calculation using the operative strength is identical to the modified static calculation using the fully remoulded strength through the majority of the route section, for this particular soil and lay condition (Figure 6.16b). However, use of the operative strength

captures the observed embedment through the lay down zone better than use of the intact or remoulded strength, using $\kappa = 3$ in Equation 6.18.

6.4.7 Discussion of results

The performance of the different calculation methods indicates the techniques that are most applicable for practical use. While field data are limited by the accuracy of the as-laid survey measurements and the supporting geotechnical data, these surveys provide a better benchmark of dynamic lay effects than model tests, which do not fully mimic the lay process.

For drained conditions, soil is swept aside with each oscillation of the hanging pipe. A practical approach to assess static pipe penetration in drained soil uses the cone resistance, based on previous studies. The model is used to assess the dynamic embedment based on a cycle-by-cycle accumulation of incremental static penetration, representing the sweeping process. This method has a more logical basis than a reliance on a simple static embedment calculation multiplied by an arbitrary f_{dyn} factor.

For undrained conditions, soil is softened (and potentially displaced) with each pipe oscillation. In areas where lay effects are negligible, the as-laid embedment can be captured well by using the intact shear strength in the undrained bearing capacity model. In areas where lay effects are present, i.e. normal lay conditions, the as-laid embedment can be captured well by using the fully remoulded shear strength to approximately account for dynamic lay effects. These trends agree with previous field studies (Westgate et al. 2010c). An operative undrained shear strength, linking the strength degradation response from cyclic T-bar tests to cumulative pipe displacement during laying, provided better overall agreement with the observed embedment when combined with an idealised model of the attenuation of lay effects through the lay down zone.

For partially-drained conditions, which appear to occur in soils exhibiting between 5% to 95% dissipation of excess pore pressure during each cycle of pipe motion, the expected as-laid embedment could be bracketed by separate calculations using drained and undrained methods. The stated transition limits were based on locations where the calculated embedment departed from the observed embedment in each region. As shown in Figure 6.16, this occurred at about 3.9 km in Region A, and at about 1.6 km in Region B.

6.5 CONCLUSIONS

Field survey data of as-laid pipeline embedment for two well-characterised, 5 km sections of a pipeline route through carbonate soils were analysed, and linked to the relevant metocean conditions, vessel motions, and pipe lay geometry. The lay process was monitored in sufficient detail for the effects of the catenary shape, pipe tension and lay rate to be assessed. Improved methodologies were proposed, which have provided good agreement with the observed embedment. The offset distance where the pipeline embedment is measured is important, and consideration of the effects of soil heave (or trench formation) and local undulations in the seabed topography on the measured values may be required.

In drained conditions, video footage indicated that the additional embedment arises from sweeping of soil aside during each cycle of motion. A cycle-by-cycle embedment model was proposed that sums the incremental static 'swept' pipe embedment, using the number of pipe motions determined from the lay rate, the characteristic pipeline length and the swell period, as well as the bearing capacity derived from cone penetration resistance

In undrained conditions, where lay effects were present, the observed embedment was approximately captured using the fully remoulded soil strength. Where the pipeline was lowered to the seabed using a cable, the back-calculated soil strength increased progressively from the fully remoulded value towards the intact value, due to the attenuation of lay effects. The full response was captured using an operative soil strength, calculated from the pipe motions in the touchdown zone and linked to cyclic T-bar tests.

In summary, this detailed case study has highlighted the limitations of current practice for predicting as-laid pipeline embedment. The methodologies proposed represent a better basis for assessing as-laid pipe embedment in carbonate soils than the use of empirical f_{dyn} factors to account for lay effects. The methodologies can also be applied to other soil types, being linked back to soil properties (cone resistance for drained soil conditions and shear strength for undrained conditions).

Table 6.1. Pipe and lay parameters

Parameter	Units	Region A	Region B
Pipeline outer diameter, D	[mm]	640	634
Concrete coating thickness	[mm]	40	-
Pipe bearing pressure, W'/D	[kPa]	3.3	1.5
Bending stiffness, EI	[MN.m^2]	229.6	214.6
Lay angle, ϕ	[degrees]	64	64
Water depth, z_w	[m]	100 – 140	240 – 830
Bottom tension, T_0	[kN]	300	100 – 500
Characteristic length, λ	[m]	27	21 – 46
Significant wave height, H_s	[m]	1.1 – 1.9	1.5 – 2.5
Swell period, t_{swell}	[s]	8 – 11	8 – 13
Lay rate	[m/hr]	30 – 220	30 – 110

Table 6.2. As-laid embedment summary

Embedment measurement	Lateral offset from pipe (m)	Region A			Region B		
		Min.	Avg.	Max.	Min.	Avg.	Max.
'Far' embedment	8 m	0.05D	0.12D	0.19D	0.06D	0.36D	0.66D
'Near' embedment	2 m	0.02D	0.06D	0.11D	0.06D	0.29D	0.68D
'Local' embedment	0.5 m	0.03D	0.08D	0.15D	0.05D	0.29D	0.66D

Table 6.3. Soil parameters

Parameter	Units	Region A	Region B
Percent coarse fraction	[%]	> 70	< 30
Percent fine fraction	[%]	< 30	> 70
Percent calcium carbonate	[%]	> 95	86 – 90
Effective unit weight, γ'	[kN/m^3]	> 10.5	4.5 – 6
Coefficient of consolidation, c_v	[m^2/yr]	400,000 – 700,000	10 – 1,000
Net cone resistance gradient, k_{qnet}	[kPa/m]	3,000 – 6,000	60 – 600
T-bar resistance gradient, k_{Tbar}	[kPa/m]	-	40 – 400
Undrained shear strength gradient, $k_{su\text{-}ini}$	[kPa/m]	-	4 – 38
Soil sensitivity, S_t	[-]	-	7

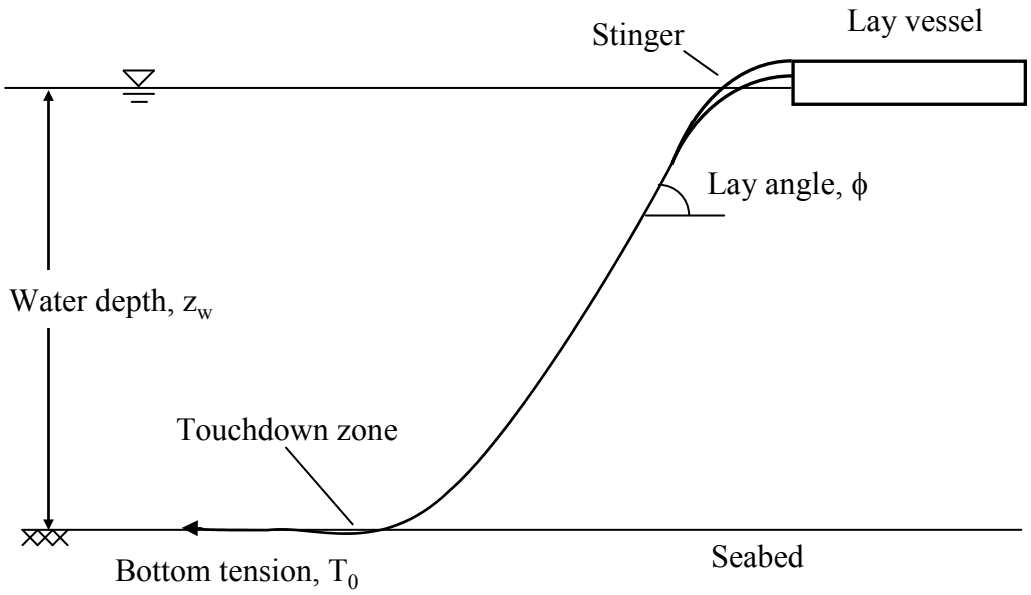

Figure 6.1. Illustration of typical S-lay pipeline catenary

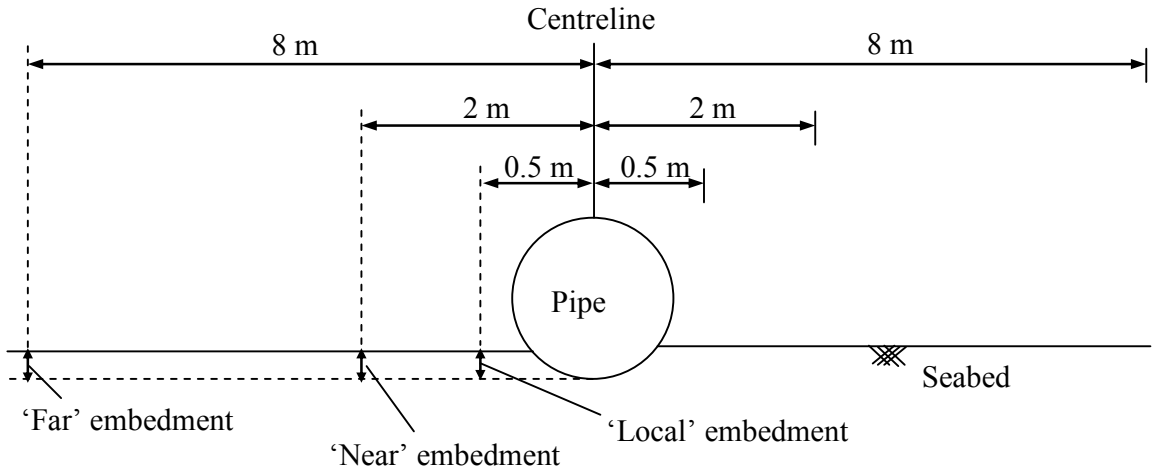

Figure 6.2. Location of as-laid embedment measurements (not to scale)

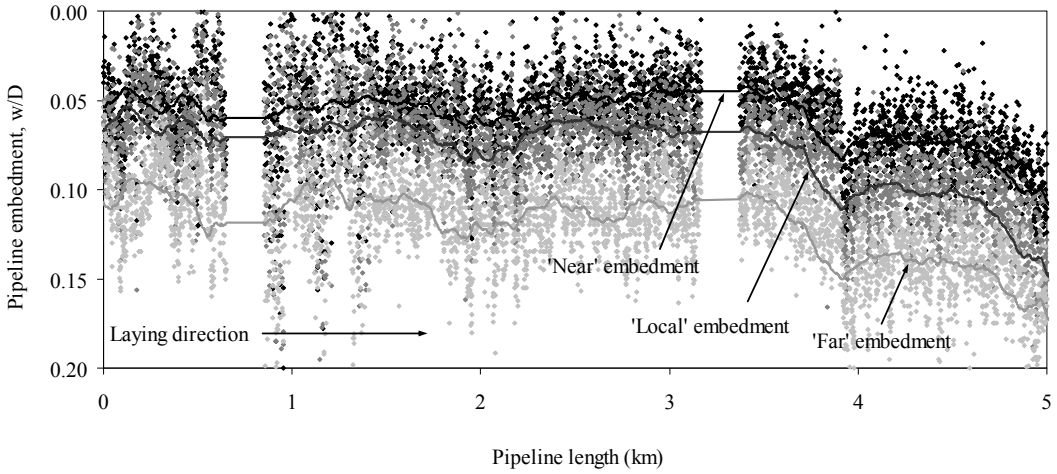

(a)

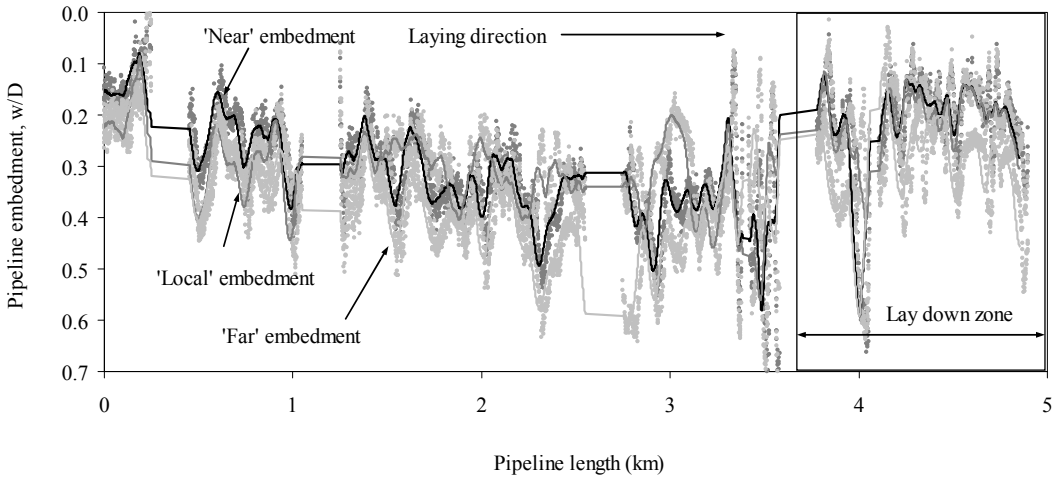

(b)

Figure 6.3. Measured as-laid pipeline embedment through (a) Region A and (b) Region B (note different vertical scales)

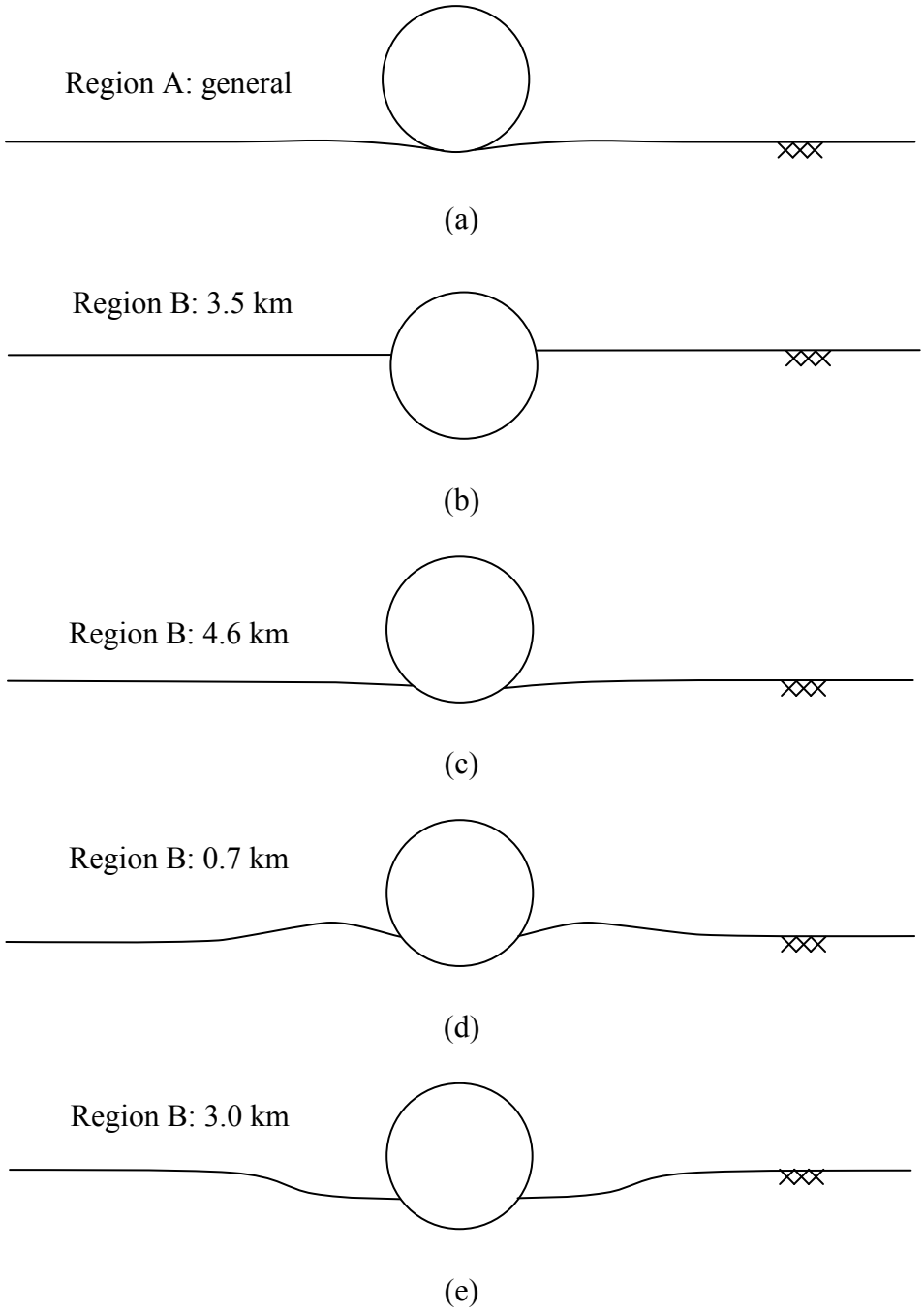

Figure 6.4. Illustrative cross-sections of pipe embedment along routes

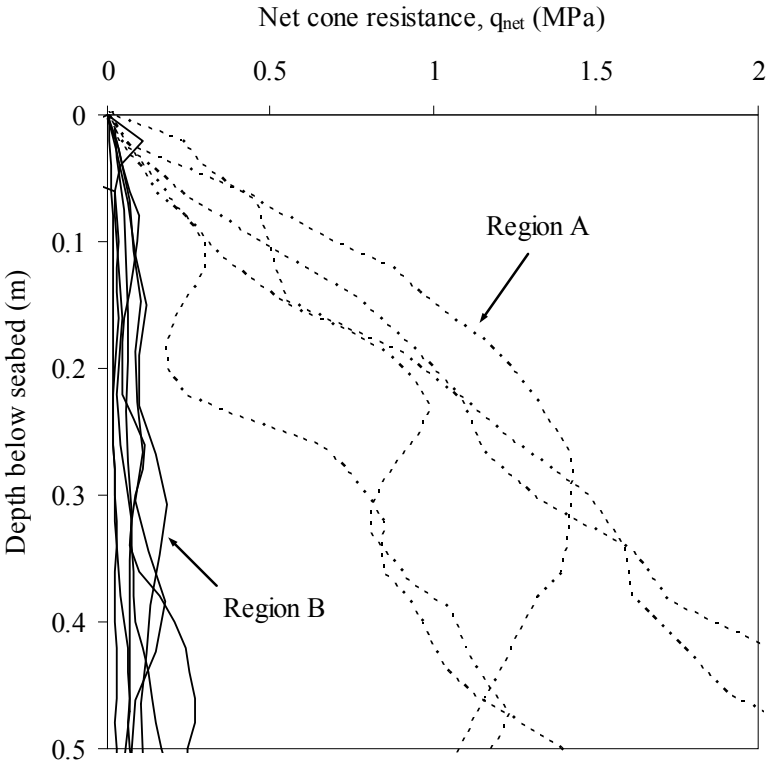

Figure 6.5. Net cone penetration resistance profiles

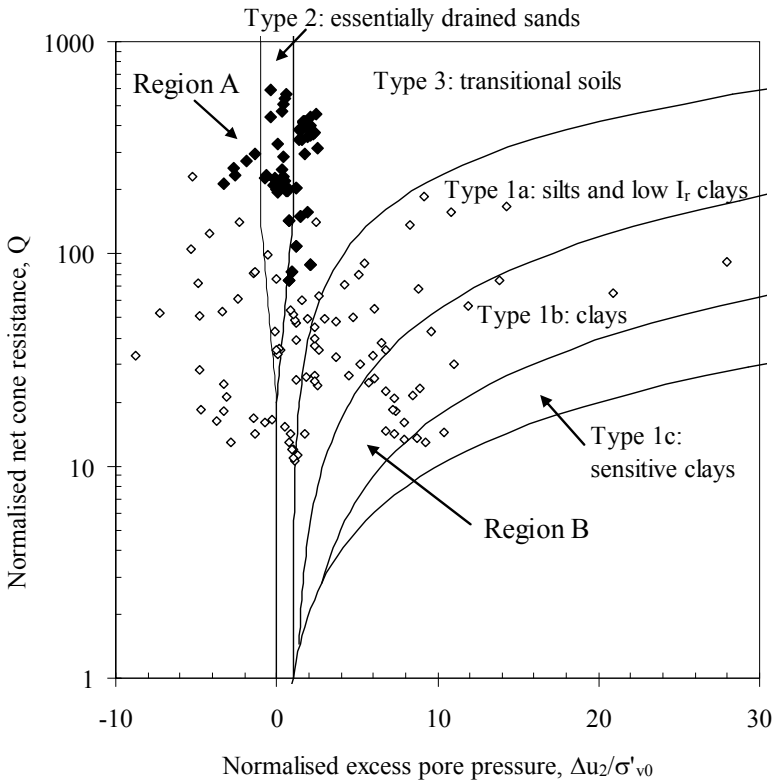

Figure 6.6. Cone test results plotted on Schneider et al. (2008) classification charts

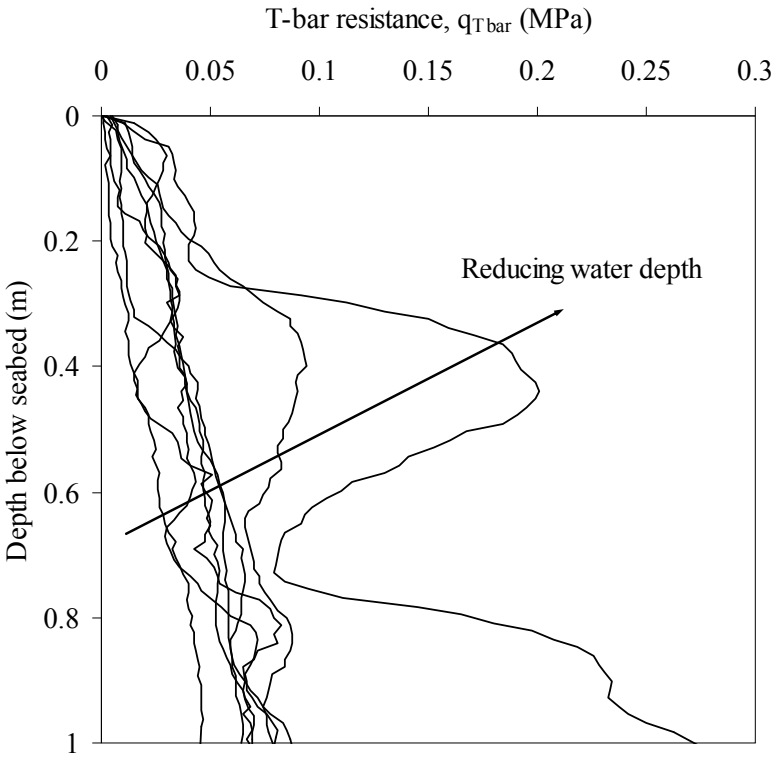

Figure 6.7. T-bar penetration resistance profiles

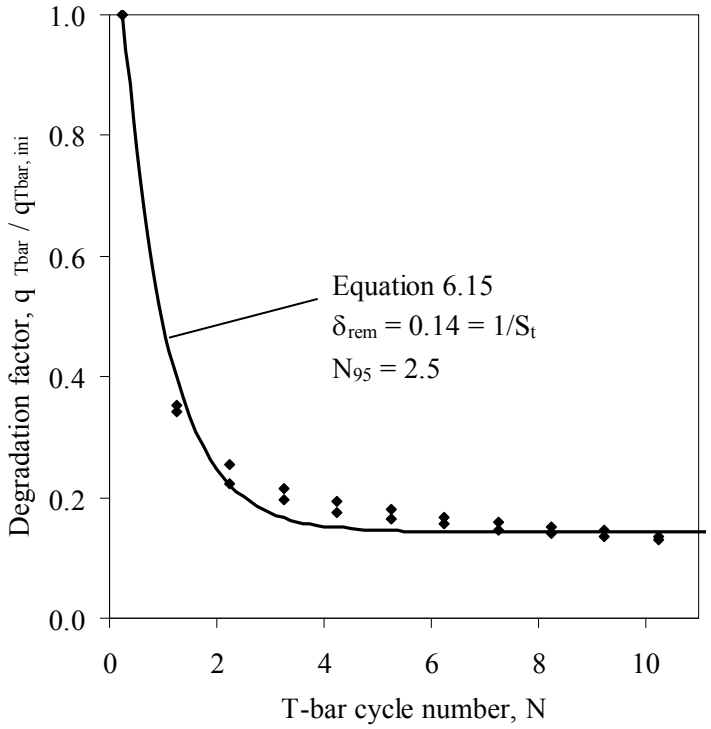

Figure 6.8. T-bar penetration resistance degradation with cycling

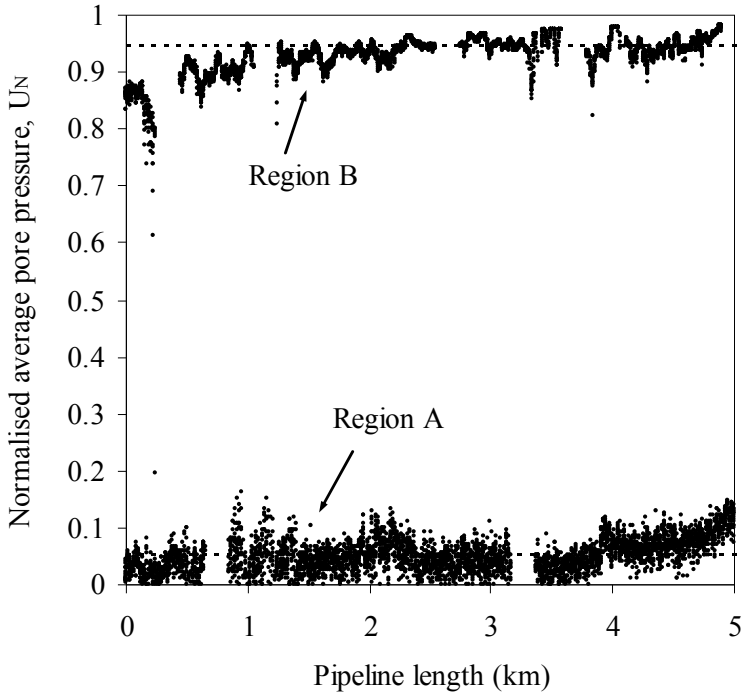

Figure 6.9. Average pore pressure dissipation around pipe

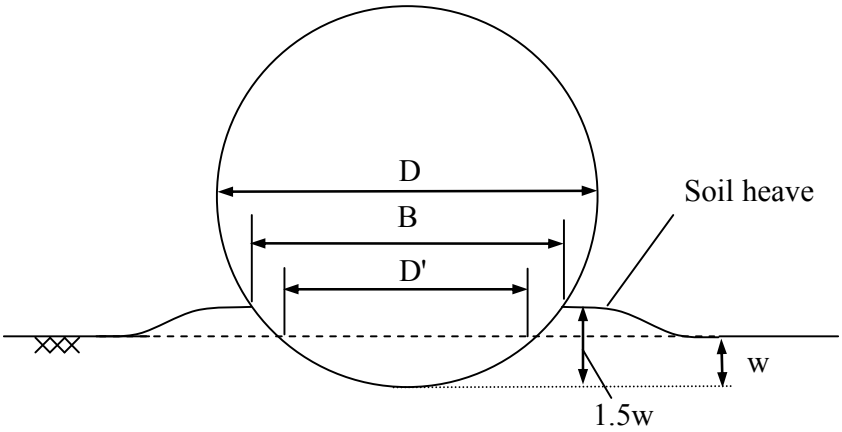

Figure 6.10. Definition of pipe-soil contact width and length

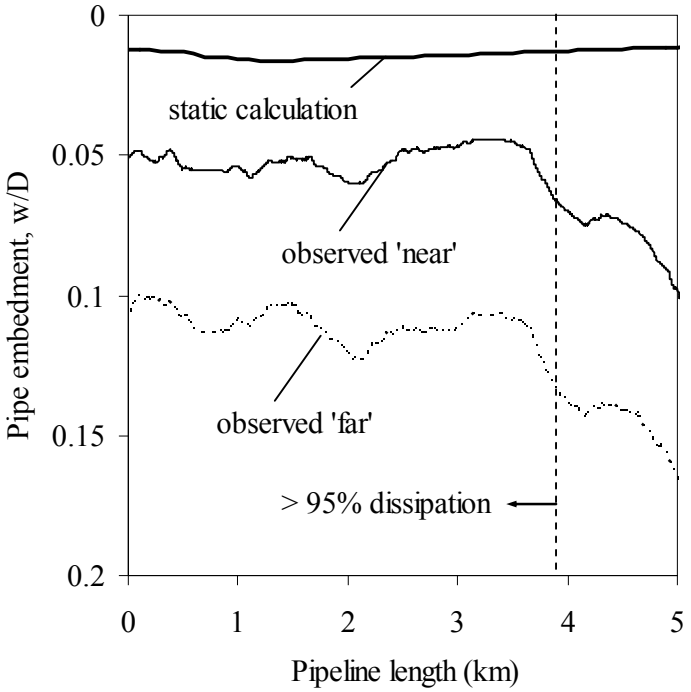

(a)

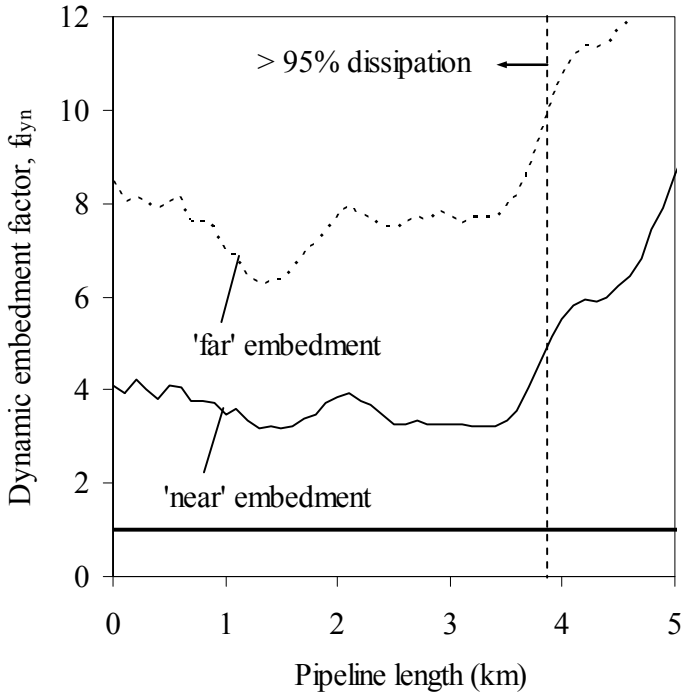

(b)

Figure 6.11. Region A back-analysis showing (a) comparison of static calculation to observed pipe embedment and (b) dynamic embedment factor

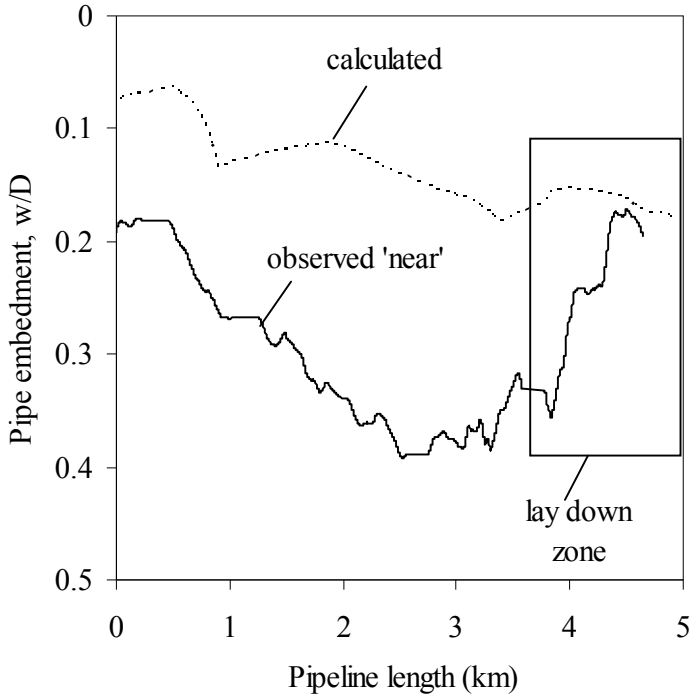

(a)

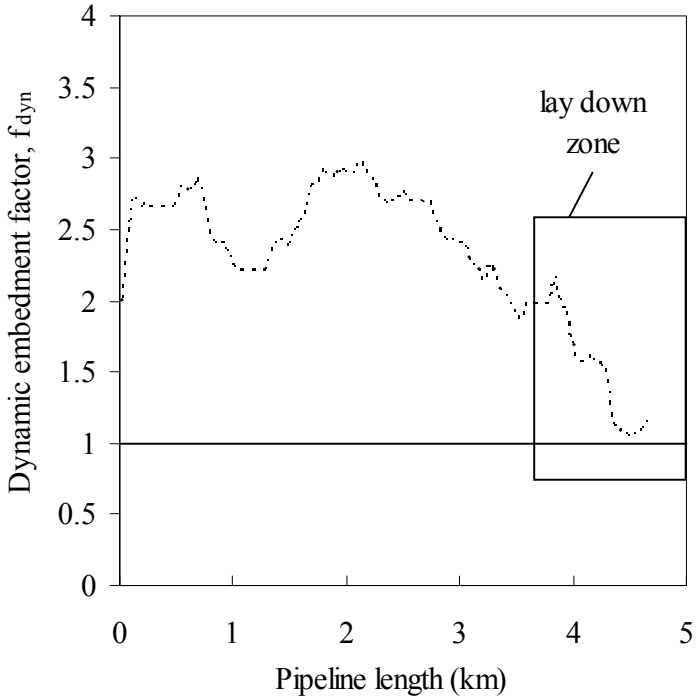

(b)

Figure 6.12. Region B back-analysis showing (a) comparison of static calculation to observed pipe embedment and (b) dynamic embedment factor

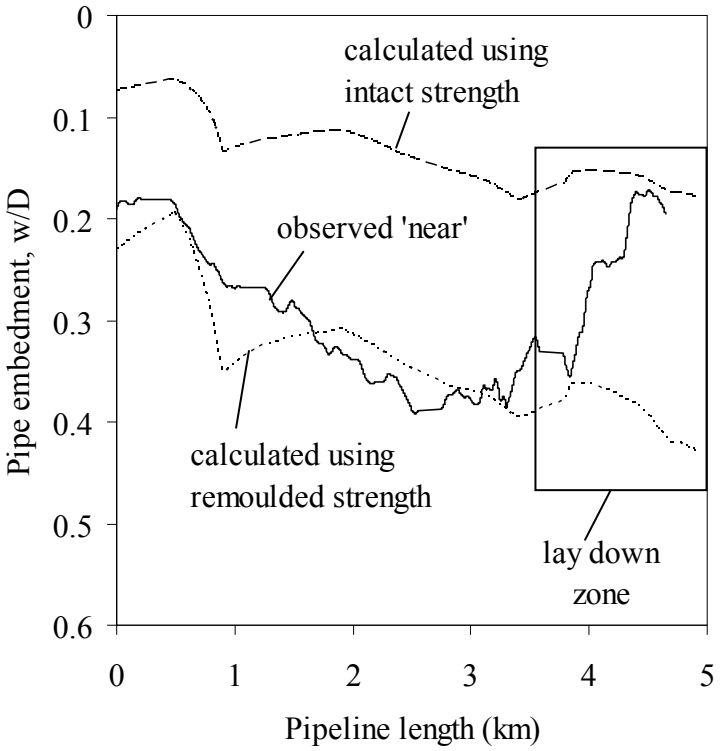

Figure 6.13. Region B back-analysis showing comparison of static and modified static calculations to observed pipe embedment

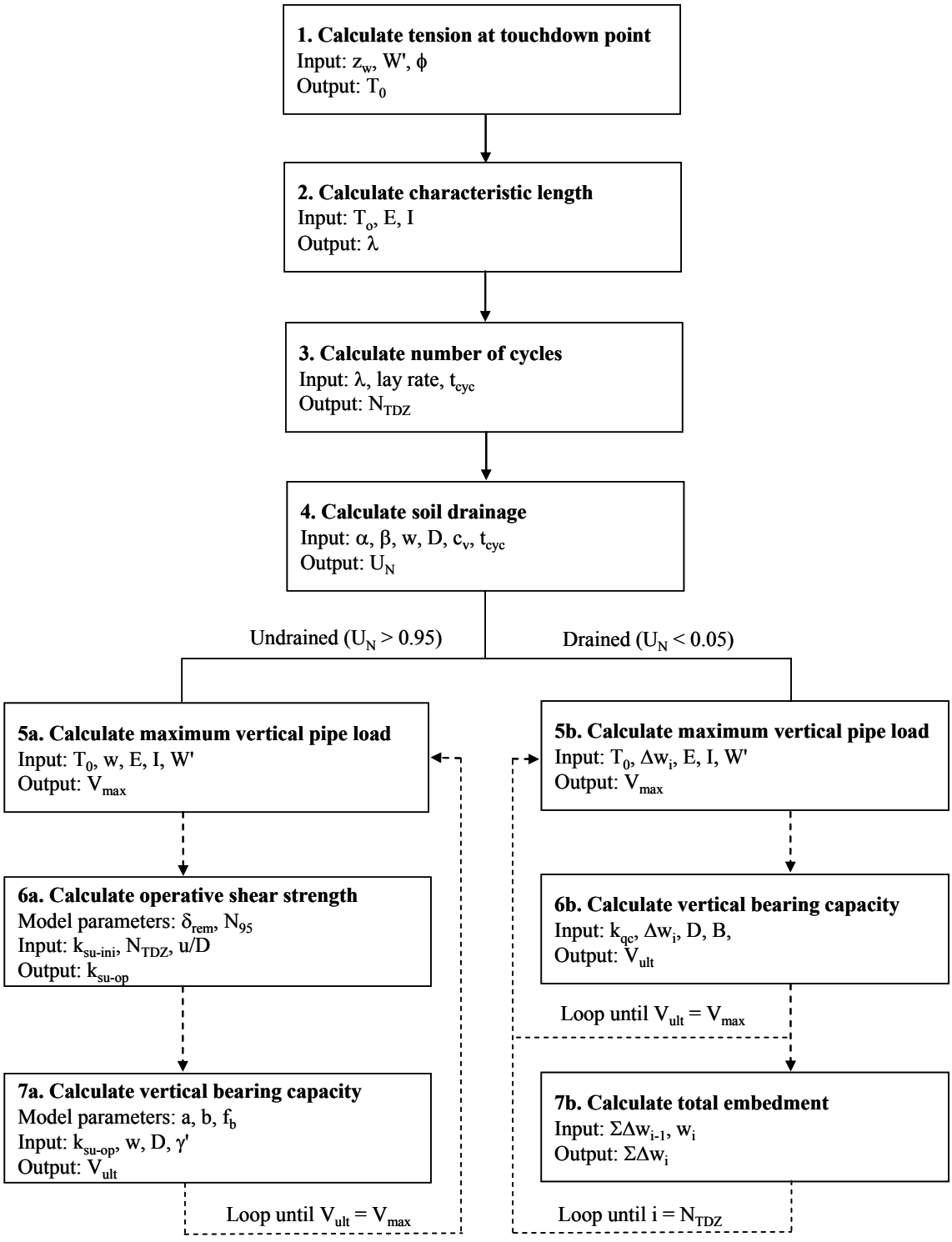

Figure 6.14. Flowchart of cycle-by-cycle calculation framework

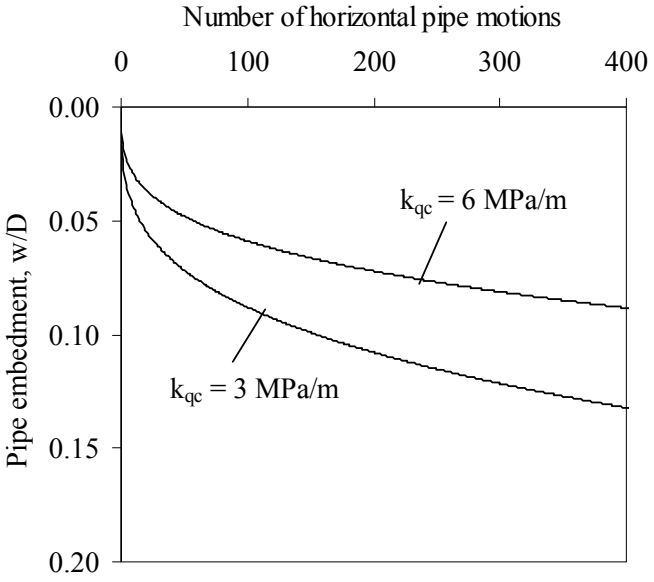

(a)

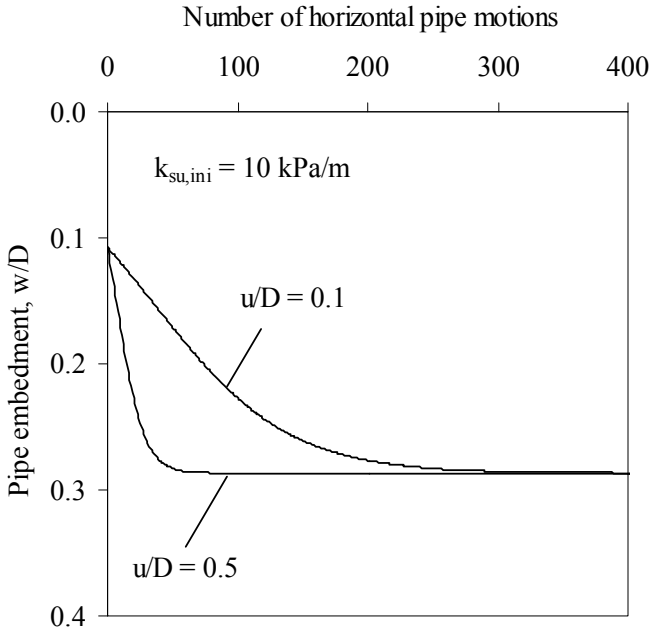

(b)

Figure 6.15. Example cycle-by-cycle embedment profiles for (a) drained embedment and (b) undrained embedment

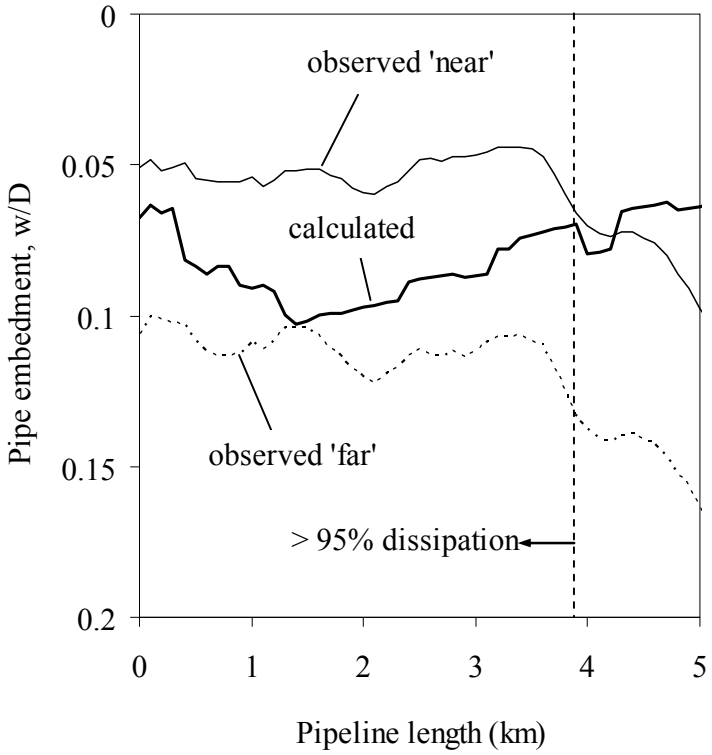

(a)

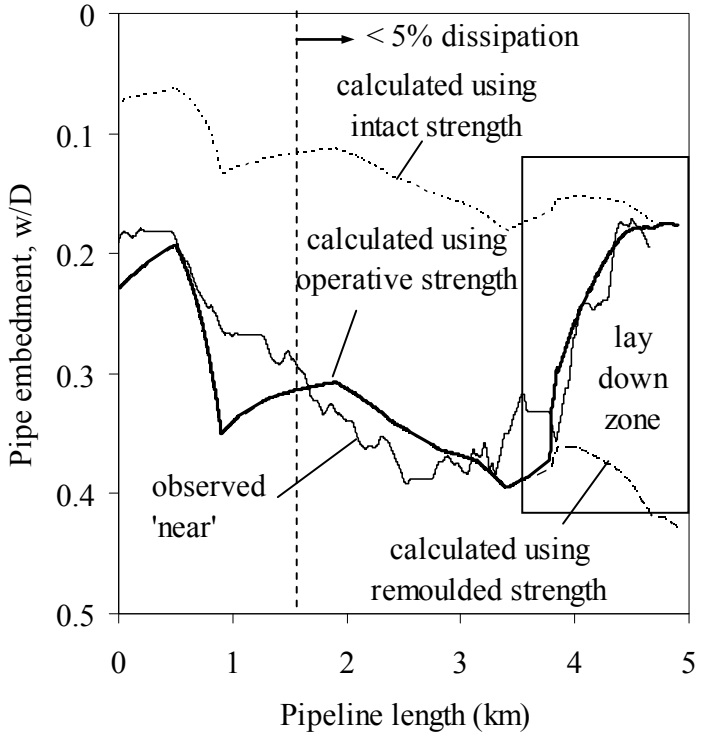

(b)

Figure 6.16. Comparison of cycle-by-cycle calculations to observed pipe embedment in (a) Region A using drained method and (b) Region B using undrained method

CHAPTER 7. MODELLING THE EMBEDMENT PROCESS DURING OFFSHORE PIPE LAYING ON FINE-GRAINED SOILS

The paper presented in this chapter describes a suite of centrifuge model tests that were performed to investigate the different contributions from soil softening and combined vertical and horizontal loading lay effects on dynamic pipe embedment in soft clay soil. The motivation for the work stemmed from the limitations on quantifying lay effects using field data alone. Similarly, numerical simulations, while useful to perform parametric analyses, are limited in the manner in which the soil is modelled and consequently responds. Model testing in a geotechnical centrifuge allowed the different embedment mechanisms to be isolated, and therefore the effects of soil softening and combined loading were more closely investigated and quantified.

The insights from the model tests allowed for development and calibration of a simple model, extended from work by others, to track pipe embedment through cycles of vertical loading and horizontal displacement. The model incorporates the soil softening contributions to embedment as described in Chapter 6, and has links to plasticity theory to quantify the contribution to dynamic embedment resulting from horizontal movements. The model is compared to the observed as-laid embedment from the field studies. It is shown to provide a useful framework to assess as-laid pipeline embedment in fine-grained soils that represents a significant improvement to existing design methods, capturing an appropriate balance between theory and empiricism.

Westgate, Z.J., White, D.J. & Randolph, M.F. (2013). Modelling the embedment process during offshore pipe laying on fine-grained soils, *Canadian Geotechnical J.*, Vol. 50, No. 1, pp. 15-27.

7.1 ABSTRACT

Subsea pipelines are becoming an increasingly significant element of offshore hydrocarbon developments as exploration moves into deep water environments further from shore. During the lay process, pipelines are subject to small amplitude vertical and horizontal oscillations, driven by the sea state and lay vessel motions. Centrifuge model tests have been used to simulate these small amplitude lay effects, with varying degrees of idealisation relative to the real lay process. In the soft soils found in deep water, pipe embedment can exceed a diameter or more, thus significantly affecting the lateral pipe-soil interaction, axial resistance, and thermal insulation.

In this paper, results from centrifuge model tests are used to calibrate a model for calculating the dynamic embedment of a subsea pipeline. The model uses elements of plasticity theory to capture the effects of combined vertical and horizontal loading, and incorporates the softening of the surrounding soil as it is remoulded due to the pipeline motions. Influences from the lay rate, lay geometry and sea state are included in the calculation process. The model is compared to observed as-laid pipeline embedment data from field surveys at three different offshore sites. Using site-specific soil parameters obtained from in situ testing and idealised pipe loads and motions to represent the load and displacement patterns during offshore pipe laying, the model is shown to capture well the final as-laid embedment measured in the field surveys.

7.2 INTRODUCTION

As offshore hydrocarbon developments have advanced into deeper water, subsea pipelines have become a larger component of project cost. The as-laid embedment of a subsea pipeline is an important design parameter, influencing the hydrodynamic response, lateral buckling, axial walking, and thermal insulation (Cathie et al. 2005, Bruton et al. 2006). During the lay process, the pipeline is subject to vertical and horizontal oscillations that are driven by the sea state and vessel motion. These oscillations, or dynamic lay effects, cause the soil to soften and displace, resulting in increased pipeline embedment. The length of pipeline-seabed contact where lay effects occur is termed the touchdown zone, illustrated in Figure 7.1. Near the front of the touchdown zone – towards the lay vessel – the pipeline experiences cycles of seabed separation, influenced by the severity of the sea state. The vertical loading and

horizontal oscillations attenuate through the touchdown zone due to the increasing restraint associated with pipeline embedment. Quantifying the influence of these dynamic effects on the as-laid pipeline embedment is challenging.

7.2.1 Static penetration of pipes

The static bearing capacity of a pipeline on undrained soil is well established, based on plasticity solutions (Murff et al. 1989, Randolph & White 2008b), finite element analyses (Aubeny et al. 2005, Merifield et al. 2009, Chatterjee et al. 2012), and model testing (Dingle et al. 2008). Figure 7.2 shows the general shape of the relationship between the normalised pipe embedment w/D and the normalised pipe bearing capacity V/s_uD, where V is the vertical pipe-soil load, s_u is a characteristic undrained soil shear strength, and D is the pipe diameter. For a pipeline being laid from a vessel, the maximum value of V within the touchdown zone is greater than the submerged pipe weight W' due to the catenary effect. This stress concentration can be estimated from the lay tension, pipe bending stiffness and the seabed response (Pesce et al. 1998, Lenci & Callegari 2005, Randolph & White 2008a, Palmer 2009).

7.2.2 Dynamic lay effects

Dynamic lay effects increase the as-laid embedment beyond simply the penetration under the maximum static pipe-soil load. These mechanisms include:

- increased vertical pipe-soil load from the vertical oscillations of the pipeline catenary;
- reduced soil strength due to remoulding and disturbance;
- reduced vertical bearing capacity for combined vertical-horizontal loading; and
- generation of a trench around the pipe, locally lowering the seabed.

Pipeline oscillations in the touchdown zone soften the soil and also entrain water, which leads to a further reduction in strength. Studies of purely vertical pipe movements have shown that both the rate and magnitude of soil softening is significantly increased due to water entrainment (Gaudin & White 2009). In rough sea states, transient reductions in lay tension can occur which increase the vertical load, or pipe bearing pressure, as shown by numerical simulations (Westgate et al. 2010a) and field monitoring (Westgate et al. 2012). Combined loading reduces the available vertical bearing capacity of the soil, as shown through theoretical plasticity analysis for planar contacts (Green 1954)

and also shallowly-embedded pipes under horizontal loading (Randolph & White 2008b) and axial loading (Yan et al. 2011). Lastly, horizontal oscillations can displace the seabed soil laterally, creating a trench by lowering the seabed elevation adjacent to the pipe, as shown via experimental simulations in a geotechnical centrifuge (Cheuk & White 2011) and via field observations (Lund 2000b, Westgate et al. 2010c).

Existing models for assessing dynamic pipe embedment

Quantifying dynamic lay effects is complicated by the nature of the lay process, where the presence of each mechanism, and its relative influence, changes as an element of pipeline moves through the touchdown zone. Experimental studies have supported a tentative model in which dynamic pipe embedment can be assessed on a cycle-by-cycle basis (Cheuk & White 2011). The model links progressive soil softening to cumulative horizontal pipe displacements, at a rate related to the strength degradation measured in cyclic T-bar tests. The progressive embedment of the pipe is then assessed from the combined vertical-horizontal bearing capacity for the present soil strength. Similar strain-based strength degradation models are common in offshore foundation design (e.g. Andersen 1991), and combined loading models have been proposed for monotonically loaded pipelines in fine-grained soils (e.g. Hodder & Cassidy 2010). However, the complexity of deformations around an oscillating pipe makes such models cumbersome for assessing as-laid pipeline embedment. Models for cyclic pipe-soil interaction purely in the vertical plane have been developed for steel catenary riser behaviour (Bridge et al. 2004, Clukey et al. 2005, Aubeny et al. 2008, Randolph & Quiggin 2009). However, these models do not include any influence of horizontal motions. More general models that incorporate the effects of combined vertical and horizontal pipe motions on pipe embedment have not been developed.

7.2.3 Objective and focus of study

The objective here was to investigate pipe embedment on fine-grained soils by systematically isolating each of the dynamic lay effect mechanisms through simulations in a geotechnical centrifuge. Different types of dynamic lay processes were simulated, with the aim of separating the effects listed previously. The results of the simulations were then back-analysed to calibrate a modified version of the cycle-by-cycle model for pipe embedment proposed by Cheuk & White (2011), providing a framework that quantifies the different effects separately. The modified model has been evaluated

against as-laid pipeline embedment from field surveys, based on idealisations of the vertical loads and horizontal motions of the pipeline at the seabed (Westgate et al. 2010c, Westgate et al. 2012).

7.3 EXPERIMENTAL TEST PROGRAMME

7.3.1 Test apparatus

Centrifuge model tests were performed using the beam centrifuge at the University of Western Australia (Randolph et al. 1991). A 20 mm diameter by 120 mm length model pipe was tested at a centrifuge acceleration of 25 g, resulting in a prototype pipe diameter of 0.5 m. The equivalent prototype depth of the soil model was 3.0 m. Vertical and horizontal actuators controlled the pipe motions through an instrumented loading arm capable of recording the vertical and horizontal load applied to the pipe. Data acquisition and control was through in-house software capable of modelling sophisticated sequences of pipe motions (Gaudin & White 2009, De Catania et. al. 2010).

7.3.2 Soil sample preparation

The soil sample was prepared by mixing kaolin powder with water to approximately twice its liquid limit (~120% water content), then pouring it into the strongbox over a 10 mm (model scale) sand drainage layer covered with a geotextile. The sample was spun at 100 g in the centrifuge for 2 days, after which the upper 10 mm (model scale) of the sample was removed and the sample was spun at the lower acceleration of 25 g, creating a lightly overconsolidated clay sample with a small mudline strength intercept.

7.3.3 Strength characterisation

A 5 mm diameter, 30 mm long T-bar penetrometer was used to characterise the strength of the soil after the preparation was complete. The undrained shear strength, s_u, was determined from the T-bar penetration resistance, $q_{T\text{-}bar}$, using a T-bar bearing factor, $N_{T\text{-}bar,}$ of 10.5 (Stewart & Randolph 1994) with an adjustment to this factor applied near to the soil surface, following White et al. (2010). The resulting initial strength profile was idealised as a linear variation with mudline strength intercept, s_{um}, and strength gradient, k_{su}, as:

$$s_{u-ini} = 0.8 + 3z \text{ kPa} \tag{7.1}$$

where z is the depth below the soil surface in metres. Cyclic sequences of T-bar penetration and extraction were performed to quantify the softening response of the soil. Deep cycles were performed where the T-bar remained buried below the soil surface by several diameters, as well as surface cycles where the T-bar was fully extracted from the soil during each cycle. The rate of T-bar penetration and extraction was sufficient to ensure undrained soil conditions, with velocity, v, equal to 1 mm/s, normalised as $vd_{T\text{-}bar}/c_v$ (with $d_{T\text{-}bar}$ being the T-bar diameter equal to 5 mm, and c_v the consolidation coefficient of the soil not greater than 0.1 mm^2/s) (e.g. Randolph & Hope 2004).

The degradation in strength during cyclic T-bar testing can be modelled using an exponential decay function linked to the number of cycles, which is a proxy for the accumulated shear strain (Einav & Randolph 2005, Zhou & Randolph 2009). The model may include an additional more brittle component of degradation that can be attributed to the structure of the soil (Randolph et al. 2007). The strength degradation response can therefore be expressed as:

$$\delta_{op} = \frac{s_{u-op}}{s_{u-ini}} = \delta_{rem} + \left(1 - \delta_{rem} - \delta_{str}\right)e^{-3N/N_{95,rem}} + \delta_{str}e^{-3N/N_{95,str}} \tag{7.2}$$

where δ_{rem} is the fully remoulded strength degradation factor, defined as:

$$\delta_{rem} = \frac{1}{S_{t,cyc}} \tag{7.3}$$

and δ_{str} is the component of strength degradation due to the loss of soil structure, defined as:

$$\delta_{str} = 1 - \frac{1}{S_{t,in-out}} \tag{7.4}$$

The cyclic sensitivity, $S_{t,cyc}$ (in terms of resistances) is the ratio of the initial penetration resistance to the stable penetration resistance after many cycles. $S_{t,in\text{-}out}$ is the ratio of the initial penetration resistance to the initial extraction resistance. By definition, the cycle number for loss of structure, $N_{95,str}$, is 0.75, corresponding to the first cycle of penetration and extraction and noting that the initial penetration represents cycle number N = 0.25 (Randolph et al. 2007). The cycle number, $N_{95,rem}$, for 95% resistance degradation is obtained by fitting the measured degradation response. Example fits to the T-bar test data in the kaolin clay centrifuge sample, for both deeply-cycled and

surface-cycled tests, are shown in Figure 7.3, with the corresponding degradation parameters listed in Table 7.1. As indicated, the degradation responses are markedly different for deep and surface cycling and can also vary significantly for different soil types, as shown by Gaudin & White (2009) for high plasticity clay and carbonate silt.

7.3.4 Testing programme

The test programme comprised a baseline test (Test A) in which the pipe was statically penetrated to a depth of 1 diameter, as well as four dynamic pipe laying simulations (Tests B to E), in which specific embedment mechanisms were sequentially introduced. For each dynamic simulation, the pipe was initially penetrated statically to approximately one third of the pipe diameter. A relatively heavy pipe was modelled in order to generate significant dynamic embedment under the small amplitude horizontal oscillations. Axial oscillations were not considered in this study and it is expected that the effects of axial loading on the vertical bearing capacity during pipe laying are minor compared to the relatively larger horizontal oscillations.

The total number of vertical or horizontal cycles varied from 120 to 1200, which represents the typical range of oscillations that a pipe will be subjected to as it passes through the touchdown zone while being laid, with the upper value representing a situation where a period of downtime delays laying. In all tests the rate of initial monotonic penetration was equal to 0.1 mm/s, which ensured undrained conditions during monotonic penetration (i.e. $vD/c_v > 10$, Randolph & Hope 2004). The pipe displacement rate during cycling ranged from 0.25 to 3 mm/s, or cyclic periods, t_{cyc}, ranging from about 7-16 s. This corresponds to dimensionless times generally less than $T = 0.001$, where $T = t_{cyc}c_v/D^2$, which result limit the dissipation of excess pore pressures generated during cyclic loading (Randolph & Hope 2004, Westgate et al. 2012).

The test details are presented in Table 7.2. Test B targeted soil softening and water entrainment during large amplitude vertical pipe motions. The pipe in this test was fully extracted from the soil during each cycle and was penetrated to a target vertical load of $V/D = 5.7$ kPa, all in the absence of horizontal motions. Tests C and D targeted soil softening and combined vertical and horizontal loading. In both of these tests the pipe remained in contact with the soil during cycles of fixed-amplitude horizontal motions, minimising water entrainment. In Test C, the pipe was held under a constant vertical

load of V/D = 5.7 kPa. Test D varied from Test C by including vertical load cycles, with an average value equal to the static vertical load in Test C. Within each cycle of horizontal motion, the pipe was subjected to two cycles of vertical loading between 3.5 kPa and 8.0 kPa, representing a peak-to-peak amplitude of about 75% of the static V/D. This pattern of loading for Test D is presented in Figure 7.4a, which shows that the experimental data consistently follow the demanded profiles of vertical load and horizontal displacement. The resulting cyclic accumulation of pipe embedment and increase in horizontal resistance during Test D is shown in Figure 7.4b. All imposed oscillations – both vertical load and horizontal displacement – were sinusoidal in time.

Test E was the most onerous laying simulation, targeting soil softening and water entrainment combined with cyclic vertical loading and horizontal displacement. The pipe in this test underwent one cycle of extraction from the soil and vertical loading to a load of only V/D = 4.4 kPa during each cycle of horizontal motion. The change in soil consistency during the modelled lay effects is shown in Figure 7.5. While the soil breaks into blocks of intact material for a statically-penetrated pipe (Test A, Figure 7.5a), in Test E the soil surrounding the pipe degrades into slurry due to the extremely onerous cyclic motions (Figure 7.5b). Tests B, C and D represent intermediate cases relative to these two extremes.

7.4 MODELLING DYNAMIC PIPE EMBEDMENT

Before presenting the remaining test results, the model used to interpret and back-analyse the results is described. The model is based on that presented by Cheuk & White (2011), modified to allow tracking of the full pipe displacement throughout cyclic vertical loading and horizontal oscillations of varying amplitude; by contrast the original model was limited to tracking pipe embedment on a cycle-by-cycle basis. The modelling approach utilises theoretical V-H yield surfaces for partially embedded pipes, combined with a soil softening model calibrated to cyclic T-bar tests. Full details are provided in Cheuk & White (2011) and are summarised below, together with the proposed modifications. The model parameters are listed in Table 7.3.

7.4.1 Model description

The dynamic embedment process is modelled using features of yield surfaces for V-H bearing capacity in undrained conditions, an example of which is shown in Figure 7.6

(Merifield et al. 2008). Yield surfaces have been derived analytically based on plastic limit analysis and through numerical modelling, and depend on pipe roughness, strength heterogeneity, bonding of the pipe-soil interface, and pipe embedment (Randolph & White 2008b). The bearing capacity under purely vertical load is defined as V_{max}. The parallel point, $(V/V_{max})_{pp}$, corresponds to the vertical load level that results in purely horizontal movement at failure, and can be assessed from the failure envelopes by invoking normality. $(V/V_{max})_{pp} = 0$ for fully bonded or deeply buried pipes, and increases to $(V/V_{max})_{pp} = 0.5$ for an unbonded pipe on the soil surface. In this paper, $(V/V_{max})_{pp}$ is taken as a constant value of 0.5, reflecting the unbonded condition. The basis for this assumption is that there is unlikely to be significant tension sustainable at the pipe surface, due to soil softening and the tendency for weak surface soils to be carried downward by the pipe during laying.

For the undrained conditions being modelled here, the assumption of normality (and the neglect of elastic behaviour) allows the slope of the yield surface to be used to define the pipe trajectory during horizontal motion. The parameter that controls the direction of the pipe motion at failure, λ, varies approximately linearly with load level, V/V_{max}, in the range $0.2 < V/V_{max} < 0.8$ (Cheuk & White 2011) allowing the direction of pipe movement to be written as:

$$\left(\frac{dw}{du}\right)_f = \lambda\left(\frac{V}{V_{max}} - \left(\frac{V}{V_{max}}\right)_{pp}\right) \tag{7.5}$$

leading to increments of pipe embedment given by:

$$\frac{\Delta w}{D} = \left(\frac{dw}{du}\right)_f\left(\frac{\Delta u}{D}\right) \tag{7.6}$$

where $\Delta u/D$ is the incremental horizontal pipe displacement.

The vertical bearing capacity of the soil is affected by the soil strength and soil buoyancy, and is expressed as:

$$\frac{V_{max}}{D} = N_c s_{u-op} + N_b \gamma' w \tag{7.7}$$

where $s_{u\text{-}op}$ is the operative undrained shear strength at depth, w (Equation 7.2), γ' is the soil effective unit weight, and w is the pipe invert embedment. N_c and N_b are bearing

capacity factors for soil strength and soil buoyancy, respectively. N_c can be approximated as:

$$N_c = a\left(\frac{w}{D}\right)^b \tag{7.8}$$

where fitting parameters a and b capture the influence of soil strength heterogeneity, pipe roughness, pipe penetration rate and strain softening (Aubeny et al. 2005, Merifield et al. 2009, Chatterjee et al. 2012). N_b can be written as:

$$N_b = \frac{f_b A_s}{Dw} \leq \frac{\pi D}{4w} \tag{7.9}$$

where the buoyancy factor f_b captures the influence of the soil heave adjacent to the pipe, with a value of 1.5 being commonly adopted (Merifield et al. 2009), and A_s is the area of the pipe within the soil.

The effect of the softened soil strength on the bearing capacity due to remoulding can be assessed using a modified form of Equation 7.2, substituting the cumulative pipe movement for the number of T-bar cycles, so that the operative strength is expressed as:

$$\delta_{op} = \delta_{rem} + \left(1 - \delta_{rem} - \delta_{str}\right)e^{-3\alpha_N(rem)} + \delta_{str}e^{-3\alpha_N(str)} \tag{7.10}$$

where α_N accounts for the cumulative pipe displacement, expressed as:

$$\alpha_N = \zeta^r \frac{\Sigma(s/D)}{(\Sigma s/D)_{95}} \tag{7.11}$$

where s/D is the total pipe displacement per cycle, for $w > 0$ (when $w < 0$ the pipe is above the soil, so it is not remoulding it). The sum of the pipe displacement required to cause 95% strength degradation, $(\Sigma s/D)_{95}$, is analogous to the parameter N_{95} from the cyclic T-bar test. Zhou & Randolph (2009) showed that the vertical extent of the failure mechanism around a penetrating T-bar is approximately 1.5 diameters, so it can be assumed that the remoulding during a single pass of a T-bar penetrometer is equal to the remoulding caused by a cumulative pipe movement of 1.5D. Since 1 cycle involves two passes of the T-bar, $(\Sigma s/D)_{95} = 3N_{95}$ (Cheuk & White 2011). A discounting parameter, ζ, is included in Equation 7.9 to reflect that, as the pipe embeds, the soil below the oscillating pipe is less affected by the earlier oscillations and so the cumulative damage

is lower than if all cycles had remoulded the same zone of soil. The depth-discounting parameter, ζ, is defined as:

$$\zeta = \frac{w_{avg}}{w} = \frac{0.5(w + w_{static})}{w} \tag{7.12}$$

A fitting parameter r is included to moderate the depth-discounting effect (Equation 7.11), as a simplification to the more complicated procedure of tracking the cumulative degradation through different soil horizons over the depth of embedment.

7.4.2 Back-analyses using modified embedment model

The modified model performance was assessed in three ways. First, a base case comparison was performed that only considered soil softening in the calculation of embedment, i.e. the effects of horizontal pipe movement on the pipe penetration were ignored. Instead, Equations 7.10-7.12 were used to assess the operative soil strength around the pipe throughout the lay process, and the resulting embedment was calculated based on V_{max}, from Equations 7.7-7.9. This calculation used either the deep or surface T-bar parameters (Table 7.1) without any empirical adjustment to the softening response, i.e. r = 0 in Equation 7.12. This back-analysis was done for all four lay simulations.

Second, a base case comparison was performed using both soil softening and the flow rule (to add the increasing embedment that results from combined V-H loading), with either the deep or surface T-bar parameters and r = 0 (i.e. no depth-discounting effect). This back-analysis was performed for Tests C and D, where the pipe remained in contact with the soil (so V/V_{max} was always defined).

Lastly, an optimised comparison was performed for Tests C and D using both soil softening and the flow rule, based on the average of the deep and surface T-bar parameters (Table 7.1), and with the parameter r calibrated to the observed embedment. The adopted parameters in each of these back-analyses are listed in Table 7.4. The bearing capacity was approximated using Equation 7.8 by fitting the parameters a and b to the pipe penetration response from the static penetration case (Test A), resulting in a = 7 and b = 0.3. This simplified penetration resistance profile approaches $N_c = 10.5$ at a pipe embedment of about 3D, and is consistent with the expected profile for this particular soil strength to weight ratio ($s_u/\gamma'D$) (White et al. 2010).

Back-analysis 1: soil softening only

Comparisons of the observed pipe embedment and the calculated pipe embedment using only soil softening are shown in Figure 7.7. In these calculations, the embedment reached in each cycle is calculated from the softened soil strength (using Equations 7.7-7.12) and the maximum vertical load in that cycle.

The rate of pipe embedment is slightly overestimated during the large-amplitude vertical displacements of Test B (Figure 7.7a), suggesting that a portion of the pipe displacement near the soil surface does not contribute to strain accumulation. The observed embedment eventually reaches the calculated embedment using the deep T-bar degradation parameters, suggesting that the softening model alone (excluding any element of water entrainment) is sufficient for simulating dynamic embedment during vertical pipe motions in isolation. However, with continued cycling some element of water entrainment may develop, as the pipe embedment gradually continues towards that calculated using the surface T-bar degradation parameters.

For Test E, the calculated rate of embedment is very rapid, with the combined vertical and horizontal oscillations causing the operative strength to reach the fully remoulded value (excluding water entrainment) within a small number of cycles (Figure 7.7b). In contrast to Test B, the observed embedment rapidly exceeds the calculated embedment using the deep degradation response, and continues to increase towards the calculated embedment using the surface degradation response (i.e. the minimum credible remoulded strength), suggesting a significant water entrainment component. The observed embedment eventually exceeds the surface degradation response at very high cycle numbers ($N > 1000$), reflecting the additional destabilising influence of the horizontal loading which is neglected in this back-analysis case. Due to the complexity of the pattern of pipe loads and motions in Test E, which do not lend themselves to simulation using the proposed model, no further back-analyses were performed for this test.

For Test C, the observed pipe embedment exceeds the calculated embedment based on softening alone, even when using the surface degradation parameters (Figure 7.7c). The observed pipe embedment for Test D is similar to that of Test C (Figure 7.7d), but the calculated values are greater due to the higher vertical load.

From these comparisons, two clear observations can be made. First, the observed embedment for tests with combined horizontal and vertical loading generally exceeds the calculated embedment at the end of each test, showing that soil softening alone is not sufficient to explain the observed high embedments; an additional embedment mechanism must be present. Second, the observed rate of embedment is slower than calculated by direct analogy with T-bar tests. This supports the explanation that the remoulding action of the pipe movement is not concentrated within a single zone of soil, but is progressively transferred to new soil that is encountered at greater depth as the pipe moves downwards. This is the depth-discounting effect modelled by Equation 7.12, and the 'r' parameter in Equation 7.11.

Back-analysis 2: soil softening and combined loading

To improve on the first set of back-analyses, the influence of the combined V-H loading was introduced (via Equations 7.5 and 7.6), while retaining r = 0 (i.e. no depth-discounting is applied to the cumulative softening). The comparisons of the observed pipe embedment and the calculated pipe embedment using both soil softening and the flow rule are shown in Figure 7.8. In both Tests C and D, the calculated rate of embedment still remains too high compared to the observed response, but the final embedment is better predicted, progressing towards a steady state embedment between the embedment calculated using the deep and surface degradation responses. This shows that inclusion of the combined loading effect improves the accuracy of the predicted final embedment.

A further improvement in the prediction accuracy is achieved by using the average of the deep and surface degradation parameters in Equation 7.10, coupled with a depth-discounting adjustment using r = 4 in Equation 7.11 (Figure 7.9a, b). The depth-discounting effect does not change the final embedment, only the rate at which this is approached. This further improvement appears to indicate that the depth-discounting aspect of the model is necessary in order to scale from the softening rate observed in the T-bar test to the rate occurring during the lay process.

The pipe trajectory during embedment in Tests C and D is shown in Figure 7.10. The general shapes of the two pipe trajectories are captured using the optimised model, even though the rate of pipe embedment in Test C is overpredicted during the initial cycles (Figure 7.10a). For Test D, which included a varying vertical load, the pipe trajectory

shows greater non-linearity, and the model, due to the assumptions of constant $(V/V_{max})_{pp}$ and λ, does not accurately capture the detailed trajectory (Figure 7.10b).

7.5 SIMULATING AS-LAID PIPELINE EMBEDMENT

The agreement between the centrifuge test simulations and the calculated pipe embedment using the modified model is encouraging, given the complex nature of the pipe-soil interaction during the simulations. In this section, the modified model is used to simulate pipeline laying in the field using an idealised pattern of constant vertical loading and cyclic horizontal pipe displacement through the touchdown zone. The results are then compared to the measured embedment from as-laid pipeline surveys.

7.5.1 Modelling the pipeline loads and motions

During pipe laying, the patterns of pipeline loads and motions are highly irregular. These vertical loads and horizontal oscillations can be modeled numerically, but require some site-specific details such as the sea state and lay vessel response. For the current analysis, the changing vertical load and horizontal displacement through the touchdown zone has been idealised in a simple manner, as described below.

Static profiles of the pipe-soil catenary force can be calculated theoretically (e.g. Lenci & Callegari 2005, Palmer 2009). However, these profiles depend on the seabed secant stiffness, which varies through the touchdown zone due to the non-linearity of the load-penetration response. The effect of the changing seabed stiffness for a typical deep water pipeline is shown in Figure 7.11, with stiffness, k, defined as the pipe-soil contact force, V, divided by the pipe embedment, w. As the stiffness reduces, two effects are observed: (i) the location of the peak force moves further away from the touchdown point, and (ii) the length of the touchdown zone increases, which increases the number of motions that an element of pipe is subjected to during laying. A parameter to quantify the length of the touchdown zone is the characteristic length, λ_{TDZ}, (Pesce et al. 1998), calculated as:

$$\lambda_{TDZ} = \sqrt{\frac{EI}{T_0}} \tag{7.13}$$

where E is the elastic modulus of the pipeline, I is the second moment of area and T_0 is the bottom tension in the pipeline.

For the example pipeline in Figure 7.11, λ_{TDZ} captures the length of the touchdown under the initially higher stiffness values. Randolph & White (2008a) relate this parameter to the static peak catenary force, V_{max}, along the touchdown zone for a given seabed stiffness, expressed as

$$\frac{V_{max}}{W'} = 0.6 + 0.4\left[\frac{\left(\lambda_{TDZ}^{\ 2}\right)k}{T_0}\right]^{0.25} \tag{7.14}$$

where W' is the submerged pipeline weight. During pipe laying, the catenary-induced force changes due to changes in the pipe tension, resulting in transient increases in V that can exceed the static V_{max} value. Numerical simulations based on field conditions have shown that the dynamic peak catenary force, V_{dyn}, can attain nearly twice the value of V_{max} in severe sea states (Westgate et al. 2010a, Westgate et al. 2010c).

As with V_{max}, the dynamic peak catenary force, V_{dyn}, also depends on the seabed stiffness, which itself depends on the achieved embedment. It is therefore necessary to use an iterative process. For a given ratio, V_{dyn}/V_{max}, V_{dyn} was first calculated from the static V_{max} value for an estimated soil stiffness (Equation 7.14). The as-laid embedment was then calculated, and used to update k, V_{max}, V_{dyn} and hence the embedment, and the process repeated until convergence.

It is assumed that the normalised horizontal pipe displacement amplitude, u/D, attenuates to zero at the end of the touchdown zone (where V stabilises at the pipe weight), and can be idealised using a sinusoidal relationship linked to the period of pipe motion, t_{cyc}. In this study, the horizontal motion was modelled as:

$$\frac{u}{D} = \frac{u_{max}}{D} - \left[\sin\left(\frac{t}{t_{cyc}}\right)\right]\left(1 - \frac{t}{t_{TDZ}}\right)^{\beta} \tag{7.15}$$

where u_{max}/D is the maximum horizontal displacement amplitude occurring at the front of the touchdown zone (i.e. the vessel end) and β is an attenuation factor. Based on numerical simulations of pipe laying presented in Westgate et al. (2010a), β was taken as 3. The time, t, in Equation 7.15 represents the time during which a pipe element passes through the touchdown zone. The total time in the touchdown zone, t_{TDZ}, is calculated from the lay rate and the touchdown zone length, λ_{TDZ}.

7.5.2 Summary of field surveys

Three sets of as-laid field survey data were back-analysed and linked to the variation in lay conditions and soil parameters along the different pipeline routes. The field surveys represent a range of pipe laying conditions across three major offshore oil and gas producing regions. The pipelines at these sites ranged from 0.33 to 0.63 m in diameter, with submerged pipe weights between 0.22 and 0.95 kN/m, laid in fine-grained sediments with undrained shear strength gradients between 4 and 38 kPa/m (and negligible strengths at the mudline).

Calculations of pipe embedment using the soil softening and combined loading model components proposed in this paper, including the discounting parameter 'r' in Equation 7.11, were performed for each site using the pipeline properties, soil conditions, and model parameters representative of the site-specific lay conditions, which are listed in Table 7.5. Three calculations of the embedment process were performed for each site, representing the range in observed sea state. The parameters that are linked to the sea state are (i) the maximum horizontal displacement amplitude, u_{max}/D, and (ii) the ratio of the maximum dynamic vertical load to the maximum static vertical load, V_{dyn}/V_{max}. The adopted values for each site were based on video footage of pipe motions in the touchdown zone and numerical simulations of pipe laying. Full back-analyses of the as-laid embedment at each site are detailed in Westgate et al. (2010a, 2010c, 2012).

7.5.3 Comparisons of as-laid embedment to calculated embedment

The ranges of calculated embedment values are compared to histograms of as-laid embedment for each site in Figure 7.12. In all cases, the agreement between the calculated embedment and the observed embedment is excellent, capturing both the average embedment (when using the best estimate parameters) and the range of embedment (when using the extreme minima and maxima parameters).

As well as providing the as-laid embedment of the pipeline, the calculation process also leads to an estimate of the operative soil strength around the pipe at the end of laying, through Equations 7.10 – 7.12. The final degree of remoulding associated with the operative strength is given by δ_{op}, which is shown in the bottom row of Table 7.5. In general, δ_{op} is greater than the fully remoulded condition, given by δ_{rem}, although in the most severe lay conditions $\delta_{op} \sim \delta_{rem}$.

Since δ_{op} is considered directly within the calculations, and is linked quantitatively to the sea states and pipe motion inputs, it is possible to identify the relative influences of the soil softening embedment mechanism and the combined vertical and horizontal loading. In relatively benign conditions, where pipe motions are small, the soil strength is only slightly degraded (δ_{op} is close to 1), but the combined loading effect leads to significantly greater embedment than if the pipe were simply placed statically onto the seabed.

It is important to emphasize that this comparison is limited to typical pipe laying conditions in fine-grained soils. Conditions that were absent from the centrifuge simulations that may lead to further dynamic embedment processes include (i) longer downtime events during pipe laying where a larger ($N >> 1000$) number of cycles is imposed, causing the growth of a trench around the pipe, (ii) extreme lateral movements (e.g. of an SCR during a storm) in which the pipe can translate laterally to a new touchdown alignment, re-commencing the embedment process, (iii) episodes of reconsolidation prior to further cyclic loading, such as the whole life response at an SCR touchdown zone, (iv) dynamic embedment in partially-drained conditions, reducing the level of soil softening, and (v) scouring erosion of soil due to the pumping action of the oscillating pipeline.

Notwithstanding these limitations, the model represents a significant improvement to the assessment of as-laid pipeline embedment in fine-grained soils. The model could potentially be implemented as a pipe-seabed element response, for use in numerical simulations of pipe laying and SCR response. Currently, models for this behavior do not incorporate explicitly the soil softening and combined loading behaviour (Randolph & Quiggin 2009). However, both of these effects are shown in this study to be important, having a significant effect on the pipe embedment process.

7.6 CONCLUSIONS

This paper has presented data from centrifuge model simulations of pipeline laying in soft fine-grained soils. The simulations comprised different combinations of isolated or concurrent vertical and horizontal lay effects, which represent varying degrees of realism relative to the pipe lay process occurring in the field. The results of the centrifuge tests were used to calibrate a simple model for dynamic pipe embedment,

which is a modified version of a cycle-by-cycle model originally proposed by Cheuk & White (2011).

The model was then compared to as-laid field survey data from three locations that comprised a variety of lay conditions, pipeline properties, and soil conditions representative of typical offshore pipe laying in fine-grained soils. Realistic estimates were made of the pipe motions and loading at the seabed, quantified from detailed field observations and numerical modelling of the lay process. The model was shown to capture the average and range of observed as-laid embedment at each site, illustrating the approximate contributions from soil softening and combined vertical and horizontal loading on the as-laid embedment.

The model provides a simple approach for assessing as-laid pipeline embedment in fine-grained soils that explicitly accounts for dynamic lay effects, linked to the lay rate and sea state. This type of model could be incorporated into a pipe-seabed interaction element to be used in numerical modelling of pipe laying and steel catenary riser behaviour, encapsulating the effects of soil softening and combined loading behaviour in the touchdown zone.

Table 7.1. Centrifuge test sample: T-bar resistance degradation parameters

Parameter (field scale)	Value
Deep remoulding degradation factor, $\delta_{rem\text{-}deep}$	0.45
Deep remoulding degradation cycle number, $N_{95,rem\text{-}deep}$	3
Deep structure degradation factor, $\delta_{str\text{-}deep}$	0.14
Deep structure degradation cycle number, $N_{95,str\text{-}deep}$	0.75
Surface remoulding degradation factor, $\delta_{rem\text{-}surface}$	0.25
Surface remoulding degradation cycle number, $N_{95,rem\text{-}surface}$	4
Surface structure degradation factor, $\delta_{str\text{-}surface}$	0.15
Surface structure degradation cycle number, $N_{95,str\text{-}surface}$	0.75

Table 7.2. Centrifuge pipe embedment test details

Test ID	Vertical lay effects				Horizontal lay effects		Simulated dynamic embedment mechanism(s)
	Pipe bearing pressure, V/D (kPa)			Number of vertical cycles	Horizontal pipe displacement, u/D	Number of horizontal cycles	
	V_{min}/D	V_{avg}/D	V_{max}/D				
A	-	-	12	-	-	-	-
B	< 0	2.8	5.7	120	-	-	Soil softening with water entrainment
C	5.7			-	±0.05	420	Horizontal loading
D	3.5	5.7	8.0	280	±0.05	140	Combined vertical and horizontal loading
E	< 0	2.2	4.4	1200	±0.05	6000	Combined vertical and horizontal loading with water entrainment

Table 7.3. Calculation model parameters for centrifuge back-analysis

Parameter	**Symbol**	**Unit**	**Value**	**Comments**
Mudline strength intercept	s_{um}	[kPa]	0.8	Fit to T-bar test
Intact shear strength gradient	k_{su}	[kPa/m]	3	
Discounting factor	r	[-]	4	Fit to test data
Effective unit weight	γ'	[kN/m^3]	6	Assumed based on typical values
Fitting parameter (to strength profiles)	a	[-]	7	Fit to static pipe penetration response
Fitting parameter (to strength profiles)	b	[-]	0.3	
Parallel point	$(V/V_{max})_{pp}$	[-]	0.5	Assumed constant for simplicity
Flow rule parameter	λ	[-]	1.5	

Table 7.4. List of centrifuge back-analyses performed

Parameter	Symbol	Unit	Back-analysis case		
			Base case softening	**Flow rule and base case softening**	**Flow rule and optimised softening**
Mudline strength intercept	s_{um}	[kPa]	0.8	0.8	0.8
Intact shear strength gradient	k_{su}	[kPa/m]	3	3	3
Discounting factor	r	[-]	Not used (0)	Not used (0)	4
Effective unit weight	γ'	[kN/m^3]	6	6	6
Bearing capacity parameter (modified to suit strength profile)	a	[-]	7	7	7
Bearing capacity parameter (modified to suit strength profile)	b	[-]	0.3	0.3	0.3
Parallel point	$(V/V_{max})_{pp}$	[-]	Not used	0.5	0.5
Flow rule parameter	λ	[-]	Not used	1.5	1.5

Table 7.5. Site-specific pipeline and soil properties for field study comparisons

Parameter	Site A Westgate et al. 2010a			Site B Westgate et al. 2010c			Site C Westgate et al. 2012		
	A1	A2	A3	B1	B2	B3	C1	C2	C3
Outer pipe diameter, D (m)	0.39			0.33			0.63		
Submerged bearing pressure, W'/D (kPa)	0.56			1.4			1.5		
Bending rigidity, EI (MN/m^2)	37			44			230		
Water depth, z_w (m)	140			1350			600		
Lay angle, ϕ (deg)	68			84			64		
Bottom tension, T_0 (kN)	19			73			447		
Significant wave height, H_s (m)	0.3 to 4			0.7 to 2.5			1.5 to 2.6		
Wave / swell period, T_p (s)	5			13			10		
Lay rate (km/day)	2.5			1			2		
Number of cycles in touchdown zone, N_{TDZ}	306			192			98		
Assumed maximum horizontal oscillation amplitude, u_{max}/D	0.05	0.25	0.5	0.001	0.025	0.05	0.05	0.25	0.5
Dynamic amplification factor, V_{dyn}/V_{max}	1	1.25	1.5	1	1.25	1.5	1	1.25	1.5
Soil type	silty clay			high plasticity clay			carbonate silt		
Shear strength gradient, s_u/z (kPa)	10			20			10		
Strength degradation factor, δ_{rem}	0.33			0.25			0.14		
Degradation cycle number, N_{95}	4			3			2.5		
Discounting parameter, r	4			4			4		
Effective unit weight, γ' (kN/m^3)	7.5			3			5		
Operative strength factor, δ_{op} (Equation 7.10)	0.69	0.45	0.37	0.98	0.81	0.73	0.64	0.32	0.21

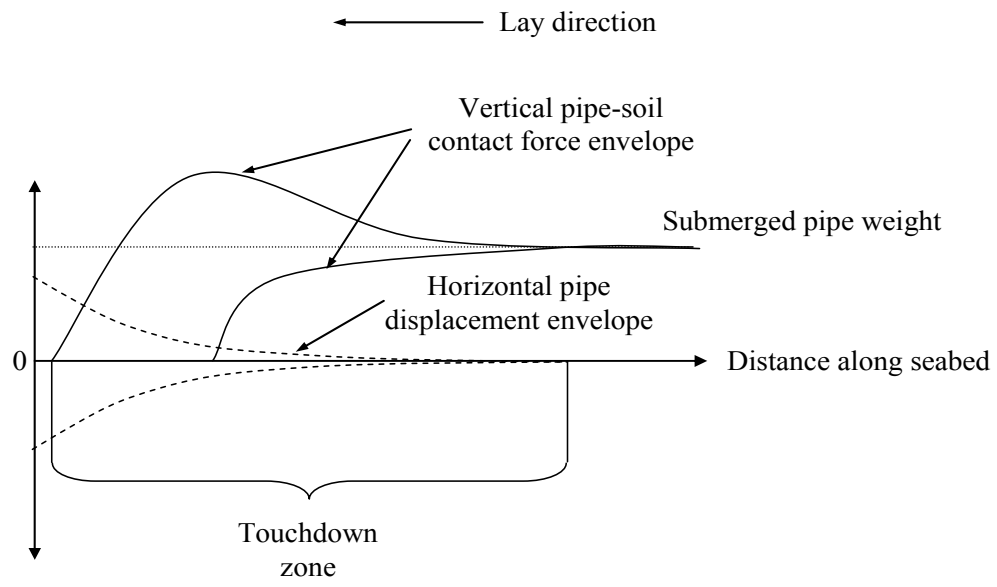

Figure 7.1. Idealisation of pipeline motions within touchdown zone during laying

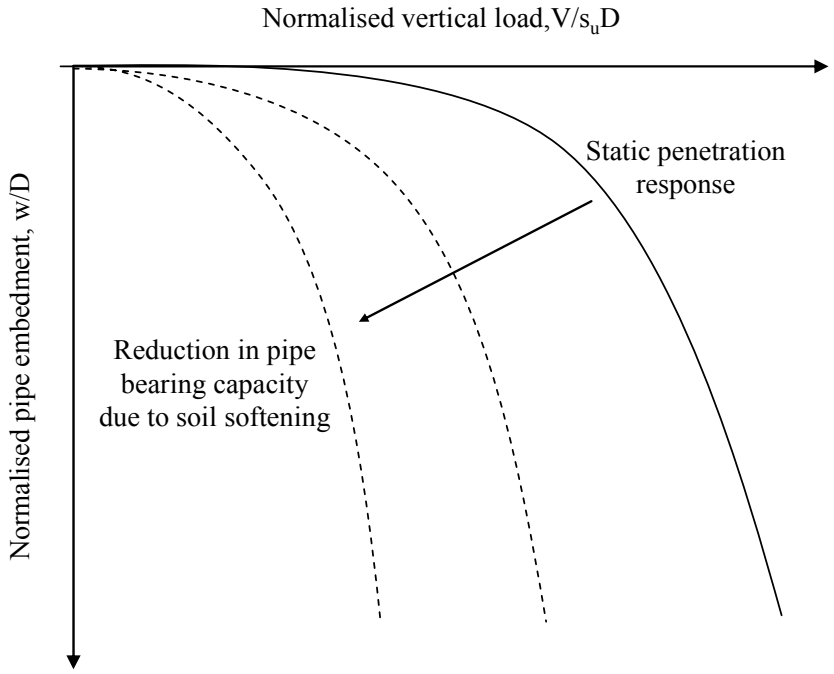

Figure 7.2. Pipe penetration response in fine-grained soil

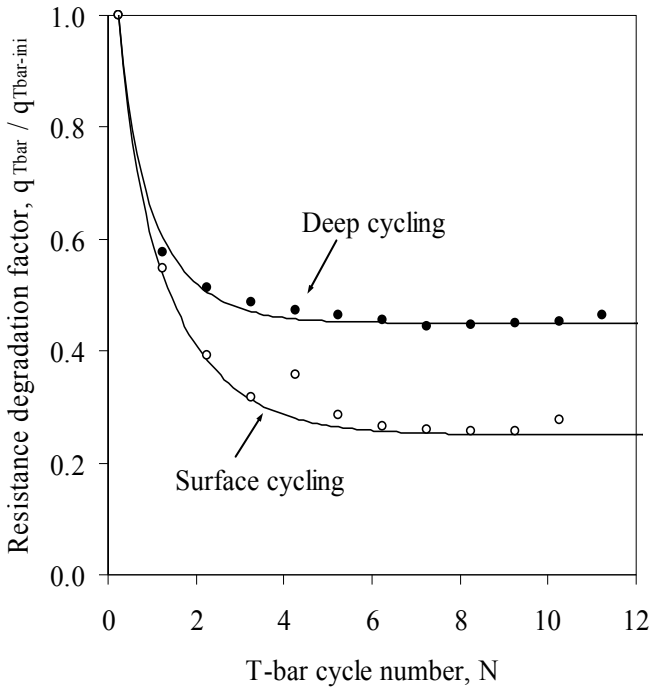

Figure 7.3. Penetration resistance degradation during T-bar cycling in kaolin clay

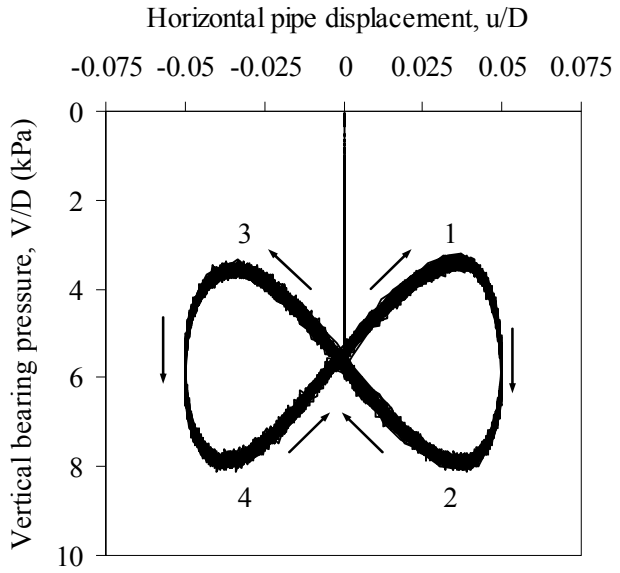

(a)

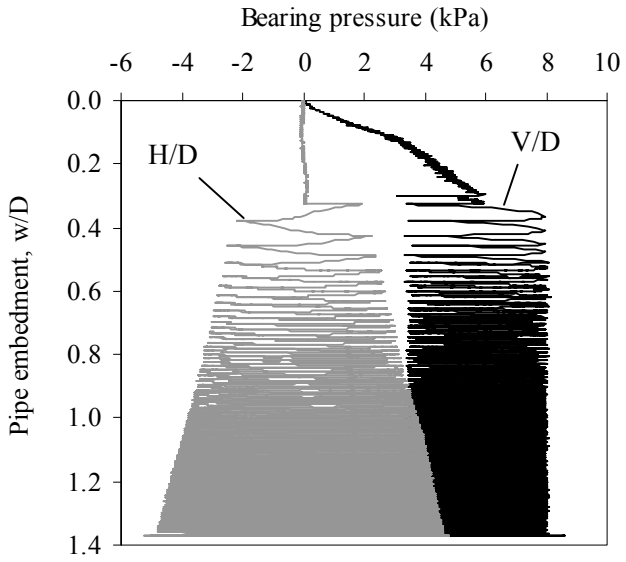

(b)

Figure 7.4. Example pipe laying simulation results (Test D) showing (a) vertical load and horizontal displacement path and (b) vertical and horizontal bearing pressure

(a) (b)

Figure 7.5. Images of soil remoulding following (a) static pipe penetration during Test A and (b) dynamic pipe penetration during Test E

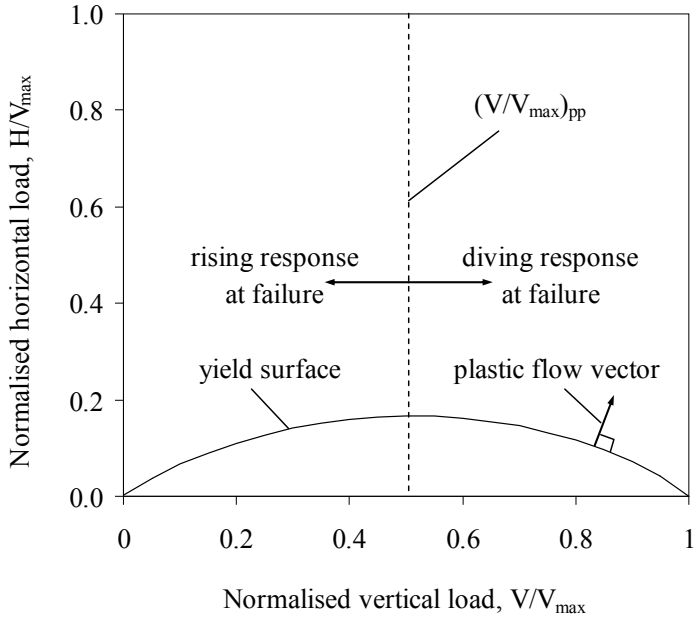

Figure 7.6. Example yield surface for pipe-soil interaction

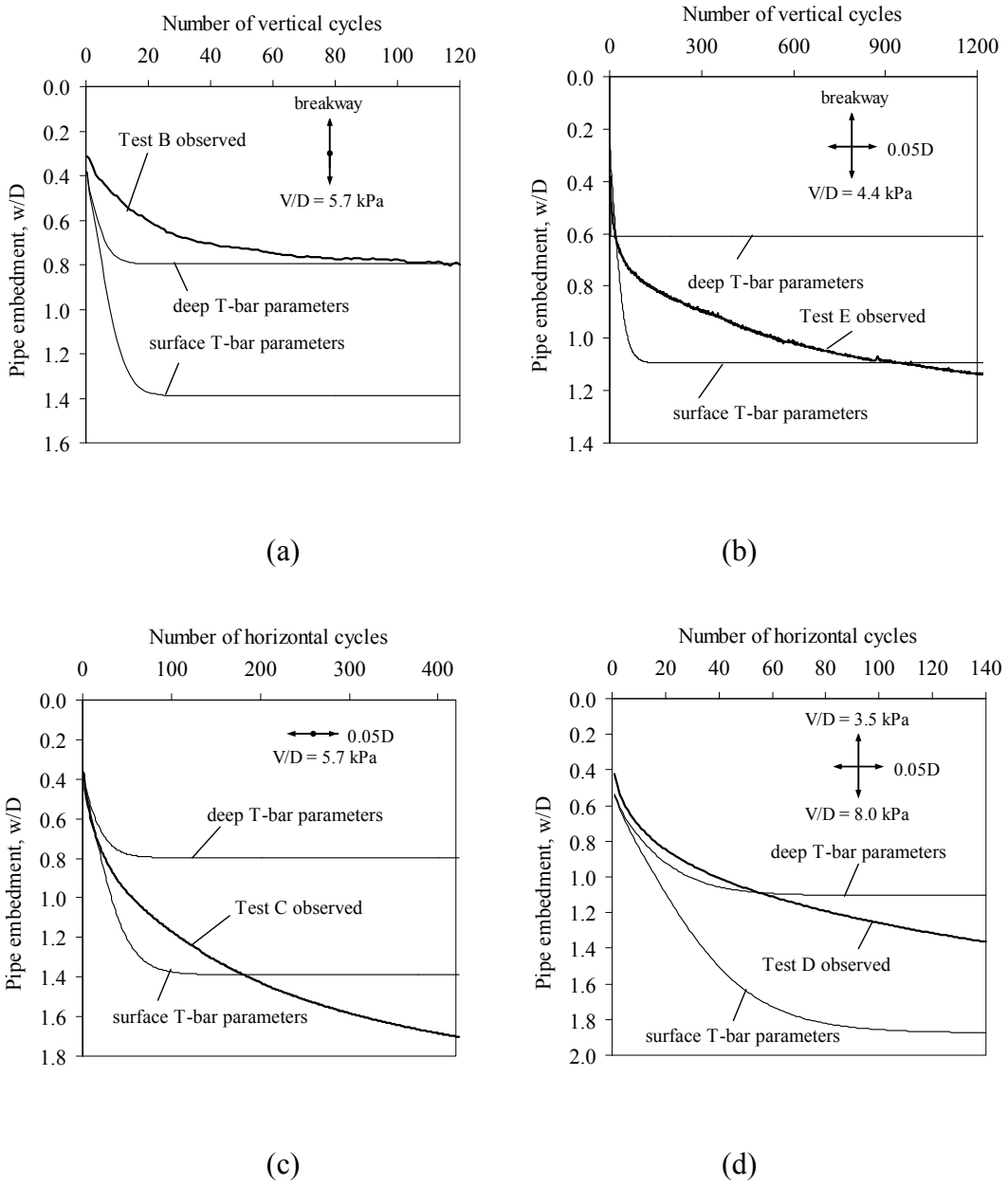

Figure 7.7. Calculations using base case softening law versus observed pipe embedment for (a) Test B, (b) Test E, (c) Test C and (d) Test D

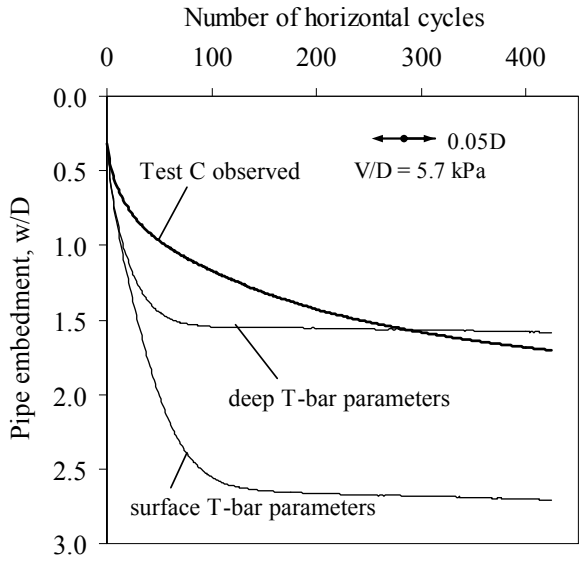

(a)

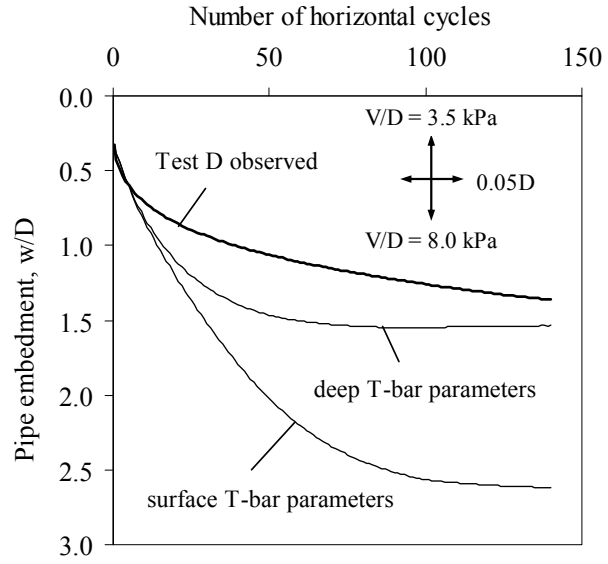

(b)

Figure 7.8. Calculations using flow rule and base case soil softening law versus observed pipe embedment for (a) Test C and (b) Test D

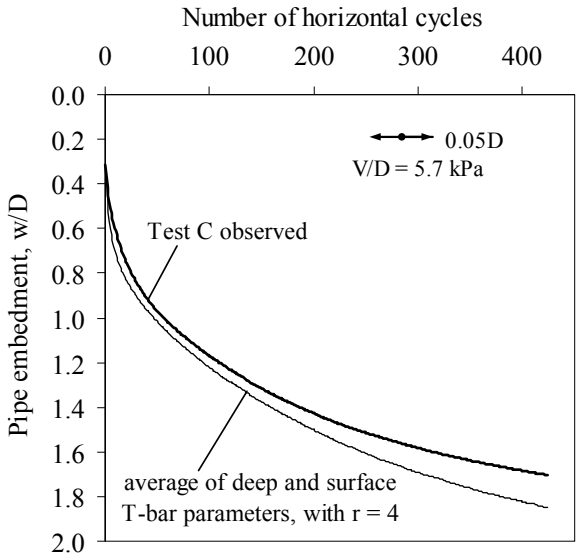

(a)

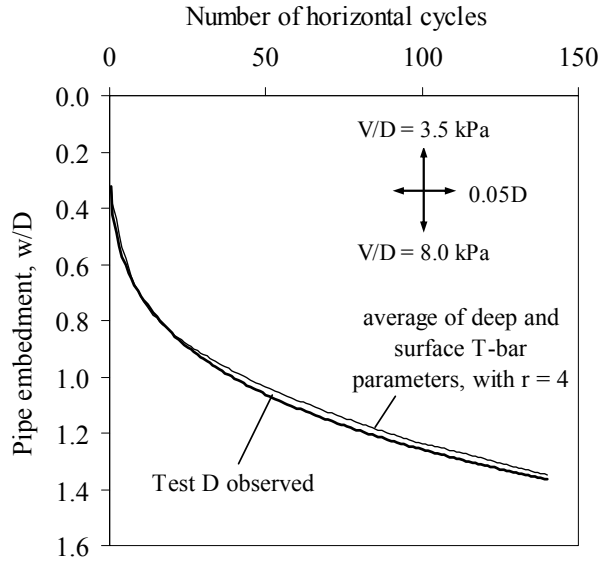

(b)

Figure 7.9. Calculations using flow rule and optimised soil softening law versus observed pipe embedment for (a) Test C and (b) Test D

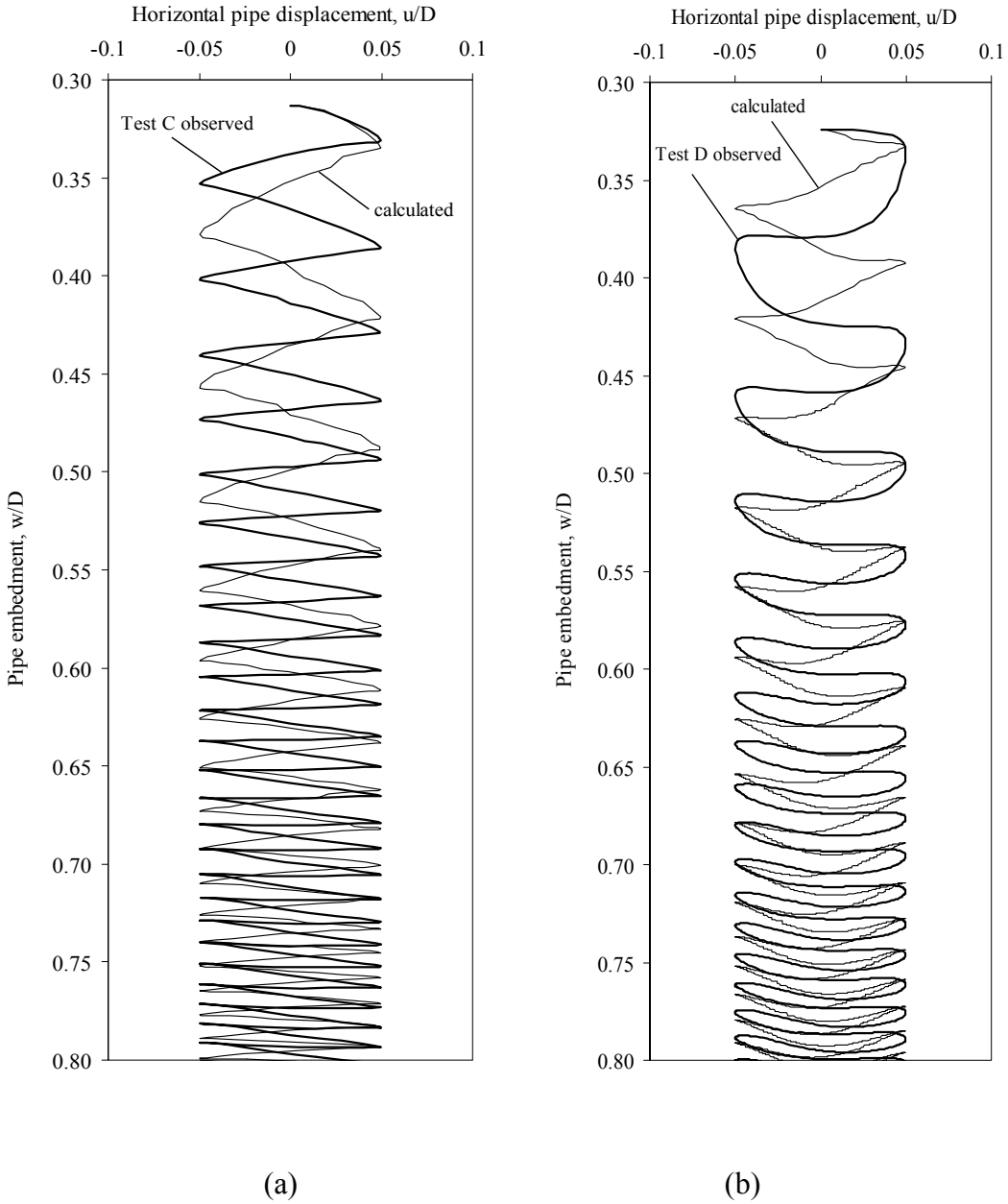

Figure 7.10. Calculations of observed pipe trajectory for (a) Test C and (b) Test D

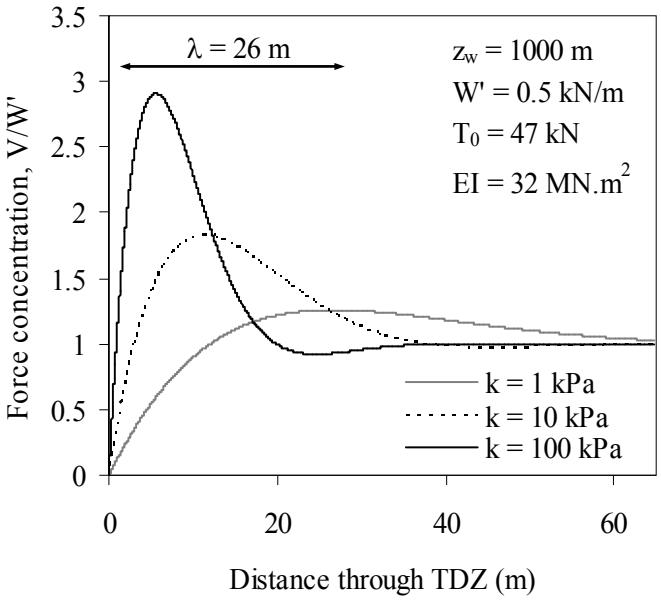

Figure 7.11. Effect of seabed stiffness on pipe-soil contact stress through touchdown zone

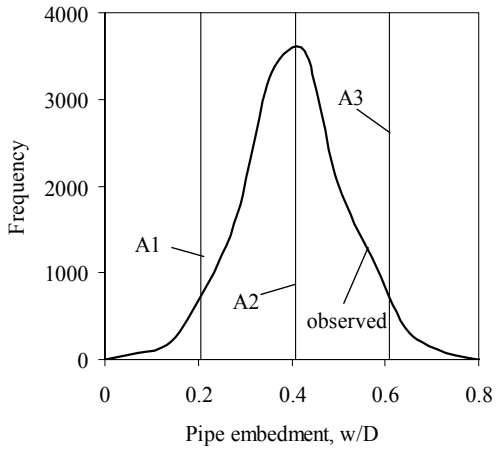

(a)

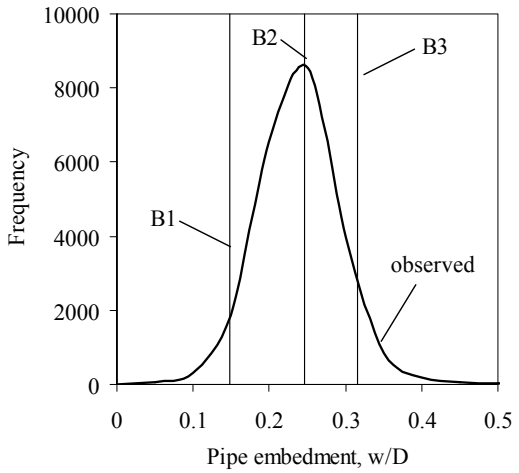

(b)

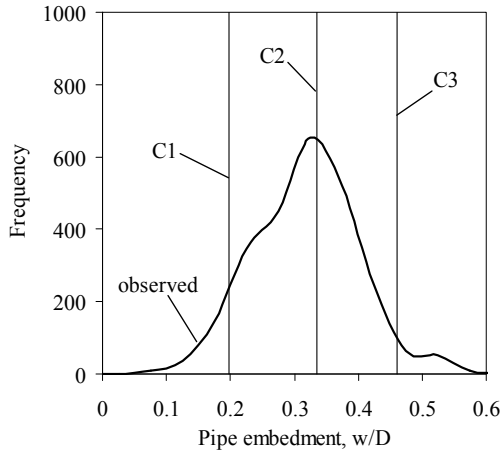

(c)

Figure 7.12. Comparisons of calculated and observed pipe embedment for (a) Site A, (b) Site B and (c) Site C

CHAPTER 8. CONCLUSIONS

This conclusions chapter (i) provides a summary discussion of the outcomes from the research presented throughout the previous chapters, (ii) highlights the key conclusions arising from this work, and (iii) describes suggested activities for further research.

8.1 SUMMARY DISCUSSION

The following sections provide a brief discussion and synthesis of the work carried out for this thesis. The aim of this section is to:

1. Highlight the complexities of assessing as-laid pipeline embedment.
2. Present the key factors affecting as-laid embedment, as identified during this research.
3. Discuss the various approaches to assess as-laid embedment, including their advantages and limitations.

8.1.1 Complexities of assessing as-laid embedment

Accurate prediction of as-laid pipeline embedment has remained notoriously difficult as noted by many publications over the past decade (e.g. Lund 2000b, Cathie et al. 2005, Bruton et al. 2006, White & Randolph 2007, Randolph & White 2008a, Carneiro et al. 2010, Oliphant et al. 2011). The following six factors have contributed to this:

1. The poor quality of the experimental database from early work on dynamic pipe embedment related to on-bottom stability;
2. The lack of as-laid embedment data available in the public domain to benchmark existing solutions;
3. The limited capability of conventional site investigation tools to accurately quantify the undrained shear strength at the seabed surface and assess the effects of water entrainment on surface soil conditions;
4. The complex influences from the sea state on the lay vessel and pipeline dynamics ;
5. The large deformations and disturbances at the seabed during laying, including the influence of soil remoulding and trenching, around the pipeline;

6. The uncertainties in assessing the drainage conditions in the soil around the pipe, which influence the mobilised strength and any tendency for soil softening and strength recovery due to reconsolidation, as the pipe interacts with the seabed.

To overcome these limitations, this thesis has quantified the factors that control as-laid embedment, which were previously uncertain (Section 8.1.2), and has proposed improvements to the basis on which as-laid embedment is estimated (Section 8.1.3). This has led to two distinct new approaches for the calculation of as-laid embedment, with differing levels of complexity (Section 8.1.4).

8.1.2 Key factors affecting as-laid embedment

Effect of the sea state

The field studies presented in this thesis illustrate the different pipe laying characteristics from a wide range of lay vessels. These include a hybrid S-lay / J-lay vessel in shallow water (see Chapters 2 and 3), a J-lay vessel in deep water (see Chapters 4 and 5), and an S-lay vessel capable of laying in shallow and deep water (see Chapter 6). The nature of the pipeline motions at the seabed are highly influenced by the severity of the sea state, and also by the lay vessel characteristics as well as the lay geometry. For example, when the lay ramp is located at the stern of the vessel, the heave motions are exacerbated by the vessel pitch, which increases the amplitude of vertical pipe motions in the touchdown zone and increases the effects of water entrainment on the soil softening response. Conversely, for a centrally located lay ramp, the effects of the vessel motions are attenuated, which reduces the amplitude of pipe motions at the seabed. Often, the type of lay vessel is not known until late in the pipeline design stage, and therefore a wide range of lay vessels (and associated lay rates and sea state effects) may need to be considered when assessing as-laid embedment.

The tension in the pipeline also influences the embedment. Tensioners on the lay vessel restrict the range of tension available in the pipeline, which is set to specific values that safeguard the pipe from excessive bending within the catenary. While the tension settings are often limited to a small range around a target value (~10 to 20%), transient oscillations in tension due to the sea state can exceed this range, significantly increasing the vertical pipe-soil contact force at the seabed, which leads to localised variations in as-laid embedment.

Effect of exposure period

The exposure period of the pipeline to cyclic movements in the touchdown zone significantly affects the as-laid embedment. Extreme examples of this are presented in Chapter 4, showing profiles of embedment during downtime events, or periods when lay vessel progress was halted due to poor weather or mechanical repairs, for example. Such exposure periods can often exceed several hours, resulting in several hundreds to thousands of additional pipe motions at the seabed. This increased exposure increases the cyclic degradation in the soil strength to a state where the soil can become slurry, with the consistency of a liquid, as observed during the centrifuge testing presented in Chapter 7 as well as by others (e.g. Cheuk & White 2011).

In addition to increased strength loss, the soil is displaced and can erode during longer exposure periods, resulting in a net loss of soil in the vicinity of the touchdown zone and thus increasing the pipe embedment through a reduction in the local seabed elevation. This mechanism is referred to as trenching. Trenching has been observed in several field studies, including both pipe laying video surveys (see Chapter 2) and video surveys of steel catenary riser (SCR) response (e.g. Bridge & Howells 2007). For SCRs, the exposure period is cumulative over the design life of the riser, with trenches around the riser reported to exceed several diameters in depth and width due to exposure to successive storm events. Pipeline laying essentially mimics the very early life of a catenary riser, and the initial embedment process is similar.

Effect of soil drainage

The drainage in the soil affects the strength mobilised as the pipe interacts with the seabed. For slow draining soils (e.g. clays), a fully undrained response is typical during laying, allowing use of undrained calculation methods such as those presented in Chapters 4, 6 and 7 to assess pipe embedment. For faster draining soils (e.g. sands), a fully drained response can be assumed, allowing the approach described in Chapter 6, for example, to assess pipe embedment. In drained conditions, the very high static vertical bearing capacity means that the pipe embedment is instead controlled principally by the soil being swept aside (rather than penetrated into). Methods for determining the boundaries between these drainage regimes have been proposed, which are linked to the period of pipe motion, the pipe diameter, and the coefficient of consolidation of the soil.

For partially-drained soils (e.g. silts), it remains unclear what method is most appropriate for assessing as-laid embedment, i.e. an undrained or drained approach. The field study in carbonate soils presented in Chapter 6 suggests that partially-drained embedment may best be assessed using a modified undrained approach, although a reduction in the as-laid embedment may result from reconsolidation and associated strength recovery in the soil. Approximate methods for assessing the competing effects of remoulding and reconsolidation have been proposed (e.g. White & Hodder 2010), but these are difficult to apply to pipe embedment calculations. For routine assessment of as-laid embedment, a more practical approach is to perform calculations using both undrained and drained approaches, adopting the results that are more conservative for the particular design application.

8.1.3 Basis for calculations of as-laid embedment

Traditional approach: dynamic embedment factors

The industry standard approach to assess as-laid embedment, when this thesis was begun, was to apply a multiplicative dynamic embedment factor, $f_{dyn,}$ to the static pipe embedment, calculated using the intact soil strength and submerged weight of the pipe factored up to account for the stress concentration at the touchdown point. Using this approach, the back-calculated dynamic embedment factors from the field observations collated in the thesis range from 2 to 10 for typical pipeline laying conditions. While these values broadly agree with published f_{dyn} values (Lund 2000b, Bruton et al. 2006), which were back-calculated using slightly different bearing capacity formulae, they remain wholly empirical and are not linked to any soil property, pipeline property, sea state condition, or lay rate variation. They also show a wide variation, so if this range is used in design, the predicted embedments have a wide uncertainty band.

Revised approach aspect 1: use of degraded soil strength

It is well known that during undrained cyclic loading of soil, the strength of the soil degrades, or softens, such as during hydrodynamic loading of large offshore foundations (e.g. Andersen 1991). However, large foundations disturb the soil to a lesser degree than an oscillating pipeline. Conversely, a cyclic T-bar test performed through the seabed disturbs the soil to a much greater degree than during the same number of small amplitude cycles by a pipeline. A T-bar test fully remoulds the soil within only a few cycles of motion.

This process of soil softening can be accounted for in as-laid embedment calculations in two ways. Firstly, it can be assumed *a priori* that the soil around a pipe is fully remoulded by the lay process. Using this assumption, the as-laid embedment can be calculated directly from the fully remoulded soil strength. Alternatively, the level of remoulding can be calculated through some simulation of the lay process – either an assumed sequence of pipe motions during laying, or a full numerical model of the process – which then results in a softened value of soil strength which may equal or exceed the remoulded strength depending on the duration and severity of the lay motions.

To support this latter approach, the progressive softening during a cyclic T-bar test can be scaled to the soil softening process around a pipe since they share the same shape (Cheuk & White 2011). However, unlike a T-bar test, the pipe movements are at the seabed surface (where water entrainment can occur), are small in amplitude, and involve progressive movement down into fresh soil that was less (or not) affected by previous cycles, so such scaling is somewhat idealised. However, the T-bar degradation response at least provides a basis to estimate the progressive change in the operative soil strength around a pipe during laying, either on a cycle-by-cycle basis (Cheuk & White 2011) or throughout the full displacement path, as proposed in Chapter 7 of this thesis.

Revised approach aspect 2: use of plasticity theory to model combined loading effects

An additional aspect of an improved model for pipe embedment in a cycle-by-cycle approach is to incorporate the effect of the horizontal pipe motion on the bearing capacity. This type of calculation approach uses aspects of plasticity theory, and is more rigorous theoretically. The combination of both vertical and horizontal pipe-soil loading causes additional embedment compared to purely vertical loading. Theoretical failure envelopes can be used to assess the combined vertical-horizontal bearing capacity and the principle of associated flow – which applies in undrained conditions – allows the rate of pipe embedment to be calculated for a given pattern of horizontal oscillation under a specified vertical loading.

Several aspects of this approach require further detailed study. Theoretical aspects include the detailed shape of the failure envelope, particularly the location of the parallel point (which controls the ultimate embedment state), and the treatment of elastic components of pipe movement. However, the use of a simple form of failure

envelope combined with a single empirical fitting parameter within the soil softening model has shown good predictive success. This type of calculation approach can capture well the full process of pipe embedment through experiments that simulate laying, as well as the final embedment value. This shows that the model can incorporate effects associated with the severity of the lay process – such as the lay rate and the amplitude of pipe movements in the touchdown zone – as well as the detailed form of the soil softening response, into estimates of as-laid embedment. The same model, with unchanged parameters, was shown to provide good estimates of both the average and the range of as-laid embedment observed in the field studies.

8.1.4 Improved approaches for calculation of as-laid embedment

Simple method: fully remoulded soil strength and static bearing response

A simple method proposed in the thesis to assess as-laid embedment in undrained conditions is to use the fully remoulded strength in a static vertical bearing capacity assessment that accounts for the stress concentration at the touchdown point. The method captures reasonably well the embedment values observed in the field. Across a wide database of field observations, the approach is accurate, on average, albeit with some scatter. However, the approach can result in wide ranges of plausible embedment due to the uncertainties in assessing the fully remoulded soil strength, and does not provide a basis to capture the known effects of other parameters, such as the lay rate or sea state. Overall, the method appears to be successful due to compensating errors: the soil is assumed to be too weak – fully remoulded – while other lay effects, such as the weakening effect of combined vertical-horizontal loading, are overlooked.

Complex method: analysis of progressive softening and combined V-H response

The second, more complex class of approach proposed in the thesis involves the as-laid embedment emerging from an idealised analysis of the lay process. For undrained conditions, this analysis explicitly calculates the progressive soil softening during the lay process and also considers the effect of the combined vertical-horizontal loading between the pipe and the seabed. The approach is shown to be theoretically more rigorous than the assumption of a fully remoulded strength, based on careful back-analysis of model tests (Chapter 7). It is shown that the operative soil strength around the pipe, for typical levels of dynamic lay effect, lies between the intact and fully

remoulded values. The approach also captures the reduced vertical bearing capacity that is associated with the concurrent horizontal pipe-soil load.

Although this complex method requires the pipe movements in the touchdown zone to be idealised in some manner, it is a more robust calculation approach. Using recent advances in the numerical modeling of lay dynamics shown in Chapter 3 and 5, it has become more straightforward to estimate the touchdown zone movements during laying. However, in some extreme laying conditions additional factors are relevant such as the growth of a trench around the pipe, and so even this complex calculation method represents an over-simplification of the lay process.

8.2 KEY CONCLUSIONS

The following key conclusions have resulted from this work, which represent original contributions to research and scholarship:

1. *Mechanisms of dynamic pipe embedment*. The three principal mechanisms controlling as-laid pipeline embedment in fine-grained soils comprise (i) soil softening, where the strength of the soil is reduced due to remoulding and water entrainment, (ii) combined vertical and horizontal loading of the pipe on the seabed, and (iii) trenching, where soil in the touchdown zone is displaced or eroded.

2. *Seabed profiles around laid pipes.* Seabed heave adjacent to the pipeline is most evident during calmer sea states and short exposure periods, and is up to 50% as high as the nominal embedment. Under more onerous sea states and longer exposure periods, the seabed profile transitions from heave to trench formation adjacent to the pipeline. The trenches can exceed over one pipe diameter in depth for typical periods of downtime during normal pipe laying.

3. *Drainage conditions during laying.* Excess pore pressure is generated when soft fine-grained seabed soils are sheared. Drainage leads to dissipation of excess pore pressures in the soil, which results in recovery of effective stress and therefore soil strength. Soil drainage can be assessed based on the consolidation properties of the soil relative to the period of pipe motion and the size of the pipeline. Fully undrained conditions appear to occur when excess pore pressure

dissipation remains less than about 10%, while fully drained conditions appear to occur when excess pore pressure dissipation remains greater than about 90%.

4. *Conventional undrained embedment predictions: the dynamic embedment factor*. Back-analyses of six different pipelines across three different sites, installed with different types of lay vessels, showed that during typical laying conditions the as-laid embedment is about 2 to 10 times greater than the static embedment, calculated using the intact soil strength and the enhanced submerged pipe weight to account for the static stress concentration created by the pipeline catenary. This range broadly agrees with previously published dynamic embedment factors. It shows the significant uncertainty associated with this conventional prediction method, which has been widely used by industry in the past.

5. *Simple method for improved undrained embedment predictions: full soil remoulding.* Dynamic lay effects can be simplistically accounted for by use of the fully remoulded shear strength of the soil (at the pipe invert) in a static bearing capacity analysis that includes the effect of pipeline catenary, i.e. the touchdown lay factor. During severe sea states or slower lay rates, this approach may underestimate the as-laid embedment. During calm sea states or for highly sensitive soils or heavy pipelines, the approach may overestimate the as-laid embedment.

6. *Complex method of improved undrained embedment predictions: progressive remoulding and plasticity modelling.* The undrained soil softening response of an oscillating pipeline, based on cyclic T-bar penetration tests, was utilised in a complex model that calculated the full pipe displacement through cycles of vertical loading and horizontal displacement, using elements of plasticity theory. Incorporating only a single empirical fitting parameter, calibrated to physical model tests of pipe laying, the model was shown to capture the average and range of as-laid embedment observed from field surveys, using idealised patterns of loads and motions through the touchdown zone.

7. *Complex method of improved drained embedment predictions*. For pipe laying on a drained seabed, the dynamic embedment occurs through the sweeping of soil aside during each cycle of pipe motion. Cycle-by-cycle summation of the 'swept' pipe embedment based on the static bearing capacity derived from cone

penetration resistance, was shown to capture well the observed field embedment using estimates of the number of pipe motions determined from the lay rate, the characteristic pipeline length and the period of pipe motion.

8. *Comparison of methods of embedment prediction.* Overall, the simple and complex methods described in this thesis offer significant improvements over the conventional method of using dynamic embedment factors. They can be performed relatively simply, without recourse to numerical analysis of the whole lay catenary.

8.3 FUTURE RESEARCH

During this research, areas of work considered to be secondary to the main focus of this thesis were identified, which warrant further investigation. These potential areas of further research generally involve extension of the embedment modelling to cover greater potential depths of embedment – to simulate SCR touchdown behaviour, as well as pipeline laying – and a move away from 'lumped' modelling of the soil properties towards explicit inclusion of the spatial variation in strength and other properties.

Future research activities include:

1. *Quantification of soil remoulding through different soil horizons within and beyond the depth of pipe embedment*. The models in the thesis are based on the magnitude of soil remoulding at the pipe invert elevation, which is considered by previous studies to be the representative depth most strongly influencing vertical pipe-soil interaction. A more accurate assessment of the spatial distribution of soil strength, including the contribution from water entrainment, as a pipe dynamically embeds may remove the need for empirical adjustment parameters, such as discussed in Chapter 7, in these models.

2. *Dynamic pipeline embedment in partially drained soils*. The study has identified a large spectrum of soil, pipeline and lay conditions where as-laid embedment may be influenced by partial drainage, based on the work presented in Chapter 6. Under these conditions, the as-laid embedment is expected to be less than for fully undrained conditions, due to the recovery of soil strength as excess pore pressures dissipate between cycles of loading. Similarly, the as-laid embedment

is expected to be greater than for fully drained conditions, due to the reduction in effective stress during excess pore pressure generation.

3. *Implementation of dynamic embedment calculation models into pipeline modelling or structural analysis software*. The offshore modelling programme OrcaFlex, developed by Orcina Ltd., is capable of modelling non-linear vertical pipe-soil interaction during cyclic pipe motion. This, or similar, software, could be augmented by incorporating a model that quantifies the development of as-laid pipeline embedment, for example using links to plasticity theory and the number and amplitude of horizontal pipeline motions in the touchdown zone, such as proposed in Chapter 7. This has the advantage that the pipe loads and displacements from the numerical simulation can be properly accounted for through the touchdown zone, i.e. incorporating the effects of the three-dimensional lay process such as discussed in Chapter 5.

4. *Coupling the dynamic embedment mechanisms of soil softening, combined loading, and trenching*. The soil softening and combined loading embedment mechanisms have been incorporated into a cycle-by-cycle model for fine-grained soils, as presented in Chapter 7, while the trenching embedment mechanism has been incorporated into a cycle-by-cycle model for coarse-grained soils, as presented in Chapter 6. However, trenching, i.e. lowering of the local seabed elevation, has been shown to occur in fine-grained soils as well, as illustrated in Chapter 4. It is thought that the trenching mechanism is at least in part related to seabed erosion, especially during prolonged exposure to dynamic lay effects (e.g. during downtime), whereby sediments are agitated into suspension by the pumping action of the oscillating pipeline and dispersed across the seabed due to the prevailing current. It is anticipated that coupling these three mechanisms may allow for more accurate assessments of the deeper as-laid embedment observed during these prolonged cyclic pipeline motions. This is particularly relevant to SCRs, which are exposed to significant erosion effects, resulting in much deeper embedment than for typical as-laid pipelines.

REFERENCES

Allen, D.W., Lammert, W.F., Hale, J.R. & Jacobsen, V. (1989). Submarine pipeline on-bottom stability: recent AGA research, *Proceedings of the Offshore Technology Conference*, Houston, Paper OTC6055.

American Petroleum Institute. (2007). Errata and supplement 3 to recommended practice 2A-WSD: recommended practice for planning, designing and constructing fixed offshore platforms – working stress design, 21st Edition, American Petroleum Institute, Washington, D.C.

An, H., Cheng, L. & Zhao, M. (2011). Numerical simulation of a partially buried pipeline in a permeable seabed subject to combined oscillatory flow and steady current, *Ocean Engineering*, Vol. 38, pp. 1225-1236.

Andersen, K.H. (1991). Foundation design of offshore gravity structures. In *Cyclic loading of soils: From theory to design* (eds. M.P. O'Reilly & S.F. Brown), pp. 122-173. Glasgow: Blackie.

Aubeny, C.P. & Dunlap, W.A. (2003). Penetration of cylindrical objects in soft mud. *Proceedings of IEEE OCEANS 2003*, San Diego, pp. 2068-2073.

Aubeny, C.P., Biscontin, G. & Zhang, J. (2006). Seafloor interaction with steel catenary risers: Final Project Report, OTRC Library 9/06A173, 35p.

Aubeny, C.P., Gaudin, C. & Randolph, M.F. (2008). Cyclic tests of model pipe in kaolin, *Proceedings of the Offshore Technology Conference*, Houston, Paper OTC19494.

Aubeny, C.P., Shi, H. & Murff, J.D. (2005). Collapse loads for a cylinder embedded in trench in cohesive soil, *International Journal of Geomechanics*, ASCE, Vol. 5, No. 4, pp. 320-325.

Aubney, C.P. & Shi, H. (2007). Effect of rate-dependent soil strength on cylinders penetrating into soft clay, *IIIE Journal of Oceanic Engineering*, January, Vol. 32, No. 1, pp. 49-56.

Bai, Y. (2001). *Pipelines and risers,* Elsevier Ocean Engineering Book Series, Vol. 3, Bhattacharyya & McCormick, 526p.

Barbosa-Cruz, E.R. & Randolph, M.F. (2005). Bearing capacity and large penetration of a cylindrical object at shallow embedment, *Proceedings of the 1st International Symposium on Frontiers in Offshore Geotechnics*, Perth, pp. 615-621.

Boreas Consultants (2007). SAFEBUCK JIP: Safe design of pipelines with lateral buckling – pipe soil interaction, Report No. BR06071 to SAFEBUCK JIP Participants, 44p.

Brennodden, H., Lieng, J.T., Sotberg, T. & Verley, R.L.P. (1989). An energy-based pipe-soil interaction model, *Proceedings of the Offshore Technology Conference*, Houston, Paper OTC6057, pp. 147-158.

Brennodden, H., Sveggan, O., Wagner, D.A. & Murff, J.D. (1986). Full-scale pipe soil interaction tests, *Proceedings of the Offshore Technology Conference*, Houston, Paper OTC5338, pp. 433-440.

Bridge, C. (2005). Effects of seabed interaction on steel catenary risers, PhD Thesis, University of Surrey, 519p.

Bridge, C., Laver, K., Clukey, E.C. & Evans, T.R. (2004). Steel catenary riser touchdown point vertical interaction model, *Proceedings of the Offshore Technology Conference*, Houston, Paper OTC16628.

Bridge, C.D. & Howells, H.A. (2007). Observations and modeling of steel catenary riser trenches, *Proceedings of the 17th International Offshore and Polar Engineering Conference*, July 1-6, Lisbon, pp. 803-813.

Brinch Hansen, J. (1970). A revised and extended formula for bearing capacity, Bulletin No. 28, Danish Geotechnical Institute, Lyngby.

Bruton, D.A.S., Carr, M.C. & White, D.J. (2007). The influence of pipe-soil interaction on lateral buckling and walking of pipelines – The SAFEBUCK JIP, *Proceedings of the 6th International Offshore Site Investigation and Geotechnics Conference: Confronting New Challenges and Sharing Knowledge*, September 11-13, London, pp. 133-150.

Bruton, D.A.S., White, D.J., Carr, M.C. & Cheuk, C.Y. (2008). Pipe-soil interaction during lateral buckling and pipeline walking: the SAFEBUCK JIP, *Proceedings of the Offshore Technology Conference*, Houston, Paper OTC19589.

Bruton, D.A.S., White, D.J., Cheuk, C.Y., Bolton, M.D. & Carr, M.C. (2006). Pipe-soil interaction behaviour during lateral buckling, including large amplitude cyclic displacement tests by the SAFEBUCK JIP, *Proceedings of the Offshore Technology Conference*, Houston, Paper OTC17944.

Bræstrup, M.W. & Andersen, J.B. (2005). *Design and installation of marine pipelines*. Wiley-Blackwell, 342p.

Callegari, M., Carini, C.B., Lenci, S., Torselletti, E. & Vitali, L. (2003). Dynamic models of marine pipelines for installation in deep and ultra-deep waters: analytical and numerical approaches, *Proceedings of the 16th AIMETA Congress of Theoretical and Applied Mechanics*.

Carneiro, D., Gouveia, J. & Parrilha, R. (2010). Feedback analyses of pipeline embedment over as-laid survey results, *Proceedings of the Ocean, Offshore and Arctic Engineering Conference*, June 6-11, Shanghai, Paper OMAE2010-20410, pp. 505-509.

Cathie, D.N., Jaeck, C., Ballard, J-C. & Wintgens, J-F. (2005). Pipeline geotechnics – state of the art, *Proceedings of the 1st International Symposium on Frontiers in Offshore Geotechnics*, Perth, pp. 95-114.

Chatterjee, S. Randolph, M.F., White, D.J. & Wang, D. (2010). Large deformation finite element analysis of vertical penetration of pipelines in seabed, *Proceedings of the 2nd International Symposium on Frontiers in Offshore Geotechnics*, Perth.

Chatterjee, S., Randolph, M.F. & White, D.J. (2012). The effects of penetration rate and strain softening on the vertical penetration resistance of seabed pipelines, *Géotechnique*, Vol. 62, No. 7, pp. 573-582.

Cheuk C.Y. & White D.J. (2011). Modelling the dynamic embedment of seabed pipelines, *Géotechnique*, Vol. 61, No. 1, pp. 39-57.

Cheuk, C.Y. & White, D.J. (2008). Centrifuge modelling of pipe penetration due to dynamic lay effects, *Proceedings of the ASME 27th International Conference on Offshore Mechanics and Arctic Engineering, OMAE2008*, June 15-20, Estoril, Paper OMAE2008-57923.

Cheuk, C.Y., White, D.J. & Dingle, H.R.C. (2008). Upper bound plasticity analysis of a partially-embedded pipe under combined vertical and horizontal loading, *Soils and Foundations*, Japanese Geotechnical Society, Vol. 48, No. 1, pp. 133-140.

Clark, A.R. & Walker, B.F. (1977). A proposed scheme for the classification and nomenclature for use in engineering description of Middle Eastern sedimentary rocks, *Géotechnique*, Vol. 27, No. 1, pp. 93-99.

Clukey, E.C., Haustermans, L. & Dyvik, R. (2005). Model tests to simulate riser-soil interaction in the touchdown point region, *Proceedings of the 1st International Symposium on Frontiers in Offshore Geotechnics*, Perth, pp. 651-658.

Davis, E.H. & Booker, J.R. (1973). The effect of increasing strength with depth on the bearing capacity of clays, *Géotechnique*, Vol. 23, No. 4, pp. 551-563.

De Catania, S., Breen, J., Gaudin, C. & White, D.J. (2010). Development of a multiple-axis actuator control system, *Proceedings of the 7th International Conference on Physical Modelling in Geotechnics*, Vol. 1, Zurich, pp. 325–330.

Det Norske Veritas. (1988). Recommended Practice E305: On-bottom stability design of submarine pipelines, Det Norske Veritas, Hovik, Norway.

Det Norske Veritas. (1992). Classification Notes 30.4: Foundations. Det Norske Veritas, Hovik, Norway.

Det Norske Veritas. (2006). Recommended Practice F105: Free spanning pipelines. February, Det Norske Veritas, Hovik, Norway.

Det Norske Veritas. (2007). Recommended Practice F109: On-bottom stability design of submarine pipelines. October, Det Norske Veritas, Hovik, Norway.

Dingle, H.R.C., White, D.J. & Gaudin, C. (2008). Mechanisms of pipe embedment and lateral breakout in soft clay, *Canadian Geotechnical Journal*, Vol. 45, No. 5, pp. 636-652.

Dunlap, W.A., Bhojanala, R.P. & Morris, D.V. (1990). Burial of vertically loaded offshore pipelines in weak sediments, *Proceedings of the Offshore Technology Conference*, Houston, Paper OTC6375.

Einav, I. & Randolph, M.F. (2005). Combining upper bound and strain path methods for evaluating penetration resistance, *International Journal of Numerical Methods Engineering*, Vol. 63, pp. 1995-2016.

Finnie, I.M.S. & Randolph, M.F. (1994). Punch-through and liquefaction induced failure of shallow foundations on calcareous sediments, *Proceedings of the International Conference on Behavior of Offshore Structures, BOSS'94*, Boston, pp. 217-230.

Fontaine, E., Nauroy, J.F., Foray, P., Roux, A. & Gueneneux, H. (2004). Pipe-soil interaction in soft kaolinite: vertical stiffness and damping, *Proceedings of the International Conference on Offshore and Polar Engineering*, Toulon, pp. 517-524.

Frazer, I. (2006). Polaris J-lay system overhauled for next generation of ultra-deep projects, *Offshore*, October 1, Vol. 66, No. 10.

Gaudin, C. & White, D.J. (2009). New centrifuge modelling techniques for investigating seabed pipeline behaviour, *Proceedings of the 17th International Conference on Soil Mechanics and Geotechnical Engineering*, Alexandria, October 5-9.

Ghazzaly, O.I. & Lim S.J. (1975). Experimental investigation of pipeline stability in very soft clay, *Proceedings of the Offshore Technology Conference*, Houston, Paper OTC2277, pp 315-326.

Gourvenec, S.M. & White, D.J. (2010). Elastic solutions for consolidation around seabed pipelines, *Proceedings of the Offshore Technology Conference*, Houston, Paper OTC20554.

Green, A.P. (1954). The plastic yielding of metal junctions due to combined shear and pressure, *Journal of Mechanics and Physics of Solids*, Vol. 2, pp. 197-211.

Hale, J.R., Lammert, W.F. & Allen, D.W. (1991). Pipeline on-bottom stability calculations: comparison of two state-of-the-art methods and pipe-soil model verification, *Proceedings of the Offshore Technology Conference*, Houston, Paper OTC6761, pp. 567-582.

Hale, J.R., Lammert, W.F. & Jacobsen, V. (1989). Improved basis for static stability analysis and design of marine pipelines, *Proceedings of the. Offshore Technology Conference*, Houston, Paper OTC6059, pp. 171-181.

Hale, J.R., Morris, D.V., Yen, T.S. & Dunlap, W.A. (1992). Modelling pipeline behavior on clay soils during storms, *Proceedings of the Offshore Technology Conference*, Houston, Paper OTC7019, pp. 339-349.

Harrington, P.K. (1985). Formation of pockmarks by pore-water escape, *Geo-Marine Letters*, Vol. 5, pp. 193-197.

Hodder, M.S. & Cassidy, M.J. (2010). A plasticity model for predicting the vertical and lateral behaviour of pipelines in clay soils, *Géotechnique*, Vol. 60, No. 4, pp. 247-263.

Hodder, M.S., White, D.J. & Cassidy, M.J. (2008). Centrifuge modeling of riser-soil stiffness degradation in the touchdown zone of a steel catenary riser, *Proceedings of the ASME 27th International Conference on Offshore Mechanics and Arctic Engineering, OMAE2008*, Estoril, June 15-20, Paper OMAE2008-57302.

Hodder, M.S., White, D.J. & Cassidy, M.J. (2010). Analysis of soil strength degradation during episodes of cyclic loading, illustrated by the T-Bar penetration test, *International Journal of Geomechanics*, Vol. 10, No. 3, pp. 117-123.

Hu, Y. & Randolph, M.F. (1998). A practical numerical approach for large deformation problems in soil, *International Journal of Numerical and Analytical Methods in Geomechanics*, Vol. 22, pp. 327-350.

Jewell, R.J. & Khorshid, M. (1988). *Proceedings of the 1st International Conference on Engineering for Calcareous Sediments*, Perth, Balkema.

Karal, K. (1977). Lateral stability of submarine pipelines, *Proceedings of the Offshore Technology Conference*, Houston, Paper OTC2967, pp. 71-78.

Krost, K., Gourvenec, S. & White, D.J. (2011). Consolidation around partially-embedded seabed pipelines, *Géotechnique,* Vol. 61, No. 2, pp. 167-173.

Lammert, W.F., Hale, J.R. & Jacobsen, V. (1989). Dynamic response of submarine pipelines exposed to combined wave and current action, *Proceedings of the Offshore Technology Conference*, Houston, Paper OTC6058, pp. 159-170.

Lehane, B.M., O'Loughlin, C.D., Gaudin, C. & Randolph, M.F. (2009). Rate effects on penetrometer resistance in kaolin, *Géotechnique*, Vol. 59, No. 1, pp. 41-52.

Lenci, S. & Callegari, M. (2005). Simple analytical models for the J-lay problem, *Acta Mechanica*, Vol. 178, pp. 23-39.

Low, H.E., Randolph, M.F., Rutherford, C.J., Bernard, B.B. & Brooks, J.M. (2008). Characterization of near seabed surface sediment, *Proceedings of the Offshore Technology Conference*, Houston, Paper OTC19149.

Lund, K.M. (2000a). Effect of increase in pipeline soil penetration from installation, *Proceedings of the ETCE/OMAE2000 Joint Conference*, New Orleans, February 14-17, Paper OMAE2000-PIPE5047.

Lund, S. (2000b). Developments of subsea pipeline technology for Norwegian waters, *Journal of Offshore Mechanics and Arctic Engineering*, February, Vol. 122, pp. 33-39.

Malahy, R.C. (1996). *OFFPIPE User's Guide.* Version 2.05.

Martin, C.M. & Randolph, M.F. (2006). Upper-bound analysis of lateral pile capacity in cohesive soil, *Géotechnique*, Vol. 56, No. 2, pp. 141-145.

Merifield, R., White, D.J. & Randolph, M.F. (2008). The ultimate undrained resistance of partially embedded pipelines, *Géotechnique*, Vol. 58, No. 6, pp. 461-470.

Merifield, R., White, D.J. & Randolph, M.F. (2009). Effect of surface heave on response of partially embedded pipelines in clay, *Journal of Geotechnical and Geoenvironmental Engineering,* Vol. 135, No. 6, pp. 819-829.

Morris, D.V., Webb, R.E. & Dunlap, W.A. (1988). Self burial of laterally loaded offshore pipelines in weak sediments, *Proceedings of the Offshore Technology Conference*, Houston, Paper OTC5855.

Morris, D.V., Yen, T.S., Dunlap, W.A. & Hale, J.R. (1992). Pipeline storm behavior on clay soils, *Proceedings of the International Conference on Civil Engineering in the Oceans V*, College Station, November 2-5, pp. 560-570.

Murff, J.D., Wagner, D.A. & Randolph, M.F. (1989). Pipe penetration in cohesive soil, *Géotechnique*, Vol. 39, No. 2, pp. 213-229.

Oliphant, J. & Yun, G.J. (2011). Pipeline embedment prediction using as-laid data, *Proceedings of the International Conference on Ocean, Offshore and Arctic Engineering*, Rotterdam, June 19-24, Paper OMAE2011-50095.

Orcina. (2009). *OrcaFlex User Manual*, Version 9.2e.

Palmer, A. (2009). Touchdown indentation of the seabed, *Applied Ocean Research*, Vol. 30, No. 3. pp. 235-238.

Palmer, A.C. & King, R.A. (2008). *Subsea Pipeline Engineering,* Pennwell, 624p.

Palmer, A.C., Hutchinson, G. & Ells, J.W. (1974). Configuration of submarine pipelines during laying operations, *Journal of Engineering for Industry: Transactions of the ASME*, November, pp. 1112-1118.

Paul, M.A. & Jobson, L.M. (1991). Geotechnical properties of soft clays from the Witch Ground Basin, central North Sea, *Geological Society, London, Engineering Geology Special Publications*, Vol. 7, pp. 151-156.

Perinet, D. & Frazer, I. (2007). J-lay and steep S-lay: complementary tools for ultradeep water, *Proceedings of the Offshore Technology Conference*, Houston, Paper OTC18669.

Pesce, C.P., Aranha, J.A.P. & Martins, C.A. (1998). The soil rigidity effect in the touchdown boundary layer of a catenary riser: static problem, *Proceedings of the International Offshore and Polar Engineering Conference*, Montreal, May 24-29, pp. 207-213.

Prandtl, L. (1921). Über die Eindringungfestigkeit Plastischer Baustoffe und die Festigkeit von Schneiden, *Zeitschrift für Angewandte Mathematik und Mechanik*, Vol. 1, No.1, pp. 15-20.

Randolph, M.F. & Hope, S. (2004). Effect of cone velocity on cone resistance and excess pore pressures, *Proceedings of the International Symposium on Engineering Practice and Performance of Soft Deposits*, Osaka, Yodogawa Kogisha Co. Ltd., pp. 147-152.

Randolph, M.F. & Houlsby, G.T. (1984). The limiting pressure on a circular pile loaded laterally in cohesive soil, *Géotechnique*, Vol. 34, No. 4, pp. 613-623.

Randolph, M.F. & Quiggin, P. (2009). Non-linear hysteretic seabed model for catenary pipeline contact, *Proceedings of the International Conference on Offshore Mechanical and Arctic Engineering*, Honolulu, Paper OMAE2009-79259.

Randolph, M.F. & White, D.J. (2008a). Pipeline embedment in deep water: processes and quantitative assessment, *Proceedings of the Offshore Technology Conference*, Houston, Paper OTC19128-PP.

Randolph, M.F. & White, D.J. (2008b). Upper-bound yield envelopes for pipelines at shallow embedment in clay, *Géotechnique*, Vol. 58, No. 4, pp. 297-301.

Randolph, M.F., Jewell, R.J., Stone, K.J.L. & Brown, T.A. (1991). Establishing a new centrifuge facility, *Proceedings of the International Conference on Centrifuge Modelling*, Boulder, pp. 2-9.

Randolph, M.F., Low, H.E. & Zhou, H. (2007). In situ testing for design of pipeline and anchoring systems, *Proceedings of the 6th International Conference on Offshore Site Investigation and Geotechnics*, Society for Underwater Technology, London, pp. 251-262.

Reese, L.C. & Casbarian, A.O.P. (1968). Pipe soil interaction for a buried offshore pipeline, *Offshore Operations and Technology, SPE 2343, Society of Petroleum Engineers of AIME, 43rd Annual Fall Meeting*, Houston, Sept 29 - Oct 2.

Schneider, J.A., Randolph, M.F., Mayne, P.W. & Ramsey, N. (2008). Analysis of factors influencing soil classification using normalised piezocone tip resistance and pore pressure parameters, *Journal of Geotechnical and Geoenvironmental Engineering*, Vol. 134, No. 11, pp. 1569-1586.

Sinclair, F., Carr, M., Bruton, D. & Farrant, T. (2009). Design challenges and experience with controlled lateral buckle initiation methods, *Proceedings of the Offshore Mechanics and Arctic Engineering Conference*, Honolulu, Paper OMAE2009-79434.

Skempton, A.W. (1951). The bearing capacity of clays, *Proceedings of the. Building Research Congress*, Vol. 1, pp. 180-189.

Small, S.W., Tamburello, R.D. & Piaseckyj, P.J. (1971). Submarine pipeline support by marine sediments, *Proceedings of the Offshore Technology Conference*, Houston, Paper OTC1357.

Stewart D.P. & Randolph M.F. (1994). T-Bar penetration testing in soft clay, *Journal of the Geotechnical Engineering Division*, ASCE, Vol. 120, No. 12, pp. 2230-2235.

Stewart, D.P. & Randolph, M.F. (1991). A new site investigation tool for the centrifuge, *Proceedings of the International Conference on Centrifuge Modelling 91*, Boulder, pp. 531-538.

Swanson, R.C. & Jones, W.T. (1982). Mudslide effects on offshore pipelines, *Transportation Engineering Journal*, ASCE, Vol. 108, No. TE6, pp. 585-600.

Thethi, R. & Moros, T. (2001). Soil interaction effects on simple catenary riser response, *Proceedings of the Deepwater Pipeline and Riser Technology Conference*, Houston.

Tian, Y., Cassidy, M.J. & Gaudin, C. (2010). Advancing pipe-soil interaction models in calcareous sand, *Applied Ocean Research*, Vol. 32, pp. 284-297.

Tucker, M.J. & Pitt, E.G. (2001). *Waves in ocean engineering,* Elsevier Ocean Engineering Series, Vol. 5.

Verley, R. & Lund, K.M. (1995). A soil resistance model for pipelines placed on clay soils, *Proceedings of the Offshore Mechanics and Arctic Engineering Conference*: *Pipeline Technology*, Vol. 5, ASME, pp. 225-232.

Verley, R.P.L. & Sotberg, T. (1994). A soil resistance model for pipelines placed on sandy soils, *Journal of Offshore Mechanics and Arctic Engineering*, Vol. 116, pp. 145-153.

Wagner, D.A., Murff, J.D., Brennodden, H. & Sveggen, O. (1987). Pipe-soil interaction model, *Proceedings of the Offshore Technology Conference*, Houston, Paper OTC5504.

Wang, D., White, D.J. & Randolph, M.F. (2010). Large deformation finite element analysis of pipe penetration and large-amplitude lateral displacement, *Canadian Geotechnical Journal*, Vol. 47, pp. 842-856.

Wantland, G.M., O'Niell, M.W., Reese, L.C. & Kalajian, E.H. (1979). Lateral stability of pipelines in clay, *Proceedings of the Offshore Technology Conference*, Houston, Paper OTC3477, pp. 1025-1034.

Westgate, Z.J., Randolph, M.F., White D.J. & Li, S. (2010a). The influence of seastate on as-laid pipeline embedment: a case study, *Applied Ocean Research*, Vol. 32, No. 3, pp 321-331.

Westgate, Z.J., Randolph, M.F., White, D.J. & Brunning, P. (2010b). Theoretical, numerical and field studies of offshore pipeline sleeper crossings, *Proceedings of the 2nd International Symposium on Frontiers in Offshore Geotechnics*, Perth.

Westgate, Z.J., White, D.J. & Randolph, M.F. (2009). Video observations of dynamic embedment during pipelaying in soft clay, *Proceedings of the Offshore Mechanics and Arctic Engineering Conference*, Honolulu, June 1-5, Paper OMAE2009-79814.

Westgate, Z.J., White, D.J. & Randolph, M.F. (2012). Field observations of as-laid pipeline embedment in carbonate sediments, *Géotechnique* Vol. 62, No. 9, pp. 787-798.

Westgate, Z.J., White, D.J., Randolph, M.F. & Brunning, P. (2010c). Pipeline laying and embedment in soft fine-grained soils: field observations and numerical simulations, *Proceedings of the Offshore Technology Conference,* Houston, Paper OTC20407.

Westgate, Z.J., White, D.J. & Randolph, M.F. (2013). Modelling the embedment process during offshore pipe laying on fine-grained soils, *Canadian Geotechnical Journal*, Vol. 50, No. 1, pp. 15-27.

White D.J. & Hodder M. (2010). A simple model for the effect on soil strength of remoulding and reconsolidation, *Canadian Geotechnical Journal*, Vol. 47, pp. 821-826.

White, D.J. & Gaudin, C. (2008). Simulation of seabed pipe-soil interaction using geotechnical centrifuge modelling, *Proceedings of the Deep Offshore Technology Conference (Asia-Pacific)*, Perth, December 3-5.

White, D.J. & Randolph, M.F. (2007). Seabed characterisation and models for pipeline-soil interaction, *Journal of Offshore and Polar Engineering*, Vol. 17, No. 3, pp. 193-204.

White, D.J., Gaudin, C., Boylan, N. & Zhou, H. (2010). Interpretation of T-bar penetrometer tests at shallow embedment and in very soft soils, *Canadian Geotechnical Journal*, Vol. 47, pp. 218-229.

White, D.J., Take, A.W. & Bolton, M.D. (2003). Soil deformation measurement using particle image velocimetry (PIV) and photogrammetry, *Géotechnique*, Vol. 53, No. 7, pp. 619-631.

Yan, Y., White, D.J. & Randolph, M.F. (2011). Penetration resistance and stiffness factors for hemispherical and toroidal penetrometers in uniform clay, *International Journal of Geomechanics*, Vol. 11, No. 4, pp. 263-275.

Zhang, J., Stewart D.P. & Randolph M.F. (2002). Modelling of shallowly embedded offshore pipelines in calcareous sand, *Journal of the Geotechnical Engineering Division*, ASCE, Vol. 128, No. 5, pp 363-371.

Zhou, H. & Randolph, M.F. (2009). Numerical investigations into cycling of full-flow penetrometers in soft clay, *Géotechnique*, Vol. 59, No. 10, pp. 801-812.

Zhou, H., White, D.J. & Randolph, M.F. (2008). Physical and numerical simulation of shallow penetration of a cylindrical object into soft clay, *GeoCongress 2008: Characterization, Monitoring, and Modeling of GeoSystems (GSP 179)*, Vol. 311, No. 14.